5-2014

Predictions of NOx emissions in pulverized coal combustion.

Niko Hachenberg 1981-
University of Louisville

Recommended Citation

Hachenberg, Niko 1981-, "Predictions of NOx emissions in pulverized coal combustion." (2014). *Electronic Theses and Dissertations.* Paper 557.
https://doi.org/10.18297/etd/557

PREDICTIONS OF NO_X EMISSIONS IN PULVERIZED COAL COMBUSTION

By

Niko Hachenberg
Dipl.–Ing. (FH), University of Applied Science Cologne, 2006
Dipl.–Wirt.–Ing. (FH), University of Applied Science Cologne, 2007
M.S., University of Louisville, 2011

A Dissertation
Submitted to the Faculty of the
J. B. Speed School of Engineering of the University of Louisville
in Partial Fulfillment of the Requirements
for the Degree of

Doctor of Philosophy

Department of Industrial Engineering
University of Louisville
Louisville, Kentucky

May 2014

PREDICTIONS OF NO_X EMISSIONS IN PULVERIZED COAL COMBUSTION

By

Niko Hachenberg
Dipl.–Ing. (FH), University of Applied Science Cologne, 2006
Dipl.–Wirt.–Ing. (FH), University of Applied Science Cologne, 2007
M.S., University of Louisville, 2011

A Dissertation Approved on

March 3, 2014

by the following Dissertation Committee:

Dr. William E. Biles, P.E., Dissertation Director

Dr. Suraj M. Alexander, P.E.

Dr. Ki–Hwan G. Bae

Dr. Angela K. Thompson

To my family,

ACKNOWLEDGEMENTS

I offer my deepest gratitude to Dr. William E. Biles, whose interest, patience and instruction enabled this dissertation to be completed. During the entire research work he kindly granted me his outstanding support at any time.

I would like to sincerely thank the other committee members Dr. Suraj M. Alexander, Dr. Ki–Hwan G. Bae and Dr. Angela K. Thompson for their efforts in reviewing this research work.

Many thanks to my fellow students for all the support and encourage that they gave to me to accomplishing this goal.

Last, but certainly not least, I would also like to thank the University of Louisville and all the Professors who provided me the opportunity to pursue this research and further my education.

Niko Hachenberg

University of Louisville in Kentucky, USA

March 2014

ABSTRACT

PREDICTIONS OF NO_X EMISSIONS IN PULVERIZED COAL COMBUSTION

Niko Hachenberg

March 3, 2014

The purpose of this research work was to develop a transferable mathematically simple model which gives the possibility to make fast and easy predictions regarding the NO_x emission behavior of a broad–spectrum of coals within a certain combustion environment. In this context, this thesis is a further step of a common ongoing investigation focused on predicting NO_x emissions from self–sustaining, pulverized coal combustion in dry bottom firing systems. A comprehensive literature research focused on already published NO_x prediction approaches from scientific publications based on fundamental quantitative relationships or empirical algorithms and statistical relationships was also carried out in this context.

This research concentrated on three specific areas which were found to constitute a major gap in the knowledge of NO_x formation in industrial full–scale applications: the fuel properties; the dependence of furnace geometry factors; and the specific operating conditions. The developed model shows a strong statistical significance with a coefficient of determination of 0.9876 and a standard error of 28 mg / m³ STP_{dry} at 6 % O_2 based on 142 observations coming from 28 utility boilers. Direct comparisons between model history and observations reported by other researchers have also shown very good conformities.

For that background, this thesis form a good basis for identifying individual factors which contributes to system related NO_x emissions in order to investigate how variations in the process parameters affect the emission level. Perhaps, as contribution to the understanding of NO_x formation during coal combustion what is still an imperfectly understood phenomenon, or as basis for possible process optimization which might find application on pulverized coal–fired boilers to make the world a little bit more green.

Key words:

NO_x; Low–NO_x; NO_x prediction; NO_x formation; NO_x emissions; Pulverized coal combustion; Coal–fired utility boilers; Combustion optimization; Effective volatiles;

TABLE OF CONTENTS

PAGE

LIST OF TABLES

PAGE

LIST OF FIGURES

PAGE

PREFACE

In order to avoid confusion and errors with the thesis at hand, it should be noted that the entire work based on the International System of Units (SI). Furthermore it incorporates to the reference conditions of the German Institute for Standardization (DIN; Deutsches Institut für Normung e.V.) DIN 1343:1990–01. These standard conditions referred to a temperature of 273.15 K (0 °C, 32 F) and an absolute pressure of 101,325 Pa (1 atm, 1,013.25 mbar). Two different reference cases under these conditions exist for the definition of the reference gas state. First, the reference condition for dry gas (0 % relative air humidity) and second the reference condition for wet gas which contains 6.2 g/kg H_2O per kg dry air [1]. Every unit which referred to one of these conditions is termed by the shortcut 'STP' (standard temperature and pressure) and extended by the subscript 'dry' or 'wet' respectively.

Furthermore, the development of the here presented NO_x predictive technique is based on consistent, plausible and complete field data coming from various power plants located all over the world. These data sets have been acquired by own on site measurements, have been requested and provided by operators or have been published within other research works. All NO_x concentrations reported in this thesis are average values of several hours of stable operation of utility boilers, and they were obtained under dry gas conditions. These data sets have been mostly anonymized in order to protect all specific process data against competition espionage and social engineering.

I. INTRODUCTION

Coal as an Energy Source

The use of coal dominates the world–wide energy production and accounted for nearly half of the increase in global energy use over the past decade. The respective share of world energy consumptions was in 2010 nearly 30 % and thus the highest since 1970 [2] compared with 23 % in 2000. Coal is the backbone of global electricity generation and accounts for over 40 % of electricity output in 2010. Even in the OECD[1], coal fueled more than one–third of electricity generation in 2010. In non–OECD countries, where coal resources are often abundant and low cost, coal is the most important fuel. It accounted for 35 % of total primary energy use, 36 % of total industry consumption and nearly half of total electricity generation in 2010 [3].

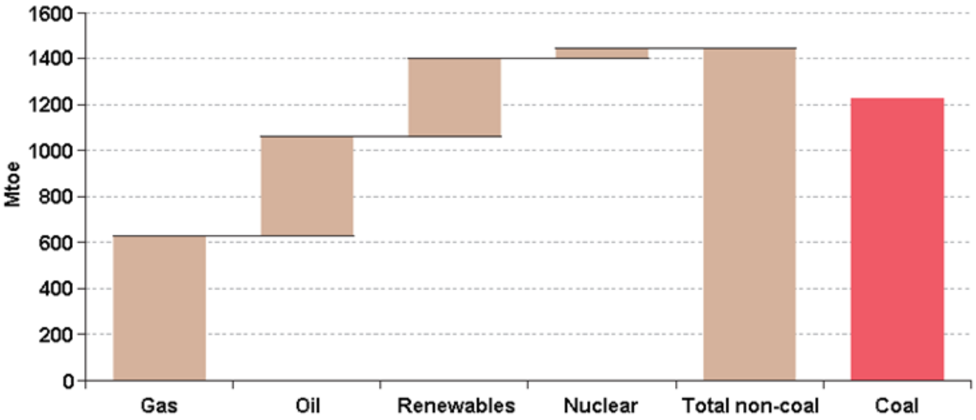

Figure 1. Incremental worlds primary energy demand by fuel, 2000–2010 [3]

---

[1] Current OECD member countries (as of September 1, 2011) are the United States, Canada, Mexico, Austria, Belgium, Chile, Czech Republic, Denmark, Finland, France, Germany, Greece, Hungary, Iceland, Ireland, Italy, Luxembourg, the Netherlands, Norway, Poland, Slovakia, Slovenia, Spain, Sweden, Switzerland, Turkey, the United Kingdom, Japan, South Korea, Australia, and New Zealand, Israel, Estonia.

In the last years the respect for the environment has become the main target for all and especially for coal–fired power plants in the world. However in the absence of international agreements which would limit or reduce greenhouse gas emissions, coal is still a major energy source throughout the world. The US Energy Information Administration projected an average annual increasing rate of approximately 1.5 % of their consumption from 40.7 sextillion kWh (139 quadrillion Btu) in 2008 to 61.2 sextillion kWh (209 quadrillion Btu) in 2035 [4]. This substantial increase in coal consumption is being justified by the strong economic growth in China and India.

Environmental Effects

There is a long history of public concern about the major environmental impacts which are coming from fossil power generation. Whenever fossil fuels are burned carbon dioxide (CO_2), sulfur oxides (SO_x) and additionally nitrogen oxides (NO_x) released into the atmosphere leading ultimately to a wide range of environmental impacts, including damage to forests and soils, fish and other living things, materials, and human health. All over the world are emission standards becoming more stringent due to increased concerns about the local, regional, and transboundary effects of coal–fired plant emissions. Nitrogenous oxides or also referred as 'NO_x' undergo a series of complex chemical processes into acids which effects the environment dramatically [5]. Dispersed in the atmosphere, it reacts to form secondary pollutants, including ground–level ozone and acid rain. Chemical reactions between volatile organic compounds (VOCs) (hydrocarbon radicals) and NO_x create ground–level ozone a major ingredient of smog. The control of acid rain has focused primarily on reducing SO_2 emissions because NO_x is estimated to contribute less than one–third of the acid rain generated but also one third is out of the question significant. For this background the European environmental legislation has tighten the emission limits for coal–fired power stations for power plant operations post the year 2016 as follows [6, 7].

Table 1. NO_x limits after year 2016 [6]

Thermal power (MWt)	**NO_x limit based on 6 % O_2, dry gas**
≥ 50 MWt to 500 MWt	300 mg / m³ STP_{dry} 400 mg / m³ STP_{dry} in case of pulverized lignite combustion
100 MWt to 300 MWt	200 mg / m³ STP_{dry}
> 300 MWt	150 mg / m³ STP_{dry} 200 mg / m³ STP_{dry} in case of pulverized lignite combustion

These restrictions forced plant owners and operators to decide whether to invest in their power stations to comply or to stop further operations and shut down. Therefore almost all the efforts are currently focused on the reduction of CO_2, NO_x and $SO_{x.}$ In which CO_2 and SO_x are unfortunately process dependent and cannot be reduced only by modifying the combustion itself. These emissions need to be reduced by the help of additional systems, like flue gas denitrification– and scrubber desulphurization plants. Also the nitrogenous emissions can be limited by the help of catalysts or by direct injection of ammonia inside the flue gas flow but in contrast to SO_x, NO_x can significant reduced by the modification of the combustion settings and surroundings at sources [8].

The Future of Coal

Power generation remains the main driver of global coal demand and will therefore play a significant role in meeting the global energy needs. According to the

International Energy Outlook [3] there are about 150 years of known world coal reserves economically exploitable with current technology at present consumption rates. Estimated undiscovered resources expand world energy supply from coal to about 3,000 years and as market conditions change and technology advances, more coal will be proven over time. The International Energy Agency (IEA) as well as the US Environmental Protection Agency (EPA) expected in the new policies scenario, that coal–fired plants are expected to account for around 27 % of the total new additions to generating capacity worldwide between 2011 and 2020, and around 22 % between 2011 and 2035 [3, 9].

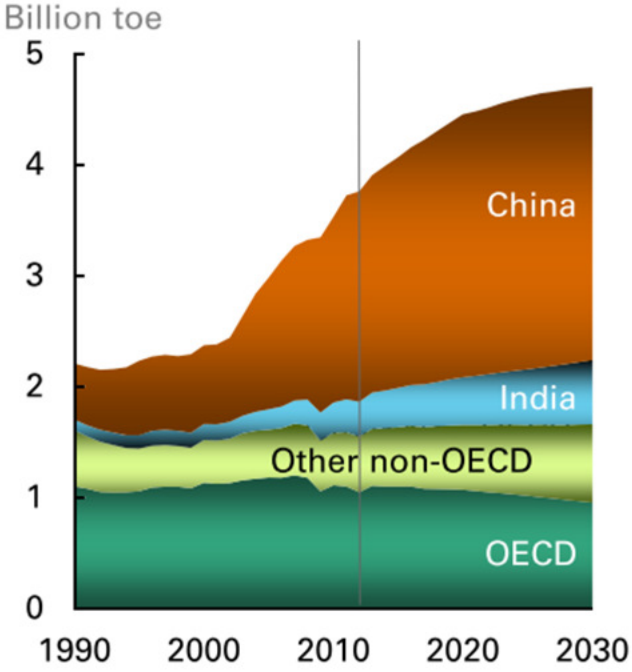

Figure 2. Perspective of the global coal demand by region [9]

The strong economic growth and large domestic coal reserves in China and India lead to a substantial increase in their coal use for electric power and industrial processes. Installed coal–fired generating capacity in China nearly doubles in the projected time period from 2008 to 2035. That means, the use of coal in Chinas industrial sector grows by 67 % [4]. China is currently the biggest coal producing and consuming country in the world. Coal is accounting for almost 75 % of the energy supply in the countries which means that the composition of energy consumption will not change much in the decades to come [10].

For all the talk about natural gas and renewable energy, coal–fired utilities are the largest electricity provider in nearly every country in the world and accounted for nearly half of the increase in global energy use over the past decade. Global coal demand accelerated by 4.4 % per year and the future steady supply is due to enormous reserve ensured. A bigger increase in both volume and percentage terms than for any other fuel category, including renewables. Coal is thus the backbone of global electricity generation, alone accounting for over 40 % of electricity output in 2010 which was almost 55 % higher than in 2000 [3]. While the price for a large proportion of coal output is relatively stable, the internationally traded coal prices tend roughly to fluctuate due to the importance of oil in coal mining operations and the cost of transporting coal over long distances the price roughly in line with oil prices over short periods. The prospects for international coal prices are not consistent throughout the literature and therefore uncertain. The most critical factor is the development of the Chinese imports, which could account for a large share of international coal trade.

It can be concluded that due to the projections described above nearly every economic engine is fueled primarily by coal, a trend that will continue for several decades. Therefore coal will continue to be one of the major sources of electricity generation for indefinite time for the world but it needs to be reliable, economical and definitely ecological too in order to protect life, environment and ensure climate stability.

II. PULVERIZED COAL COMBUSTION

Coal Characterization

Coals are complex substances that are geologically formed from ancient vegetation by the combination of time, pressure, and heat of the earth over several millennia. It is a highly heterogeneous material where the chemical composition and properties vary from sort to sort depending on how long the vegetable matter has been subjected to these conditions. For this background coal is being classified by a variety of methodologies. The common method sorts coal by its carbon content from low (45 wt.–%, lignite) to high (95 wt.–%, anthracite) and is termed as 'coal rank' [11]. The standard method of distinguish the coal by its rank is based to their progressive alteration in the natural metamorphosis from low (lignite) to high (anthracite). The classification is according to fixed carbon and gross calorific value calculated to a mineral–matter–free basis [12]. Mineral matter is the parent material from which ash is being generated during combustion. Therefore it is not the same and results in generally lower weight for ash than for its source minerals. The amount of mineral matter in the coal is a measure for the coal quality. Sulfur content, ash behavior at high temperatures, and quantity of trace elements in the coal are also used to describe the grade of coal. Although formal classification systems have not been developed around the grade of coal, the grade is more important for the power plant. In addition there are two different kinds of moisture incidents distinguish when coal is being analyzes. The moisture, mineral–matter–free basis (moist, mmf) for coal analysis which is calculated from the coal sample and expressed the natural inherent moisture is present but does not include visible water on the surface and the dry–mineral–matter–free basis (dmmf) which expressed the total moisture excluded [13]. Since the rank of the coal, its quality, and burning behavior is most important for the coal industry, almost every coal–producing country has developed its own economic coal classification. These classification methods based mainly on certain rank parameters which have been defined under the jurisdiction of several organizations for standardization, e.g. the American Society for Testing and Materials (ASTM) or the International Organization for Standardization (ISO). The volatile content and the carbon and hydrogen content are often used to classify coals. The following Figure 3 gives an overview [14].

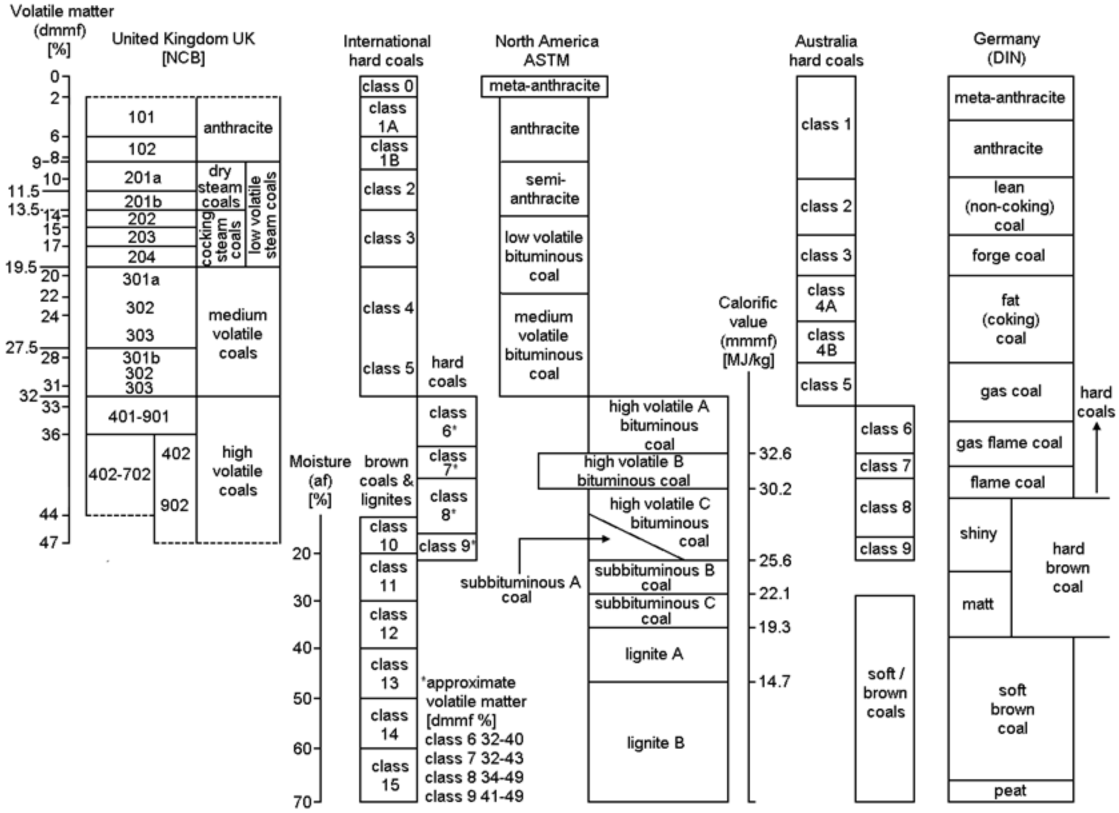

Figure 3. Coal classification systems [14]

Coal characterization shall help to predict the combustion behavior. The proximate and ultimate analysis of coal provides important information as specific energy, inert fraction (ash), moisture content, volatile matter content, and elementary components [15].

Proximate Analysis

The proximate analysis of coal is a commonly applied characteristic test which yields: total moisture, inherent moisture, volatile matter, ash and fixed carbon. The total moisture content is measured by the weight difference of a specific coal sample size between before and after heating under reducing conditions (N_2) for 3 hours at 105 – 110 °C. Moisture determination is important because the moisture content of coals varies widely. The highest moisture content is with the low–rank coals. Moisture levels provide an indication of the drying required in the handling and pulverizing portions of the boiler coal feeding system [16]. The remaining moisture after surface drying is the inherent moisture which is measured with another sample that first heated to 35 °C under same atmospherically conditions for drying the particle surface water. 1 gram of air–dried sample is placed into a furnace at temperature of 105 – 110 °C for 30 minutes. The weight difference before and after this heating phase is the inherent moisture content.

The volatile matter content is that portion that is driven off in gas or vapor form (exclusive of moisture). The main constituents of volatile matter are hydrogen, oxygen, carbon monoxide, methane, other hydrocarbons, and that portion of moisture that is formed by chemical combination during thermal decomposition of the coal. The volatile matter content is measured by the weight loss before and after heating of 1 gram coal with particle size < 200 μm under reducing conditions to a temperature of 900 °C, corrected for inherent moisture [17]. Volatile matter is also used to determine the coal rank, an indicator of ease of ignition and if a supplemental fuel will be necessary for flame stabilization, and used as a basis for selling and purchasing of coal.

The ash content is the resulting mass after a sample of 1 gram with particle size < 200 μm has been heated in air at 815 °C. The weight of ash is usually slightly less than that of the mineral matter originally present before burning. The ash content indicates the load under which the collection system for boiler bottom ash and fly ash must operate and is used for assessing shipping and handling costs [16].

The fixed carbon content is the combustible residue after driving off the volatile matter. Therefore it can be calculated as the difference of one minus the sum of moisture, ash and volatiles. It is not all carbon and represents that portion of the coal that must be burned in a solid state. Fixed carbon is used to determine coal rank and is a guide in the choice of fuel–firing equipment [16].

Ultimate Analysis

The ultimate analysis determines the elemental compositions of the organic fraction as proportion of carbon, hydrogen, nitrogen, oxygen, sulfur and others by laboratory standard procedures. Oxygen is determined by the difference, i.e., subtracting the total percentages of carbon, hydrogen, nitrogen, and sulfur from one because of the complexity in determining oxygen directly. However, this technique does accumulate all the errors in determining the other elements into the calculated value for oxygen. The ultimate analysis is used with the heating value of the coal to perform combustion calculations including the determination of coal feed rates, combustion air requirements, and weight of products of combustion to determine fan sizes, boiler performance, and sulfur emissions [16]. Table 2 gives an overview of some typical values for different coal ranks [18].

Table 2. Typical coal compositions [18]

US Geological Survey Sample No.		D 165564	D 163186	D 169557	D 176167	D 176165	D 171211
As received basis		**Lignite**	**Sub–bituminous**	**Bituminous**			**Anthracite**
				High VM	**Med. VM**	**Low VM**	
Heating Value	MJ/kg	16.637	21.796	26.583	31.462	31.137	30.184
Proximate Analysis							
Volatile Matter	wt.–%	29.20	27.50	37.80	24.70	18.10	6.30
Fixed Carbon	wt.–%	31.90	46.30	42.40	63.30	70.10	80.30
Moisture	wt.–%	34.60	19.70	4.20	1.80	3.50	1.50
Ash Content	wt.–%	4.30	6.50	15.60	10.20	8.30	11.90
Ultimate Analysis							
Carbon	wt.–%	42.80	56.40	63.40	76.80	78.80	80.30
Hydrogen	wt.–%	6.80	5.50	5.00	4.70	4.40	2.70
Oxygen	wt.–%	10.30	10.70	8.60	3.20	2.20	2.30
Nitrogen	wt.–%	0.70	0.80	1.40	1.70	1.70	0.80
Sulfur	wt.–%	0.50	0.40	1.80	1.60	1.10	0.50

The coal quality has a significant impact on the boiler performance, with respect to efficiency, emissions, fly ash quality, slagging and fouling behavior. Maintenance and availability are also influenced. Therefore, coal properties have to be determined in order to assess if a specific coal or coal blend maybe fired in a particular unit.

Coal Combustion

The combustion of coal involves a complex series of different reactions. Principally it is the oxidation of organic material in coal. Solid and gas phase chemical reaction as well as complex structural changes occur during the burning process [19]. The combustion of coal takes place in three stages:

• Devolatilization	Release of volatile matter due to rapid heating of the coal particle.
• Char oxidation	Heterogeneous combustion of the solid core (char) after the gaseous components have been driven off.
• Volatile reaction	Homogeneous gas–phase combustion of the devolatilized products.

The composition of the used coal is important for the formation of NO_x within a furnace because it primarily influences the local environment and temperature profiles [20]. Ohtsuka et al. [21] and Mori et al. [22] demonstrated that the molecular nitrogen (N_2) content in the flue gas was greatly promoted when various pulverized coals were doped with iron from precipitated $FeCl_3$ solutions and pyrolyzed in a fluidized bed reactor. Leppälahti et al. [23] also found under pyrolysis conditions at 900 °C that the presence of iron catalyzed the destruction of NH_3 and HCN from coal nitrogen and promote the formation of N_2. That means higher iron contents in the coal leads basically to a less NO_x production rates.

Devolatilization

As mentioned describes the devolatilization process the initial phase of particle heating. It is a process in which coal is transformed at elevated temperatures to split into gaseous, char and tar compounds [24]. This elevation of temperature necessary occurs during combustion process within a certain furnace by radiation and convention. During the heat–up of the coal particles dominates the convection because of the hot recirculated gas zones which belongs to the axial pulse of the outcoming volume flows at the burner outlet. The resulting heating rate during this process are known to be of the order of 10^4 to 10^6 K / s [25] with peak temperatures of 1,800 to 1,900 K [26]. After the particle reached a certain temperature the volatile material starts to exorcise and ignites rapidly at higher temperatures in the presence of oxygen. The total amount of volatiles and the rank of coal give an indication about their ignition behavior and are thus an important factor for the stability of self–sustaining pulverized coal flames. The yield of volatiles depends on the coal type and combustion conditions, such as temperatures, heating rate and particle size [27]. Different products released at different temperatures and just a porous char matrix is left after the devolatilization process which contains high carbon content in relation to the remaining particle weight. This char pattern burns heterogeneously in the postflame region. Essenhigh [25] described for example, that as higher the rank of a coal the more volatiles are released as tar which formed more HCN and NH_3 during the devolatilization and secondary cracking [24] which are generally an indicator for tendencially higher NO_x emissions. The higher a coal is being ranked as more tar will be released during the devolatilization process. The tar proportion will be cracked into lighter components and under an oxygen deficiency environment soot will be formed [28].

Char Oxidation

As the name suggest diffuses oxygen into the pores of the particle and reacts with the fixed carbon. The conversion is proportional to the internal surface area. The main driver for the rate of this chemical kinetics is the temperature. At temperatures below 600 °C (~ 1100 F) the reaction rate is comparatively slow and the oxygen can completely penetrates the pores of the particle. At high temperatures the diffusion velocity of oxygen into the pores becomes the limiting factor. During the burning process at the outer surface the particle shrinks over the time because of the oxidation of the bound carbon [29].

Char combustion and loss of volatile matter occur simultaneously and is compared with the devolatilization a slow process. Determining by the char reactivity, particle size, density and the combustion environment the total time required for a full burnout can be up to 3 seconds and determines therefore mainly the size of the boiler [27]. Therefore is the initial particle size distribution of importance. As smaller the particle as faster the burning rate and as better the chemical conversion [16]. A change in the particle size distribution affects the heat generation and heat loss of the particle mixture because possible maceral disproportionation during grinding leads to differences in oxidation rates between the size fractions [30, 31] and results therefore in a change in the thermal equilibrium conditions and temperature [32].

Volatile Reaction

Volatile matters are the organic decomposition products which emerge as gas or steam during heating up of coal substance under air exclusion. The reference temperature on this occasion is 900 °C (~ 1,650 F). Essentially the volatile constituents consist of different hydrocarbons as carbon monoxide (CO), CO_2, H_2O, methane, ethane, ethylene and tar [33, 34]. With advancing coalification the content of volatile components bound in the particle decreases and as a logical result the proportion of elemental fixed carbon increase. These particles tend more to lose their overall density instead of shrinking during devolatilization [16].

It can be concluded that the rank of a coal reflects their coalification properties, that means the proportion of volatiles are generally proportional to the coal age/–rank. As a result has the geological relatively young lignite a high proportion of non–condensibles because due to the lower pressure during the coalification process it have not converted so much vegetable matter into fixed carbon and are substantially woody [11], while higher rank/–older coals have lower proportions of non–condensibles [35].

Pulverized Coal–Fired Boilers

Due to over 100 years of service pulverized fuel–fired boilers have the highest combustion efficiency than any other boilers. These kinds of boilers have burnt almost every type of coal across the world. It is the most dominant type because of its great versatility and scalability [36]. In the field of pulverized coal combustion it can be distinguish between slag–tap firing and dry bottom firing systems.

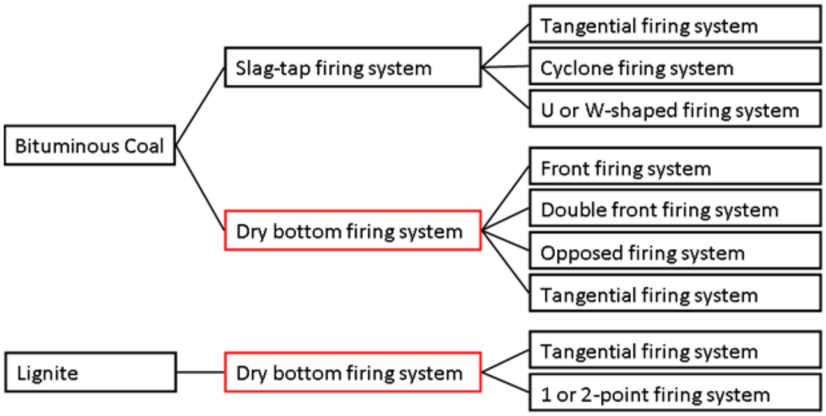

Figure 4. Pulverized coal firing system applications

The boiler philosophy of both combustion systems is the same. It is a device that boils water to produce steam. More scientifically, it converts the chemical bound energy in fuel into the heat energy in steam, or the heat energy of hot gases into the heat energy of steam when no firing is involved. The type of power plant boilers are being designed for the specifically application with its fuel composition, its calorific value and ash characteristics. The combustion furnaces are made in various shapes and sizes to burn a variety of fuels with the end purpose of producing varying amounts of steam for either process or power or both [36, 37]. Pulverized fuel combustion systems involve a sequence of plant auxiliaries and equipment which consist of coal size reduction and drying in mills, transportation from mills to burners and the final injection through burners into the furnace for combustion. In general there are two kinds of pulverized coal firing principles available which depends on the characteristics of the used coal and their respective milling plant and requirements

- Bituminous coal–fired units
- Lignite coal–fired units

Due to the significant difference between slag–tap firing systems and dry bottom firing systems it will not be successful to compare these two combustion applications directly and due to the fact that widely most applications are being based on the dry bottom principle has the actual work being focused them. Dry bottom principle means that the furnace temperature is kept below the ash melting point.

Bituminous–fired Systems

The functional principle of a pulverized bituminous coal–fired boiler is generally characterized by a pneumatic transport of pulverized fuel (PF) with a certain portion of the combustion air (about 20 %) into a combustion chamber (furnace). The necessary hot air being pulled by a primary air fan from the air heater outlet through the mill and picks up the ground coal from the mill to deliver the mixture to the burners. The temperature of this primary air (PA) depends on the necessary energy to dry and preheat the wet and cold coal inside the milling plant. For that hot air is suitably mixed with ambient air to meet the mill outlet temperature requirements which are usually at around approximately 90 to 120 °C.

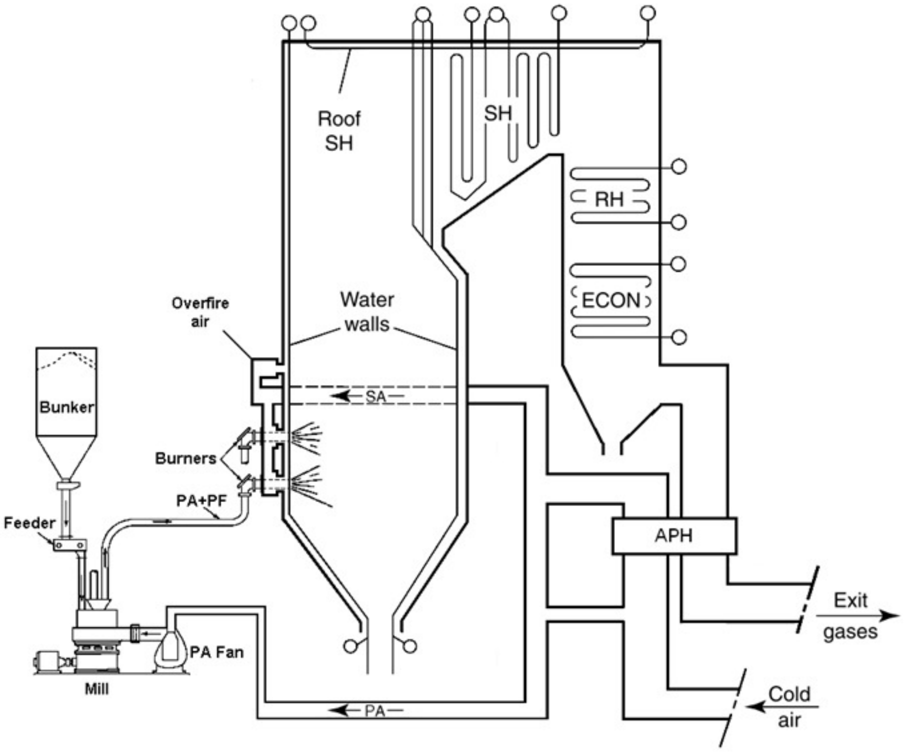

Figure 5. Typical configuration of a pulverized bituminous coal–fired boiler

The coal is transported through pipes as a PF / PA mixture from the mill to burners along with the moisture of the incoming coal that is heated and dried before grinding. The amount of primary air is keeping constant at a certain ratio of coal at full load, whereas the moisture can vary [37]. The larger part of the combustion air (secondary air) is preheated at a high temperature level (up to 340 °C) and enters through separate duct works. Pulverized coal is injected into the furnace through burners. Generally, the design of a burner can be quite different but generally two main types for pulverized coal burners can be identified: swirl burners and yet burners. The respective design depends on the coal properties and also on the specific configuration of the combustion system involved. Each burner creates its own flame, and there is limited physical interaction between the flames of the e.g. wall–fired burners [16].

Most bituminous coals can be fired in dry–bottom firing systems. Only coals with a volatile content lower than 20 % are typically burned in slag–tap firing systems or, in the case of high ash initial softening temperatures, in downshot–fired furnaces.

Lignite–fired Systems

The main difference to bituminous coal–fired units is that the coal has a significant higher amount of moisture content than higher ranked coals have. Therefore is much more energy needed for the drying and grinding process. Flue gas is used for drying and conveying, in preference to air, especially for low–rank fuels which contains high moisture contents (up to 70 %). This milling process is determined by a significant amount of recirculated hot flue gas from the furnace, suitably mixed with air from the air preheater (APH) exit. Another important difference is that there is no need for impact for these fuels. Attrition is sufficient and provided by a high–speed beater wheel that works also as a suction fan for the flue gas.

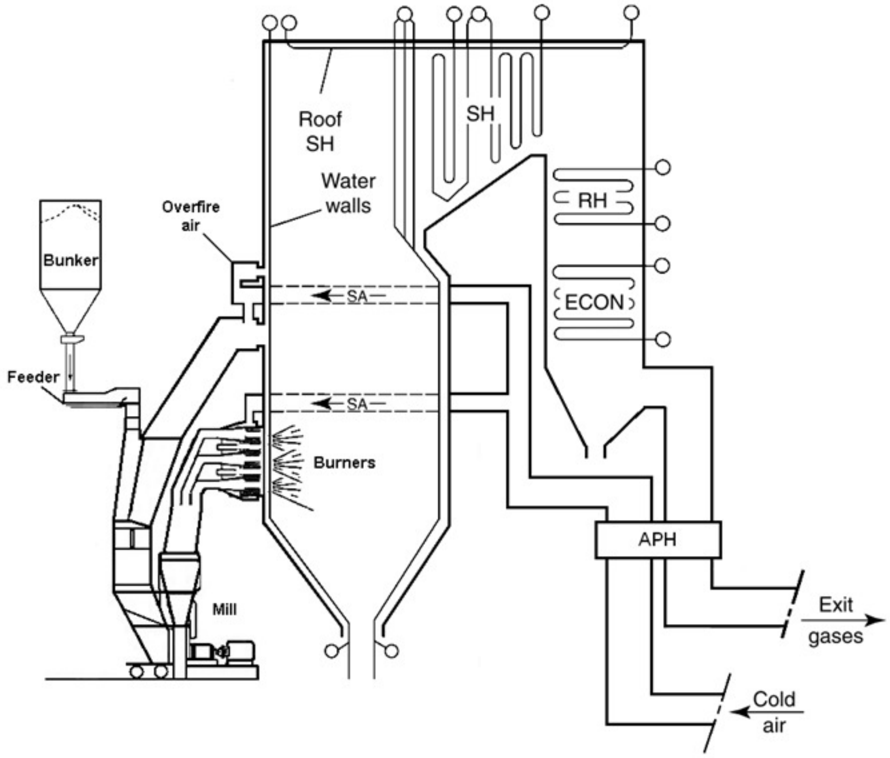

Figure 6. Typical configuration of a pulverized lignite–fired boiler

The classifier on the discharge side returns larger pieces to the inlet. The burner and the type of firing and, accordingly, the need for the inclusion of the classifier determine the fineness which is affected by the several boundary requirements [37]. After grinding the coal is typically injected into the furnace through yet burners. There is mostly no swirling of air in principle. The SA introduced into the furnace through burners in several small alternate streams. These streams make use of the entire furnace to generate a cyclonic motion, thereby providing the necessary scrubbing.

The burning philosophy, arrangement, and effects of these combustion system, superheater (SH), and attemperator system differ from bituminous coal fired units but exhibit no difference in efficiency and performance.

NO_x Emissions

The global emissions of NO_x into the atmosphere have been increasing steadily since the middle of the last century. Although there are important natural sources for NO_x is a significant amount of the increased emissions attributed to human activities, especially by the combustion of fossil fuels [38]. The term NO_x refers to the sum of seven main compounds [5].

Table 3. NO_x composition

Valence	Name	Formula	Properties
1	Nitrous oxide	N_2O	Colorless gas, water soluble
2	Nitric oxide Dinitrogen dioxide	NO N_2O_2	Colorless gas, slightly water soluble
3	Dinitrogen trioxide	N_2O_3	Black solid, water soluble, decomposes in water
4	Nitrogen dioxide Dinitrogen tetroxide	NO_2 N_2O_4	Red–brown gas, very water soluble, decomposes in water
5	Dinitrogen pentoxide	N_2O_5	White solid, very water soluble, decomposes in water

Nitrous oxide (N_2O) also termed laughing gas occurs only in very negligible amounts in the flue gas at the boiler outlet. It arises from the nitrogen content in the combustion air only within the primary reaction zone. In this area N_2O occurs nearly complete as an intermediate reaction until it responds to NO, N_2 and O_2 at the end of the reaction zone. The traces of N_2O at the furnace end are not serious measurable because the actually present quantity is still smaller than the tolerance area of the measurement device itself [39]. Therefore it is commonly not taken into consideration while talking about NO_x emissions. The components dinitrogen dioxide (N_2O_2), dinitrogen trioxide (N_2O_3), dinitrogen tetroxide (N_2O_4) and dinitrogen pentoxide (N_2O_5) however, can only be generated on the basis on nitrogen oxide (NO) and nitrogen dioxide (NO_2). NO is also an intermediate reaction because within the atmosphere this compound is in the presence of oxygen and at temperatures above 20 °C very unstable and will further react to NO_2. This reaction can be expressed as follows:

$$\boldsymbol{O_3 + NO \leftrightarrow NO_2 + O_2} \tag{II–1}$$

Equation (**II–1**) means, under the availability of ozone (O_3) from the atmosphere NO will further react to NO_2 at the stack outlet. From the environmental point of view is therefore NO_2 the important magnitude and because it contributes to the production of photochemical smog and acid rain [40]. Taking the average ozone concentration within the atmosphere into account is the typical reaction time of the process described in equation (**II–1**) around 1 minute [41].

The fraction of NO_2 in total NO_x is about 50 % on low–temperature low–NO_x flames due to the high ratio of H to NO [42] and about 90 % under fuel–rich conditions [43]. This circumstance builds the foundation for the fact that only the molar mass of NO_2 is being used for the determination of the emitted NO_x quantity of a power plant unit at the stack outlet instead of a complex or individual molar mass calculation.

Mechanisms of NO_x Formation during Coal Combustion

During coal combustion nitrogen oxides are produced by potentially tens of species and hundreds of reactions involved which are closely linked with the coal combustion mechanisms of devolatilization, char combustion, and volatile burning in a typically turbulent two–phase flow condition with significant heat releases [44]. These complex mechanisms have been classified into two basic groups which produced NO_x during homo– and heterogeneous reactions [45–62].

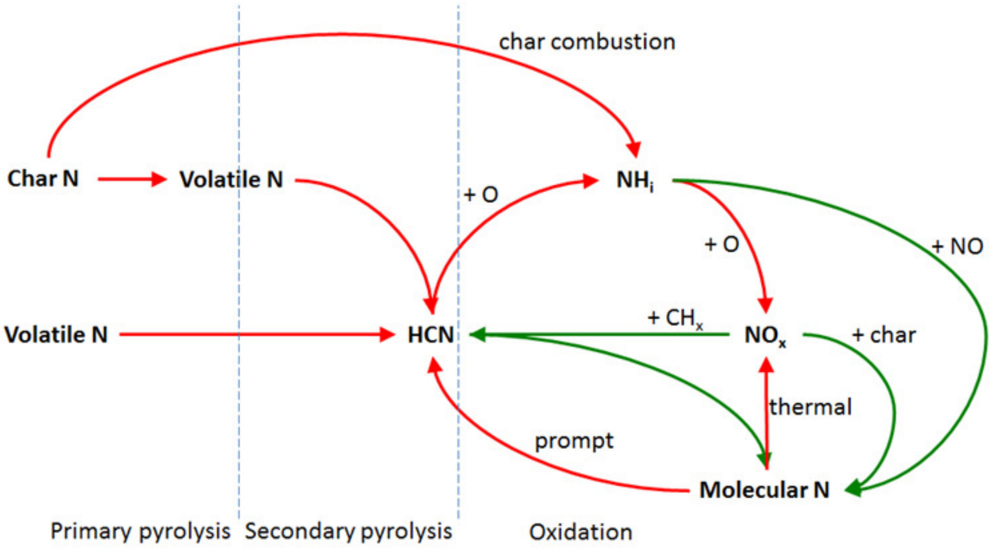

Figure 7. Simplified NO_x formation pathways during coal combustion [63]

The molecular nitrogen (N_2) of the combustion air and the fuel–bound organic nitrogen are being based as causal sources for the formation of NO_x [63–67]. The total amount of NO_x emissions resulting from solid–fuel combustion can be described by the summation of the three main identified reaction pathways [6]. They consist of two dominant and one devote mechanism depending on their shares in the total amount and the source of nitrogen and chemical kinetics.

• Thermal–NO_x	The fixation of atmospheric nitrogen by atomic oxygen, the latter formed by splitting of the molecular oxygen and nitrogen due to high available temperatures within the combustion zone.
• Fuel–NO_x	The fuel–bound organic nitrogen reacts with available hydrocarbons (CH_x).

- Prompt–NO_x The in the combustion air bound nitrogen reacts with available hydrocarbons or hydrocarbon fragments that originated in thermal decomposition in a reducing atmosphere.

Thermal–NO_x

Thermal–NO_x results from the oxidation of nitrogen present in the combustion air under strong temperature dependencies. Generally it accounts for 20 % to 50 % of the total NO_x generated [40]. This is due to the fact that during the combustion process the existing O_2 is being dissociated by the local temperature profiles and the emerging free oxygen atoms attacks the available nitrogen molecules to form mainly NO and NO_2. For this purpose, the necessary temperatures prevail predominantly within the secondary combustion zone. Zeldovich [45] has described the oxidation of nitrogen and discovered the following eponymous mechanism:

$$\boldsymbol{O + N_2 \leftrightarrow NO + N} \qquad \text{(II–2)}$$

$$\boldsymbol{N + O_2 \leftrightarrow NO + O} \qquad \text{(II–3)}$$

The first reaction hereby controls the system but as this reaction needs very high activation energy it is mentioned that it is slow at low temperatures. The cracking of the stable N_2–binding required a very high activation energy which means temperatures above 1,200 °C [39]. These reactions occur even rapidly at combustion temperatures over 1,538 °C [40]. Therefore the main formation of thermal–NO_x occurs at the portion of the flame close to the burner, where the peak flame temperature is the highest in combination with available oxygen. For pulverized coal combustion, especially in fuel–rich flames, the two–step mechanism underpredicts the real NO_x level. Fenimore and Jones [46] referred that to the higher concentration of hydrocarbon radicals within the reaction zone and Bowman and Seery [68] extend the Zeldovich [45] mechanisms by a third elementary step in order to consider this effect.

$$\boldsymbol{N + OH \leftrightarrow NO + H} \tag{II–4}$$

The NO_x production rate dependents upon the availability of oxygen in the flame and is found to be exponentially dependent, upon the temperature resulting in that area so, that temperature peaks within the flame structure substantially stronger determine the rate of formation as the level of the average temperature profile [39]. For this background it can be assumed that the generation of thermal–NO_x could be reduced by optimizing the furnace and burner design.

Fuel–NO_x

The organic nitrogen which is chemically bound in the coal is the main source for the total exhaust NO_x emissions from coal flames [69, 70]. Generally coal consist of a few percent nitrogen which results in much larger NO_x emissions of flames compared to those from gas or oil flames [71]. It results from the oxidation of nitrogen which is organically bound in the fuel and can contribute over 75 % (up to 95 %) of the total NO_x formed during the devolatilization process and char burnout [72]. The production of nitrogen oxides and molecular nitrogen is either as a homogenous gas phase reaction or as heterogeneous reaction which involves the coal char surface [73]. In this connection are the most important reactions on the char surface described by the following reaction equations:

$$\boldsymbol{C_{Char} + \frac{1}{2}O_2 \leftrightarrow CO_{Char}} \tag{II–5}$$

$$\boldsymbol{N_{Char} + \frac{1}{2}O_2 \leftrightarrow NO + Char} \tag{II–6}$$

$$\boldsymbol{NO + 2CO_{Char} \leftrightarrow N_2 + 2CO_2 + Char} \tag{II–7}$$

These mechanism indicated that the amount of NO_x generated by fuel–bond nitrogen increase when the residence time of the burning particle increase likewise. Fenimore [74] stated that these relations can be observed as long as the reaction occurs at temperatures above 800 °C. An additional rise of NO_x generated by fuel–bond nitrogen is caused by the rise of oxygen content in the flame which leads to fuel–lean conditions. Under these circumstances leads the higher partial pressure of the molecular oxygen to more available atomic oxygen in the flame front and favor therefore the formation of NO from HCN, whereas under fuel–rich conditions the generation of N_2 would be preferred. A similar set of reactions can be written for NH_3, where fuel–lean conditions are favoring NO and fuel–rich conditions are favoring N_2 [73]. They can be found in the work of Nordin et al. [73].

Prompt–NO_x

Due to the fact calculations based only on the above given mechanisms would generally under predict the total amount of NO_x generated especially when no fuel–bound nitrogen is involved, e.g. natural gas firing systems, leads to the assumption that must be also another reaction pathway. This chemical mechanism describes the prompt–NO_x as formation of molecular nitrogen in the air combining with these in the fuel under fuel–rich conditions with short flame–residence times at temperatures between 1,600 °C (~ 2900 F) and 2,100 °C (~ 3800 F) [75]. The formation is being initiated through various hydrocarbon fuel fragments like CH and CH_2 which results by the devolatilization process. The molecular nitrogen is being attacked by these hydrocarbons and due to the reaction zone and velocity it occurred very rapidly [6]. Fenimore [47, 76] has described this phenomenon as follows:

$$\boldsymbol{N_2 + CH \leftrightarrow HCN + N} \tag{II–8}$$

With a contribution of [58]:

$$\boldsymbol{C + N_2 \leftrightarrow CN + N} \tag{II–9}$$

These reactions occur mainly in fuel–rich regions where hydrocarbon radicals increase the formation of HCN through the following reactions [73, 75]:

$$\boldsymbol{N + O_2 \leftrightarrow NO + O} \tag{II–10}$$

$$\boldsymbol{N_2 + CH_2 \leftrightarrow HCN + NH} \tag{II–11}$$

$$\boldsymbol{N + CH_3 \leftrightarrow HCN + H_2} \tag{II–12}$$

The nitrogen then oxidizes along with the fuel and becomes NO_x during combustion, just like fuel–NO_x [5] and the HCN oxidized to NO depending on the prevailing conditions. Add to this, a significant fraction of the nitrogen compounds under the prompt mechanism is being converted to diatomic nitrogen (N_2) inside the boiler [27, 40]. For this background is a distinction between these two formation mechanisms in the further course of the reaction no longer possible and as such it has until now not being considered in more detail. This might be due to the fact that it is assumed that the portion of prompt–NO_x contributes to less than 5 % of the total NO_x generated during coal combustion.

III. PROBLEM STATEMENT

Combustion research started back on half a million years and thus it seemed to be the oldest scientific engineering research altogether [77]. But only since the middle of the last century becomes the awareness before environmental impacts and health effects sources by nitrogenous pollutants from industrial coal combustion systems more and more significant. Coal combustion generates high quantities of NO_x which are a significant driver for photochemical smog and acid rain [78, 101]. The formation of NO_x during coal combustion is a very complex process and obeys hundreds of elementary chemical reactions which are still been investigated since the industrial use of utility steam generators began over 100 years ago. Fundamental investigations to determine the mechanism of NO_x formation during coal combustion have been done and despite such essential work of person like Yakov Borisovich Zel'dovich and Charles Paine Fenimore it is not fully understood. An enormous amount of literature has been published so far but up to now it is not possible to calculate NO_x emissions for a practical coal combustion situation based on solving individual reaction rate equations, even using computers. This may come by the fact that all identified primary influence factors on NO_x emissions, as temperature (as activation energy), concentrations of oxygen and nitrogen (partial pressure), C–N bonds in fuel (as reactants), and / or the respective residence time within the reaction zone [79], enter and alter each other which means, if any one of these factors changed the NO_x production rate will also change immediately.

Many unknowns have to be coupled to understand the influence of a certain parameter within a specific combustion environment and there are numerous techniques available to influence NO_x emissions. Some of these techniques involving substantial capital investment and others may only consist of changings in the operation settings of the system. Mathematical models can help to understand the combustion process in order to design and / or optimize burner or furnace. In addition they raise the understanding for various predictions, e.g. the influence of another coal quality on the combustion performance in a specific boiler which is an important factor for the procurement strategy of the international power generation industry [80].

Therefore is the objective of this study to gain the possibility to make fast and easy predictions regarding the combustion behavior of certain solid fuels within a certain combustion environment in order to identify the individual factors contributing to NO_x formation and investigates how variations in the process parameters affect the emissions as basis for possible process optimization at lowest cost. Such model could be used to find an optimum in combustion efficiency and hence emissions at highest possible process efficiency, and for sure to understanding the different influence factors and their interaction within a specific furnace environment to gain the possibility to optimize combustion systems with respect to efficiency and reliability under environmental awareness. Any results could contribute to the understanding of the entire reaction chain and thus such approach could be a useful tool for science and the industry.

IV. LITERATURE REVIEW

Predicting NO_x emissions from coal combustion is considerably difficult. Many important aspects of chemistry and physics have to be coupled in a way that allows realistic prediction of NO_x formation of practical coal–fired utilities with reasonable computational effort. Considerable work has been done to identify the major influence factors and their contribution to the overall NO_x emissions. Relating to the prediction of NO_x generation in a coal–fired power station it can generally classify into four groups [81]:

- Fundamental quantitative relationships.

  Investigations regarding nitrogen content in coal, coal rank, relevant physical and chemical properties, nitrogen partitioning, formation and fate of nitrogenous species, combustion behavior and effects.
- Empirical algorithms and statistical relationships.

  Models which have been usually developed of a certain boiler configuration and coal properties on a relatively small set of data.
- Computational Fluid Dynamic (CFD) and kinetic modeling.

  Physical and/ or chemical 3D steady state and time–dependent modeling of the combustion process [82–86 and others].
- Artificial neural–networks (ANN) and fuzzy systems

  Expert systems and neural networks are increasingly applied for the NO_x

> prediction since the early 1990s. The systems are an information processing system that imitates biological brain structure and function. The network seek iteratively for patterns and trends between the defined input and output data set [87].

NO_x emissions from practical coal combustion situations are the most difficult pollutant of all generating emissions. Actually, there is no method available which examines certain predictions on NO_x generation. For this background was the objective of this study to develop a practical, fast and easy to use engineering approach and therefore the last two categories had not be covered in this thesis. Details on the operation and use of the other modeling approaches have been reported elsewhere.

NO_x Prediction Approaches

Over the past decades there has been an increasing interest in a prediction possibility of NO_x emissions for coal combustion utilities. This is due to the fact, that at this time it is not possible to calculate the NO_x emission level based on solving individual equations, even using computers. However, the prediction of NO_x formation from coal combustion systems is very complicated by the complexity of the factors involved. Several scientists have dealt with the issue and based on fundamental quantitative relationships or empirical algorithms and statistical relationships, a considerable number of approaches have been identified. It shall be remarked that the found NO_x prediction techniques will be described in their mode of operation in the following, including a comparison summary at the end of this section.

Bartok et al. (1971)

Bartok, Crawford and Piegari [88] were the first pioneers who had tried to find a statistical relationship between NO_x emissions and a simple and general applicable system indicator to determine NO_x emission by fossil fuel type and boiler design, mainly for the reason of estimating the applicability of a potential combustion modification. This indicator should be as easy as possible to determine but anyhow reflect the individual boiler utilization for different load cases. The authors investigate therefore the correlation between boiler gross load $(\boldsymbol{MW})$ per furnace firing wall $(\boldsymbol{FFW})$ and measured data from 7 coal–fired boilers by a linear regression analysis. The following correlation had been identified based on the observed boilers at full load operation (5 data points):

$$\boldsymbol{NO_x = 569 + 2.76 \left(\frac{MW}{FFW}\right)} \tag{IV–1}$$

Where $\boldsymbol{NO_x}$ are the NO_x emissions in ppm corrected to 3 % O_2 on a dry basis, and $\boldsymbol{MW/FFW}$ as the load per furnace fixing wall. The authors found that one boiler (‘C’) had unusual design features which are not comparable with the others. They concluded that boiler ‘C’ was designed to be operated as a slag–tap bottom furnace at low load levels, fired with high slagging temperature coals which results in high flame temperatures, and for maintaining the slag molten in relatively slow heat absorption in the lower furnace. What is in line with the assumptions made in this thesis (see chapter ‘Pulverized Coal–Fired Boilers’). The authors found that the correlation for the other boilers could significantly improve by eliminating the data from boiler ‘C’ (4 data points). The new regression equation was:

$$\boldsymbol{NO_x = 293 + 3.65 \left(\frac{MW}{FFW}\right)} \tag{IV–2}$$

Due to the fact that the load of each considered boiler varied over a wide range had the regression analysis been adapted to all available data points from all loads (15 data points) as follows:

$$\boldsymbol{NO_x = 423 + 3.49\left(\frac{MW}{FFW}\right)} \tag{IV–3}$$

Without boiler ‘C’ (12 data points) the following deviation:

$$\boldsymbol{NO_x = 252 + 3.82\left(\frac{MW}{FFW}\right)} \tag{IV–4}$$

In addition, by the findings from the elimination of boiler ‘C’, boiler ‘Q’ had also been omitted because of its design principles. Boiler ‘Q’ operates as a cyclone furnace. The last regression equation which considered only the dry bottom–fired systems at all loads was than evaluated from 10 data points as follows:

$$\boldsymbol{NO_x = 256 + 3.68\left(\frac{MW}{FFW}\right)} \tag{IV–5}$$

The number of equivalent furnace walls for the large, 705 MW cyclone fired boiler ‘Q’ was arbitrarily to set at 3.

Crawford et al. (1974)

Crawford and Bartok [89] emulated their work from 1971 [88] and developed together with a third researcher (E.H. Manny) on the basis of more data a new regression equation on unchanged basic requirements:

$$\boldsymbol{NO_x = 386 + 1.263\left(\frac{MW}{FFW}\right)} \tag{IV–6}$$

The correlation between NO_x emissions and gross load $(\boldsymbol{MW})$ per furnace firing wall $(\boldsymbol{FFW})$.

Pershing (1976)

Pershing [72, 90] postulated that the dominant NO_x contribution factor in coal fired boilers arises through the oxidation of chemically bound nitrogen in the fuel but the NO_x emissions could not be correlated with fuel bound nitrogen content alone. Therefore the author investigated the influence to the conversion of fuel nitrogen in coal during coal combustion and developed on the basis of his experimental results a dimensionless emission coefficient 'psi' $(\boldsymbol{\Psi})$ which correlates the actual emissions of the system.

$$\boldsymbol{\Psi = \frac{NO}{NO@SR = 1.15} = (2 * SR - 1.32)} \qquad \text{(IV–7)}$$

The stoichiometric ratio $(\boldsymbol{SR})$ acts as variable. The reference point for $\boldsymbol{SR}$ has been set to 1.15, which was approximately the midway between the normal testing limits of the experiments ($\boldsymbol{SR}$ = 1.03 to 1.3). It has been shown that the correlation found was acceptable for a wide variety of fuels within the drop–tube furnace and constant aerodynamic conditions but for the full–scale systems unsuitable.

Therefore the author continued the investigation in a laboratory combustor to investigate the contribution of fuel–bound nitrogen to NO_x as main driving factor for NO_x formation. Fuel–NO_x was isolated by experimentation by replacing the combustion air with an artificial atmosphere containing argon instead of N_2. In order to describe the conversion rate of char containing nitrogen to NO_x the author investigated the burning behavior of a char sample and developed the following empirical equation for the conversion of char nitrogen:

$$\boldsymbol{CR_C = (2 * SR - 1.32) * \frac{1}{1 + \beta_C * N_{Char}}} \qquad \text{(IV–8)}$$

With $\boldsymbol{\beta_C = 540}$, which represents the single conversion coefficient determined by correlation of the experimental data on char combustion on the particular condition. $\boldsymbol{SR}$ is the stoichiometric ratio (air / fuel) and $\boldsymbol{N_{Char}}$ terms the char nitrogen content. The author stated furthermore that since the effective pyrolysis temperature within the actual coal flame is not known the fractional proportion of relating nitrogen volatiles to total volatiles is being assumed to be linearized according to the respective mass portion proportion. The conversion ratio for the volatile containing nitrogen portion had been formulated as follows:

$$\boldsymbol{CR_V = \frac{1}{1 + \beta_V * N_{Volatile}}} \qquad \text{(IV–9)}$$

$\boldsymbol{\beta_V}$ as the empirical volatile nitrogen conversion coefficient and $\boldsymbol{N_{Volatile}}$ terms the volatile nitrogen content. Unfortunately the author stated not the exact value for $\boldsymbol{\beta_V}$ which would complicates the traceability of results.

Lim et al. (1980)

Lim et al. [91] investigated on behalf of the US Environmental Protection Agency (EPA) possible NO_x control assessments for utility boiler combustion systems. As part of this work the authors created NO_x correlation equations based on several field test experiments in unstaged industrial steam generators. Key boiler design and operating variables, burner characteristics, and fuel properties were identified to contribute to NO_x formation. The authors carried out multiple regression analysis differentiated according to boiler firing types, tangential, single wall, and opposed wall–fired. For tangentially coal–fired boilers, the following correlation equation had been published:

$$\begin{aligned}\boldsymbol{NO_x} &= \mathbf{184 + 1.09 * 10^{-7}}(\boldsymbol{x_1})(\boldsymbol{x_2}) - \mathbf{1.67 * 10^{-5}}(\boldsymbol{x_1}) \\ &\quad + \mathbf{2.49 * 10^{-6}}(\boldsymbol{x_3})(\boldsymbol{x_4}) + \mathbf{6.54 * 10^{-14}}(\boldsymbol{x_1})^{\mathbf{2}}\end{aligned} \tag{IV–10}$$

With $\boldsymbol{NO_x}$ NO$_x$ emission (ppm dry at 3 % O$_2$)

$\boldsymbol{x_1}$ Heat input per active burner (W)

$\boldsymbol{x_2}$ Air ratio at active burners (–)

$\boldsymbol{x_3}$ Surface heat release rate (W / m²)

$\boldsymbol{x_4}$ Total air ratio of the furnace (–)

It can be seen that the most important parameters governing NO$_x$ formation are burner stoichiometry and heat release rate. Thus, equation (**IV–10**) based on fundamental principles as stoichiometry affects both thermal and fuel–NO$_x$ while heat release rate should mainly affect thermal–NO$_x$ which is in line with the findings provided by Bartok et al. [88] and Pershing [72].

The multiple regression analysis was also applied to horizontally opposed coal–fired boilers. 6 boilers were tested under various operational conditions, e.g. excess air, boiler load, off–stoichiometric combustion (OSC), and flue gas recirculation (FGR). The regression analysis yielded the following equation:

$$\begin{aligned}\boldsymbol{NO_x} &= \mathbf{-471 + 5.38}(\boldsymbol{x_1}) + \mathbf{4.24 * 10^{-6}}(\boldsymbol{x_2}) + \mathbf{7.41}(\boldsymbol{x_3}) \\ &\quad - \mathbf{5.84}(\boldsymbol{x_4}) - \mathbf{66.4}(\boldsymbol{x_5}) + \mathbf{24.6}(\boldsymbol{x_6})\end{aligned} \tag{IV–11}$$

With $\boldsymbol{NO_x}$ NO$_x$ emission (ppm dry at 3 % O$_2$)

$\boldsymbol{x_1}$ Air ratio at active burners (–)

$\boldsymbol{x_2}$ Heat input per active burner (W)

$\boldsymbol{x_3}$ Number of burners firing (–)

$\boldsymbol{x_4}$ Flue gas recirculation (%)

$\boldsymbol{x_5}$	Number of division walls (–)
$\boldsymbol{x_6}$	Furnace excess oxygen (%)

Equation (**IV–11**) indicates that NO_x increases with increasing burner stoichiometry, increasing boiler load, number of burners in service, and total excess oxygen level. Whereas NO_x decrease with increasing flue gas recirculation amount and number of division walls. These results are, in general, in agreement with other theoretical considerations within the literature.

The authors also applied a multiple regression analysis to single wall coal–fired boilers with data coming from eight boilers. The data included tests under baseline conditions with changings in excess air, boiler load, and OSC.

$$\begin{aligned}\boldsymbol{NO_x} &= \mathbf{-140 + 0.198}(\boldsymbol{x_2})(\boldsymbol{x_3}) + \mathbf{6.95 * 10^{-5}}(\boldsymbol{x_1})(\boldsymbol{x_5}) \\ &\quad + \mathbf{4.5 * 10^{-6}}(\boldsymbol{x_1})(\boldsymbol{x_2}) - \mathbf{7.57 * 10^{-8}}(\boldsymbol{x_2})(\boldsymbol{x_4}) \\ &\quad - \mathbf{1.02 * 10^{-11}}(\boldsymbol{x_1})(\boldsymbol{x_4})\end{aligned} \tag{IV–12}$$

With	$\boldsymbol{NO_x}$	NO_x emission (ppm dry at 3 % O_2)
	$\boldsymbol{x_1}$	Surface heat release rate (W / m²)
	$\boldsymbol{x_2}$	Air ratio at active burners (–)
	$\boldsymbol{x_3}$	Number of burners firing (–)
	$\boldsymbol{x_4}$	Heat input per active burner (W)
	$\boldsymbol{x_5}$	Furnace excess oxygen (%)

The authors stated that the air ratio at active burners has a marked large positive correlation with NO_x emissions. The number of firing burners, heat input per active burner, and the furnace excess oxygen level correlated also positive with NO_x emissions. Although these positive correlations are consistent with theoretical considerations known from experience, the authors clearly pointed out that the developed equations are only valid within the range of conditions of the original data base, so that any generalization should be made with caution.

Chen et al. (1982)

Chen et al. [92] investigated the char–N conversion and its contribution to total NO_x emissions. A heated wire grid reactor (HTWM = high temperature wire mesh) was used to determine the nitrogen content in the char. The chars were produced under conditions simulating the conditions in pulverized coal boilers. The resulting NO_x emissions from 50 coals covering a wide range of coal rank burning in a test rig and a full–scale boiler were measured and correlated with the char NO_x. A multi–variable regression algorithm yielded for the char relating nitrogen conversion was developed by assuming that all the char containing nitrogen converts to NO_x.

$$\boldsymbol{NO_{Char} = 318 + 702 * N_{Coal} + 0.188 * HCN - 0.347 * N_{Char}} \qquad \text{(IV–13)}$$

Where $\boldsymbol{N_{Coal}}$ is the nitrogen content in the original coal (wt.–%, daf), $\boldsymbol{HCN}$ is the inert pyrolysis HCN yield (ppm, equivalent) and $\boldsymbol{N_{Char}}$ is the modified ASTM solid nitrogen (ppm, equivalent). The resulting correlation for the exhaust NO_x emissions from the burning system was found to be:

$$\boldsymbol{NO_x = 0.87 * SR * NO_{Char} + \frac{0.67}{1 + 0.004 * (HCN + NH_3)} * (HCN + NH_3) + 0.27 * (1 - SR)^{0.5} * N_{Char}} \qquad \text{(IV–14)}$$

Where $\boldsymbol{SR}$ is the stoichiometric ratio (air / fuel). The inert pyrolysis HCN yield and the non–volatile N yield were used to develop a predictive relationship for NO_x based on the coal–N content. International experience with this relationship had not been successful but anyhow been used as basis for the NO_x predictor in the Electric Power Research Institute (EPRI) Coal Quality Impact Model (CQIM). Later attempts to apply this technique, e.g. in an Australian context had also not been successful. Results obtained in the ACIRL[2] boiler simulation furnace under a set of standard conditions show a poor dependence of NO_x produced on coal–N content [93].

Nakazawa and Kawamura (1982)

Nakazawa and Kawamura [94] investigated the influence of coal quality on NO_x emissions at the Japanese Matsushima power station. The power station consists of two tangential–fired 500 MWe boilers which have been designed by Mitsubishi[3] / Sulzer[4]. The boilers are air–staged and equipped with SGR burners (separate gas recirculation). The grade of air staging is herewith 30 % of the total combustion air was being supplied by the overfire air ports. The authors stated that a change in NO_x emissions could be attributed to the change in coal quality by the correlation to fuel ratio[5] and the nitrogen content between the design coal of the boiler and the respective change in quality.

$$\boldsymbol{NO_x = 100 * (N_{db} - N_0) + A * (FR - FR_0) + NO_{x0}} \qquad \text{(IV–15)}$$

With $\boldsymbol{NO_x}$ as the expected NO_x emissions (ppm, as measured), $\boldsymbol{N_{db}}$ as nitrogen content of coal (db), $\boldsymbol{N_0}$ as nitrogen content of design coal (db) = 0.8, $\boldsymbol{FR}$ the fuel ratio of the coal, $\boldsymbol{FR_0}$ as the fuel ratio of the design coal = 2.0, $\boldsymbol{NO_{x0}}$ are the NO_x emission of the design coal (ppm) = 250 ppm, and $\boldsymbol{A}$ is for $\boldsymbol{FR} \geq 1.6 = 50$ and for $\boldsymbol{FR} \leq 1.6 = 80$.

For the background that the original coal design properties of the observed combustion systems could be unknown it may assumed that any actual fired coal in a

---

[2] ACIRL Pty Ltd. is a private company which provides analytical and coal technology services.
[3] Mitsubishi Heavy Industries Ltd.
[4] Sulzer Ltd., a Swiss corporation.
[5] Quotient of the bound carbon content (char) and the volatile ingredients according to Kluger et al. [135].

certain combustion system is within the original design criteria. Therefore can the first consistent data set to be assumed as reference for the equation context. In addition it needs to be clarified that only different data from more than one trial run could be considered for the model application because the equation is just based on a change of the respective coal parameters but not for a change in the furnace design or boiler operation conditions.

Pohl et al. (1983 & 1987)

Pohl et al. [95, 96] developed two empirical correlation equations for the production rate of NO_x on the basis of coal properties. The experiments showed for staged and unstaged flames the nitrogen content, volatile matter content and the fixed carbon content of the coal correlated with the observed NO_x emissions. The authors developed for both conditions a correlation equation. The relationship for unstaged (diffusion) flames was formulated as:

$$\boldsymbol{NO_F = 340 + 835 * \left(\frac{N_{daf}}{1.5}\right) + 20 * \left(\frac{VM_{daf}}{40}\right) * \left(\frac{NO_{Max}}{3200}\right) - 395 * \left(\frac{FC_{daf}}{60}\right) * \left(\frac{NO_{Max}}{3200}\right)} \tag{IV–16}$$

For staged flames:

$$\boldsymbol{NO_F = 150 + 80 * \left(\frac{N_{daf}}{1.5}\right) + 30 * \left(\frac{VM_{daf}}{40}\right) * \left(\frac{NO_{Max}}{3200}\right) - 100 * \left(\frac{FC_{daf}}{60}\right) * \left(\frac{NO_{Max}}{3200}\right)} \tag{IV–17}$$

Where $\boldsymbol{NO_F}$ is the expected NO_x emission level (ppm, dry, stoichiometric (0 % O_2)), $\boldsymbol{N_{daf}}$ is the nitrogen content in the coal (daf), $\boldsymbol{VM_{daf}}$ is the volatile matter (wt.–%, daf), FC_{daf} is the fixed carbon content (wt.–%, daf) and NO_{Max} maximum NO concentration from the nitrogen in the coal (ppm, dry, 0% O_2).

As first researcher on the field of developing a NO_x prediction technique the authors considered the influence coming from the thermal load inside the furnace referred to the heat release per burner area in kBtu/hr–ft² $(HRBZ)$ additional to the influence coming from the coal parameters. The heat release impact had been formulated as:

$$HR_I = 0.34 * e^{(0.003*HRBZ)} + 0.076 * e^{(0.008*HRBZ)} \qquad \text{(IV–18)}$$

$HRBZ$ is defined by the six sided box from the bottom burner to 10 ft above the top burner and across the width of the boiler. Furthermore the findings of Pershing [90] according to the significant influence of excess air level had also been included as the excess air impact.

$$O_{2_I} = 0.6 + 0.135 * O_2 \qquad \text{(IV–19)}$$

O_2 is the flue gas oxygen content (Vol.–%, dry). The predicted NO_x emission level for the considered system is than determined by:

$$NO_x = NO_F * HR_I * O_{2_I} \qquad \text{(IV–20)}$$

The approach mentioned here had been developed under unstaged furnace conditions and would not consider significant sub–stoichiometrical zones within the furnace and therefore only limited applicable.

Nakata et al. (1988)

Nakata et al. [97] investigated the impact of coal properties on NO_x emissions and unburned carbon content (UBC). 28 bituminous coal types were burned in two burners, a swirl burner (23 coals) and a parallel flow burner (5 coals) in a test furnace under unstaged operating conditions. For both burners an empirical formula was derived by means of linear regression analysis on the basis of a conversion ratio of fuel nitrogen to NO_x. For the swirl burner was expressed as:

$$\boldsymbol{NO_x = NO_{x_{Max}} * \left(10.94 * \frac{FR}{N_{ar}} + 6.77\right)} \tag{IV–21}$$

For the parallel flow burner as:

$$\boldsymbol{NO_x = NO_{x_{Max}} * \left(4.89 * \frac{FR}{N_{ar}} + 4.57\right)} \tag{IV–22}$$

$\boldsymbol{NO_x}$ is the expected NO_x emission level in the respective unit in ppm, $\boldsymbol{NO_{x_{Max}}}$ is the maximum NO_x concentration from the nitrogen in the coal (equation (**IV–23**)), $\boldsymbol{FR}$ the fuel ratio of the coal and $\boldsymbol{N_{ar}}$ is the nitrogen content in the coal (wt.**–**%, as received). The function coefficients seemed to be represents the function adjustment to the observed combustion environment. If so, these coefficients can / needs to be adjusted to any other system which shall be considered. The $\boldsymbol{NO_{x_{Max}}}$ maximum NO_x concentration possible from the pure nitrogen in the coal (in ppm) can be calculated as follows:

$$\boldsymbol{NO_{x_{Max}} = N_{ar} * \frac{V_0}{M_N} * \frac{10^4}{V_{FG_{dry}}}} \tag{IV–23}$$

With $\boldsymbol{N_{ar}}$ nitrogen content in coal (wt.–%, ar)

$\boldsymbol{M_N}$ nitrogen atomic weight (14.0067 kg/kmol)

$\boldsymbol{V_0}$ ideal gas volume (22.414 m^3 / kmol, STP_{dry})

$\boldsymbol{V_{FG_{dry}}}$ flue gas volume per kg raw coal (m^3 / kg, STP_{dry})

The here presented approach based on the idea to assume that a certain furnace under same operating conditions would have a constant nitrogen conversion ratio regarding the total possible nitrogen level if all fuel bounded nitrogen would be converted. Therefore it can be concluded that if the reference basis for the predicted NO_x

level only referred on fuel–N, it must be assumed that thermal–NO_x formation is not been considered within such approach. That means that a change in the coal properties which results necessarily in a change in the combustion behavior and temperatures would only been considered a change in the fuel–NO_x mechanism but not in thermal–NO_x pathways. Certainly is especially for coal combustion the fuel–NO_x proportion much more significant than the thermal ones but on the other hand the prediction accuracy would certainly decrease the more the coal rank of the observed coals apart. Nevertheless, it can be concluded that a change in coal properties would result necessarily in a change in the predicted NO_x emission level which makes the approach principally usable for coal procurement strategies.

Shimizu et al. (1992)

Shimizu et al. [98] developed a model for the prediction of NO_x formation from coal combustion based on 9 different coals combusted in a fixed bed reactor. The combustor consists of a quartz tube with a quartz sintered plate gas distributor. The reactor was heated by an electric furnace in an argon stream in order to eliminate the thermal–NO_x formation. This approach describes the effects of pyrolysis conditions and coal rank of the parent coal on conversion of char–bound nitrogen to NO_x using the nitrogen and carbon content in the coal in relation to the measured emissions of CO, CO_2 and NO_x in the flue gas.

$$\boldsymbol{CR_{Fuel_N}} = \frac{\boldsymbol{NO_x}}{(\boldsymbol{CO} + \boldsymbol{CO_2})\left(\frac{\boldsymbol{N}}{\boldsymbol{C}}\right)_{\boldsymbol{Coal}}} \qquad \text{(IV–24)}$$

Where $\boldsymbol{NO_x}$, $\boldsymbol{CO}$ and $\boldsymbol{CO_2}$ are the individual measured concentrations in the flue gas. $\boldsymbol{N/C}$ as the molar ratio of nitrogen and carbon content in the char. For the determination of the char containing nitrogen the authors assumed that nitrogen and carbon dispersed uniformly.

Similar to the assumption made by Nakata et al. [97] is the here listed prediction technique based on a nitrogen conversion ratio $\left(\boldsymbol{CR_{Fuel_N}}\right)$ and the major problem is the exact definition of the partitioning between volatile and char containing nitrogen content. Due to the fact that the authors stated a fairly well explanation of the experimental results obtained by equation (**IV–24**) it can be assumed, that a specific change in the conversion ratio $\left(\boldsymbol{CR_{Fuel_N}}\right)$ value would lead to a statistic relevant change in the NO_x emission level which would it makes possible to predict the NO_x formation for other coals based on a reference situation. Nevertheless, the approach based exclusively on the assumptions that only char containing nitrogen is being converted to NO_x under constant operating conditions and do not consider any thermal contribution.

Alfonso et al. (1993)

Alfonso et al. [99] developed a semi–empirical model for predicting NO_x emissions on the basis of three independent factors comparing the predictions made with measurements made in 4 power plants firing 9 different coals. The model is defined by coal properties, burner design and operation, and boiler design and operation. Each influence is assumed to be independent of the others and thus it seemed to be contradicts the assumption that the final NO_x level is the result of the interaction of all of these influence factors.

$$\boldsymbol{\frac{NO}{NO_R} = \left(\frac{NO}{NO_R}\right)_{Coal}\left(\frac{NO}{NO_R}\right)_{Burner}\left(\frac{NO}{NO_R}\right)_{Boiler}\left(\frac{NO}{NO_R}\right)_{Fineness}} \qquad \text{(IV–25)}$$

Each of the factors had been displayed by the following graphs (see Figure 8). The respective coal term for the influence of coal quality is based on the relation developed by Pohl [95]. The factor depends on nitrogen content and volatile matter content of the coal. The burner factor depends on primary air velocity and swirl number as known from the work of others, e.g. Michelfelder et al. [100]. The boiler influence is based on the influence of oxygen concentration outside the flame region and the influence of time–temperature history in a boiler on nitrogen oxide formation correlated with the heat release in the burner zone area (HRBZA)[6] for unstaged conditions. The last quotient represents the influence of the coal fineness determined by the tentative relationship between coal fineness and NO_x emission for several limiting flame mixing condition.

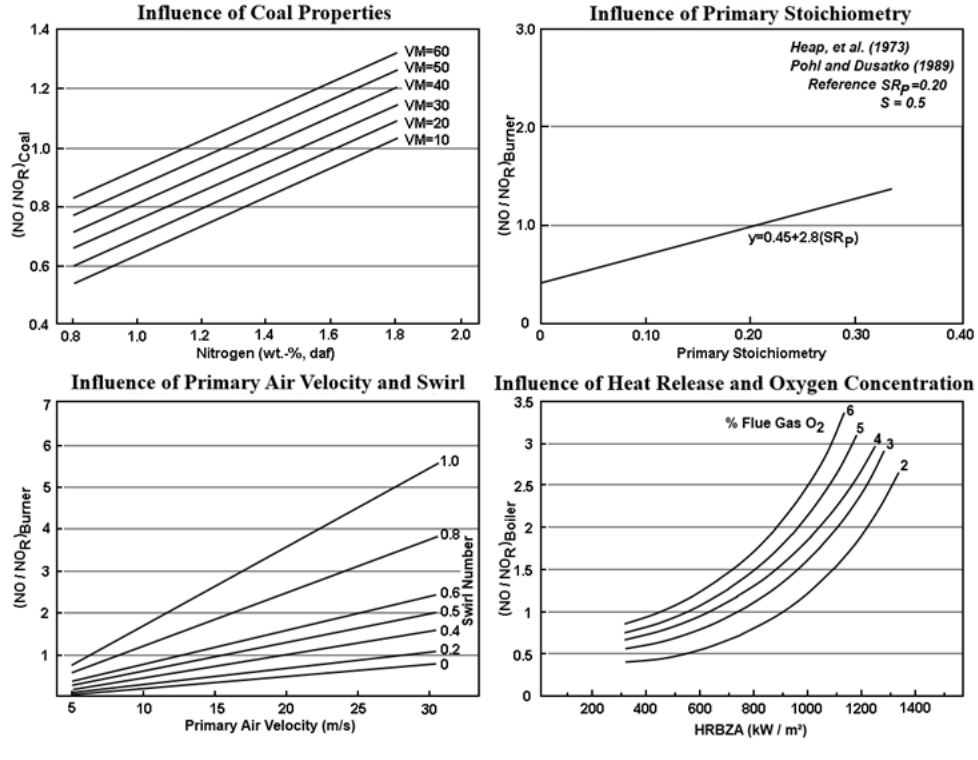
Influence of Coal Properties

Influence of Primary Stoichiometry

Influence of Primary Air Velocity and Swirl

Influence of Heat Release and Oxygen Concentration

Figure 8. Influence factors according to Alfonso et al. (1993)

---

[6] In Btu divided by the area of walls in the burner zone plus 10 feet above plus the area of planes across both ends of the burner zone.

The authors stated that due to the limited data available it is recommended that the influence of coal fineness for tangential fired boilers is set to be 1 (no influence) and for boilers equipped with swirl burners the value should be approximated as follows:

$$\left(\frac{\boldsymbol{NO}}{\boldsymbol{NO_R}}\right)_{\boldsymbol{Fineness}} = \mathbf{0.8} + \mathbf{0.003} * (\% < \mathbf{200}\boldsymbol{m}) \tag{IV–26}$$

However, the authors stated that the assumption of independent influence factors is a reasonable first approximation which is partially compensated by the use of empirical data. Furthermore the authors concluded that more data and refinement are required to estimate the accuracy of the above mentioned assumptions. Thereunto it should be remarked, that similar to Pohls work [95] the approach presented here had also been developed under unstaged furnace conditions and would not consider significant sub–stoichiometrical zones within the furnace and is therefore only limited applicable for todays application.

Kambara et al. (1995)

Kambara et al. [101] found a relationship between nitrogen functionality and NO_x emissions. The authors investigated the thermal decomposition behavior of fuel bound nitrogen during rapid pyrolysis of different coal samples in a quartz tube reactor to develop a general index which estimates the NO_x levels for coals over a wide range of rank by the use of the NH_3 / HCN ratio within the volatile nitrogen. This NO_x index is described by:

$$\boldsymbol{NO_x\,Index} = \frac{\left(\boldsymbol{QN} + \boldsymbol{PdN} + \frac{\boldsymbol{PrN}}{\boldsymbol{C}}\right)\boldsymbol{QN}}{\boldsymbol{PdN} + \frac{\boldsymbol{PrN}}{\boldsymbol{C}}} \tag{IV–27}$$

With $\boldsymbol{QN}$ is the fraction of quaternary nitrogen (wt.–%, daf), $\boldsymbol{PdN}$ as pyridinic nitrogen (wt.–%, daf), $\boldsymbol{PrN}$ as pyrrolic nitrogen (wt.–%, daf) and $\boldsymbol{C}$ as the carbon content (wt.–%, daf). The different nitrogen fractions have been measured by the use of the X–ray photoelectron spectroscopy (XPS) technique.

This predictor is based on nitrogen functionality in coals and the respective release during pyrolysis and combustion. Therefore could this approach presumably be used for procurement strategies (choosing coals) on the basis of NO_x formation potential as long as XPS investigations would be performed. Nevertheless, it should be remarked that measurements by X–ray photoelectron spectroscopy is very sensitive to sample preparation. In addition, also furnace or operational parameter had not been considered which makes the given approach only limited applicable.

Rozendaal et al. (1997)

Rozendaal et al. [102, 103] investigated the impact of coal quality changes on the NO_x emission level, especially based on using coal blends for 2 different boilers of three independent power stations located in the Netherlands. 2 tangentially–fired units and 1 opposed wall–fired unit. The work was based on pure statistical relationships. The interpolation between NO_x emissions and coal characteristics was analyzed by linear regression analysis. Scatter diagrams of NO_x emissions versus various coal characteristics (volatile matter and fuel ratio) were plotted and for each combination the coefficient of determination and the regression coefficients were calculated. But only the tangentially–fired units showed a statistical relevance for which reason only these two evaluations are being considered further. The best regressor from statistical point of view for the first boiler (Maasvlakte, NL) yields the following relationship according to $O_2 = 3\%$, wet basis:

$$\boldsymbol{NO_x = 1006 - 17.6 * VM_{db}} \tag{IV–28}$$

For the second boiler (Amer, NL):

$$\boldsymbol{NO_x = 704 - 11.8 * VM_{db}} \tag{IV–29}$$

$\boldsymbol{VM_{db}}$ is the volatile matter content on a dry basis. The equations had been developed for tangential–fired units with special attention to stable boiler conditions for all blends. The results published from the linear regression analysis shows for equation (**IV–28**) a good statistic relevant relationship and in that, that the regression coefficients adjust the reference figure $(\boldsymbol{VM_{db}})$ according to the observed furnace it can be assumed that the general methodology can be derived also to other tangential–fired units. Nevertheless is the approach being based on coal properties only and therefore only limited applicable.

van der Kooij et al. (1997)

van der Kooij et al. [104] took the developed approach by Rozendaal et al. [102] and adjusted the function coefficients by a linear regression analysis towards the boundary conditions of two other power plants burning coals of an unreported rank:

$$\boldsymbol{NO_x = 1509 - 26 * VM_{db}} \tag{IV–30}$$

A good example of transferring the Rozendaal approach to another boiler which confirmed the previous made assumption.

Niksa et al. (1997)

Niksa et al. [105] investigated the influence of changing coal qualities on the NO_x emissions and loss of ignition (LOI) and build herewith the basis for EPRIs[7] NO_x / LOI Predictor™[8]. The approach is termed as FLASHCHAIN™ model which determines the volatile gas yield, volatile tar yield, tar nitrogen yield and HCN production. The results of the FLASHCHAIN™ model [106–112] are used for a series of correlations to predict the NO_x level for an alternate coal based on the assumptions from the baseline coal which is, in some way similar to the application possibility of the Shimizu et al. [98] approach but other than that based the FLASHCHAIN™ model on the standard data coming from proximate analysis, ultimate analysis, and Hargrove grindability index. These data are connected to a few measured values of NO_x emissions and LOI from a particular boiler at known load and excess air.

Unfortunately it is not possible to review the overall approach methodology because of the lack of information published which is certainly due to the intentional commercial application of the NO_x / LOI Predictor™. But it can be assumed that the approach developed by the authors works on the principle of predicting a possible change in NO_x emissions by estimating of the varying in coal parameters which is being confirmed by the fact, that only coal parameter are required to evaluate a possible change in NO_x emissions based on a set of fuels being screened when they are burned under the same firing conditions that were used when the data were collected. Therefore the model would apparently not address design considerations and is also only of limited applicability.

---

[7] Electric Power Research Institute.

[8] Software for change prediction in emissions from fuel switching or blending.

Schlessing (1998)

Schlessing [113] postulated that the NO_x level to be expected from a new and unknown coal within a known combustion system can be derived from the experience from a known used coal in the respective system. The NO_x emissions from the new coal will be in a specific relation to the measured NO_x level from the known coal unless the operating parameters of the system will not be changed, as similar to the approaches of others [94, 97, 98, 101–105]. The developed empirical correlation for the expected NO_x level from the new coal has been addressed as:

$$\boldsymbol{NO_{x_N}} = \frac{\boldsymbol{NO_{x_R} * VM_R}}{\boldsymbol{VM_N}} \qquad \text{(IV–31)}$$

Where $\boldsymbol{VM_R}$ are the volatile matter content of the reference coal, $\boldsymbol{NO_{x_R}}$ are the associated emission profile and $\boldsymbol{VM_N}$ are the volatile matters of the new (unknown) coal.

The approach uses the same main NO_x indicator as basis as Rozendaal et al. [102] but the difference here is that Schlessing did not considered any variation in the furnace design. Also a difference in the operational parameters had not been investigated. All that let suggest that the approach had been developed for procurements strategies of a specific power plant owner. Thus, this approach is also of limited applicability while it considers only coal properties as basis for predictions.

Makino et al. (1999)

Makino et al. [114, 115] further developed the approach established by Nakata et al. [97]. In contrast to Nakata based the approach of Makino on the assumption that the nitrogen content estimated by the ultimate analysis on a water free basis gives more reasonable estimates regarding a correlation to the NO_x performance data of a boiler as the ‘as received’ basis would suggest. Just like the approach established by Nakata et al. [97] also a potential influence coming from boundary conditions, e.g. boiler and operation conditions is been considered by two additional parameters which needs to be adjusted to achieve best suitable prediction result. If the NO_x level of at least two coals are known for a given boiler configuration the model coefficients can be calculated by a regression analysis.

$$\boldsymbol{NO_x = NO_{x_{Max}} * \left(a_1 * \frac{FR}{N_{dry}} + a_2\right)} \qquad \text{(IV–32)}$$

With $\boldsymbol{NO_x}$ NO_x emission level at the furnace end of the respective boiler

$\boldsymbol{FR}$ fuel ratio of the coal

$\boldsymbol{N_{dry}}$ is the nitrogen content in the coal (wt.–%, dry basis)

$\boldsymbol{a_1}$ and $\boldsymbol{a_2}$ function coefficients

The best suitable values for the coefficients $\boldsymbol{a_1}$ and $\boldsymbol{a_2}$ must be re–estimated for every new combustion situation. The author determined these parameters for each burner, i.e. 0.00109, 0.00677 for burner A; 0.000489, 0.0457 for burner B. $\boldsymbol{NO_{x_{Max}}}$ is the maximum NO_x concentration from the nitrogen in the coal as described in equation (**IV–23**).

Summarized it can be concluded that also the approach presented by Makino based on the idea to assume that a certain furnace under same operating conditions would have a constant nitrogen conversion ratio regarding the total possible NO_x emission level if all fuel–bounded nitrogen would be converted. This implies, as concluded earlier (see Nakata et al. (1988)), that the thermal–NO_x formation is not considered but due to the fact that a change in coal properties would result necessarily in a change in the predicted

NO_x emission level makes the approach principally usable for coal procurement strategies.

Jung et al. (2001)

Jung et al. [116] performed a series of controlled combustion experiments in a drop tube reactor with 9 bituminous coals that represent the types of coals typically used from the State of Ohio, and 1 bituminous coal from Kentucky with a higher percentage nitrogen content. The NO_x emissions were compared to the coals composition, including their volatile matter, fixed carbon, and nitrogen content. A relationship was developed based on the coal's compositional factors.

$$\boldsymbol{FF = \alpha * \left(\frac{FC}{VM}\right) - \beta * N_0} \tag{IV–33}$$

$\boldsymbol{FF}$ is the coal fuel factor, $\boldsymbol{\alpha}$ and $\boldsymbol{\beta}$ are function coefficients, $\boldsymbol{FC}$ is the coal's fixed carbon, $\boldsymbol{VM}$ is the volatile matter, and $\boldsymbol{N_0}$ is the nitrogen percentage on a dry ash–free (daf) basis respectively. The coefficients had been determined relative to the NO_x emission values of the 10 coals by normalizing the actual NO_x emissions for each coal to the concentration of the coal with the lowest measured NO_x concentration when the values of $\boldsymbol{\alpha}$ and $\boldsymbol{\beta}$ are 550 and 92, respectively. The authors concluded that when the heat contents of the coals were considered, a linear relationship still exists between the relative NO_x emission levels and the coals chemical properties and therefore it may be possible to lower total NO_x emissions for a given combustor by replacing one coal with another coal with a lower fuel factor value.

Similar to the approaches presented by Nakata et al. [95], Rozendaal et al. [102], and Makino [114] based also this NO_x prediction model on the influence of coal properties on NO_x formation for similar ranked coals under the condition of stable boiler operating conditions. What means, that the functions coefficients needs to be adjusted for any other systems.

Bennett (2001)

Bennett [117] investigated the impact of coal properties at pilot–scale furnaces on the variations in the NO_x emissions. The approach consists of two individual terms. The basis of the first is the idea that the outcoming approximations from Pohl's approach [95] could be modified by replacing the proximate volatile matter by the high temperature volatile yield as established by Badzioch and Hawksley [118], in order to include the impact of the differences in the thermal environments of pilot–scale and full–scale furnaces which Pohls original correlation had not been considered. On the basis of a few single coal results the developed empirical correlation fitted to the data and the developed correlation was found to be:

$$\boldsymbol{NO_x = a * VM_{HT} * N_{daf} + b * e^{\left(\frac{c}{VM_{HT}}\right)}} \qquad \text{(IV–34)}$$

$\boldsymbol{N_{daf}}$ is the nitrogen content in the coal (wt.–%, daf), $\boldsymbol{VM_{HT}}$ is the high temperature volatile matter (wt.–%, daf) and $\boldsymbol{a}$, $\boldsymbol{b}$, $\boldsymbol{c}$ are coefficients which had been fitted to the test results of the single coals. Similar to Nakata et al. [97] approach represent the coefficients the influence of the interaction between the system design and operation conditions of the furnace environment. Therefore it can be concluded that, the first approach (equation (**IV–34**)) can give estimates of possible NO_x changings regarding a change in coal quality.

The second term has been developed on the basis of the findings from the empirical correlation above. This simple reaction engineering model is based on the NO_x, oxygen, and temperature dependence and helps to draw assumptions regarding the possible grade of changes in the observed combustion system instead of changes in the fuel.

$$\boldsymbol{NO_x = a * Log(O_2) + b * e^{\left(\frac{c}{HR}\right)} + d * HR} \tag{IV–35}$$

$\boldsymbol{O_2}$ is the oxygen level and $\boldsymbol{HR}$ is the sum of each burner volumetric heat release rate. The four coefficients $\boldsymbol{a}$, $\boldsymbol{b}$, $\boldsymbol{c}$, and $\boldsymbol{d}$, are not discussed in detail but it can be assumed that they represent the influence of unknown interactions within the entire system and can / need therefore to be adjusted to every initial state (see Nakata et al. [97]).

Kurose et al. (2004)

Kurose et al. [119] combusted 6 high fuel–ratio coals in order to developed the NO_x conversion rate $(\boldsymbol{CR})$ which based on the general assumption made by Nakata et al. [97]. This figure evaluates the conversion effectiveness of fuel containing nitrogen to NO_x as follows:

$$\boldsymbol{CR_{Ref} = \frac{NO_{x_{Ref}}}{\left(\frac{10^6 * V_0 * \frac{N_{ar_{Ref}}}{M_N}}{V_{FGdry_{Ref}}}\right)} * 10^2} \tag{IV–36}$$

with	$\boldsymbol{NO_{x_{Ref}}}$	NO_x concentration at the furnace exit (mg / m³, STP_{dry})
	$\boldsymbol{N_{ar_{Ref}}}$	nitrogen content in the reference coal (wt.–%, ar)
	$\boldsymbol{M_N}$	nitrogen atomic weight (14.0067 kg/kmol)
	$\boldsymbol{V_0}$	ideal gas volume (22.414 m³ / kmol, STP_{dry})
	$\boldsymbol{V_{FGdry_{Ref}}}$	dry flue gas volume per kg raw coal (m³ / kg, STP_{dry})

If the rate is being considered as constant, also for other coals, than the almost linear relationship could allow the prediction of NO_x levels for other similar–rank coals within the observed combustion environment. That would require one consistent data set in order to calculate the reference conversion rate $\left(CR_{Ref}\right)$ of a system as basis for the NO_x prediction for other model parameters by transposing equation (**IV–36**).

$$NO_x = CR_{Ref} * 10^4 * V_0 * \frac{N_{ar}}{\left(M_N * V_{FG_{dry}}\right)} \tag{IV–37}$$

Where NO_x are the predicted NO_x emissions at the furnace exit in mg / m³, STP_{dry}, N_{ar} is nitrogen content (wt.–%, ar), and $V_{FG_{dry}}$ is dry flue gas volume per kg raw coal (m³ / kg, STP_{dry}) of the new coal respectively.

Although the basic idea is the same as known from Nakata et al. [97] which implies that also this relationship based on the assumption that only fuel–N converts to NO_x which excluded the thermal–NO_x generation, there is a crucial difference. In contrast to Nakatas approach is the dry flue gas volume per kg raw coal $\left(V_{FG_{dry}}\right)$ considered. This figure depends directly on the excess air level and thus includes an operational parameter which describes the oxygen dependence.

Conclusion

Although a lot of research has been undertaken is the formation process of NO_x emissions not fully understood or even calculable. A valuable contribution to the problem had been made using a combination of fundamental analysis, empirical algorithms and statistical relationships but even with 40 years of effort to understand NO_x formation in coal combustion systems, it remains difficult to predict the effectiveness of low–NO_x combustion systems. A good example would be the work of Kokkinos et al. [120] or Stamey–Hall [121]. The later attempted to correlate the NO_x emissions with the nitrogen content and the respective fuel ratio of certain coals. The author investigates thirty units at eleven coal–fired power plants but could not found any certain correlation which is certainly due to the reason, that the significant relationships between various constituents comprise each single influence factor and masked the NO_x emissions by the impact of the other factors. Therefore is a generalization of the published NO_x prediction approaches so difficult. The known and unknown related compensating effects which could or had been occurred during the measurements of the data sets cannot be traced in necessary detail. For this reason, it was not attempted to recalculate every existing approach during the here described research work. Rather, the existing approaches were investigated according to their possible application towards the major objective of this thesis. Table 4 summarized these findings.

Table 4. Summarization of NO_x prediction approaches

Reference	Test–scale	Full–scale	Comment
Bartok et al. (1971)		X	High furnace load dependency No coal parameter 10 data points for dry bottom fired utilities
Crawford et al. (1974)		X	Based on Bartok et al. (1971) [88] High furnace load dependency No coal parameters considered
Pershing (1976)	X		Drop–tube experiments unsuitable for full–scale applications [90] The traceability of the test–rig results is very complicated No furnace design or load considered

Reference	Test–scale	Full–scale	Comment
Lim et al. (1980)		X	No coal parameters considered Unstaged industrial furnace conditions Correlation equations based on specific boiler firing types
Chen et al. (1982)	X		NO_x as a function of coal N content only (the inert pyrolysis HCN yield and the non–volatile N yield) No thermal–NO_x considered No furnace design or load
Nakazawa and Kawamura (1982)		X	No thermal–NO_x considered No furnace design or operating parameters
Pohl et al. (1983 & 1987)	X		20 coals Based on unstaged furnace conditions
Nakata et al. (1988)	X		Only constant operating parameters No thermal–NO_x considered Based on unstaged furnace conditions
Shimizu et al. (1992)	X		Single particle consideration Considered only char–N conversion No thermal–NO_x considered No furnace design or operating parameters
Alfonso et al. (1993)		X	Relatively small set of data (4 furnaces and 9 coals) [99] Only staged mixing swirl burner considered Based on unstaged furnace conditions

Reference	Test–scale	Full–scale	Comment
Kambara et al. (1995)	X		Inconsistent with other research results on nitrogen release [93] Necessary X–ray photoelectron spectroscopy investigations No boiler design or operating parameters
Rozendaal et al. (1997)		X	Derived from Nakazawa and Kawamura (1982) [94] Only constant operating parameters Only for tangential–fired units No boiler design or operating parameters
van der Kooij et al. (1997)		X	Approach of Rozendaal et al. (1997) [102], just the regression coefficients have been recalculated
Niksa et al. (1997)		X	Coal pyrolysis model for nitrogen release. No boiler design or operating parameters
Schlessing (1998)		X	Based on Rozendaal et al. (1997) [102] assumption regarding the VM significance Only constant operating parameters No boiler design or operating parameters
Makino (1999)	X		Approach of Nakata et al. (1988) [95], just the coal nitrogen reference basis had been changed and the regression coefficients were recalculated No thermal–NO_x considered Only constant operating parameters
Jung et al. (2001)	X		9 Ohio bituminous coals and 1 from Kentucky Drop–tube experiments unsuitable for full–scale applications [90] Only constant operating parameters

Reference	Test–scale	Full–scale	Comment
Bennett (2001)	X		Based on Pohl et al (1983) [95] and on Nakata et al. (1988) [95] Considered either coal quality or operating conditions but not both together
Kurose et al. (2004)	X		6 coals Based on Nakata et al. (1988) [95] No thermal–NO_x considered No furnace design or load

Most of the published predictive techniques based on the correlation approach and perform poorly when used under conditions even slightly different from those for which the correlations were originally developed. The consensus is that they offer little predictive ability for coals burnt in a wide variety of international power stations. This may be due to the fact that most detailed studies had been performed in single–burner test facilities, and may not capture significant burner–to–burner interactions that would influence NO_x emissions too. Other NO_x prediction models had been developed on the basis of laboratory–scale and pilot plants but industrial relevant quantitative results were only being reliable in cases where the model had been validated for similar cases at full–scale applications.

The decision whether full–scale or laboratory–scale test facilities serve as the most practicable basis for application depends on the attitude of the respective researcher. The main substantiation is that laboratory–scale test facilities seemed to be easier to control, and thus ensure better accuracy throughout the experiments but on the other hand scaling problems will certainly arise due to the large amount of assumptions which have to be made. It is certain that any deviation would cause discrepancies in the applicability.

Although, a number of modelers have been reported successful results at predicting NO_x, it can be concluded that none of the approaches listed in Table 4 provides the ability to draw conclusion on coal properties, furnace design and operational settings respectively at the same time. These models are not capable to handle changings in geometrical, operational parameters or coal quality at the same time. It is only possible to examine one or the other but not all together.

Hence the development of improved techniques for the prediction of NO_x formation from coal combustion is a high priority worldwide it needs to be further investigated because such a model would be of great significance. Because it would allow detailed investigations regarding the individual influence factors as well as allow to analysis running combustion system regarding possible improvements and optimizations.

V. MODEL BASIS

Approach

Due to the fact that every combustion process depends on an individual and unique dynamic it is up to now not possible to calculate NO_x emissions for a practical coal combustion situation based on solving individual reaction rate equations. Numerous influence factors are responsible for the formation quantity of NO_x emissions and some of these have been identified starting approximately forty years ago [122]. The approach used to develop an empirical technique to predict NO_x formation was not to determine the major influence variables rather than the approach was to investigate on what factors they depend. Therefore the combustion kinetic process as occurring under real furnace conditions had been split into three independent factors which are generally accepted as NO_x formation main causes.

- Coal properties
- Furnace design
- Operational settings

These three influence factors describe sufficiently (after Smouse et al. [123]) the respective reaction condition and simplify the overall assumption of the individual und unique combustion condition. For thus it can be assumed that the total NO_x production rate of a certain pulverized coal combustion system is the result of the interaction between these three major groups. That means, the results of one influence will enter and alter the other. More specifically, if one influence producing NO_x emissions it will reduce the potential for production by the others.

Assumptions

The considered systems are always unique. Location, environmental conditions, system design, dimensions, geometry, capacity, fuel properties, operating conditions and so on are always changing between different power stations. It is possible to find similar conditions at the most within one power station with a couple of identical units but even then all operating conditions must be closely examined to ensure comparability. Therefore is the best way to compare complex and unique systems by the help of a simple mathematical formulation which helps to describe such processes and to interpretate the differences between the observed systems. Some process parameter are so unique and difficult to calculate, if it is at all possible like temperature and pressure within the furnace, that they needs to be defined as identical in order to create a comparative basis for any power station unit. Table 5 summarized the principle assumptions made for the methodology.

Table 5. Principle model assumptions

Model assumptions
• Equalized and uniform distribution of air (over the furnace width)
• Equalized and uniform distribution of coal (over the furnace width)
• Equalized and uniform distribution of the flue gas composition within the flue gas duct
• Flue gas recirculation has no effect on the combustion reactions (as it is inert)
• Coal particle fineness equal and uniform for all applications

Model assumptions

- Burner–to–burner interactions has been neglected (all burner in service injects the same coal/ air massflow)
- Average furnace temperature for a better comparison between the different boilers.
  For bituminous coal: 1,400 °C (full load)
  For lignite 1,200 °C (full load)
- Model is time independent (The model considers just one moment. That means that all figures which have been taken into account belongs to the same time).
- Controlled negative pressure at the furnace exit (by the ID fan): – 0.5 mbar

Basis

A number of different information regarding different power plant units is needed to ensure that the amount of data is large enough to guarantee precise estimates on relationships, dependencies and interactions. These data sets are consistent, plausible and complete field data coming from various power plants located all over the world and they have been acquired by own on site measurements, have been provided by operators (on request) or have been published as part of other research works.

To simplify the management and analysis of these related data were the extensive calculations with formulas and functions organized and performed in a spreadsheet program. This allows the evaluation of logical operations of different known input measures with calculated results by the help of graphically visualization in diagrams. Microsoft® Excel® has been chosen as best suitable software for the data analysis because it is the most common and usually the most versatile software to enter and organize data and perform a wide variety of number–crunching tasks. In addition, is Microsoft® Excel® and as part of the Microsoft Office® package nearly on every computer available or at least installable. Excel® is very suitable for modeling and visualization and through programming in Visual Basic for Applications (VBA) the functionality can be extended according to nearly all particular requirements.

Architecture

The principle structure is to combine the basics of statistical analysis, empirical models and industrial experience to bring out a contribution to the understanding of the individual influence factors to gain the possibility to optimize really complex chemical reactions and physical properties. The main task and at the same time the goal is to analyze the interaction between furnace settings and coal parameters on the formation of nitrogen pollutants from pulverized coal–fired boilers under certain conditions by the help of field measurements. These available information needs to be organized in a way which allows being comparable, flexible and extendable to each other. Comparable between different measurements of one specific boiler and also comparable between different power plant units. Flexible in a way that allows easily to combine any known parameter from one certain system to another and extendable in order to have the possibility to further extent any data for an improvement of the prediction technique as well as to allow further estimation of additional power plant units and their process parameter.

An appropriated way in describing all necessary and consequent information about a combustion system and its process conditions is shown in Figure 9. It represents not only the spreadsheet model architecture but also the methodology within this thesis.

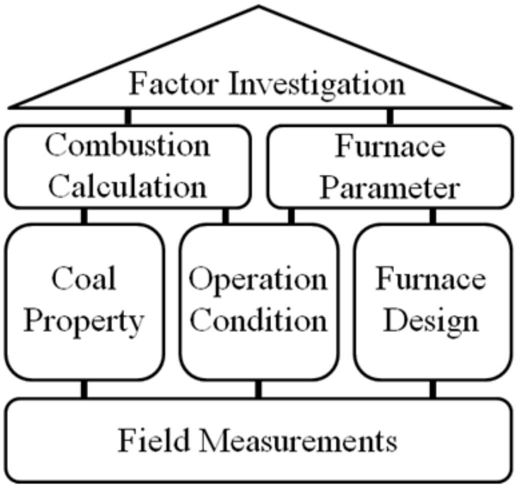

Figure 9. Basic model architecture

The basis builds three individual worksheets, analogously to the identified main causes: coal properties, furnace design and operation conditions. All required information known from a system are to be inserted in the respective working sheet. Important is that these data sets are clean, correct and useful to get no negatively effect on the model process execution during the time of model validation. It should be mentioned that all necessary input data are coming from the system (field measurements) and describe the actual conditions under a certain NO_x level had been measured or at least observed. Therefore it must be ensured that these data sets are unchanged for a proper model validation. Because if a specific power plant unit burns a specific coal under certain operational settings and results in a certain NO_x quantity at the same time than will any deviation in one of these figures lead to a significant interference in identifying reasonable dependencies. That means, the effect of one influence will enter and alter the other.

In order to describe the full scope of this linkage were two other worksheets created. This level consists of two additional dependent worksheets. A combustion calculation based on chemical properties[9] and a calculation of the resulting process parameters (e. g. furnace load ratios) which calculation figures represent the effectiveness of the combustion process and can provide indications about improvements. These two working sheets are termed as depended because they are the result of the calculation based on the input data coming from the three basis sheets.

Summary

As stated earlier, the combustion of coal involves a complex series of different reactions. The general mechanism of the reaction of a coal particle with individual size dimensions within potential reaction zones have been investigated and described by Robert H. Essenhigh, David W. Pershing, Jost O.L. Wendt and others [90 124–126, etc.]. This thesis focused on describing a way for a reliable but easy in use engineering model which makes it possible to estimate the relationships, dependencies and interactions between those factors which are important for the prediction of nitrogen oxides from dry bottom firing utilities.

Generally it can be concluded that all physical and chemical processes occurring in a pulverized coal–fired utility boiler depends on three determining causes: coal properties, furnace design, and operational settings. For thus the described spreadsheet model has been developed in the same manner. All necessary input parameter for the development of the new NO_x prediction approach are based on consistent, plausible and complete field data coming from various power plants located all over the world. These data sets have been acquired by own on site measurements, have been requested and provided by operators or have been published as part of other research works. These field

---

[9] A detailed explanation of the reactions as well as the equations to be used can be found elsewhere.

measurements define the principle conditions of the considered actual state at a specific moment. That means a specific power plant unit burns a specific coal under certain operational settings and results in a measured NO_x quantity at the same time. Mathematically expressed as:

$$\boldsymbol{NO_x = Furnace_i + Coal_j + Settings_k} \tag{V–1}$$

Such structure makes it possible to extend the model with minimal effort. That means any reasonable amount of variations can be connected to reference values. For example, full–scale experimental results are published where a specific boiler had been fired with different coal qualities lead to the fact that only one furnace design will be connected to the respective coals, and if the experimental information indeed that operational system changes had been made too, they can also easily connected to the reference value.

As more data available and inserted in the model as precise the influence factor investigation will be. All these known data are being inserted in individual worksheets act as reference and officiate as basement for any further investigation.

VI. MODEL DEVELOPMENT

The most obvious approach would certainly be to investigate the problem via a peripheral regression analysis and much works have already been published on identifying any reasonable statistical relationship between the pollutants emitted and various system related state variables with more or less success depending on the scope of consideration [88–90, 92–96, 97, 114–116, 117, 127]. With the intention not to follow the above mentioned investigations it has been concluded that a general statistical relevance would only be found by using several different factors which belongs to the assumed major driver for NO_x formation in pulverized coal–fired utilities: the fuel properties; the dependence of furnace geometry factors; and the specific operating conditions. The methodology was to bring these particular individual factors in a direct dependency where all factors are set in relation according to their influence size to each other in order to generate an individual estimation factor. Generally expressed as:

$$\boldsymbol{NI} = \prod_{i=1}^{n} \boldsymbol{h_i}, \qquad \boldsymbol{h_i} > \mathbf{0} \tag{VI–1}$$

With $\boldsymbol{NI}$ as the parent NO_x indicator, $\boldsymbol{h_i}$ are the respective individual helping factors, and $\boldsymbol{n}$ are the amount of helping factors necessary for a statistic relevant prediction. It has been found to be most practicable to define a certain index $(\boldsymbol{NI})$ instead of predicting absolute values because such individual estimation factor can be further adjusted by a peripheral regression analysis towards the reference NO_x values. This circumstances have the advantage that any further available data set which will increase the prediction model reference data basis will lead to a continuous improvement of the overall regression equation and for thus to a continuous improvement of the prediction performance at any time.

Concerning the helping factors $(\boldsymbol{h_i})$ it has been assumed due to statistical evaluations of several empirical attempts which have been developed according to the experimental results of previous studies, own statistical analyzes and industrial knowhow, that the product of five identified specific helping factors $(\boldsymbol{h_i})$ would bring out the strongest statistical relationship between measured NO_x reference values and the predicted ones from the observed coal–fired power station units. These factors are:

- $\boldsymbol{h_1}$ – Coal influence
- $\boldsymbol{h_2}$ – Excess air influence
- $\boldsymbol{h_3}$ – Air staging influence
- $\boldsymbol{h_4}$ – Burner influence
- $\boldsymbol{h_5}$ – Furnace influence

The general processes of the identification process were done during statistical and empirical experiments on a try and error basis where these five helping factors have been proven to be sufficient to describe any dry bottom coal–fired utility boiler with respect to estimate the NO_x value to be expected as well as to predict changings in the NO_x level influenced by changing individual influence conditions and will therefore be described in more detail in the following.

Coal Influence

The majority of possible NO_x relationships published in literature belong to coal parameter such as volatile matter, fuel ratio[10] and / or nitrogen content. One good example is the essential work of David Walter Pershing [90] who showed the importance of fuel nitrogen conversion in self–sustaining pulverized coal flames and its contribution to NO_x generation. Only about 20 – 40 % of the nitrogen bound in the fuel results in NO_x formation but it contributes up to 95 % of the total NO_x generated, depending on how the coal is burned [73, 128, 129]. The remaining nitrogen portion produces molecular N_2 in the further reaction process. During the course of combustion process the rates of nitrogen release can change significant and will vary according the coal type [130].

Several attempts have been reported in which correlations between coal properties and NO_x emissions have been tried to identify. The reason why until now no certain correlation has been found could on the one hand be the fact, that the influence factors of the environment and operation mode cannot be neglected, as well as that most experiments are being based on the volatile matter content (VM) known from the proximate analysis of one specific coal. A few research works stated that the VM content coming from standard measuring procedure e.g. DIN 51720 [131] or ASTM D3175 [132], would be not representative when considering the differences between the standard laboratory and the real in–furnace conditions. Because the volatile evolution, the rate, and amount of volatiles releases during the pyrolysis of the coal particles not only depend on the coal rank, it is also strongly impacted by the heating environment conditions as well. As a result it was observed in some experiments that the real weight loss under real flame conditions typically exceeds the proximate VM content by 10 to 100 % [103, 133].

---

[10] Quotient of the bound carbon content (char) and the volatile ingredients according to Kluger et al. [135].

Winkler and Neumann [134] considered the burning behavior of different coals based on the fuel ratio developed by Kluger et al. [135]. The authors observed that the unburnt carbon content (UBC) in the ash increased as they had mixed a South Africa coal with German Ruhr coal. The UBC value increased significant as the South African coal portion reached more than 8 % of the total fuel massflow. They concluded that the coals must have a different ignition and burnout behavior although these two coals had nearly the same proximate VM content. Table 6 shows a selection of appropriate coal compositions.

Table 6. Typical bituminous coal compositions

		South Africa		Germany	
	Unit (ar)	New Clydesdale	Tselentis	Auguste Victoria	Ruhr
Volatile Matter	wt.–%	32.30	27.90	33.20	33.70
Moisture	wt.–%	7.60	9.00	9.50	8.90
Ash Content	wt.–%	11.90	11.70	8.20	6.60
Carbon	wt.–%	67.00	66.70	70.20	72.00
Hydrogen	wt.–%	3.83	3.44	4.34	4.50

The authors found the greatest difference of the coals in the respective hydrogen content and assumed that the hydrogen content of a coal must be an important indicator for the ignition and burnout behavior to be expected. This conclusion had been confirmed by conducted boiler operation experiments on which basis they proposed to modify the original fuel ratio by determining the quotient of the bound carbon content (char), the volatile containing carbon and the hydrogen ingredients according to their mol mass proportion. But unfortunately the integration of the approach presented by Winkler and Neumann [134] into the investigation done within this thesis had not shown significant improvements concerning correlations between coal properties and NO_x emissions. It was the combination with the work of Fisher [136] which brought out a significant improvement in the correlation coefficient and the herewith resulting statistical dependency. The result was the assumption, that if the reaction behavior of the total volatile content of a coal is being influenced by a certain amount of proportionally volatile ingredients (hydrocarbons (C_xH_x)) than the VM content estimated by standard proximate analysis needs to be adjusted according to the fraction of highly combustible ingredients based on the total atomic mass proportion in Dalton[11].

$$\boldsymbol{VM_{Ratio}} = \frac{\boldsymbol{C_{VM} + H}}{\boldsymbol{VM_{Atomic}}} \left[\frac{\boldsymbol{Da}}{\boldsymbol{Da}}\right] \tag{VI–2}$$

Where $\boldsymbol{C_{VM}}$ is the fractional carbon volatile content, $\boldsymbol{H}$ is the VM containing hydrogen, and $\boldsymbol{VM_{Atomic}}$ are the total volatile content according to ASTM [132] proximate analysis based on the respective atomic weight. The resulting quotient of the laboratory measured VM content and the result of equation (VI–2) makes it possible to evaluate the given VM content by standard method of any coal regarding their ‘effective’ VM content in order to estimate the ignition and burning behavior under real furnace conditions.

$$\boldsymbol{VM_{Eff}} = \frac{\boldsymbol{VM}}{\boldsymbol{VM_{Ratio}}} \tag{VI–3}$$

The approach indicates always more volatile content as total volatile content measured in the proximate analysis (see Figure 10). The reason is that the $\boldsymbol{VM_{Ratio}}$ must

---

[11] Dalton (symbol: Da) is the standard unit which is used for indicating mass on an atomic scale (unified atomic mass unit).

be always less than one because every coals contains also other volatile ingredients. The reasoning behind the better correlation result might be the conclusion done by Essenhigh [25]. He stated, that the higher the rank of a coal the more volatiles are released as tar which formed more HCN and NH_3 during the devolatilization and secondary cracking [24] which are generally an indicator for tendencially higher NO_x emissions. Based on equation (**VI–3**) means that, the higher the rank of a coal the more tends $\boldsymbol{VM_{Ratio}}$ to one and thus, the less exceeds the real weight loss under flame conditions the proximate VM content and lower VM content are generally an indicator for tendencially higher NO_x emissions [25, 97, 102, 113, 114, 116, 117, 137].

Due to the fact that coals cannot have more volatiles than total volatilizing mass available the following condition must be met:

$$\boldsymbol{VM_{Eff} \leq 100 - MM} \tag{VI–4}$$

With $\boldsymbol{MM}$ as the coal containing mineral matter content, i.e. the maceral (carbonaceous) material which is unrelated for ranking purposes of the coal. The respective formula used to estimate the original mineral matter in the coal is according to ASTM D388 [12] as follows:

$$\boldsymbol{MM = 1.08 * A + 0.55 * S} \tag{VI–5}$$

With $\boldsymbol{A}$ is the ash yield[12] and $\boldsymbol{S}$ as the total sulfur content[13] in weight percent.

A comparison of the approach presented in this thesis regarding the VM content and the standard VM value available from the reference field measurements are given in Figure 10.

---

[12] According to ASTM Test Method D 3174.

[13] According to ASTM Test Method D 3177.

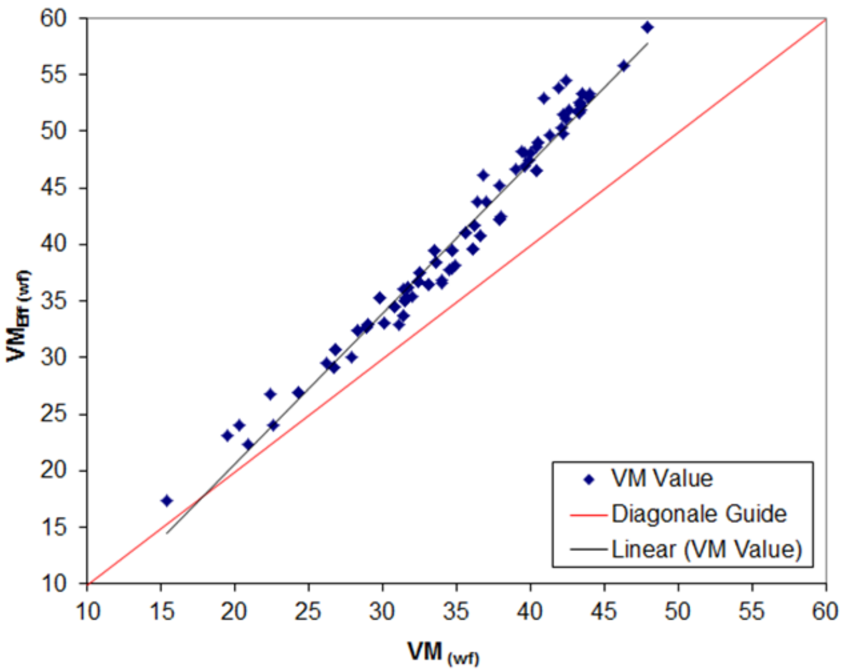

Figure 10. Relation between $VM_{Eff(wf)}$ and $VM_{(wf)}$ of various coals

Figure 10 shows the observed deviation of the yield factor between $\boldsymbol{VM}$ and $\boldsymbol{VM_{Eff}}$ is around 1.165 which is in good agreement with the results of Winkler and Neumann [134], and Fisher [136]. Previous studies showed under laboratory conditions even higher values, e.g. Rozendaal [103] observed a ratio of 1.4 and Badzioch and Hawksley [118] stated values between 1.3 and 1.8. Also the conclusions of Visona and Stanmore [138] support the assumption that the effective VM content of a coal is always greater than this measured by the standard test. The authors observed that the volatile ingredients do not always burn in a homogeneous mode but also in diffusion mode in and around a coal particle. That would mean that the real oxidation process leads to more reactivity than could occur if only one of both modes is being considered which is additionally confirmed by the findings of Badzioch and Hawksley [118]. They confirmed that the weight loss between the original coal and the char produced during their experiments was always greater than the change in the proximate volatile matter of coal and char.

The establishment of equation (**VI–3**) lead to a further development of the original fuel ratio established by Kluger et al. [135] by using the new estimated effective VM content instead of the given proximate value according to the proportion of volatile containing hydrocarbons.

$$\boldsymbol{FR_{Eff} = \frac{C_{Fix}}{VM_{Eff}}} \tag{VI–6}$$

With:

$$\boldsymbol{C_{Fix} = 100 - VM - A - H_2O} \tag{VI–7}$$

The correlation of the new effective fuel ratio $\left(\boldsymbol{FR_{Eff}}\right)$ with the field reference data show that more coal dependent parameter would be needed to identify a proper correlation. The next plausible additional parameter was the established major contribution factor, the fuel nitrogen content [90, 139] and its significant contribution on NO_x emission [139, 140]. For thus equation (VI–6) has been supplemented by the fact, that more fuel nitrogen would lead to more emissions and therefore to a higher helping factor. Which increase the nitrogen indicator $(\boldsymbol{NI})$ likewise.

$$\boldsymbol{h_1 = FR_{Eff}\left(1 + N_{wf}\right)} \tag{VI–8}$$

Where $\boldsymbol{N_{wf}}$ is the coal nitrogen content on a water–free basis in wt.–%. The results confirmed that coals with equal VM content[14] could have a significant different combustion and emission behavior than coals with equal original VM but different hydrogen and or nitrogen content. Also the work of Okazaki et al. [141] confirmed that the more nitrogen content in the coal the more fuel–NO_x will be generated. For a better

---

[14] According to the proximate analysis.

illustration of the above mentioned dependency $\boldsymbol{h_1}$ has been calculated based on several coal samples coming from the US Geological Survey Open–File Report [18].

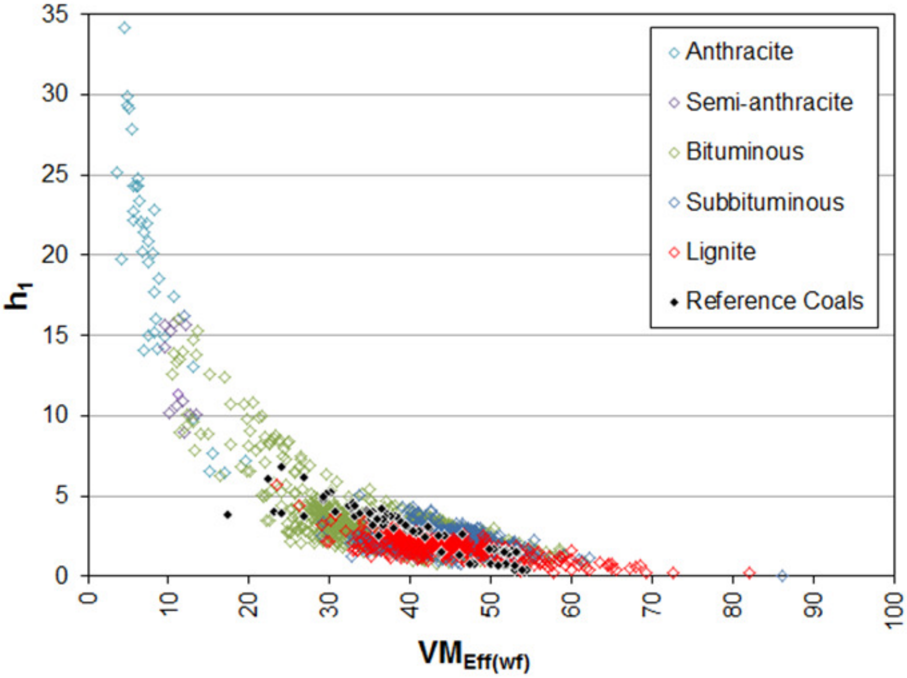

Figure 11. Relation between $VM_{Eff(wf)}$ and h_1 of various coals

Wang et al. [137] stated that higher ranked coals formed more NO from coal–N, and lower ranked coals formed more N_2 while combusting different coals in an entrained flow test reactor. Figure 11 confirmed this statement. The higher the coal rank the higher the heating value or the lower the volatile content respectively. Both results in increasing the coal influence factor $(\boldsymbol{h_1})$ and thus, in an increasing negative influence on the total NO_x emissions. Furthermore it can be postulated that according to Figure 11 coals with nearly similar effective volatile content can have significant higher NO_x tendency which encouraged the adoption that one influence factor is insufficient to draw conclusions on NO_x emission to be expected. Only the inclusion of a second factor $(\boldsymbol{N_{wf}})$ brings here the desired dependence. General means that, the higher the value of $\boldsymbol{h_1}$ the more the coal tends to NO_x.

Air Influence

The effect of stoichiometric ratio on NO_x is one of the first identified influence factors. This dependence has been investigated in test–rig studies [90], pilot–scale studies [170, 142] as well as in full–scale field tests [89, 103]. The common conclusion is that with decreasing the combustion stoichiometry the local oxygen partial pressure decreases and the NO_x formation becomes hindered. Correlations between excess air flow and the amount of NO_x generated have shown that, limiting the excess oxygen content at the end of the furnace below two percent (air ratio, $\boldsymbol{n_{Total}} < 1.1$) will strongly influence the NO_x content of flue gas. Because this influences the mutual multiple reactions in volatile–N and enhances the reduction reaction of NO_x [143, 144]. NO_x reductions of 20 % on the mean level had been achieved by reducing the total excess air by 20 % or even lower.

The major problem in identifying the oxygen correlation is to isolate the excess air influence from the other influences. Usually it is not possible to change the overall stoichiometric ratio while keeping the other parameters constant. For example, an increase of excess air results often in an increase of the amount of overfire air and thus this impact increases also and distort the result. Therefore has the dissipation of the air influence factor been based on the elementary work of David W. Pershing [90]. The investigation was done in a refractory tunnel furnace burning three different coals (Colorado, Pittsburgh, and Western Kentucky) under unstaged conditions. It is clear that due to the inhomogeneous and turbulent local conditions inside a furnace the mixing, and thus the distribution of the oxygen is not uniform at all and that the actual local stoichiometry in the primary first–stage zone is much more fuel–rich as the total excess air ratio would suggest. Otherwise the nitrogen portion in the coal would tend to a full conversion and the further reaction to molecular nitrogen does not take place, as noted in Figure 7. But due to the small number of other influence variables it was found to be more representative than results coming from full–scale applications with too many unknowns. The results of Pershings work [90] and the basis for the development of the air influence factor $\boldsymbol{h_2}$ are shown in Figure 12.

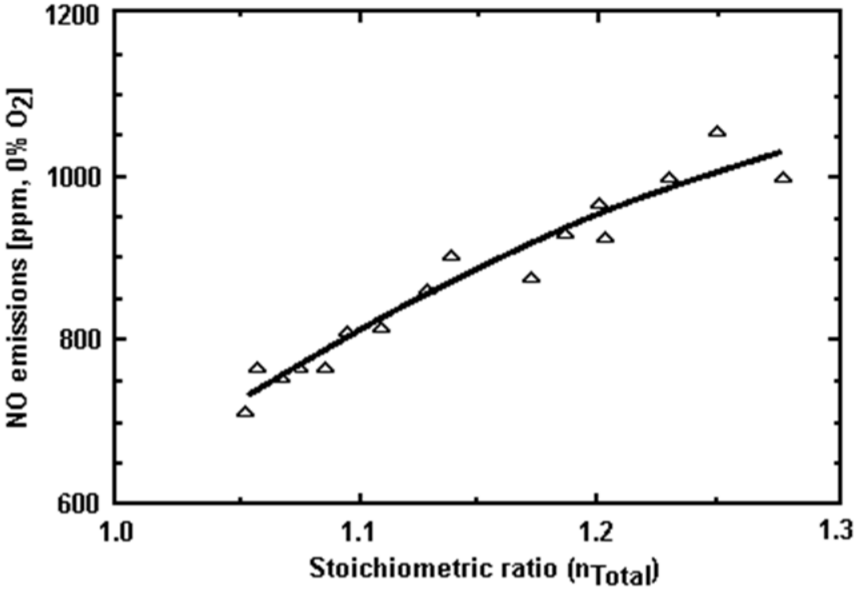

Figure 12. Influence of excess air level on the NO_x formation [90]

According to the results given in Figure 12 it can be concluded that the NO_x emissions leveled–off beyond a certain value of stoichiometric ratio and will even decrease again when the maxima of the function has been past. This effect can be explained by the fact that with rising stoichiometry the chemical reaction increases faster until the highest possible flame temperatures has been reached and until the temperature decrease through the further increasing portion of cooler oxygen carrier which prevents especially the dissociation of N_2 (thermal–NO_x) at this point.

Assuming that the regression function from Figure 12 represents the general relationship between NO_x emissions in mg / m³ STP_{dry} corrected to 6 % O_2 and total excess air ratio it can be concluded that the shape of the function becomes universally applicable for any pulverized coal system. Based on this, the grade of air ratio influence on NO_x emissions $(\boldsymbol{h_2})$ can be derived by the polynomial relationship shown in Figure 12 as Figure 13 suggest.

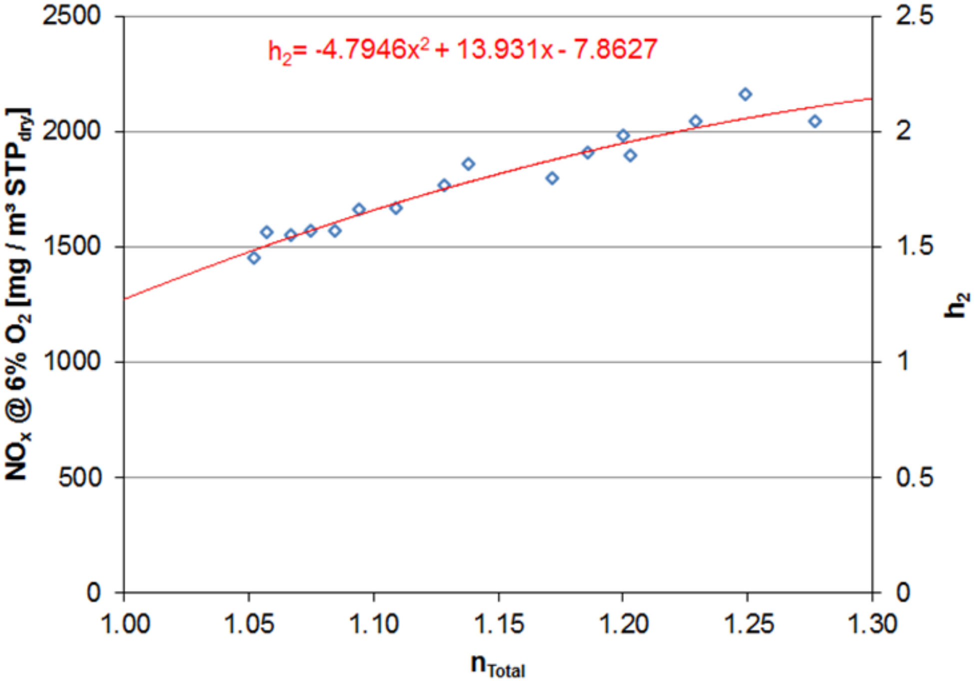

Figure 13. Advanced relation between NO_x concentration and total air ratio

Figure 13 shows the published results of D.W. Pershing converted to mg / m³ STP_{dry} at 6 % O_2 and the derived regression relationship of total excess air ratio on NO_x emissions can be expressed as follows:

$$\boldsymbol{h_2 = -4.7946 * n_{Total}{}^2 + 13.931 * n_{Total} - 7.8627} \qquad \text{(VI–9)}$$

Comparing equation (**VI–1**) with (**VI–9**) this assumption can be validated by the fact that a stable and continuous self–sustaining ignition of the coal particles can only be ensured if a certain oxygen concentration is available. Regarding equation (**VI–9**) means that, no stable self–sustaining combustion would be possible with a total air ratio below 0.75.

Air Staging Influence

Air and fuel staging promote secondary reactions of the primary coal volatiles which influence the nitrogen formation among different combustion products and therefore the overall NO_x production [145]. The influence of staged combustion on NO_x had been widely tested since its initial development in the late 1950s [146] and the level produced by pulverized coal combustion can be strongly influenced and reduced by this method [92]. Principally it uses a fuel–rich zone within the burner belt in combination with an overfire air (OFA) stage or stages where the remainder of the fuel is oxidized and the combustion being completed. The so called external air staging or furnace air staging is a method where the combustion air in the furnace is principally divided into stage–one and stage–two air which could also termed as burnout air. The stage–two air is being added as overfire air above the burner belt which targeting to reduce the stoichiometry of the primary zone [27]. It can be further understood as a furnace air staging and infect of the sub–stoichiometric atmosphere where the primary combustion is occurring, the temperature is being held down and thus the thermal–NO_x generation is being kept down [147]. Air–staged combustion is one of the most efficient technologies for reducing NO_x emissions and it has been the most widely adopted technology in coal–fired power plants around the globe [185]. A lot of laboratory, pilot–scale and full–scale research work have been carried out on NO_x generation under air–staged conditions [192, 148–160] and most tests show a continuing decrease in NO_x emissions as long as the amount of combustion air is shifted away from the burner and added as overfire air / oxidant at different levels to the furnace. This oxidant staging effect can reduce the conversion rate of coal–N to

NO_x by more than 50 % [161]. In this manner, it can be concluded that air–staging reduces both thermal– and fuel–NO_x, when:

- The air quantity that is staged increases, because shifting more combustion air to the stage–two zone means decreasing the oxygen partial pressure within the primary combustion zone where the heterogeneously reductive reaction of NO_x and coal char occurs.
- The particle residence time between the burner and the individual burnout air injection position increases.

Both conditions influence the amount and decomposition of reducing species (HCN, NH_3, NCO, etc.) and is for that conducive to NO_x destruction and therefore produce less NO_x emissions until the furnace end [154, 162, 176]. The major problem regarding the residence time is that the temperature profiles inside a furnace cannot be calculated. It needs to be interpolated, which indicates that the furnace mean temperature profiles among the furnace height are just going to be estimated and in fact such method could not produce realistically results. Also during the design procedure of a boiler are the specific temperature profiles occurring neglected. Boilers are typically designed for a specific flue gas velocity in the range of 8 to 9 m / s and this velocity is in turn based on an assumed average mean temperature which depends on the coal properties (see Table 5). This circumstance imply that any assumption concerning the residence time based on comparable mean temperatures would lead to nearly equal velocities even due to the general boiler design criteria which in fact signify that the more significant influence characteristic coming from air staging belongs to the question on what the residence time of a burning particle depend. The conclusion made was, if the residence time is the quotient of flue gas velocity (the quotient of operating flue gas volume and furnace cross section) and the respective travel distance, than it can be assumed that the vertical spacing between the highest point of coal injection and the point of air injection would be the most trusting indicator for the reduction potential. An investigation concerning this influence under constant air quantities have proven this assumption, the results can be seen in Figure 14 [163].

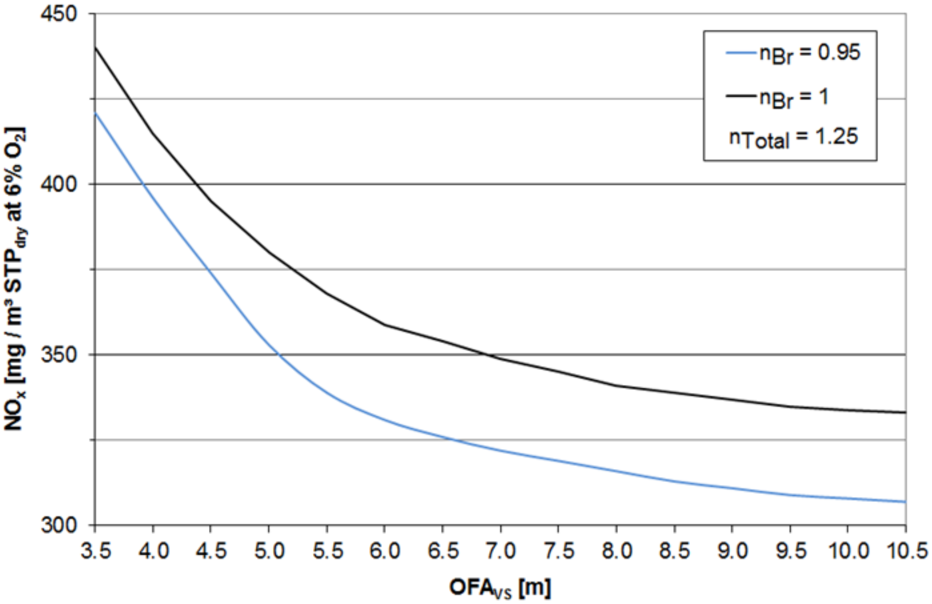

Figure 14. Influence of OFA spacing on the NO_x formation [163]

Figure 14 shows the total NO_x formation (normalized) as function of the OFA vertical spacing ($\boldsymbol{OFA_{VS}}$) for different burner air ratios ($\boldsymbol{n_{Br}}$) depending on a constant total air ratio ($\boldsymbol{n_{Total}}$) at the furnace end. It can be seen that under constant burner– and total air ratios ($\boldsymbol{n_{Br}}$ & $\boldsymbol{n_{Total}}$) with increasing distance between top active burner row and the location of OFA injection ports the NO_x reduction efficiency greatly increases at the beginning, and then leveled–off beyond 6 m. That means, that the degree of NO_x reduction by increasing the OFA vertical spacing ($\boldsymbol{OFA_{VS}}$) seemed to be limited, however, by both practical [163] and theoretical considerations [164, 165]. Glassman

[165] concluded that this phenomenon may be explained by the fact that increasing the distance between burner and OFA ports increase the residence time of flue gas in primary combustion zone, and this expands the residence time of flue gas in reducing atmosphere. However, with the further rise of flue gas flow in primary combustion zone, the concentrations of reducing species decrease, and this makes the capability of NO_x reduction weaken. For the background that the functions shown in Figure 14 indicates that this relationship approaches to zero as the distance tend to infinity the function shape has been assumed to be a power function. Furthermore have empirical tests shown that the air staging influence can be most significant described by the vertical distance to the power of air quantity which is staged according to the following expression.

$$\boldsymbol{h_3} = \prod_{\boldsymbol{i=1}}^{\boldsymbol{n}} \frac{\mathbf{1}}{\left(\boldsymbol{OFA_{VS_i}}\right)^{\left(\boldsymbol{OFA_{\%_i}}\right)}} \tag{VI–10}$$

Where $\boldsymbol{OFA_{VS}}$ is the clearance between the upper active burner plane and the individual point of OFA injection $(\boldsymbol{i})$ in meters. $\boldsymbol{OFA_{\%}}$ as the percentage of the total combustion air shifted away from the burners and added at the individual point of OFA injection $(\boldsymbol{i})$ in percent. It should be remarked that the distance of the first OFA injection level and also the amount of burnout air cannot be arbitrarily increased as equation (**VI–10**) may connote. If the distance becomes too large then the effect of the delayed combustion would be nearly negligible because the particle reaction process would be completed until the OFA nozzles are reached where additional oxidant is supplied to the combustion. The only recoverable effect would be the dilution of the flue gas and the herewith containing NO_x but under the consideration of realistic actionable distances inside a furnace the overall assumption could be postulated as valid.

Burner Influence

Nearly every supplier developed an own burner design with individual operating philosophies and thus it becomes even more complicated when considering the fact that the ongoing development of each supplier would lead to the assumption that nearly every power station in the world has special and individual conditions within the primary combustion zone at least as a result of different burner design and operational settings. For a better understanding of the complexity of a pulverized coal burner Figure 15 illustrate the Foster Wheeler[15] low–NO_x burner of the fifth generation developed in 1997.

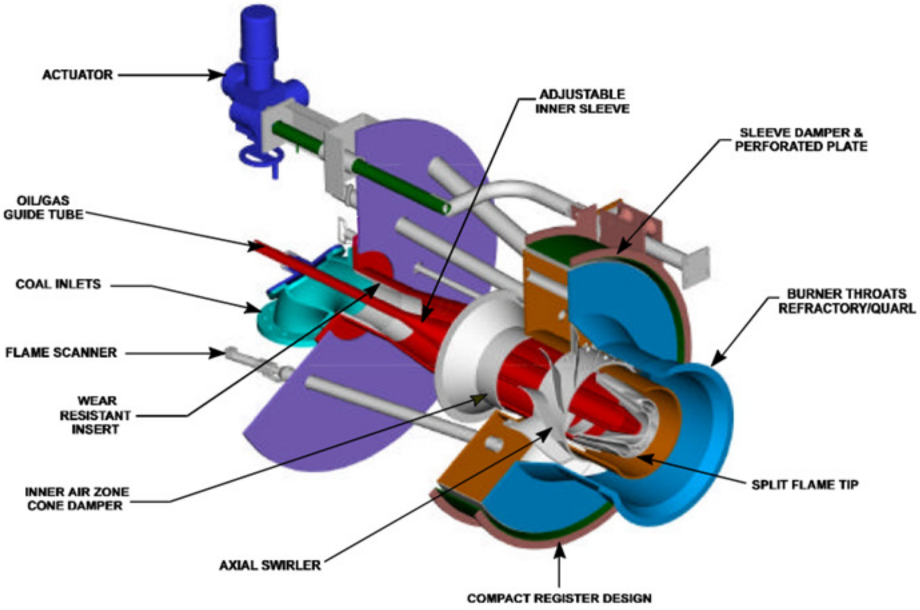

Figure 15. Foster Wheeler parallel flow split flame (VS / SF) burner [166]

For clarification purposes, it shall be remarked that while tangentially–fired utility boilers have typically coal and air nozzles rather than burners as in wall–fired boilers, the term ‘burner’ is used for both tangential and wall applications in this thesis. The exact and complete description of the working principle of pulverized coal burner can be found elsewhere [e.g. 100, 166–171] but for instance it should be noted that there are many

---

[15] Foster Wheeler Ltd. is focused on engineering, procurement, and construction in the power industry.

variations on the low–NO_x burner design of reducing NO_x and due to different kinds of coal with various properties the design of the burners may differ significant by each other which is critical because even very minor changes in the discharge configuration of the burner tip can result in NO_x changes on the order of 25 – 30 % [172]. Wang et al. [137] described that 60 to 90 % of the NO_x left after installation of low–NO_x burners originates from the char–N component. Cai et al. [173] observed something similar. Estimating 60 to 95 % of NO_x originates from char–N when using low–NO_x burners. Heap et al. [168] observed that the type and position of the fuel injection within the burner quarl box was the one of the most important factor in influencing the emissions. However, the influence of individual factors and their specific contributions are very difficult to investigate because it would require extreme effort attached to changings regarding geometry factors. Therefore it has been assumed that it is absolutely necessary to describe the fuel injection system and their respective condition in an adjustable and flexible algorithm according to individual plant unit conditions. For thus the burner design has been classified according to its burning effectiveness in combination with its coal behavior. Throughout the published literature have been the following factors identified to be the most influencing causes regarding the NO_x emissions generated by the fuel injection system.

- Excess air level within the burner zone (reducing atmosphere).
- Coal properties (ignition behavior).
- Design geometry (aerodynamic effectiveness).

These factors need to be arranged in an adjustable, reproducible, and comprehensible way in order to define the burner helping factor $(\boldsymbol{h_4})$ as part of equation (**VI–1**). The discovery process started with the definition of the general function which serves as basis of the magnitude of value determination of $\boldsymbol{h_4}$. The most common relationship concerning burner influence on total NO_x emissions is without any doubt the correlation between the air ratio within the near burner zone $(\boldsymbol{n_{BZ}})$ and the respective NO_x formation. The so called burner internal air staging or burner air staging is a method where fuel–rich zones, in which the devolatilization takes place, were created near the burner outlet and then local air–staged conditions were formed [27]. Schlessing et al. [174] published such results concerning such correlation function from a wall–fired power station unit (see Figure 16). These results are also in good agreement with these published by Daood et al. [175]. Considering the results described by both authors it was postulated for the further study, that $\boldsymbol{h_4}$ must mainly depend on the excess air level within the burner zone and further that this relationship would follow the specific function shape based on the results published by Schlessing [174], see Figure 16 (solid line).

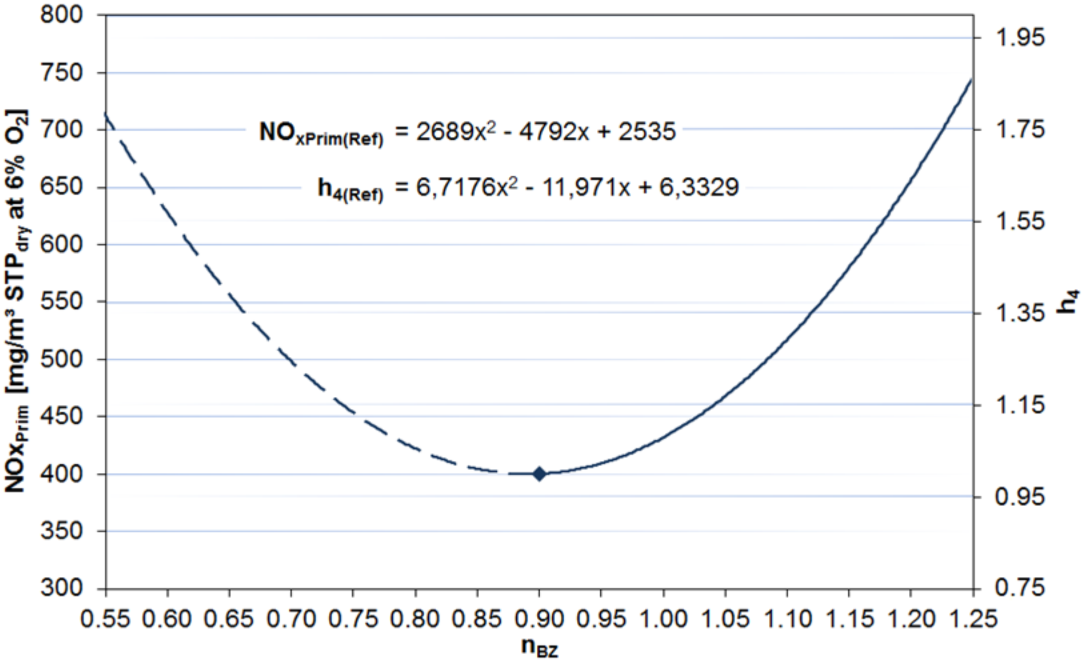

Figure 16. Relation of NO_x generation, burner air ratio, and h_4 [174]

The dotted part of the graph in Figure 16 has been interpolated by a regression analysis based on the results published. Considering the complete shape of the function than it is obvious that the function described an upwards opening U–shaped two–dimensional mirror–symmetrical curve, at least within the range of observed validity. This may be explained by fact that, if the burner air ratio is too low, the combustion is apparently incomplete within the primary combustion zone and thus increases the amount of combustion intermediates (HCN, NH_3, etc.) which then are being oxidized into NO_x in the downstream process when additional oxygen becomes available [176]. When the burner stoichiometric ratio is too high, oxygen is relative sufficient present in the primary combustion zone, and this weakens the reducing atmosphere and leads to form more NO_x. Both effects results in higher emission values. That means also, that the point on the axis of symmetry that intersects the parabola (vertex / minima) described the point of lowest possible NO_x emissions while the system operates at optimal burner air ratio ($\boldsymbol{n_{OBZ}}$). This point represents the case where the resulting helping factor coming from the burner influence ($\boldsymbol{h_4}$) results in no change on the NO_x emission level predicted by equation (**VI–1**), i.e. $\boldsymbol{h_{4(Ref)} = 1}$ which is the value of the helping factor 4 at the optimal burner air ratio ($\boldsymbol{n_{OBZ}}$). For the given function in Figure 16 means that, helping factor 4 ($\boldsymbol{h_4}$) should be equal to one (no influence) at $\boldsymbol{n_{BZ} = 0.9}$. Due to this fact is also the shape of the relationship between burner air ratio ($\boldsymbol{n_{BZ}}$) and the burner influence factor ($\boldsymbol{h_4}$) describable by the help of a regression analysis of the function coming from the work of Schlessing et al. [174] (Figure 16, secondary axis) and results in a polynomial function of the second order which can be expressed as follows:

$$\boldsymbol{h}_{\boldsymbol{4}(\boldsymbol{x})} = \sum_{\boldsymbol{i}=\boldsymbol{0}}^{\boldsymbol{2}} \boldsymbol{a}_{\boldsymbol{i}}(\boldsymbol{n}_{\boldsymbol{BZ}})^{\boldsymbol{i}} \tag{VI–11}$$

According to the above mentioned assumption it can be postulated that the equation coefficients $(\boldsymbol{a}_{\boldsymbol{i}})$ and thus the function shape are generally applicable to every combustion plant. Essential is the location of the function within the coordinate system. If $\boldsymbol{h}_{\boldsymbol{4}}$ depends on the excess air level within the burner zone than must the location of this relationship in the coordinate system depend on the volatile content of the coal (ignition behavior) as well as the design of the burner (aerodynamic effectiveness).

Ignition Behavior

The homogeneous ignition of the volatiles and oxidizer mixture occurs first followed by secondary ignition and burning of the char particle. Therefore, it is instructive to investigate the factors governing the ignition of a mixture of gaseous volatiles and oxygen under well defined surroundings. Following the derivation of Law [177], is the homogenous ignition of coal volatiles strongly influenced by the coal volatile content, heating and devolatilization rate, and oxygen concentration in the environment. These arguments can qualitatively be simplified by the fact that the heating and devolatilization rate of a particle is strongly influenced by the temperature [177, 178] and according to Table 5, this has been assumed as equal for all observed systems within this thesis in order to improve their comparability. For this background is the remaining open relation the oxygen concentration of the near burner environment depending on the volatile content of the coal. This assumption can be validated by the fact that the burning characteristic of coal varies significantly depending on its volatile content [177–184] which has already been shown in Figure 11. The existence of appropriate concentration of oxygen within the reduction zone is beneficial to NO_x reduction in deep or middle air–staged combustion [185], because of the above mentioned relationship of too low burner air ratios which causes a bigger amount of reducing species (HCN, NH_3, etc.) which enter the burnout zone and then being oxidized into NO_x [176]. Concerning to the combustion behavior of different coals means that, that a high volatile coal need more partial available oxygen as low volatile coals. That means the chemical reactions of the volatiles will need a certain amount of direct available oxygen. Therefore it needs to be ensured that after and during the homogeneous reaction enough oxygen is present at the char surface in order to lower the char consumption in the primary high temperature heating zone which comes due to the lower oxygen diffusion rate. Some researchers have observed this phenomenon, the existence of a certain concentration of O_2 will significantly enhance the extent of NO_x reduction of carbon–containing substances such as coal, char and soot [186–190]. Another side effect is that if not enough oxygen is being provided during the primary combustion process it could lead to a thermal instability of the air / coal mixture due to unburned fuel volatiles which results in strong temperature fluctuations due to 'flashovers' in the downstream process [191]. Fan et al. [192] stated that O_2 concentration close to zero leads to less surface–complex C(O) production which is not beneficial for the accelerated NO_x reduction and when the O_2 concentration is too high (more than 4 %), the O_2 tends to consume a large amount of coal char through the direct combustion reaction which produced also significant amounts of NO_x. That means that the optimum O_2 concentration around the coal particle for maximum NO_x reduction is determined by the portion and reactivity of the coal containing volatiles. Greul et al. [193] split the fuel into pyrolysis gas and residual char before being combusted in a test facility with a view to lower NO_x emissions. The authors stated that the optimum air / fuel ratio for lowest NO_x emissions increases with increasing the coal pyrolysis gas (volatiles) content. This effect supports the conclusion of the necessity of enough oxygen concentration within the primary combustion zone near the burner outlet according to the devolatilized volatile gas portion. Therefore it can be postulated that the optimum burner zone air level ($\boldsymbol{n_{OBZ}}$) depends on the amount of devolatilized volatiles.

Based on the fact that the above mentioned relationship indicates that an early full conversion of volatiles should be preferred, means that the describing function of that relationship would need to tend to one, when the volatile matter ($\boldsymbol{VM}$) content tends to one and would need to tend to zero when the $\boldsymbol{VM}$ content tends to zero. These circumstances indicate a power function shape and different empirical model trials have shown that the mentioned dependency could satisfactory described by:

$$\boldsymbol{n_{OBZ} = {VM_{Eff}}^{0.25}} \tag{VI–12}$$

With $\boldsymbol{n_{OBZ}}$ as the appropriate concentration of oxygen within the primary combustion zone with respect to $\boldsymbol{VM_{Eff}}$, which is the effective coal volatile content in kg / kg according to equation (**VI–3**). The following figure visualized this relationship.

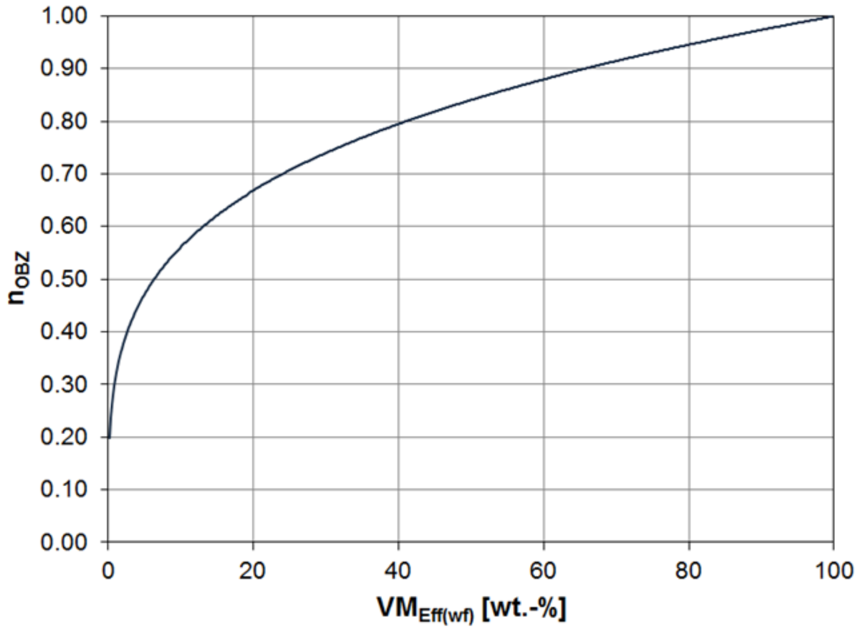

Figure 17. Relation between $VM_{Eff(wf)}$ and n_{OBZ}

The shape given in Figure 17 describes the assumption that the appropriate oxygen concentration in the nearer burner outlet (primary zone) depends on the coal properties. The result of this relationship is according to Figure 16 and equation (**VI–11**) the location of the function vertex on the x–axis inside the coordinate system and herewith the determination of $\boldsymbol{n_{OBZ}}$ for the respective coal.

The second determination of the coordinates for the global function (**VI–11**) concerning the y–axis position was postulated to depend on the design of the burner and its aerodynamic effectiveness which determined the oxygen staging and combustion delay within the primary combustion zone.

Aerodynamic Effectiveness

Before the 1970s, coal burners were designed to provide highly turbulent mixing and combustion at peak flame temperatures in order to ensure the highest possible combustion efficiency. Unfortunately these circumstances promote significant the thermal–NO_x formation [194]. Since 1971 pulverized fuel burners have undergone considerable improvements which changed the general working principle towards a more controlled aerodynamic mixing between the fuel and combustion air, whereby the combustion stoichiometry (e.g. delay mixing to create a fuel–rich primary flame) and the temperature profiles (e.g. reducing the residence at peak temperature profile) will be influenced and thus the particle heating rate occurring in the closer burner environment [195, 196]. The biggest problem relating the influence of burner parameters on primary NO_x formation is the variety of factors involved. Table 7 summarized the dominant burner design criteria which determine the influence on NO_x formation.

Table 7. Burner design factors for NO_x control

Burner design criteria
• Method of fuel injection (swirl, jet)
• Throat velocity
• Geometry of the burner exit
• Geometry of the burner quarl
• Position of fuel injector
• Type of burner exit
• Wear and tear of the burner outlet
• The degree of flame attachment to the burner outlet
• Proportion of air streams (air ratios)
• Portion of recirculated flue gas
• Swirl intensity

Due to the broadness of possible variations listed here the above mentioned assumption regarding uniqueness of every primary combustion situation of a power station is validated. But nevertheless, the individual situation in the nearer burner area must be a result of any possible combination of the above listed parameters. Therefore it can be expressed as:

$$\boldsymbol{BI} = \prod_{\boldsymbol{i}=\boldsymbol{1}}^{\boldsymbol{n}} \boldsymbol{b_i} \qquad \text{(VI–13)}$$

Where $\boldsymbol{BI}$ is the burner index which is the result of the interplay of the various burner design factors ($\boldsymbol{b_i}$) given in Table 7. The problem occurred when considering the required amount of different data needed for a detailed statistical investigation of any dependency between NO_x emissions and the different burners factors involved, it seemed to be obvious that the estimation of the individual burner index ($\boldsymbol{BI}$) needed to be simplified. A good and practical way for solving such situation is the methodology used by Pershing [72, 90], Shimizu et al. [98], Schlessing [113], and Kurose et al. [119]. The principle method was to make use of a reference scenario to draw conclusions on another. Concerning the current problem means that, if the result of equation (**VI–13**) represents the effectiveness of a specific burner than it can be assumed that the combination of all these different influence factors given in Table 7 results in a certain amount of primary NO_x level which can be compared with the reference primary NO_x level given from the work of Schlessing et al. [174] (Figure 16). That leads to the fact that equation (**VI–13**) could be also expressed as:

$$\boldsymbol{BI} = \frac{\boldsymbol{NO_{x_{Prim}}}}{\boldsymbol{400}} \qquad \text{(VI–14)}$$

$\boldsymbol{BI}$ is the quotient of the primary NO_x level of the reference scenario (400 mg / m³ STP_{dry} at 6 % O_2) and the primary NO_x emission level of the observed system $\left(\boldsymbol{NO_{x_{Prim}}}\right)$ while it operates at optimal burner air ratio $\boldsymbol{n_{OBZ}}$. The exact value of the primary NO_x emission behavior $\left(\boldsymbol{NO_{x_{Prim}}}\right)$ of the observed combustion plant has been considered as model adjustment factor which needed to be estimated either based on experience from other comparable plants (see chapter 'Burner Design') or by the help of objective factors, e.g. by an iterative investigation by setting equation (**VI–1**) equal to an observed reference field measured NO_x level from the respective system. The estimated ratio from equation (**VI–14**) indicates the aerodynamic effectiveness of a specific combustion plant based on the reference scenario and thus the necessary adjustment of the y–axis coordinate of the vertex of the function.

It shall be remarked that it was found due to several model trials that an exponential adjustment of the burner index $\boldsymbol{BI}$ tends to more realistically deviations between certain combustion systems as the normal quotient would do.

$$\boldsymbol{h_{4(n_{OBZ})} = exp^{(BI-1)}} \tag{VI–15}$$

The exponent of the relationship as described in equation **(VI–14)** needed to be subtracted by one because of the fact, that any nearly comparable system according to the reference primary NO_x emission level given from the work of Schlessing et al. [174] (Figure 16) would lead to $\boldsymbol{BI = 1}$ and in order to get sure that $\boldsymbol{h_{4(n_{OBZ})}}$ results for such cases also in one, the zero exponent is needed. $\boldsymbol{h_{4(n_{OBZ})}}$ represents according to Figure 16 and equation (**VI–11**) the location of the function vertex on the y–axis inside the coordinate system and herewith the second determination of the coordinates for the global function (**VI–11**).

Summary of the Burner Influence

Summarized, it can be stated that the above mentioned methodology postulated that the influence factor $\boldsymbol{h_4}$ as given in equation (**VI–11**) can be described by the shape of the global reference function given from the work of Schlessing et al. [174], see Figure 16. That means the function coefficients are to be expected as general applicable for all combustion systems, with $\boldsymbol{a_2 = 6.71, a_1 = 11.97}$, and $\boldsymbol{a_0 = 6.34}$. Whereas the location of the function vertex inside the global coordinate system could be described by the relationship between optimal burner air ratio $(\boldsymbol{n_{OBZ}})$ depending on the coal volatile matter (equation (**VI–12**)) and the aerodynamic effectiveness of the specific combustion configuration $(\boldsymbol{BI})$ (equation (**VI–13**)). For this background it is possible to displace the reference function by a coordination transformation in order to determine the respective helping factor $\boldsymbol{h_4}$ on the basis of the actual burner air ratio $(\boldsymbol{n_{BZ}})$.

$$\boldsymbol{h_4} = \boldsymbol{a}_2(\boldsymbol{n_{BZ}} - \Delta\boldsymbol{x})^2 - \boldsymbol{a}_1(\boldsymbol{n_{BZ}} - \Delta\boldsymbol{x}) + \boldsymbol{a_0} + \Delta\boldsymbol{y} \qquad \text{(VI–16)}$$

The corresponding displacement of the coordinates Δx and Δy are:

$$\Delta\boldsymbol{x} = \boldsymbol{n_{OBZ}} - \boldsymbol{n_{OBZ(Ref)}} \qquad \text{(VI–17)}$$

$$\Delta\boldsymbol{y} = \boldsymbol{h}_{4(\boldsymbol{n_{OBZ}})} - \boldsymbol{BI_{(Ref)}} \qquad \text{(VI–18)}$$

The reference values used according to Schlessing et al. [174] (Figure 16) are $\boldsymbol{n_{OBZ(Ref)}} = \boldsymbol{0.9}$ and for $\boldsymbol{BI_{(Ref)}} = \boldsymbol{1}$. By the help of the above described methodology (equation (**VI–12**) to equation (**VI–18**)) is it possible to adjust the global function (Figure 16) according to the effective volatile matter content of the actual coal under consideration of the respective burner mixing effectiveness in order to determine the respective helping factor $\boldsymbol{h_4}$ on the basis of the actual burner air ratio.

Furnace Influence

The so called ‘furnace’ represents the part of the boiler where the main energy reaction occurs and is normally enclosed by encircling walls of a welded fin tube construction. On the water side, these furnace walls are typically arranged as an evaporative system. The lower end of the furnace is formed by the outlet hopper with the necessary facilities for ash removal and the upper ends below the convective heating surfaces normally those of the superheater.

The rate of fuel bound nitrogen conversion is not constant. The volatile release during the heating of coal is strongly influenced by the rank of the coal and additionally by the heating environment which is can be defined by the heat density. The kind of furnace affects therefore the NO_x emissions and NO_x reduction capability [197]. Therefore it can be postulated that the grade of the primary emission level is in compliance with the heat density within the primary zone which could be confirmed by the results reported by Soud et al. [197] and Cherry et al. [198]. Soud et al. [197] showed variations in NO_x emissions versus different boiler types and sizes and Cherry et al. [198] compared operational data obtained from two power stations (Council Bluffs No. 3 and San Juan No. 1). Both publications confirmed the assumption made above. NO_x emissions generally increase with increasing thermal capacity per cubic meter furnace of a unit. Several factors are important for the formation methodology of NO_x emissions with respect to the boundary conditions determined by the furnace design. That means the dominant variables determine the energy density in the primary combustion zone which influences the NO_x emissions. Table 8 summarizes these dominant influence factors coming from the furnace.

Table 8. Dry bottom furnace design factors

Furnace influence factors on NO_x generation
• Geometry of the combustion chamber (radiant surface area / volume, flue gas velocity / residence time)
• Wall design (gas tight membrane wall, tube–and–brick, etc.)
• Wall temperature (heat flux)
• Wall cleanness (slagging)
• Process philosophy (air staging / injection points, burnout grate)
• Burner arrangement
• Burner capacity

Similar to the burner NO_x influence factors listed in Table 7 and assumptions based thereupon, can also here be assumed that due to the broad variations nearly every power station in the world has a unique situation within the furnace as a result of any possible combination of the above listed parameters. The difference between the burner– and furnace influence factors is that furnaces can be classified by the help of established thermodynamic parameters which are commonly used for qualitative comparison between different plants also for the estimation of the in–furnace conditions with respect to slagging–, fouling– and emission tendency, see Table 9.

Table 9. Furnace characteristic parameters

Furnace design parameter
• Area heat release rate Quotient of the heat input and the furnace radiant heat exchange surface

Furnace design parameter

- Volumetric heat release rate
  Quotient of heat input and furnace volume
- Burner belt heat release rate
  Quotient of heat input and burner belt area
- Burner belt volumetric heat release rate
  Quotient of heat input and burner belt volume
- Cross–sectional heat release rate
  Quotient of heat input and furnace cross–sectional area

As stated above, NO_x formation influence by the energy density within the burner belt which is described only by the burner belt volumetric heat release rate. This circumstance could be explained by the fact that the most important point regarding NO_x formation is the place where the main part of the chemical reaction happens within a specific volume which is also the place with the highest energy density, i.e. the burner belt. Generally it can be simplified: the higher the energy density within the furnace and thus the higher the thermal rating, the higher the NO_x emissions can be expected. This assumption can be validated by the fact that higher temperatures lead generally to higher NO_x values. According to Y. B. Zel'dovich [45] and C. P. Fenimore [47, 76, 74] the generation of NO_x depends exponential on temperature and happens mainly according to the limit of available oxygen. Therefore it has been assumed that also the energy density must be of exponential dependency. That means the influence factor from the furnace design can be expressed as:

$$\boldsymbol{h_5 = exp^{(BBVHR)}} \tag{VI–19}$$

Where $\boldsymbol{BBVHR}$ is the burner belt volume heat release rate which is the quotient of the total heat input to the furnace ($\dot{\boldsymbol{Q}}_{\boldsymbol{th}}$) and the burner belt volume ($\boldsymbol{BBV}$).

$$\boldsymbol{BBVHR} = \frac{\dot{\boldsymbol{Q}}_{\boldsymbol{th}}}{\boldsymbol{BBV}} \tag{VI–20}$$

It shall be remarked, that within the literature is $\dot{\boldsymbol{Q}}_{\boldsymbol{th}}$ could also related to the energy which enters the process, i.e. the fuel heat capacity release inside the furnace $(\dot{\boldsymbol{Q}}_{\boldsymbol{fuel}})$ and thus it is equivalent to the thermal power of a unit which is therefore the official characteristic parameter for energy conversion systems [199]. But related to the real energy density within the furnace, this definition is not applicable at all because it does not consider the total internal energy in the furnace which is out of the question the sum of all supplied energies. Therefore for the entire research work $\dot{\boldsymbol{Q}}_{\boldsymbol{th}}$ has been defined as the total internal energy inside the furnace which is the sum of the fuel heat and the heat capacity of all superimposed material flows (e.g. classifier stream, secondary air, false air, recirculated flue gas etc.) see Figure 18

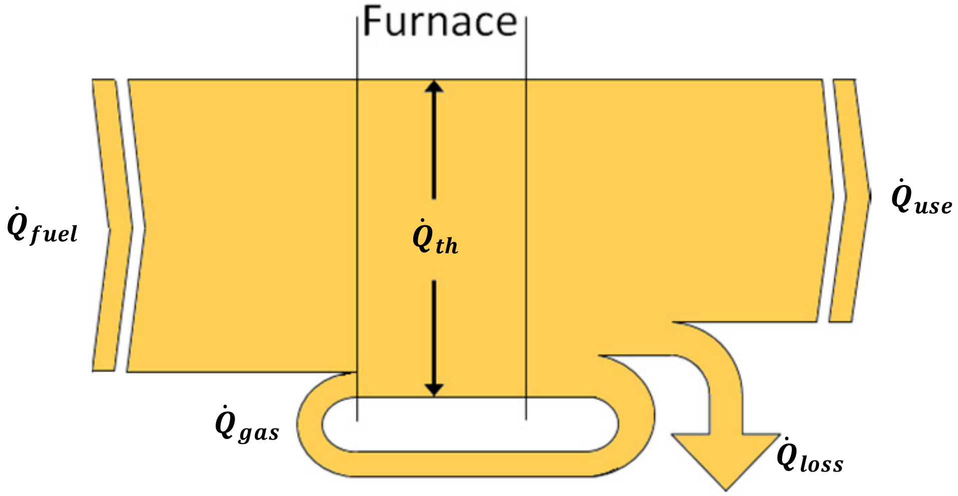

Figure 18. Sankey diagram[16] for a furnace without air staging

---

[16] Developed by the Irish engineer Riall Sankey over 100 years ago [200].

The major assumption made is that only the real volume load can give reasonable estimates regarding the actual energy density of a certain volume. According to Figure 18 can the resulting energy of all material flows inside the furnace expressed as:

$$\dot{\boldsymbol{Q}}_{\boldsymbol{th}} = \dot{\boldsymbol{Q}}_{\boldsymbol{fuel}} + \dot{\boldsymbol{Q}}_{\boldsymbol{gas}} \qquad \text{(VI–21)}$$

With $\dot{\boldsymbol{Q}}_{\boldsymbol{fuel}}$ as the product of fuel massflow [kg / s] and its lower heating value [MJ / kg] and $\dot{\boldsymbol{Q}}_{\boldsymbol{gas}}$ as the sum of all recirculated energies within the system balance limits, expressed as:

$$\dot{\boldsymbol{Q}}_{\boldsymbol{gas}} = \sum_{\boldsymbol{i}=1}^{\boldsymbol{n}} \boldsymbol{C}_{\boldsymbol{P}_{\boldsymbol{i}}} \dot{\boldsymbol{m}}_{\boldsymbol{i}} \boldsymbol{T}_{\boldsymbol{i}} \qquad \text{(VI–22)}$$

where $\boldsymbol{C}_{\boldsymbol{P}_{\boldsymbol{i}}}$ is the average specific heat capacity [J / kg K], $\dot{\boldsymbol{m}}_{\boldsymbol{i}}$ is the massflow [kg / s], and $\boldsymbol{T}_{\boldsymbol{i}}$ the temperature [K] of the respective flow $\boldsymbol{i}$. The definition of the related reference volume, termed as burner belt volume ($\boldsymbol{BBV}$) is understood as a part of the furnace internal volume between the lowermost and the top burner plane plus one additional burner vertical distance due to the significant radiation exposures in the closer area above and below a burner plane as shown in Figure 19.

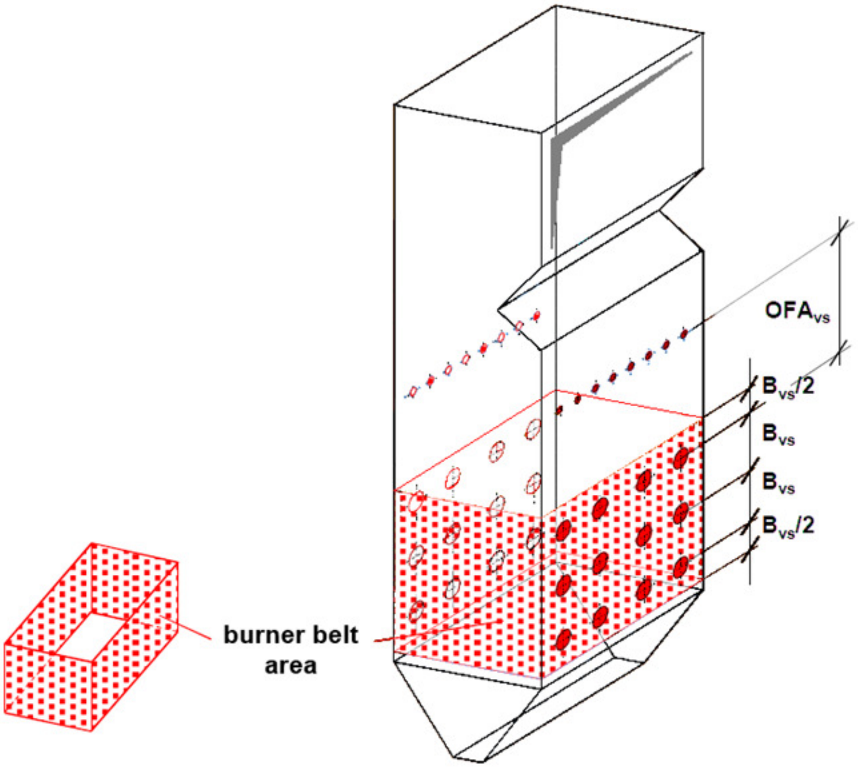

Figure 19. Definition of the furnace geometry

Figure 19 shows the definitions made regarding the encircling burner belt area, where $\boldsymbol{B_{VS}}$ is the vertical distance between two burner planes. The furnace wall area is being assumed to be a continuous heat loaded surface without wall openings, e.g. for the consumables injection. Special attention is to be made on the fact that the size of the burner belt volume can vary inside one furnace due to different variations in the mill–patter–usage, within this thesis also termed as burner–out–of–service (BOOS). Multi–burner combustion systems can have part of an array with burners which are out of service due to the fact that not all burners are required to achieve full boiler load. Burners which are out of service are not fed with fuel but supplied with small quantities of air for cooling the burner tips. Otherwise the strong temperature radiation on these burner parts lead to deformation and annealing of the material. Thus operation mode creates fuel rich combustion zones. The result can be combustion by stages with temperatures lower than when all burners are in service [201]. Such thermal energy reductions lead to lower thermal–NO_x generation and lower heat release rates within the burner belt which leads in fact to a lower average heat density within the related volume. Therefore the calculation of the real burner belt volume based on the upper and lower active burner elevation (BE).

$$\boldsymbol{BBV = (BE_{up} - BE_{low}) f_D f_W} \qquad \text{(VI–23)}$$

Where $\boldsymbol{BE_{up} - BE_{low}}$ is the number of burner elevations from the upper active to the lower active burner elevation. $\boldsymbol{f_D}$ is the furnace depth, and the $\boldsymbol{f_W}$ furnace width. This consideration would not include burner rows out of service between the active ones. Because the average heat density inside the burner belt would be the result of the highest and lowest fuel injection point where BOOS in between has negligible influence on the radiation load of the reference surface related to the supply limits.

VII. EXTRAPOLATION OF RESULTS AND DISCUSSION

Plant owners and operators are extremely interested in using simple and user–friendly as well as cost effective techniques which helps to optimize their plants but also the scientists benefit through the use of simple and fast models, e.g. for the preparation and execution of experiments. Problems may arise when such developed prediction approach based on too many assumptions which then jeopardize the reliability and accuracy of the tool. Therefore is validation an important aspect to evaluate how well approach predictions match certain observations, both qualitatively and quantitatively. The validity of the actual developed approach assessed in three ways:

- By direct comparison on a point–by–point basis of the calculated and measured data.
- By examination of the results by the help of a statistical analysis.
- By comparison of the model history with observations published in other research works.

Basis for Comparison

The Comparative Utility Units

A number of different information regarding different power plant units were needed to ensure that the amount of data is large enough to guarantee best estimates on relationships, dependencies and interactions. These data sets were consistent, plausible and complete field data coming from various power plants located all over the world and they have been acquired by own on site measurements, have been provided by operators (on request) or have been published as part of other research works [103, 202, 203]. In summary means that, the data using coming from:

- 28 utility boilers (incl. 6 boilers used before and after retrofitting).
- Located in 14 countries all over the world (Europe, Russia, China, and USA).
- With boiler capacities between 90 to 2,900 MWt.
- For different boiler loads.
- Consisting of a variety of different combustion systems (tangential–, front–, double front–, allwall–fired).
- Burning a wide range of coal quality parameters (from lignite–A to medium–volatile–bituminous coals[17]).

The reference data of the above mentioned bullet points can be found in Appendix 2. Due to the fact that also usually more than one complete data set was available the total amount of based reference scenarios could be counted to 142 and represent therefore a large enough sample to obtain precise estimates of the strength of the relationship between the NO_x indicator $(\boldsymbol{NI})$[18] value and the NO_x level measured $\left(\boldsymbol{NO_{x_{Ref}}}\right)$.

Necessary Unit Information

An optimized combustion control is essential to reduce NO_x emissions without loss in boiler performance [204]. In order to optimize a combustion system and make

---

[17] According to Figure 3. Coal classification systems [14] ASTM Standard.

[18] According to equation (**VI–1**).

serious predictions of their process parameters, some basic information have to be used which can include tabulated thermo chemical data, the results of several varieties of laboratory and field analyses concerning fuel, residue, gases in the system, and basic rate data usually, the flow rates of feed, flue gases, etc. [71]. Some of these figures can also be calculated and / or compared with real measured data know from the process in order to validate process assumptions. If the combustion process logic is understood it raises the possibility to replicate not fully known process data. That means, even if not all necessary model input are known, the missing data can be adjusted by plausible values according to target figures from the process itself or by comparing with similar datasets.

Extrapolation of Results

In order to ascertains whether a system tends to more or less emissions when changing the respective system conditions and whether it tends to more or less emissions than another, the developed NO_x indicator $(\boldsymbol{NI})$ needs to have a strong statistical relevance compared with the previous mentioned field data. One major problem occurred was the fact that the determination and / or subsequent calculation of flue gas concentrations as well as the definition and measurement of the actual operation conditions are always subject to some uncertainty. These errors are mostly systematic and other random but in any case unavoidable in full–scale applications. Systematic errors can occur with the emission monitoring equipment, stratification of the different volume flows inside the ducts, etc. In addition are also random errors which belong to the observations omnipresent. Nevertheless have all available data sets been considered as representative data samples because they are based on direct measurements on an hourly or daily average.

Regression Analysis

In order to justify the linear relationship between the NO_x indicator $(\boldsymbol{NI})$ from equation (**VI–1**) and the NO_x emission level measured $\left(\boldsymbol{NO_{x_{Ref}}}\right)$ a linear regression analysis was carried out on the basis of comparable conditions, i.e. $\boldsymbol{NO_{x_{Ref}}}$ as interpolated value according to an oxygen concentration of 6 % at dry flue gas. The linear regression method had been chosen because the independent variable $\boldsymbol{NI}$ based on measuring points and is thus not stochastic. The aim was not only to evaluate the model prediction performance $(\boldsymbol{R^2})$ further it was also the determination of the most suitable regression coefficients. Therefore equation (**VI–1**) has been extended by linear regression coefficients and used as regression function.

$$\boldsymbol{NO_{x_{Pred}}} = \boldsymbol{\beta_0} + (\boldsymbol{NI})\boldsymbol{\beta_1} \qquad \text{(VII–1)}$$

Where $\boldsymbol{\beta_0}$ and $\boldsymbol{\beta_1}$ are the regression parameters which represents the y–intercept and the slope of the relationship, respectively. Due to the direct dependency of $\boldsymbol{NI}$ from the burner mixing effectiveness (see equation (**VI–13**)) it was necessary to evaluate several coefficient combinations in order to find the respective optimal combination under which the model guaranteed most suitable prediction performance. For that background $\boldsymbol{NO_{x_{Prim}}}$ of the reference utilities had been recalculated for each run according to most precise prediction results compared with the measured $\boldsymbol{NO_{x_{Ref}}}$ before the statistical significance was evaluated. This recalculation had been done via the Microsoft Excel® Solver while setting the estimated value as constant when no change of the respective burner belt volume $(\boldsymbol{BBV})$ according to equation (**VI–23**) were reported. The used Solver settings are given in Table 10.

Table 10. Solver settings for estimating of NO_{xPrim}

Microsoft Excel® Solver settings		**Goal**
Solution method	GRG–non linear	
Objective function	Total amount of residuals for the respective burner belt volume $(\boldsymbol{BBV})$	Min
Variable	$\boldsymbol{NO_{xPrim}}$	
Constraint 1	Mean of the residuals	Zero
Constraint 2	$\boldsymbol{NO_{xPrim}}$	≥ 150
All other settings	Standard	

The sensitivity analysis had been done for $\mathbf{0} \leq \boldsymbol{\beta_0} \leq \mathbf{200}$ and $\mathbf{10} \leq \boldsymbol{\beta_1} \leq \mathbf{30}$ with a sequence of steps for $\boldsymbol{\beta_0} = \mathbf{25}$ and $\boldsymbol{\beta_1} = \mathbf{2}$ respectively. Figure 20 shows the resulting coefficient of determination $(\boldsymbol{R^2})$ of every resulting coefficient combination.

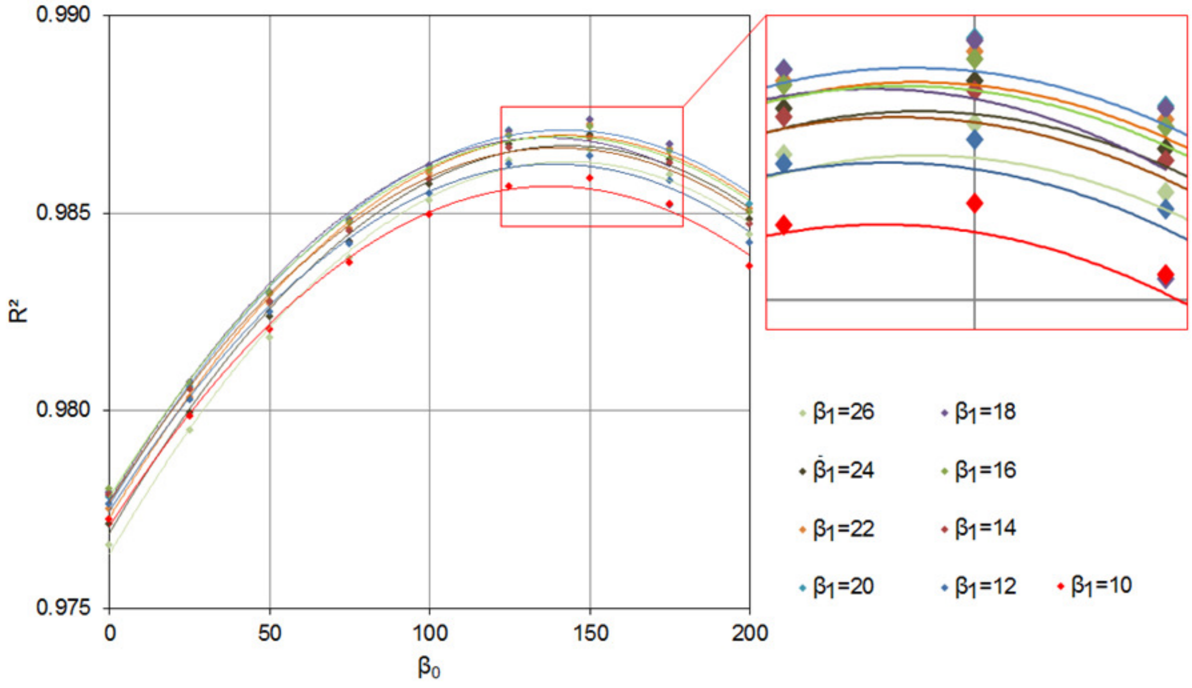

Figure 20. Sensitivity plot of investigated regression coefficients

Figure 20 shows that $\boldsymbol{R^2}$ increased with increasing the y–interception and will start to decrease for $\boldsymbol{\beta_0} > \mathbf{150}$. The dependence of the slope of the relationship in this case shows also an increasing $\boldsymbol{R^2}$ and decrease for $\boldsymbol{\beta_1} > \mathbf{20}$. In order to find the highest prediction performance, the sequence of steps for the regression coefficients had been reduced to $\boldsymbol{\beta_0} = \mathbf{1}$ and $\boldsymbol{\beta_1} = \mathbf{1}$ for the combinations between $\mathbf{135} \leq \boldsymbol{\beta_0} \leq \mathbf{155}$ and $\mathbf{16} \leq \boldsymbol{\beta_1} \leq \mathbf{22}$. Figure 21 shows the resulting $\boldsymbol{R^2}$ of every resulting coefficient combination.

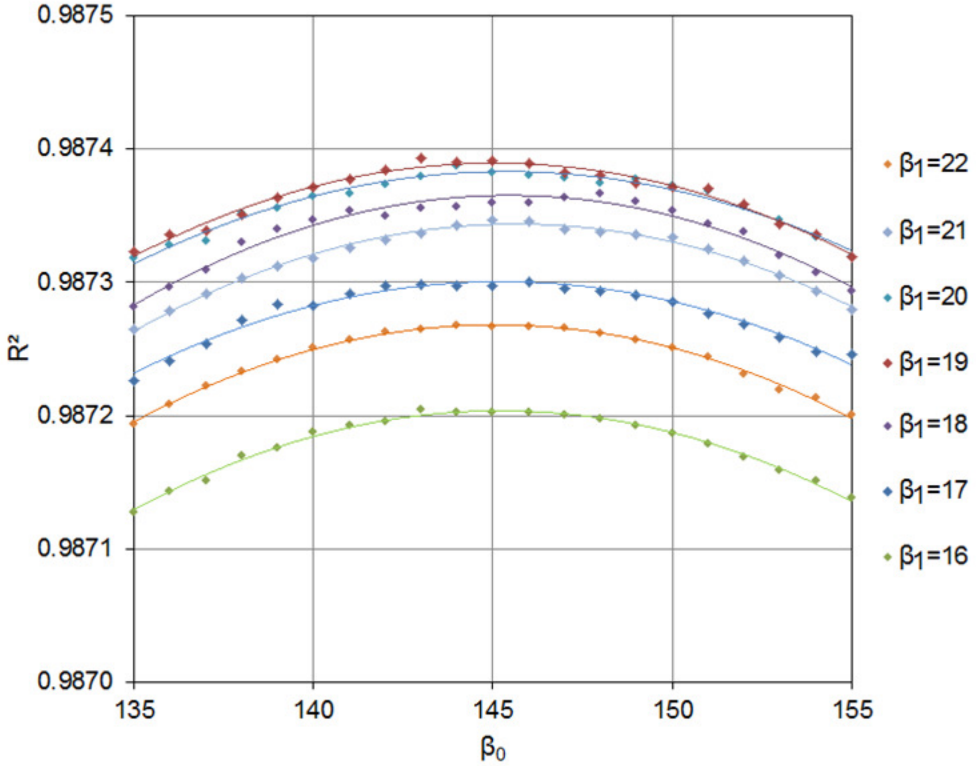

Figure 21. Sensitivity plot of restricted regression coefficients

Due to the fact that the difference between the shown $\boldsymbol{R^2}$ based only to the third digit after the decimal point, the coefficient were rounded to integer values. The main results for the observed highest $\boldsymbol{R^2}$ occurs when setting $\boldsymbol{\beta_0} = \mathbf{143}$ and $\boldsymbol{\beta_1} = \mathbf{19}$, respectively. The statistical results are listed in Table 11.

Table 11. Regression analysis of NI vs. NO_{xRef}

Regression statistics	
Coefficient Intercept ($\boldsymbol{\beta_0}$)	143
Coefficient X Variable ($\boldsymbol{\beta_1}$)	19
Multiple R	0.9938
R²	0.9876
Standard Error	28.0382
Observations	142

The input data set for the linear regression analysis are given in Appendix 3. The resulting scatter plot of the linear relationship between $\boldsymbol{NI}$ and $\boldsymbol{NO_{x_{Ref}}}$ are shown in Figure 22.

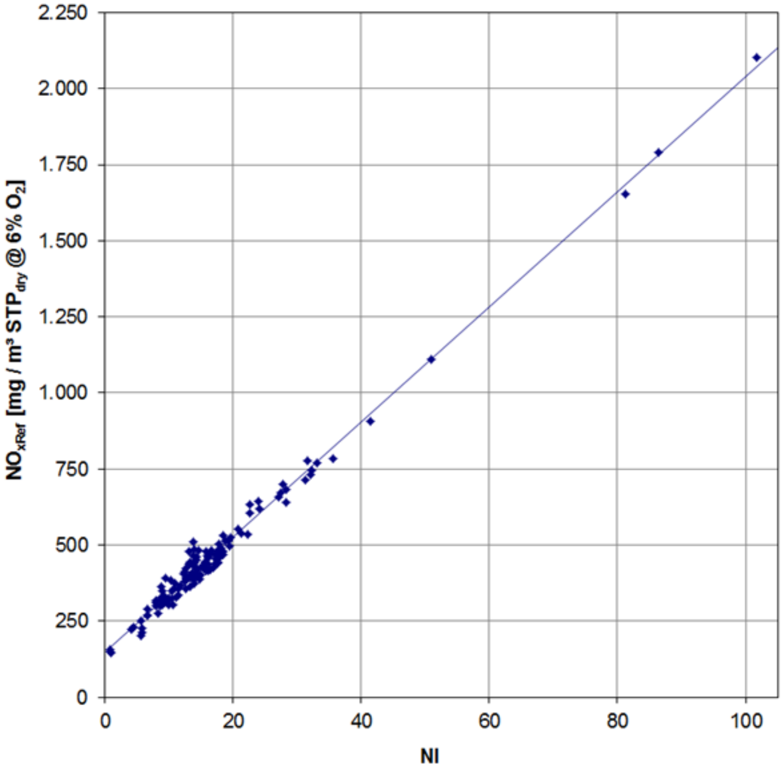

Figure 22. Scatter plot of NO_{xRef} vs. NI

In general the results of the prediction approach are in fairly good agreement with the measured reference data which highlights the model performance. The standard error estimated indicated that the difference between the measured and the predicted values turns around 28 mg / m³ STP$_{dry}$ referred to 6 % oxygen content. Therefore it can be concluded that the model predictions are fairly usable for any kind of application since the model is valid for every kind of the investigated power plants, coal qualities, and different operation conditions. Much work has already been published on identifying any reasonable statistical relationship between the pollutants emitted and various system related state variables with more or less success, depending on the scope of consideration. The major problem to be solved is that each possible single influence factor and its relationship towards NO$_x$ emissions are masked by the impact of others. Each single influence factors can consists of several sub–factors of more or less importance within a specific furnace environment. Figure 23 underline that when the scope of considering is not large enough no significant correlation would be observable.

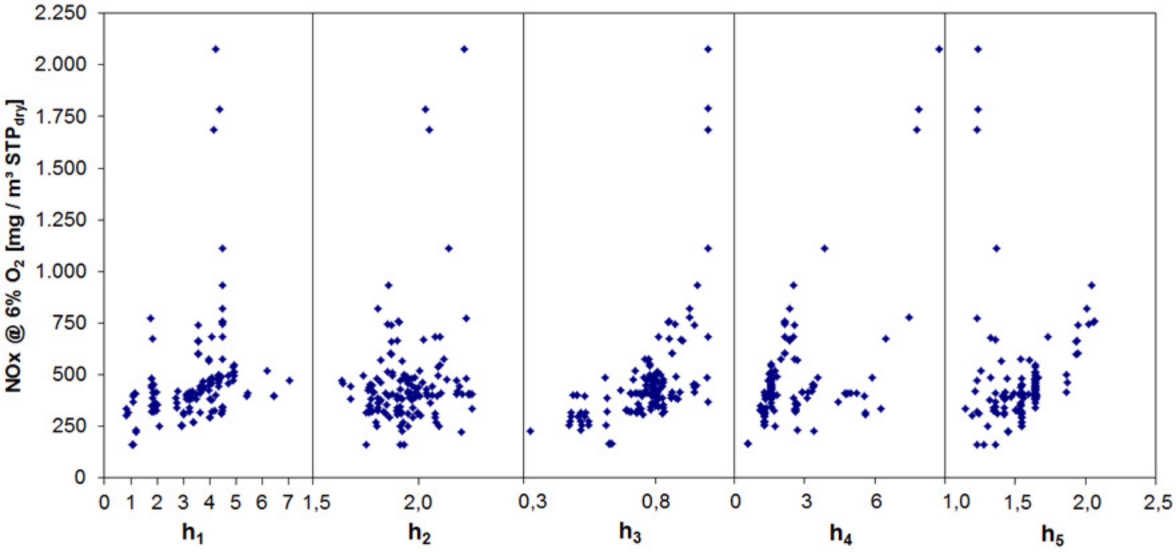

Figure 23. Matrix plot of NO_{xRef} vs. h_i

Figure 23 shows that it could be postulated that no certain statistical relationship or trend is observable when concentrating on one helping factor $(\boldsymbol{h_i})$ alone. But, if considering the product of all factors according to equation (**VII–2**) it leads to an impressively proof of a certain relationship as Table 11 and Figure 22 suggest.

Residual Analysis

In the previous section the statistical relevance of the NO$_x$ indicator $(\boldsymbol{NI})$ was proven and the most suitable regression coefficients been calculated. In order to determine how the model results fit to the data, the assumptions made on the differences between the fitted and measured NO$_x$ values had been analyzed in the following. For thus, the NO$_x$ levels have been calculated based on equation (**VII–1**) with regression coefficients $(\boldsymbol{\beta_0 = 143}, \boldsymbol{\beta_1 = 19})$ and compared with the respective measured values.

$$\boldsymbol{NO_{x_{Pred}} = 143 + (NI)19} \qquad \text{(VII–2)}$$

Where $\boldsymbol{NO_{x_{Pred}}}$ is the predicted NO$_x$ emission level in mg / m³ STP$_{dry}$ at 6 % O$_2$. Due to the fact that the model fairly predicts the target values the error term could be assumed to have a zero mean with a constant variance $(\boldsymbol{\sigma^2})$ which means that an interval estimation of the mean response can constructed in order to test the statistical hypothesis whether the means of the $\boldsymbol{NO_{x_{Pred}}}$ and $\boldsymbol{NO_{x_{Ref}}}$ are nearly equal. For the background that also the target values of $\boldsymbol{NO_{x_{Ref}}}$ should be assumed to be independent through the strong difference in the data sets could the two groups being compared via a paired t–test. Because both sample sizes are equal and the two residual distributions should have the same variance. Table 12 shows the results of the statistical test.

Table 12. Paired t–test of NO_{xPred} and NO_{xRef}

Hypothesis testing	
Confidence Interval	95 %
Margin of error	4.5815
Lower bound	– 6.201
Upper bound	2.962

The result indicated that for the 95 % confidence interval the difference in the mean of $\boldsymbol{NO_{x_{Ref}}}$ and the mean of $\boldsymbol{NO_{x_{Prim}}}$ is within 10 mg / m³ STP$_{\text{dry}}$ at 6 % O_2. Therefore it can be concluded that also the distribution and the values of the model results are in very good agreement with the reference values.

The residuals $(\boldsymbol{e})$ are the difference between the observed value $\left(\boldsymbol{NO_{x_{Ref}}}\right)$ and the corresponding fitted value $\left(\boldsymbol{NO_{x_{Pred}}}\right)$.

$$\boldsymbol{e_i = NO_{x_{Pred_i}} - NO_{x_{Ref_i}}}, \qquad \boldsymbol{i = 1, 2, \ldots, 142} \tag{VII–3}$$

The resulting differences for the observation value $(\boldsymbol{i})$, residuals, are plotted in Figure 24 against the measured NO_x level $\left(\boldsymbol{NO_{x_{Ref}}}\right)$.

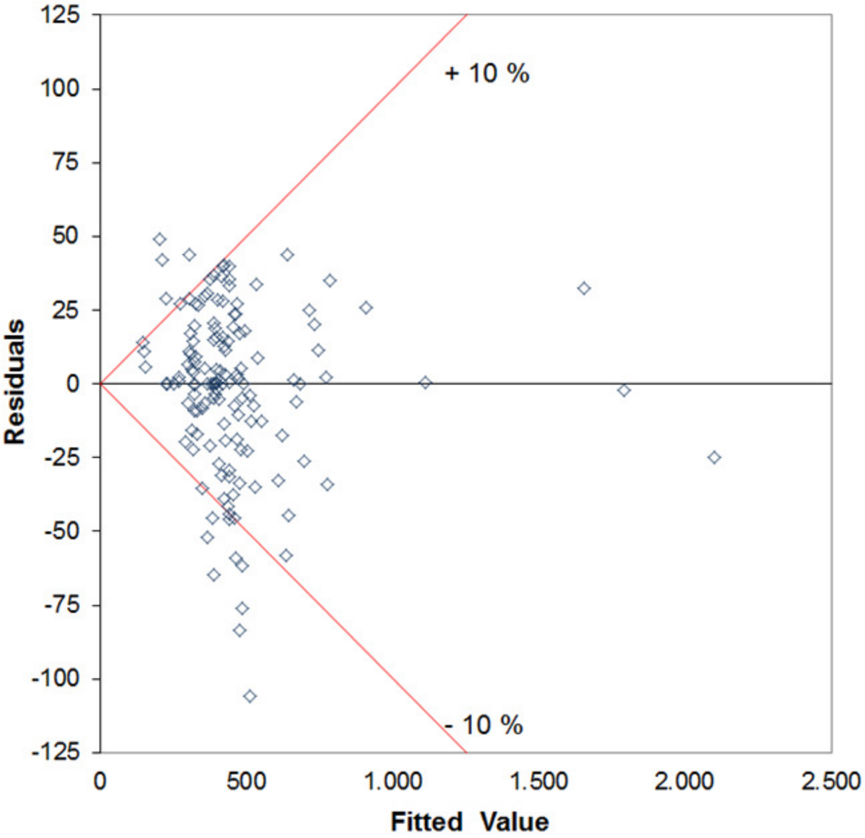

Figure 24. Residual plot of NO_{xPred} against NO_{xRef}

Figure 24 shows that the most deviations between the predicted and the reference NOx value are smaller than 10 % of the $\boldsymbol{NO_{x_{Ref}}}$ value. The model results contain only 14 out of 142 outlines. From Figure 24 can be concluded that since no systematic pattern is observable, it can be assumed that the residuals are of homoscedasticity and thus the assumption of variance homogeneity is met, which implies the validity of the linear regression results.

Comparison with the Literature

The reasoning behind the data support and the NOx prediction approach developed in this thesis are discussed in in length in the previous sections. Theoretically applications are shown in this section for practical demonstrations compared to the

Literature. In contrast to full–scale or laboratory–scale facility experiments have the theoretical research work clear advantages. It can be postulated that no errors in measurements and thus no accuracy problems would occur; no dynamic process fluctuations are possible; no need of careful process control and observation; no scaling problems; and no need for process assumptions due to missing information which certainly causes discrepancies.

The example chosen is focused on possible modifications to one of the known existing boilers rather than designing a new boiler. Because the focus is more on providing suitable engineering tools which helps plant owners and operators to optimize their existing system with respect to efficiency and reliability under environmental awareness.

Reference Plant

The application of the developed NO_x prediction model has been accomplished and investigated on the basis on the spreadsheet model described in chapter V 'Model Basis'. The reference plant used as basis had also been used and described in the research work of Hwang [202]. The author accomplished straightforward full–scale experiments with sub–bituminous coal blends at the second unit of Fayette power plant. The Fayette Power Project (FPP) is a three–unit coal–fired electricity generation facility co–owned by the Lower Colorado River Authority (LCRA) and Austin Energy (AE) located near La Grange, Texas (USA) which had been commissioned in the early 1980s. LCRA is a Texas state conservation and reclamation district that provides wholesale electricity and other services to cities and rural cooperatives in the Central Texas area. AE is a municipal electric utility owned by the City of Austin, Texas.

The main reasons for choosing this reference plant were the fact that the boiler behavior could be evaluated by the help of several accomplished tests, where each test based on different operation conditions. All variations had influence on all three identified main groups (system design, operational settings, and coal properties) and gives therefore an appreciate basis to recalculate the respective primary NO_x level $(\boldsymbol{NO_{x_{Prim}}})$ and to evaluate the goodness of fit of the complete developed model.

Another reason for choosing this reference plant was the fact that the special design of the furnace of FPP boiler 2 and its burning system would made it possible to fire a large variety of coals which would make the investigation of changing coal properties on the NO_x behavior a bit more realistic and also practicable. Especially the special design of the combustion system allows rapid manipulation of programming changes because the unit DCS (Distributed Control System) system is nearly fully flexible to adjust to nearly every possible operational specification and therefore would also studies of various operational settings on the NO_x behavior be more realistic and practicable.

FPP boiler 2 is a tangentially fired two–pass 606 MWe unit equipped with a low–NO_x technique developed by the Combustion Engineering Company (USA)[19]. It is a supercritical balanced draft boiler which rated for 1,905 t / h steam flow at a superheat outlet steam pressure and temperature of 180 bar (absolute) and 540 °C. Originally design for East Decker sub–bituminous coal, with provisions for future Texas lignite firing. Currently the unit is fired by coal from several mines in the Southern Powder River Basin (PRB) area. A side view of the boiler arrangement is shown in Figure 25.

---

[19] Since 2000 purchased by Alstom.

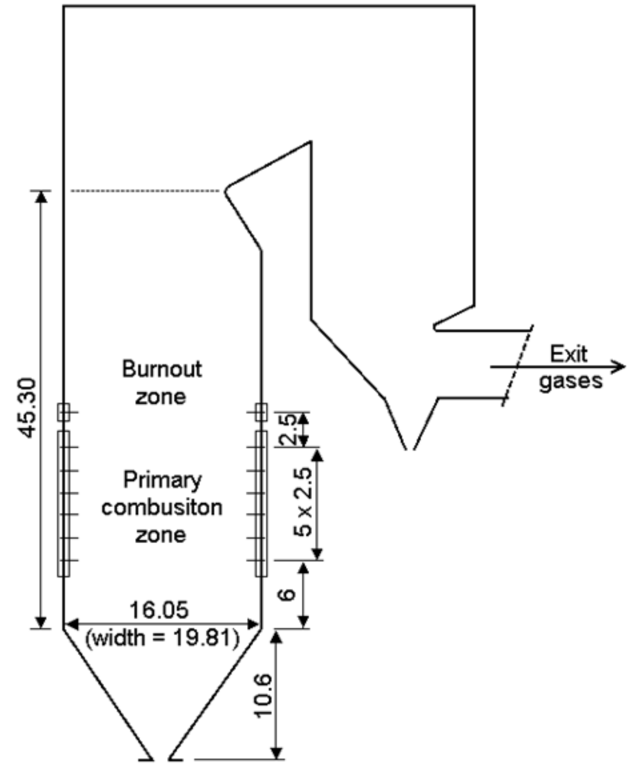

Figure 25. Dimensions of Fayette No. 2 in meters [202]

Five burner levels are required for full–load operation although the combustion system consists of six burner elevations. Originally it was even designed for seven. The unused additional bottom elevation has also been included in the original design for the event that the unit switched to a lower ranked coal in the future. The furnace had been designed as air–staged combustion with a possible shift of approximately 30 % of the combustion air through two close coupled overfire air ports. Fuel and air are introduced into the furnace through four windbox assemblies located in the corners. Each windbox contains air and coal nozzles. The air stream is split into two different parts, primary and secondary air. The secondary combustion air is admitted to the auxiliary air compartments around the fuel nozzle through a set of dampers. Each set of dampers is operated by a damper drive cylinder located at the side of the windbox. The fuel and air streams are directed toward a firing cycle in the center of the furnace in order to create a rotating vertex for most effective mixing. The primary air dries the coal as it is being pulverized and transports the mixture through the coal dust piping to the coal nozzles of the burners. It must be made sure that the outlet velocity of the primary air and coal mixture exceeds the speed of flame propagation. Behind the burner tip the stream rapidly spreads out with a corresponding decrease in velocity, especially as mixing occurs with the secondary air. More detail descriptions can be found in the work of Hwang [202].

Prediction Precision

Examining the data sets available from FPP–2 (Appendix 4) and comparing the respective $\boldsymbol{NO_{x_{Pred}}}$ with $\boldsymbol{NO_{x_{Ref}}}$ it can be concluded that the developed model fairly predict the reference values. The statistical results of the model precision concerning FPP–2 are listed in Table 13.

Table 13. Regression analysis of NI vs. NO_{xRef} for FPP–2

Regression Statistics	
Coefficient Intercept ($\boldsymbol{\beta_0}$)	143
Coefficient X Variable ($\boldsymbol{\beta_1}$)	19
Multiple R	0.9585
R Square	0.9187
Adjusted R Square	0.9142
Standard Error	18,4664
Observations	20

The plant data used for the model validation are introduced in Appendix 4. Table 13 shows the results of the correlation analysis to determine the model prediction adequateness in order to estimate the applicability of the developed approach to the real plant behavior. The regression results indicated that the demonstrated model precision seems to be a very good fit to the data based on the 20 observations available. Therefore it can be concluded that the adjusted model represents a suitable basis for further studies.

Theoretical Application

There are numerous technologies available to reduce the NO_x emissions but all these methods range significantly in cost, effectiveness, complexity and extent of modifications required to achieve NO_x reduction. When combustion modifications are planned, it is important to avoid adverse impacts on boiler operation as well as of the formation of other pollutants such as CO_2 or CO while dealing with the interactions between combustion related process conditions. Scientific and industrial research projects indicate evidence that these changeable process factors belongs to three identified main groups (coal properties, operational settings, and system design) which have considerable influence on NO_x emissions from pulverized coal–fired utilities. Very seldom is only one method or principle for NO_x reduction used alone. The choice depends upon the type of combustion system, type of boiler, type of fuel and / or other energy conversion devices used. Available technologies will be narrowed by consideration of turndown ratio, stability of combustion, availability or access to burners, air supply controls, fuel impurities, and cost among other factors which needs to be considered for every possible practical application. A myriad of constraints must be balanced to allow owners and operators of coal–fired power plants a profitability operation of their generating units.

For this background, the following exemplary application of the developed prediction approach shall be focused on the investigation of the interaction and individual influences of different single influence factors on the total NO_x emissions generated by the above described reference boiler FPP–2. The outcomes will additionally be compared to conclusions made in the literature. For thus several sensitivity analyses have been carried out by varying one parameter of the prediction model while holding the other parameters constant. The model parameters examined were given in Table 14.

Table 14. Investigation parameters

Investigation parameter	**Helping factor** $(\boldsymbol{h_i})$
Coal properties and coal blending	
Fuel ratio, based on the effective volatile content $(\boldsymbol{VM_{eff}})$	$\boldsymbol{h_1}$
Nitrogen content	$\boldsymbol{h_1}$
Volatile content	$\boldsymbol{h_1}$
Boiler operation	
Total excess air	$\boldsymbol{h}_2$
Air staging mode (overfire air)	$\boldsymbol{h}_3$
Burner operation (burner zone stoichiometry, mill pattern)	$\boldsymbol{h}_4$
Boiler load (burner belt and furnace cross section)	$\boldsymbol{h}_5$
Preheat air temperature	$\boldsymbol{h}_5$
Boiler design	
Design of overfire air system	$\boldsymbol{h}_3$
Burner–out–of–service (BOOS)	$\boldsymbol{h}_3$
Burner design (air staging effectiveness)	$\boldsymbol{BI}$[20]

---

[20] Burner index according to equation (**VI–14**)

Thereby that the theoretical model was verified by several practical generated experimental data it can be assumed that it behaves likely the real system would do and thus, it can be further assumed, that any model outcomes could be accepted as valid for the real system, at least within the calculated statistical relevance (Table 13).

Coal Properties and Blending

A thorough understanding of the coal, its respective burning characteristic, transportation inside and outside the boiler plant, its ash generation and disposal, the environmental aspects, and so on, is necessary for design, selection, operation, and maintenance of a utility boiler. All these can be attributed to the fuel properties. Therefore is perhaps no other parameter more important. A pulverized coal–fired boiler is being designed based mainly on the characteristics of the provided coal. The so called design coal or reference coal depend often on different available world–traded coals which are being mixed to specified coal blends. Whereas 20 years ago the most pulverized fuel–fired power plants have been fed by single coals which were available in the closer area around the power plant [205]. Nowadays the coal blends could have nearly every possible varying characteristic between a specified range. Consequently, the quality of the delivered coals as heating value, chemical composition, ash content and ash composition may vary significantly and can lead to higher furnace fouling rates with increasing deposits, shorten flame ignition points and promote flame impingement on walls, alter superheat and reheat distribution, promote boiler tube failures rates and other adverse factors. However, the boiler operation and performance suffer from variations in the coal properties in unscheduled outages, lower efficiency, maintenance effort, corrosion problems, increasing emission levels and consequently as an increase in generation costs, is coal blending today an attractive easy way to influence the plant performance and emissions. With respect to NO_x emissions means that, that the direct allocation of different influences is complicated by the fact that changes in the coal quality will change the combustion behavior inside the furnace.

In this section, the theoretical application of the NO_x prediction approach is conducted under consideration of varying coal properties. That means the definition of a coal parameter spectrum instead of single coal properties. The reference unit No. 2 of Fayette power station is reported to be burning coal with a heating value between 8,000 and 9,000 Btu / lb and a sulfur content of up to 1 % [206]. On the basis of the USGS Coal Quality Database [18], over 200 different coal compositions could be identified when assuming that the unit is able to burn any available coal within the above specified range limits. These types of coal are all classified as US sub–bituminous coals. The whole range of the proximate and ultimate analysis is shown in Table 15.

Table 15. Composition of used coals

Coal	**Unit**	**Range**	
	as received	max	min
Lower Heating Value (LHV)	Btu / lb	8,000	9,000
	MJ / kg	18.608	20.934
Proximate Analysis			
Volatile Matter	wt.–%	43.20	26.30
Fixed Carbon	wt.–%	43.90	27.80
Moisture	wt.–%	31.77	8.00
Ash Content	wt.–%	26.60	2.50

Coal	**Unit**	**Range**	
	as received	max	min
Ultimate Analysis			
Carbon	wt.–%	65.60	44.80
Hydrogen	wt.–%	7.00	4.60
Oxygen	wt.–%	18.50	6.40
Nitrogen	wt.–%	1.51	0.50
Sulfur	wt.–%	0.09	1.00

Table 15 shows that the selection process emphasized an interesting wide range. The volatile matter content ranged from 26 % to 43 wt.–%. The ranges of moisture, ash content and nitrogen content were from 8 to 32 wt.–%, 2.5 to 26 wt.–%, and 0.5 to 1.5 wt.–% respectively. As stated above are the most important issues concerning the applicability of a coal defined by the spectrum of lower heating value, moisture content, and ash fraction. Therefore builds the extreme values of these coal characteristics also the basis for the procurement strategy of a plant.

Figure 26 visualized the resulting permissible coal range described in Table 15.

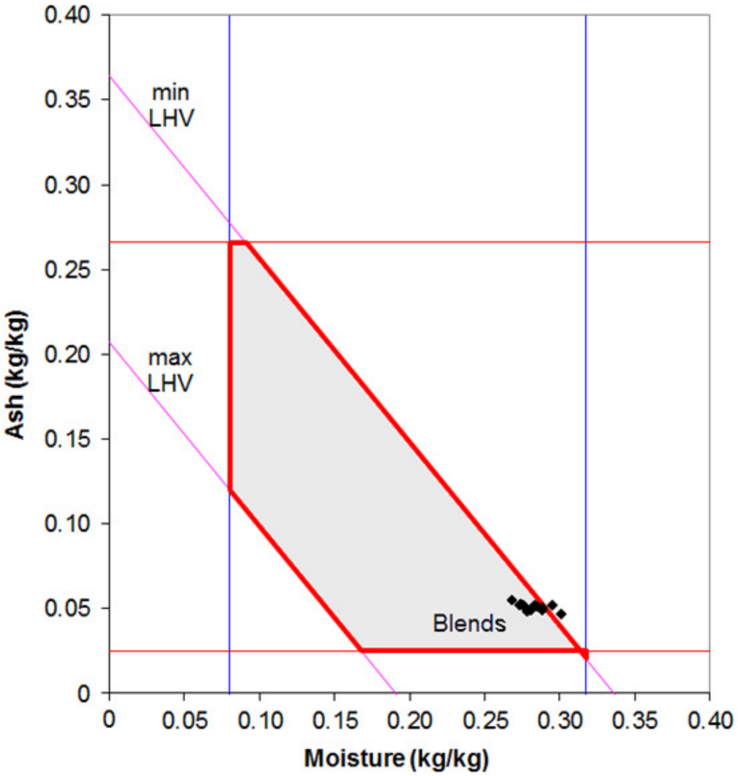

Figure 26. Schema of the specified coal range for FPP–2

The in Figure 26 inserted coal blends (black data points) are the coal properties measured during the research work of Hwang [202]. It can be seen that two blends are slightly out of the box. This is not unusual when buying different coals which are further being mixed to coal blends at the power stations coal storage. This belongs to changes in the heating value due to fluctuations in the actual ash and moisture content.

As already mentioned was the NO_x prediction approach conducted under consideration of varying coal properties under identical design surroundings and unchanged operational conditions. That means one reference scenario had been randomly selected from the research work of Hwang [202] which served as basis for all calculations within this section. The only variable according to equation (**VI–1**) was the coal helping factor. The respective plant operational data can be found in Appendix 4 or in the work of Hwang [202] were it is termed as 'Test 10B'.

Fuel Ratio

Considering the calculated NO_x emissions by using the new approach on the basis of the identified coals from the USGS Coal Quality Database [18] and plotting the results in a diagram based on the new effective fuel ratio[21] $(\boldsymbol{FR_{Eff}})$ as function of the coal containing nitrogen content $(\boldsymbol{N_{wf}})$ in wt.–% on a water free basis, than an interesting relationship could be recognized (see Figure 27).

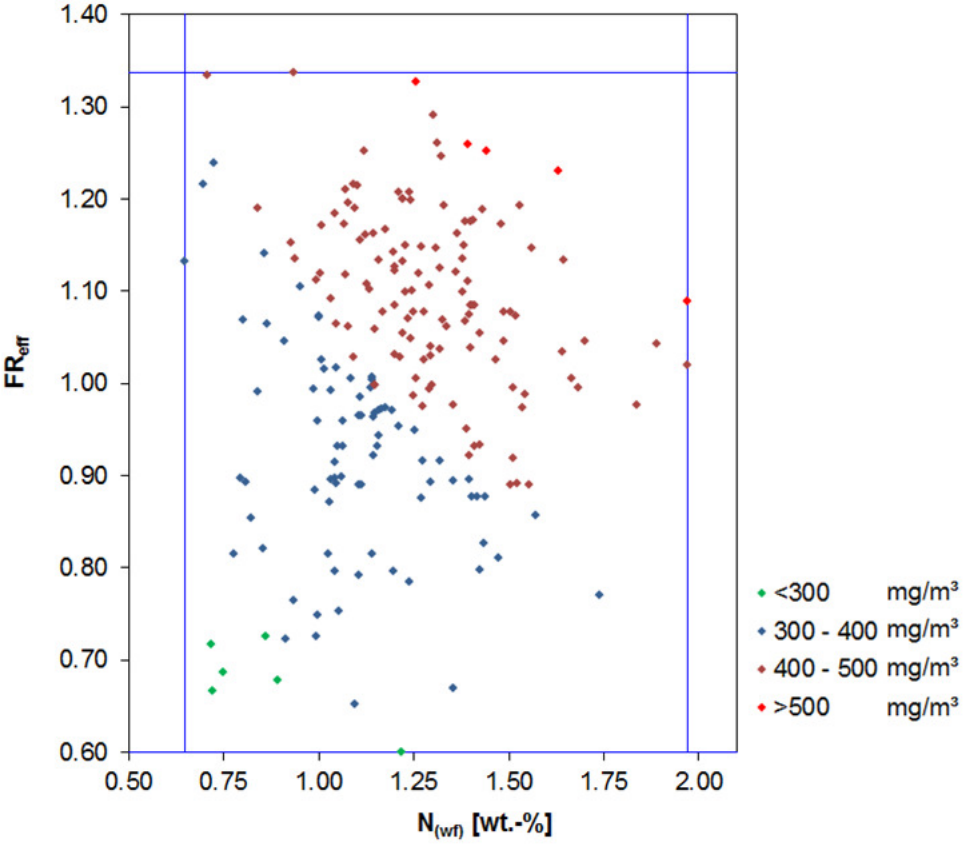

Figure 27. NO_x expectation for FPP–2 depending on coal quality

---

[21] According to equation (**VI–6**).

$\boldsymbol{N_{wf}}$ is the coal containing nitrogen in wt.–% on a water free basis, and $\boldsymbol{FR_{Eff}}$ is according to equation (**VI–6**) the new effective fuel ratio based on the corrected volatile content ($\boldsymbol{VM_{Eff}}$, equation **(VI–3)**). The blue lines define the specified permissible range properties based on Table 15 and thus describes similar to Figure 26 all possible coal qualities. All 207 different coal compositions have been entered and colored according to their predicted NO_x values (STP_{dry} at 6 % O_2). Figure 27 indicates clear boarders between the colored data points. It is obviously that NO_x emissions increase when $\boldsymbol{N_{wf}}$ and $\boldsymbol{FR_{Eff}}$ of the investigated coals increase likewise which is in principle also in line with the findings of Nakazawa et al. [94], in which he considered the original fuel ratio.

Summarized it can be stated that by the use of Figure 27 it is possible to draw conclusions on the NO_x emissions to be expected by burning a different coals under the conditions served as basis for Figure 27 (Hwangs [202] 'Test 10B'). That means in short, coals can be categorized by their constituents to different emission rates which could significant improve the procurement strategy of the power plant according to performance at lowest cost.

Furthermore it can be concluded that according to Figure 27 the general statement of some other researcher cannot confirmed. NO_x emissions not forcibly decrease when the volatile matter content of a coal increase likewise, which is also confirmed by the fact that until now no statistical evidence for a single and direct relationship could be provided. Whereas the dependency of nitrogen content and fuel ratio are impressively shown in Figure 27. NO_x emissions increase when nitrogen content and / or fuel ratio (based on the effective volatile matter content according to equation (**VI–6**)) increase.

Nitrogen Content

Although, the chemically bound organic nitrogen is the main source for the total exhaust NO_x emissions from pulverized coal combustion [69, 70] represents the measureable nitrogen content bound in the coal just a very rough and inaccurate indication on the NO_x level to be expected. From a practical point of view it is not suitable as a good predictor [92, 207]. Figure 28 illustrated the dependency between calculated NO_x emissions and the nitrogen content $(\boldsymbol{N_{wf}})$ on the basis of the selected coals based on the quality specification in Table 15.

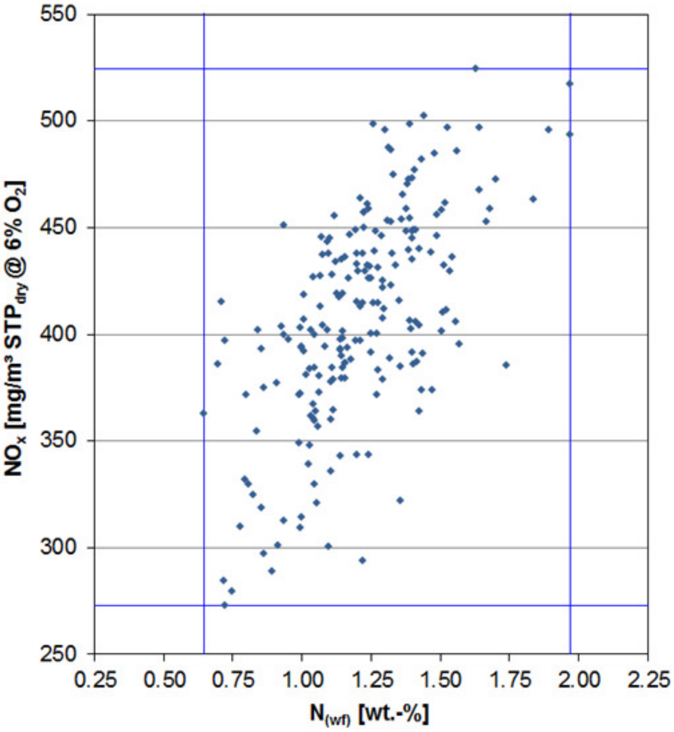

Figure 28. $\boldsymbol{NO_{xPred}}$ **vs.** $\boldsymbol{N_{(wf)}}$ **for FPP–2 depending on selected coal qualities**

Although, a certain significance can be observe it needs to be clear that the resulting relationship is mainly driven through the linear dependency of the coal nitrogen content $(\boldsymbol{N_{wf}})$ in equation (**VI–8**) and the associated direct dependency to the parent NO_x indicator $(\boldsymbol{NI})$ given in equation (**VI–1**). Nevertheless underlines this finding that obviously $\boldsymbol{N_{wf}}$ as single indicator will not be sufficient to make conclusions of the emission behavior due to the broad scattering of the data points.

Effective Volatile Matter Content

Focused on the volatile matter content it can be stated that also the most prevailing opinion regarding the fact, that higher volatile coals tends generally to lower NO_x emissions [95, 103, 208] can be confirmed. Figure 29 shows the relationship between the ASTM proximate analysis volatile content $(\boldsymbol{VM})$, the transformed effective volatile content $(\boldsymbol{VM_{Eff}})$ and predicted NO_x level $(\boldsymbol{NO_{x_{Pred}}})$ based on Hwangs [202] 'Test 10B'.

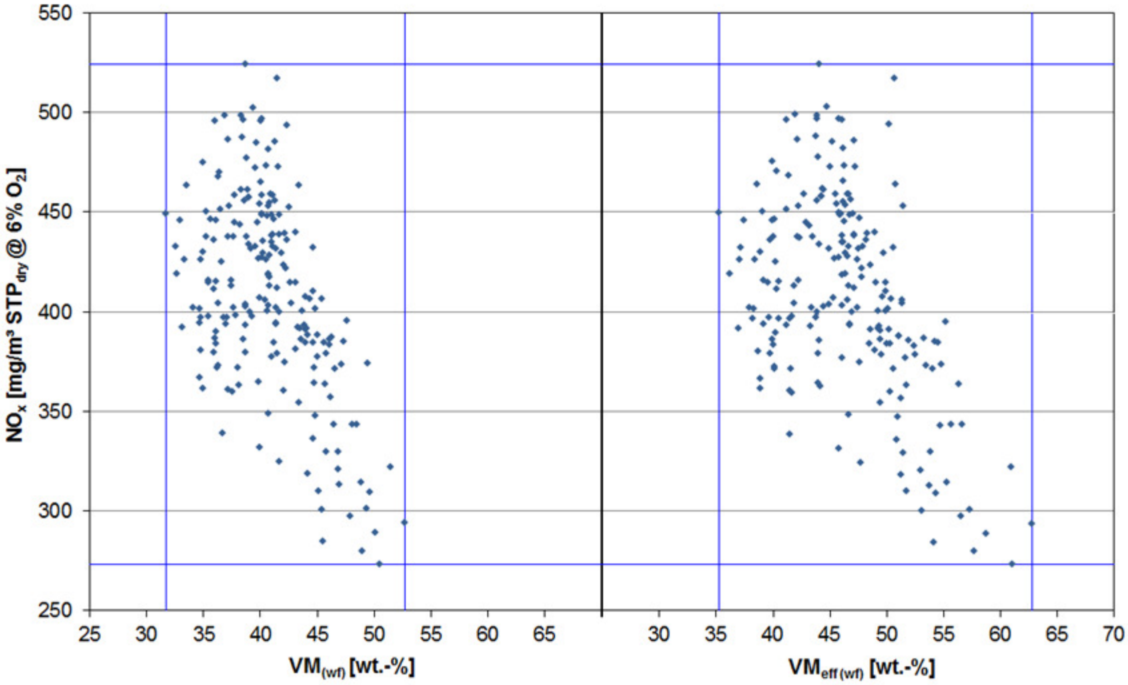

Figure 29. $\boldsymbol{NO_{xPred}}$ **vs.** $\boldsymbol{VM_{(wf)}}$ **and** $\boldsymbol{VM_{eff\,(wf)}}$ **for FPP–2 application**

On the left side are the predicted NO_x values applied to proximate $\boldsymbol{VM}$ and the right diagram shows the same NO_x values as calculated on the basis of $\boldsymbol{VM_{Eff}}$ on a water free basis. The blue vertical lines describes the range between the lowest and the highest VM value and the blue horizontal lines describes the range between the lowest and highest predicted NO_x value.

As Figure 29 indicated there is no certain relationship between NO_x and volatile matter content observable. Although, the proximate volatile matter content seems to be more statistic relevant, better prediction precision can be achieved by using the effective VM. Anyway, it should be remarked that the general statement must be questioned because although, the general relationship is statistically relevant indicate the correlation between both axis in both diagrams that the relationship does not imply that $\boldsymbol{VM}$ or $\boldsymbol{VM_{Eff}}$ causes $\boldsymbol{NO_{x_{Pred}}}$. Which may be due to the fact that also small changes in the coal properties leads to a difference in the burning characteristics of the fuel which results e.g. in different combustion temperatures and residence time in the fuel–rich zone. What might be the explanation why until now no certain dependency could be found.

Jones et al. [209] investigated the effects of coal quality on NO and unburnt carbon formation in an integrated full, pilot and laboratory–scale study. The observed coals from the US, UK, Colombia, South Africa, and Australia ranged in their nitrogen content from 1.62 – 2.01 wt.–% (wf) and in volatile matter content from 29.0 – 40.1 wt.–%. No correlation between nitrogen content or VM could be observed under staged conditions but using a function based on the coal volatile matter release at high heating rates (HTVM[22]) and on nitrogen content together, the authors had observed a correlation. This may due to the fact, that coals are not being composed of defined amounts of volatile matter and fixed carbon [210]. In fact, Saji [211] has shown that also substantial

---

[22] High temperature volatile matter content.

amounts of volatile matter may remain in the coal particles even after traveling through the furnace which had also been confirmed by the work of Badzioch and Hawksley [118]. Nevertheless, the amount and characteristic of volatile matter content depend on the combination of time and temperature acting the particles which are very complex to evaluate for a defined time.

By the theoretical dependency established in equation (**VI–8**) the finding of Jones et al. [209] can be surely confirmed because function (**VI–8**) based also on both variables, a developed transformation for the volatile matter content $(\boldsymbol{VM_{eff}})$ and on the nitrogen content on a water free basis. Figure 30 visualized the linear dependency of the coal influence $(\boldsymbol{h_1})$ under the described conditions for the selected coal properties (Table 15).

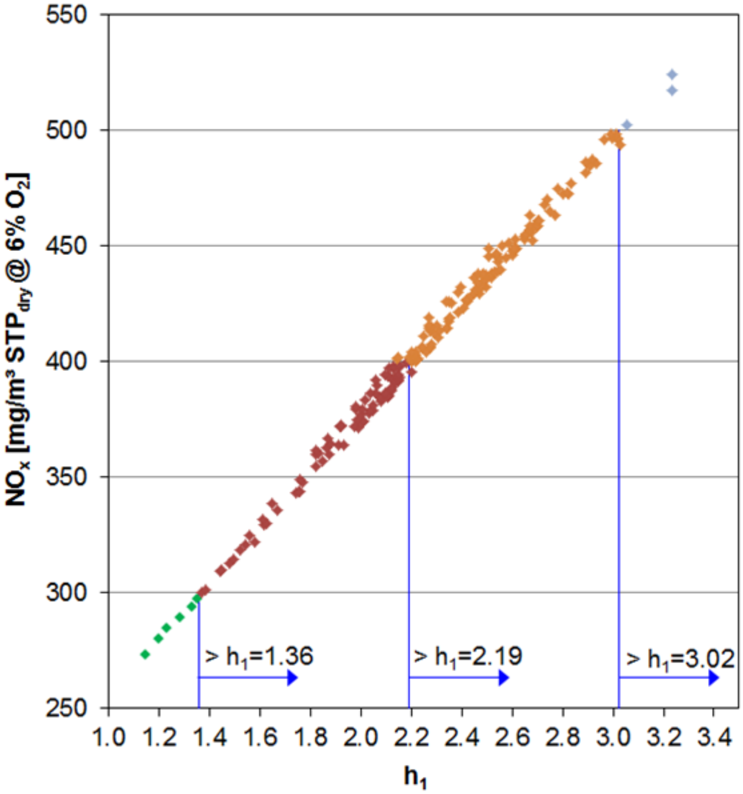

Figure 30. NO_{xPred} **vs.** h_1 **for various coals applying to FPP–2**

The single vertical lines describe different specified NO_x levels (y–axis). The scattering of the results around the theoretical regression line is due to the fact that besides the coal properties also the coal ignition behavior plays an important role. As described in chapter ‘Ignition Behavior’ is the optimum required amount of oxygen at the first combustion stage a function of the coals effective volatile content. That means, the more the actual burner air ratio is at its optimum, $\boldsymbol{n_{OBZ}}$ according to equation (**VI–12**), the less influence would occur due slightly changings in the coal effective volatile contents and the more the results shown in Figure 30 would describe a straight line. This circumstance is another good example for the superposition of different influence variables on the total NO_x emissions and the resulting difficulty of isolating individual influences. Table 16 summarized the results shown in Figure 30.

Table 16. Results of NO_{xPred} vs. h_1 for FPP–2

Predicted NO_x range	**h_1**
≤ 300 mg / m³ STP_{dry} at 6 % O_2	≤ 1.36
≤ 400 mg / m³ STP_{dry} at 6 % O_2	≤ 2.19
≤ 500 mg / m³ STP_{dry} at 6 % O_2	≤ 3.02
> 500 mg / m³ STP_{dry} at 6 % O_2	> 3.02

It should be mentioned, that Figure 30 just represents the effect of varying coal properties under absolute constant boundary conditions on NO_x emissions under the described methodology within this thesis. Nevertheless, if considering the overall model precision of the NO_x prediction approach and assuming that the individual helping factors are of similar significance, than it can be postulated that Figure 28 and Figure 30 can be used as helpful tool for the evaluation of coals which could be possibly burned at Fayette power station with respect to NO_x emissions.

Operational Settings

The boiler operating conditions specify the process boundary conditions and thus a major influence on NO_x formation. These conditions specify the overall combustion process and give the largest possible influence at lowest costs because changes at the system operational settings can be accomplished fast and easily via the control room desk. The optimal operational settings for a certain coal and a certain energy demand requested by the grid will be analyzed based on the presented model within this section. Correction curves for NO_x emissions will be created as possible system control optimization opportunities for minimal stack emissions and efficiency improvements. The mayor problem herewith, is to avoid the deterioration of the plant performance while changing these influence factors.

Excess Air Ratio

The generated energy distribution inside the furnace has besides on NO_x also a significant impact on the efficiency of the boiler and its connected turbine. From the perspective of overall cycle efficiency, the furnace exit gas temperature should be as low as practicable while superheat and reheat steam temperatures should be achieve the defined set–points. This can be realized e.g. by reducing the excess air level at the furnace end. Beside the increase of the boiler efficiency it will also improve the NO_x suppression. Unfortunately the reduction of the excess air level is limited due to significant operating impairments, as increase of the CO level and the loss of ignition[23], risk of reinforced slagging effects, and stronger furnace wall corrosion behavior and herewith decreasing of the boiler efficiency or also fouling and slagging can become problematically when the excess air level decreases [212, 213].

For this background is the primary focus while changing the air ratio with the boiler performance, i.e. the minimum excess air level with satisfactory performance. The definition of satisfactory depends herewith on the power plant owner. Considering the relatively low oxygen level during the test scenarios reported by Hwang [202] it can be assumed that the excess air level was already at its optimum. Therefore is the main objective not to define a new optimum situation rather than to investigate how the system would behave outside of the documented settings. The theoretical minimum practical level of excess air which can be achieved in FPP–2 depends on several factors but mainly on the type of coal fired. The burning behavior causes the onset of smoke or increasing CO emissions when the air ratio is reduced to levels far below the design value. Such boiler is usually being designed for achieving its required steam parameter between 80 % and 100 % boiler load at nearly constant oxygen level. The permissible excess air ratio range concerning that load range has been assumed to be $1.1 \leq n \leq 1.3$.Therefore had the investigation been concentrated on this specific boiler load– and air–range. Additionally the operational settings of ‘Test 6’ as documented by Hwang [202] have been chosen as reference basis; active burner elevations (B.E.) 1 to 5, firing coal blend No. 6. For the settings of the other air streams, e.g. overfire air (OFA) it has been assumed that the total excess air ratio of the system is controlled by the forced draft fan. That means, if the damper positions of the auxiliary air and OFA would not be changed the split between

---

[23] Unburnt carbon content in the ash (UBC).

these two air streams should be constant over the observed air range. Therefore is the OFA share of the total combustion air held constant over the investigated air range. The reported unburnt carbon content (UBC) in the ash is around 0.13 % which indicates a very efficient combustion. Figure 31 shows the results.

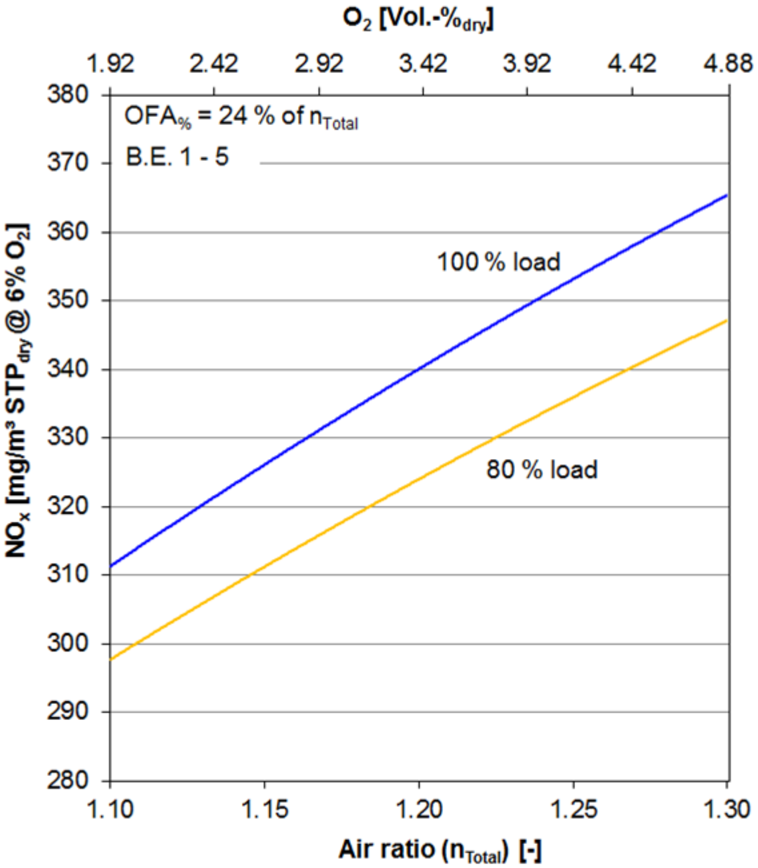

Figure 31. NO_{xPred} **vs. air ratio and** O_2 **level for FPP–2**

It can be seen that the full– and the 80 % part load operation apparently run parallel depending on the air ratio (n). However on closer inspection it is noticeable that the difference between the two load functions increase when the air ratio increase too. This could be due to the fact that the effect of the combustion air temperature on the total combustion temperature within the furnace is at lower energy densities higher than at higher energy densities. The effect of the seemingly parallel functions based on the fact that the only difference between both sensitivity analyses are the incoming energy which has obviously just a small effect on the NO_x formation because of the small effect on the average combustion temperature which is in line with the conclusion made by Okazaki et al. [141]. The authors stated that the conversion ratio from fuel–N to NO_x increases with the stoichiometric ratio and the temperature has only a small effect on this relation.

As basis condition for Figure 31 the ratio of primary air to overfire air had been held constant while changing the overall excess air ratio. This is because of the fact, that the boiler combustion system must be controlled in a way that an adequate proportioning of coal and air to all burners as well as to the air registers is guaranteed in order to avoid imperfect fuel–air mixing. Appleton and Heywood [213] stated that this could lead to inhomogeneities during the combustion which affects local stoichiometry and thus the fuel–nitrogen conversion. Therefore, it has been assumed that this definition provides most suitable predictions within an unchanged furnace air–staged environment. Furthermore, uniform distribution of coal and air to all burners has also been implied. Table 17 summarized the findings from Figure 31.

Table 17. Results of NO_{xPred} vs. excess oxygen for FPP–2

Air ratio	**O_2**	**Boiler load**	**NO_{xPred}**
–	Vol.–% dry	%	mg / m³ STP_{dry} at 6 % O_2
1.30	4.88	100	365.63
		80	347.32
1.10	1.92	100	311.21
		80	297.61

Considering the results given in Table 17 than are the predicted NO_x reduction potentials for FPP–2, 14.9 % for full boiler load and 14.3 % for 80 % load operation calculated when lowering the air ratio by 15.4 % (from 1.3 to 1.1). These values are in very good agreement with the results obtained by Pershing [90]. Who reported NO_x reductions of 20 % on the mean level by reducing the total excess air by 20 % respectively. Comparing to these results published for the reference case by Hwang [202], the results given in Table 17 fits tendencially but not in this accuracy. The author documented in his thesis that, decreasing the excess oxygen by 6 % (from n = 1.22 down to 1.15) had decreased the NO_x emissions by 20 % for the full load operation when burner elevation 1–5 were in service. This might be due to slightly different operation variables due to limitations of the control system (limited samplings of oxygen), mechanical problems (furnace wall cleanliness) or flow characteristics of the combustion gases (flow stratification). Also taking the average values over the length of the test period of at least 12 hours could cause for differences because this considers also strong short outliers.

FPP unit 2 is designed to achieve full load operation while one mill is out of service. Such design philosophy allows the mill–pattern–usage. Within this thesis also termed as burner–out–of–service (BOOS). The affected burners are removed from the coal supply and just served with a specific air flow so that the burner tips are cooled and covered against the heat radiation. This circumstances and the conclusion made above regarding the influence of different boiler loads and the herewith resulting difference in the energy density inside the furnace, on the NO_x dependency on the excess air level raises the question, how differences in the primary NO_x emission level $\left(\boldsymbol{NO}_{\boldsymbol{x}_{\boldsymbol{Prim}}}\right)$ as defined in equation (**VI–13**) would influence this relationship. For this background three different burner configurations for full load operation had been analyzed according to the information provided by the 'Test 6' experiments of Hwang [202], see Figure 32.

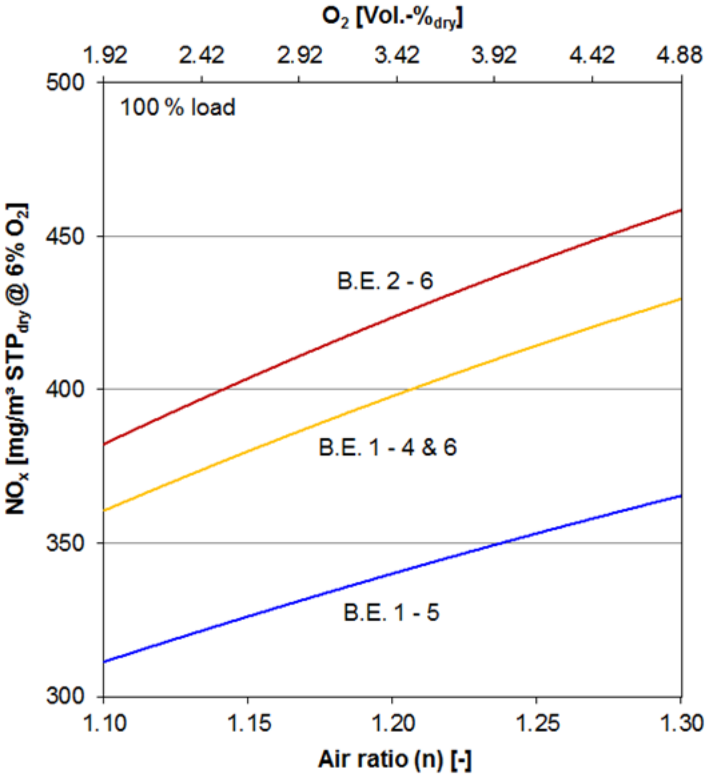

Figure 32. NO_{xPred} vs. air ratio (n) for different BOOS for FPP–2

Figure 32 shows the different NO_x dependencies on the overall stoichiometry for different burner configurations under unchanged conditions (the same operational conditions as used for Figure 31). The results are given in Table 18.

Table 18. Results of NO_{xPred} vs. excess oxygen and BOOS for FPP–2

B.E.	Air ratio	NO_{xPrim}	NO_{xPred}
–	–	mg / m³ STP$_{dry}$ at 6 % O_2	
1 – 5	1.30	785	365.63
	1.10		311.21

B.E.	**Air ratio**	$NO_{x_{Prim}}$	$NO_{x_{Pred}}$
–	–	mg / m³ STP_{dry} at 6 % O_2	
1 – 4 & 6	1.30	850	429.83
	1.10		360.49
2 – 6	1.30	860	458.78
	1.10		382.21

Hwang [202] stated that with increasing the elevation of burner configuration the NO_x emissions of the boiler increase too, i.e. $NO_{x,\text{ B.E. }2–6} > NO_{x,\text{ B.E. }1–4\&6} > NO_{x,\text{ B.E. }1–5}$, which is absolute in line with the results obtained in Table 18. Table 18 reveal for burner configurations 1 – 5, 1 – 4 & 6, and 2 – 6, NO_x reduction potentials of 14.9 %, 16.1 %, and 16.7 % respectively for the observed excess air range. That means, the more effective a primary combustion zone, the less influence takes the excess oxygen level on the NO_x emissions. This conclusion is even for low–NO_x systems an important finding, because the more effective the primary combustion situation of a boiler the less susceptible the system will respond to oxygen fluctuations during operation and the less emission peaks could be expected.

The correction curves presented in Figure 31 could optimize the process for minimal stack emissions and efficiency improvements regarding FPP–2. Especially for the background of minimizing the operational and maintenance costs by e. g. reducing the excess air level, which leads to power and stress savings at the forced and induced draft fan, therefore the presented approach could be a powerful optimization tool.

Overfire Air Mode

Furnace air staging is well proven for NO_x reduction at coal–fired power stations. The application example in this section focused on the the air–staging influence $(\boldsymbol{h}_3)$ described in the developed NO_x prediction model (equation (**VI–1**)). The helping factor $\boldsymbol{h}_3$ consist of two variables, first $\boldsymbol{OFA}_{\%}$ which is the percentage of the total combustion air shifted away from the burners and added at the individual point of OFA injection and second, $\boldsymbol{OFA_{VS}}$ which is the distance in meter between the upper active burner plane and the individual point of overfire air system (OFA) injection. This section focused on the influence resulting due to operational changings of the OFA with respect to the reference boiler FPP–2, i.e. the air ratio supplied to the existing nozzles. Not to system geometry changings, i.e. the distance $(\boldsymbol{OFA_{VS}})$. This question will be investigated in chapter 'System Modifications' in the following.

Hwang [202] performed and analyzed different test situations. The test series 10 targeted to the effect of varying OFA damper openings. The author observed during his experiments[24] that the NO_x emissions decreased from 275 ppm[25] (564.45 mg / m³ STP_{dry}) to 190 ppm[25] (389.98 mg / m³ STP_{dry}) at economizer outlet when the OFA air damper openings had been increased from 10 % to 80 % during burner elevations (B.E.) 1 – 5 were in service at full boiler load. Table 19 shows the main operational setting concerning test 10, other settings as coal properties or air distribution are given in Appendix 4 or in the work of Hwang [202], whereby 'Test 10A' had been excluded from the comparison due to a significant different burner tilt which disagreed from the other and influenced the location of the primary combustion zone inside the furnace.

---

[24] Test 10C, and Test 10D in Hwang [202].

[25] O_2 uncorrected, values given at actual O_2 level.

Table 19. OFA reference cases for FPP–2

Reference No. in Hwang [202] –	**Coal used** –	**Boiler load** [%]	**Reference oxygen level (O_2)** Vol.–$\%_{dry}$	**OFA damper opening** [%]	**Auxiliary air damper opening** [%]	$NO_{x_{Ref}}$ at 6 % O_2 mg / m^3 STP_{dry}
Test 10B	Blend 11	100.0	2.50	50	59.2	355.92
Test 10C	Blend 12	100.3	2.60	10	70.3	459.68
Test 10D	Blend 13	100.3	2.42	80	51.5	314.44

The major problem to be solved was the interpretation of the resulting secondary air proportion according to different damper positions. In order to find a traceable and reproducible solution the system design of FPP–2 needs to be considered in more detail. The main secondary air duct is the connection between the air preheater and the burners. The OFA air duct is designed as branch duct connected to the main air duct. After the OFA duct is decoupled from the main duct the remaining duct is termed as auxiliary air duct which serves the burners. This arrangement result in the situation that the auxiliary air dampers control the back pressure inside the main air duct and thus the prevailing pressure before the OFA dampers. However the auxiliary air dampers are downstream the OFA dampers is the resulting volume flowing quantity of the OFA at constant OFA damper opening nevertheless depending on the auxiliary air damper positions. The problem to be solved was herewith the interpretation of different damper positions reported by Hwang [202] according to the proportioning of the OFA and auxiliary air volume flows. Due to the fact that no air curves for FPP–2 were available there have been used known air curves of another boiler with similar arrangement as Figure 33 suggest.

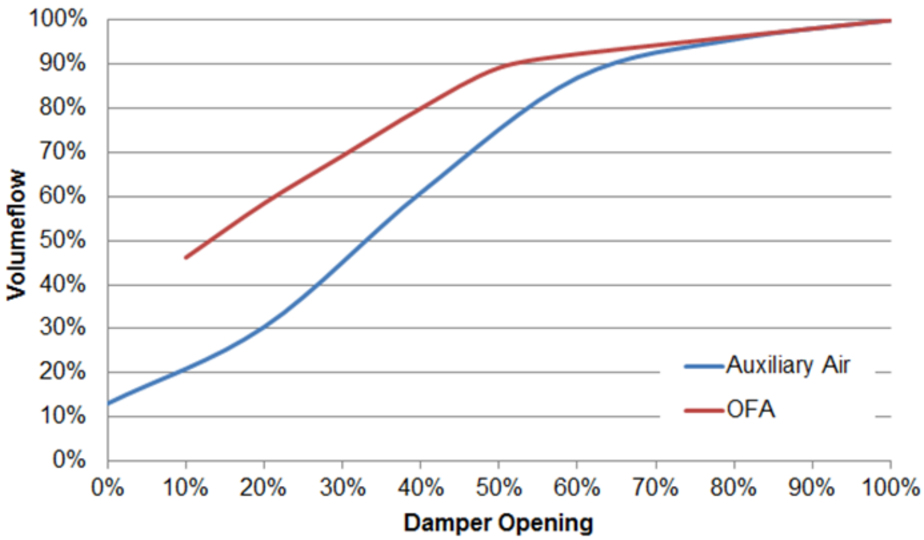

Figure 33. Air volume flow according to damper opening

Figure 33 shows the relation between resulting air stream volume as function of the respective damper opening in percent. The red colored function is the relationship assumed for the OFA and the blue colored function shows the downstream allocated auxiliary air relation. As mentioned above are both damper positions directly related and influenced by each other. For the background that the split into different air streams would have significant influence on the system NO_x emissions, due to the strong OFA influence explained in equation (**VI–10**), it has been assumed that the direct relationship between both dampers can be simplified by the following equation.

$$\boldsymbol{OFA}_{\%} = \left(\boldsymbol{1} - \boldsymbol{V}_{\boldsymbol{Aux}_{\%}}\right) * \boldsymbol{V}_{\boldsymbol{OFA}_{\%}} \tag{VII–4}$$

Where $\boldsymbol{V}_{\boldsymbol{Aux}_{\%}}$ is the resulting auxiliary air volume flow and $\boldsymbol{V}_{\boldsymbol{OFA}_{\%}}$ the resulting OFA air volume flow in percent depending on the respective damper positions according to Figure 33. Equation (**VII–4**) state, if 100 % secondary air flows through the main duct and the auxiliary air damper opening controls the system, than is the difference between secondary air and auxiliary air portion this part of the secondary air which could be served to the OFA when the OFA damper would be fully open. If the OFA damper is not 100 % open, it had been assumed to be reduced to the respective volume flow of the function given in Figure 33. In which the remaining portion of the air is back associated to the auxiliary air.

Based on Figure 33 and equation (**VII–4**) the resulting OFA air proportion of the total controlled combustion air ($\boldsymbol{OFA}_{\%}$) according to the documented damper openings had been calculated as follows.

Table 20. OFA air ratio for FPP–2 depending on damper position

Auxiliary air damper opening [%]	**Volume flow** [%]	**OFA damper opening** [%]	**Volume flow** [%]	**OFA air ratio share** [%]
51.5	78	80	96	21.1
59.2	87	50	89	11.6
70.3	93	10	46	3.2

Substituting the dependencies described above in the prediction model the following results had been produced.

Table 21. Prediction precision depending on OFA mode for FPP–2

Reference No.	**OFA air ratio share**	**OFA air ratio ($\mathbf{n_{OFA}}$)**	**Total air ratio ($\mathbf{n_{total}}$)**	$\boldsymbol{NO_{x_{Ref}}}$	$\boldsymbol{NO_{x_{Pred}}}$
–	[%]	–	–	mg / m³ STP_{dry} at 6 % O_2	
Test 10B	11.6	0.131	1.134	355.92	349.53
Test 10C	3.2	0.037	1.140	459.68	414.42
Test 10D	21.1	0.240	1.128	314.44	319.22

The experiments ‘Test 10’ done by Hwang [202] shows a measured reduction potential of 31.6 % when opening the OFA damper position from 10 % to 80 % and closing the auxiliary air damper position from 70.3 % to 51.5 %, without considering other effects coming through different coal properties, excess oxygen level, or boiler load. The results obtained by the prediction model under same conditions estimated 23 % reduction potential. The deviation might be due to errors within the assumption made on the expected air split between OFA and auxiliary air related to its damper positions. Also errors coming due to the 10 hours period of the reference measurement campaign could not be excluded. Nevertheless, compared to the results stated by Muzio et al. [214] the deviation is significantly lower. The author reported NO_x reduction potential of 25 % when using conventional OFA installations. Allen et al. [215] stated that NO_x emissions were reduced by 20 % when using 20 % over fire air amount. Both publications [214, 215] referred to experimental results of tangentially–fired boilers and to these results fit the predicted 23 % very good. One can be found in any case, the predicted NO_x values confirmed the conclusions made on the reducing effect of air staging on the NO_x emissions. The more air is shifted away from the burners the lower the emissions.

Assuming that the developed model precision concerning the OFA influence satisfied the precision expectations the investigation could go in more detail. In order to follow the methodology used so far, a sensitivity analysis on the basis of one specific reference scenario had been carried out. ‘Test 10 B’ reported by Hwang [202] had been chosen as reference case because the adjusted damper openings seemed to represent a very balanced relationship to each other and thus most transferable to the other test trials documented from a statistical point of view. Investigated was the NO_x emission behavior of the system while shifting the air away from the burners to the OFA injection nozzles. The operational data of ‘Test 10B’ used as reference for Figure 34 can be found in Appendix 4 or in the work of Hwang [202].

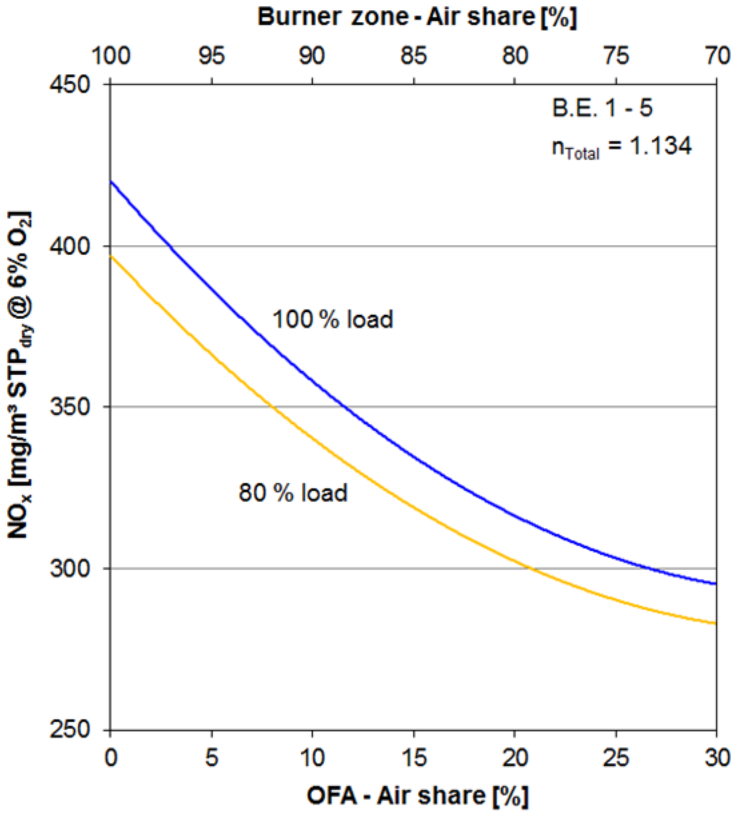

Figure 34. NO_{xPred} **vs. OFA air portion for FPP–2**

Figure 34 shows the resulting relationship between predicted NO_x emissions as function of the overfire air portion referred to the total controlled combustion air under the conditions of constant overall excess air level (n = 1.134, or O_2 = 2.5 Vol.–%, dry) when burner elevation 1 to 5 are in service for the full and for the 80 % part load operation. Considering the results given in Table 21 and these shown in Figure 34 it can be concluded that increasing the OFA air volume share would decrease the NO_x emissions but it is also well proven that this air displacement will cause in increasing CO emissions and reducing the combustion efficiency because of rising unburnt carbon content in the ash (UBC). The justification lies in the fact that a longer residence time in the fuel–rich zone caused a decrease in the conversion of coal–N to NO_x whereas too long residence times in the fuel–rich zone will cause the char burnout efficiency to decrease [161]. Unfortunately are no data available regarding the CO and UBC dependencies on air staging and total excess air level and thus it shall just be remarked that such function would look at its best like a vertically mirrored NO_x function as shown in Figure 34. Therefore this relationship cannot be analyzed and commented within this thesis but Botsford [216] documented 15 % NO_x reductions without significant impact on overall combustion stability and burnout. Referred to the function shown Figure 34 means that, 10 % of the total controlled combustion air could be shifted away from the burners before recognizing significant deterioration of UBC and CO.

Nevertheless, the relatively strong influence of the air portion supplied to the OFA injection nozzles on the NO_x reduction is another impressively example for the superposition effect of several individual influence factors. Because changing the OFA fraction while keeping the total air level constant results in changings in the primary air level (secondary x–axis in Figure 34) and on the other hand, changing the OFA air fraction while keeping the primary air level constant will change the total excess air level. That means, three of the five identified influence factors are directly related, i.e. air influence $(\boldsymbol{h_2})$, OFA influence $(\boldsymbol{h_3})$, burner influence $(\boldsymbol{h_4})$. Furthermore, if the boiler load decrease and the steam parameter will not be achieved through the insufficient flue gas volume flow, than the excess air level needs to be increased which means for part load operation that one additional influence factor will be directly connected to the others, i.e. furnace influence $(\boldsymbol{h_5})$. Therefore it can be concluded that the correlation curve presented in Figure 34 could help to operate the boiler at a previously defined acceptable emission level depending on excess oxygen, load, and burner configuration with respect to combustion efficiency.

Air staging will reduce NO_x emissions as more air is shifted away from the burner area, but at the same time it will have a negative impact on the burnout which decrease the boiler efficiency and maybe increase the fouling and slagging tendency depending on coal properties. Therefore is the major objective not only with lowest possible NO_x emissions. Rather the challenge is to balance the effects which work against each other in order to ensure the best possible boiler operation under consideration of all aspects in which the developed approach would certainly be a helpful tool.

Burner Operation

Due to the fact that only operational aspects shall be investigated during this chapter is the following application focused on changings which can be controlled by the boiler operator in the control room, i.e. burner zone stoichiometry and mill–out–of–service patterns. System design influences, i.e. burner design factors ($\boldsymbol{b_i}$) as given in Table 7, will be investigated in the following chapter 'System Modifications'.

The operational mode of a burner can limit NO_x formation by controlling the stoichiometric ratio and energy densities of the combustion process. Decreasing the availability of oxygen in the primary combustion zone inhibits fuel–NO_x conversion [171]. The resulting delayed combustion influenced both thermal– and fuel–NO_x. Figure 34 shows already the relationship between NO_x emissions and burner air portion under the conditions of constant overall excess air level at full boiler load, but based on one specific burner configuration. Therefore shows Figure 35 the results obtained in the previous section extended by two other and different active burner elevations (B.E.) on the same operational data ('Test 10B') used as reference for Figure 34 which can be found in Appendix 4 or in the work of Hwang [202].

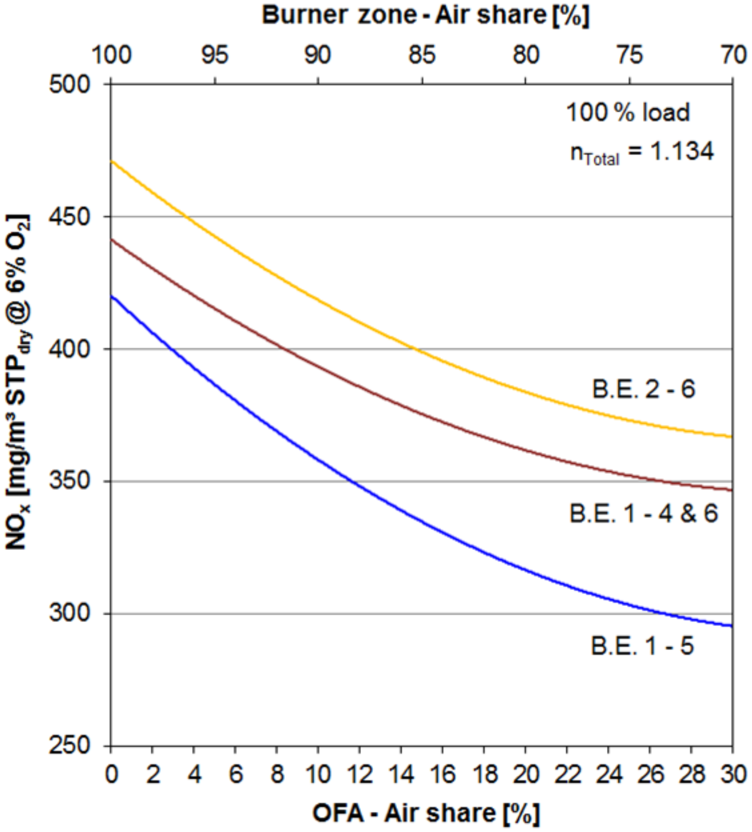

Figure 35. NO_{xPred} **vs. burner air portion for FPP–2**

As mentioned in chapter 'Excess Air Ratio' the general statement of Hwang [202] regarding the burner–out–of–service patterns, i.e. $NO_{x,\,B.E.\,2–6} > NO_{x,\,B.E.\,1–4\&6} > NO_{x,\,B.E.\,1–5}$ could be confirmed. However shows Figure 35 one more consistency. The author stated further that also the primary NO_x emission level for the different configuration goes in the same direction. This had been explained by the circumstances that the operation with B.E. 2 – 6 requires more combustion air for the burner region than the operation of B.E. 1 – 5. This conclusion can also been seen in Figure 35. The positioning of the functions inside the coordinate system shows that the function vertex based on the secondary x–axis of B.E. 2 – 6 indicate a higher value for the burner air share as for B.E. 1 – 5 which confirmed additionally the assumptions made on the primary NO_x levels made in equation (**VI–14**). Table 22 summarized the effect coming due to burner–out–of–service (BOOS) patterns shown in Figure 35.

Table 22. NO_{xPred} **vs.** n_{BZ} **and BOOS for FPP–2**

B.E.	**Total air ratio (n_{total})**	**Burner air ratio (n_{BZ})**	NO_{xPrim}	NO_{xPred}
			mg / m³ STP_{dry} at 6 % O_2	
1 – 5	1.134	0.74	785	293.83
		1.08		422.44
1 – 4 & 6	1.134	0.74	850	345.95
		1.08		442.62
2 – 6	1.134	0.74	860	366.05
		1.08		472.46

It shall be remarked that the maximum burner air ratio is assumed to be below the measured total excess air ratio. This is because of the assumption that also other areas of the boiler would be supplied with air during operation. That means the difference between the measured value at the economizer outlet and the maximum air supplied to the burners represents this part of the combustion air which is supplied to the system but not fed into the closer burner zone, e.g. various sealing air.

For the background that the developed model approach, especially the part regarding the influence of burner air ratio in equation (VI–11) based on the results reported by Schlessing et al. [174] would a comparison only provide coincidence but also the comparison with the result reported by Stamey–Hall [171] shows a very good agreement. Table 22 reveal a NO_x reduction potential of 19.7 % between burner configurations 1 – 5 and 2 – 6 for the minimum burner air ratio scenario at full load operation and 10.2 % the maximum burner air ratio scenario. Stamey–Hall [171] documented for mill–pattern–usage (termed also as BOOS) during full–scale experiments that the NO_x level varies by as much as 25 % depending upon which mill was out of service. However, it should bear in mind that the data published by Stamey–Hall [171] related to a 365 MWe single–wall coal–fired unit operating at 68 % load and firing sub–bituminous coal without any information available regarding the burner air ratio. Therefore is the basis for comparison not unequivocally but it is very likely that the boiler primary zone operated in a sub–stoichiometric environment during the experiments and therefore it could be assumed that the minimum burner air ratio scenario is adequate basis for comparison. Nevertheless, the results in Table 22 related to the tangentially–fired 606 MWe unit FPP boiler 2 operating at full load. Therefore the calculations made for Table 22 were performed again with reduced boiler load. Attention needs to be done when reducing the load down to 68 % because this would certainly increase the total excess air ratio in order to achieve furthermore the required steam parameters.

Table 23 shows the prediction results for the 68 % part load operation at an economizer outlet oxygen level of 4 %, dry gas ($n = 1.233$).

Table 23. NO_{xPred} vs. n_{BZ} and BOOS for FPP–2 for 68 % part load

B.E.	**Total air ratio (n_{total})**	**Burner air ratio (n_{BZ})**	$NO_{x_{Prim}}$	$NO_{x_{Pred}}$
			mg / m³ STP_{dry} at 6 % O_2	
1 – 5	1.233	0.813	785	290.95
		1.183		458.00
1 – 4 & 6	1.233	0.813	850	347.18
		1.183		483.28
2 – 6	1.233	0.813	860	362.61
		1.183		507.94

When considering burner configurations 1 – 5 and 2 – 6 for the minimum burner air at 68 % part load operation is the NO_x reduction potential with 19.8 % absolute comparable to the full load operation. That lead to the conclusion, that the effect of lower energy density inside the furnace is being compensated by the effect of rising oxygen content at the furnace end. Figure 35 shows the effect of different burner air level under the condition of constant total excess air level while the air is shifted away from the burners to the OFA injection points. As shown, this will increase the OFA influence according to the air ratio supplied to it. Another possibility of application is to change the burner air level under the condition of constant OFA air share based on the total excess air level as shown in Figure 31, which will eliminate the influence coming through the air staging $(\boldsymbol{h_3})$ because the value of $\boldsymbol{h_3}$ remains constant for the complete scope of consideration. That means the OFA air level will be adjusted during the sensitivity analysis according to its original share of the total excess air ratio of the reference case

‘Test 10B’, same as used for Figure 35. Table 24 summarized the results which are comparable to Table 22.

Table 24. NO_{xPred} vs. n_{BZ} and BOOS for FPP–2

B.E.	Total air ratio (n_{total})	Burner air ratio (n_{BZ})	NO_{xPrim}	NO_{xPred}
			mg / m³ STP_{dry} at 6 % O_2	
1 – 5	0.89	0.74	785	229.87
	1.28	1.08		418.36
1 – 4 & 6	0.89	0.74	850	245.84
	1.28	1.08		463.09
2 – 6	0.89	0.74	860	256.02
	1.28	1.08		494.98

Comparing the results given in Table 24 with these in Table 22 then it is striking that the ratio for the NO_x reduction potential between burner configurations 1 – 5 and 2 – 6 depending on the burner air scenario has turned. 10.2 % for the minimum burner air– and 15.5 % for the maximum burner air scenario at full load operation. That leads to the conclusion, that the air staging influence $(\boldsymbol{h_3})$, also named as OFA influence, must be the main driver for the NO_x reduction potential in Table 22 while the air influence $(\boldsymbol{h_2})$ is kept constant. The more OFA is introduced the more reduction potential on the primary NO_x emission level $(\boldsymbol{NO_{x_{Prim}}})$ is available. For Table 24 it is the other way around. The OFA influence has kept constant while the burner air ratio and the excess air ratio have been increased. That means, the more oxygen is available the more NO_x will be generated depending on its initial primary NO_x emission level and due to the fact of constant OFA share on the total combustion air is the reduction potential smaller with higher oxygen concentrations. These relationships look graphically as follows.

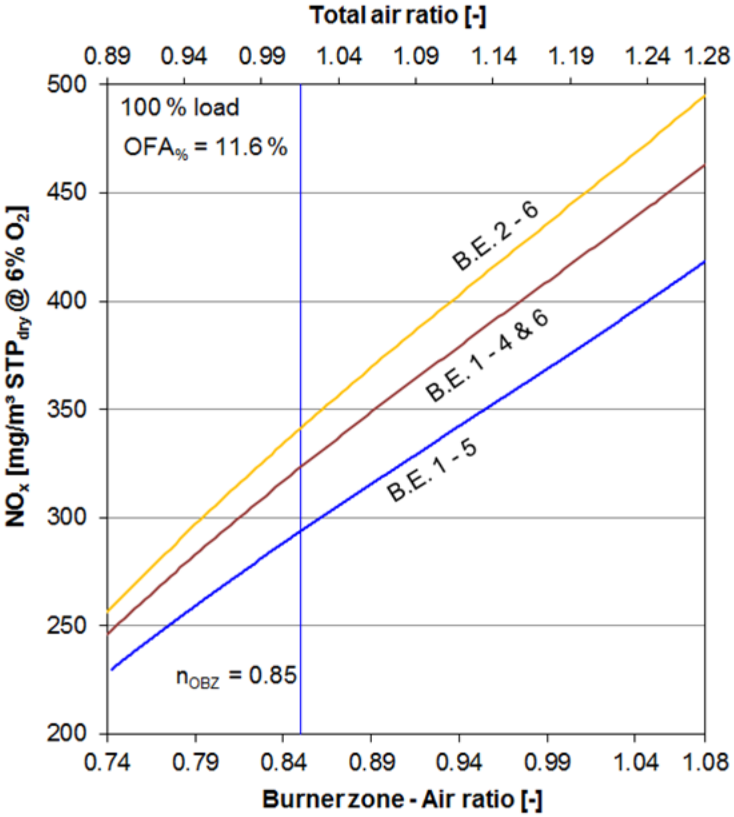

Figure 36. NO_{xPred} **vs. burner air ratio for FPP–2**

The resulting NO_x functions for the different burner configurations in Figure 36 are not linear. Three major effects describe the shape of the respective function which can be best described by a polynomial function of the third power. These effects are: air influence $(\boldsymbol{h_2})$, burner influence $(\boldsymbol{h_4})$, and furnace influence $(\boldsymbol{h_5})$. The other influence factors as coal influence $(\boldsymbol{h_1})$ and air staging influence $(\boldsymbol{h_3})$ remains constant for the complete scope of consideration. In order to get a better impression of the individual grade of influence responsible for the function shapes shown in Figure 36 the above mentioned main helping factors are plotted individually in Figure 37 for the burner configuration 1 – 5 to illustrate the relationship on the predicted NO_x values.

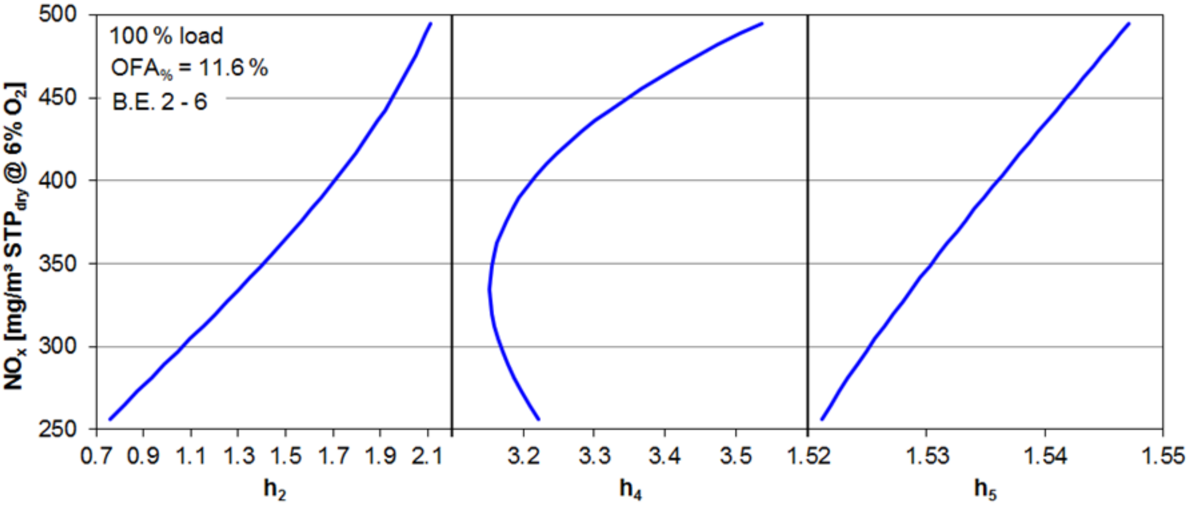

Figure 37. Matrix plot of NO_{xPred} vs. h_2, h_4, and h_4 for FPP–2

The continuously increase of the burner air ratio, while keeping the OFA air share of the total combustion air constant, lead to a rising total oxygen level which results in a continuously increasing air influence $(\boldsymbol{h_2})$. The burner influence $(\boldsymbol{h_4})$ decrease for the low air range until the optimal burner air ratio $(\boldsymbol{n_{OBZ}})$ has been reached (blue line in Figure 36) but then the function increases continually with increasing air ratio. The slightly increase of the furnace influence $(\boldsymbol{h_5})$ based on the rising heat input to the furnace due to the increasing hot secondary air massflow through the burners (see Figure 18). Interesting is that although, the influence of the burner air ratio $(\boldsymbol{h_4})$ decreases before the optimal burner air ratio $(\boldsymbol{n_{OBZ}})$ has been reached the slope of the main function $(\boldsymbol{NI})$ seemed to be steeper than after. This might be due to the strong influence of the excess air ratio $(\boldsymbol{h_2})$ which nearly doubles within the specific part, whereas the burner influences $(\boldsymbol{h_4})$ decrease. However, after $\boldsymbol{n_{OBZ}}$ was achieved all influence factors consolidate together and describe the downstream slope of the main function. Considering the grade of influence it can be concluded that the change of the value for furnace influence is very small in contrast to the complementary effect of burner $(\boldsymbol{h_4})$

and furnace influence $(\boldsymbol{h_5})$ which is possibly why these two factors are mostly named in the literature as main driver for NO_x generation, e.g. by Schlessing et al. [174] and Pershing [90]. This analogy is not surprising because the developed model approach based on the results reported by both authors. The authors investigated the influence on NO_x emissions while changing the reference O_2 concentration at different points of interest. Pershing [90] focused on the overall combustion air ratio (secondary x–axis in Figure 36) and Schlessing et al. [174] to the excess air level within the primary combustion zone (primary x–axis in Figure 36).

Precisely for this reason, could the above described relationships and illustration of superposition effects help for further investigations and experimental works to the research on the formation of NO_x emissions in pulverized coal–fired utilities. Based on the findings obtained within this chapter and the resulting possible impacts on the operational settings of the reference boiler FPP–2 it can be concluded, that the evidence obtained during the former sections could be confirmed again. A reduction in the primary zone stoichiometric ratio caused a decrease in NO_x emissions but it should also not forget that this will decrease particle burnout and increasing CO emissions.

Boiler Load

The relative importance of furnace load as one of greater predictor for NO_x generation had been identified by Bartok et al. [88] and recently been reviewed by Boyd et al. [80]. In general it can be concluded that the thermal load of a boiler has an influence on its combustion intensity which affects the flame temperature and the residence time of the coal particles in the furnace. Therefore it can be assumed that lowering the unit gross load would decrease the reactant flow rate (fuel and oxidizer) into the furnace which reduces the energy density inside the furnace (also termed as heat release rate) and thus reduces the NO_x emissions. In order to find out how this theory can be transferred to the reference unit FPP–2 the potential effect of varying boiler loads on the NO_x emissions will be investigated in this section.

For the analysis it was assumed to be most beneficial to stay with the reference conditions mentioned in ‘Test 10B’ of Hwang [202] because of the fact that this scenario was also based as reference for the work done in the previous chapters. This makes it possible to take up again the results obtained in chapter ‘Coal Properties and Blending’ for the full load operation and extended the analysis for the 80 % and 60 % boiler load operation. Additionally, as mentioned in chapter ‘Excess Air Ratio’ it has been assumed that the reference boiler FPP–2 is able to achieve the steam design conditions between 100 % and 80 % part load operation at constant excess oxygen level. For lower boiler loads it is more than likely that the controlled excess oxygen content at the evaporator outlet must be increase simultaneously. This can be explained by the fact that FPP–2 is a boiler / turbine combination with a steam reheater system and without the possibility of flue gas recirculation. That means the convective heat absorption part of the boiler needs to be served by an adequate amount of flue gas in order to meet the steam temperature defined by the turbine for both superheated steam (SH) and reheated steam (RH) flow. What is necessary to avoid imbalances inside the turbine due to temperature differences between SH and RH. Such sufficient flue gas quantity could be ensured by increasing the excess air level during lower boiler load operation. Since the necessary amount of excess oxygen content for the part load operation of such boilers depends mainly on coal properties, which has been specified in Table 15, it was determined that the oxygen content in the flue gas has to be increase for the 60 % part load operation lineally up to 5 Vol.–% O_2, dry gas at the economizer outlet according to the respective boiler load which is a plausible value for such boiler systems.

Figure 38 shows the results of the furnace influence $(\boldsymbol{h_5})$ based on 'Test 10B' for several different coals in order to provide the best possible basis for comparison with the results obtained in chapter 'Coal Properties and Blending'.

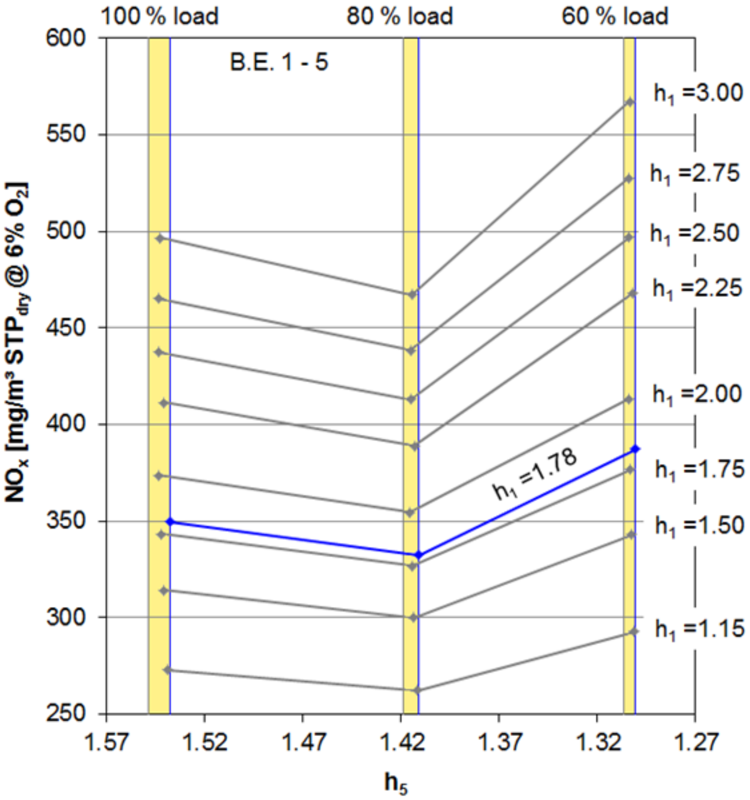

Figure 38. NO_{xPred} **vs.** h_5 **and** h_1 **for FPP–2**

The blue line in Figure 38 represents the initial situation of 'Test 10B' based on the original coal properties with a coal influence factor $(\boldsymbol{h_1})$ of 1.78 according to equation (**VI–8**). The added grew scenarios represents the effect of furnace influence $(\boldsymbol{h_5})$ on NO_x emissions based on other coal compositions from the USGS Coal Quality Database [18] which satisfy the specified condition given in Table 15. The yellow areas describe the range where the exact value of $\boldsymbol{h_5}$ could be located for respective boiler loads depending on its coal properties. That means, the grade of furnace influence $(\boldsymbol{h_5})$ is not equal for all coals, not even for the same load case. As in equation (**VI–19**) shown the furnace influence depends on the total energy supplied to the furnace which is according to Figure 18 the sum of all superimposed material flows, especially the thermal energy of the combustion air plays an important role. The necessary air flow for a constant air–fuel ratio varies between the coals because it depends on the heating value and on the oxygen demand of the specific coal compositions. The yellow range represents thus fluctuations in the thermal load due to fluctuations in the hot secondary air energy. Table 25 summarized almost some of the data shown in Figure 38 in numbers.

Table 25. NO_{xPred} vs. boiler load and h_1 for FPP–2

Boiler load		100 %	80 %	60 %
O_2 Vol.–%, dry[26]		2.5	2.5	5.0
Coal influence $(\boldsymbol{h_1})$	**Stoich. O_2 requ.**[27] kg / kg	$\boldsymbol{NO_{xPred}}$ mg / m³ STP_{dry} at 6 % O_2		
1.15	1.418	273.00	262.27	292.81
1.78	1.426	349.53	332.51	387.25
3.00	1.531	496.58	467.22	567.43

Interesting is the changing curvature behavior of the NO_x functions when the value of the coal influence $(\boldsymbol{h_1})$ increase (Figure 38). Considering the difference between full and 80 % part load scenarios for $\boldsymbol{h_1}$ = 1.15, 1.78, and 3.00, the NO_x emissions have

---

[26] At economizer outlet.

[27] Exactly the required amount of oxygen which is consumed when all fuel is burned.

been predicted to decrease by 3.9 %, 4.9 %, and 5.9 % respectively. These results are in quiet good agreement with the finding of Richards et al. [217] obtained by pilot–scale tests. The authors reported 5.8 % NO_x reduction for the respective load range. Boyd et al. [80] stated that in general NO_x emissions increase with increasing boiler load. Figure 38 confirmed that statement as long as the oxygen level is unchanged. Especially for the results given in Table 25 based on the reference unit FPP–2 are the differences between full and 60 % part load scenarios for $\boldsymbol{h_1}$ = 1.15, 1.78, and 3.00, in NO_x emissions predicted to increase by 7.3 %, 10.8 %, and 14.3 % respectively.

Therefore it can be concluded that the NO_x formation depends much more on the excess oxygen concentration as on the thermal rating of the furnace. Although the furnace influence factor $(\boldsymbol{h_5})$ decreases according to lower thermal heat input to the furnace is the NO_x suppression effect reinforced by the air influence factor $(\boldsymbol{h_2})$ which covers the effect and completely reversed the behavior of the function.

Furthermore shows Figure 38 the higher the value of the coal influence factor $(\boldsymbol{h_1})$ the more influenced the furnace energy density the total NO_x generation. Which can be explained by the fact that, if the coal influence factor increases it will both increase simultaneously the parent NO_x indicator $(\boldsymbol{NI})$ (equation (**VI–1**)) and the resulting grade of influence coming due to a load change $(\boldsymbol{h_5})$. In order to illustrate this finding Figure 30 has been extended by the results obtained during this section.

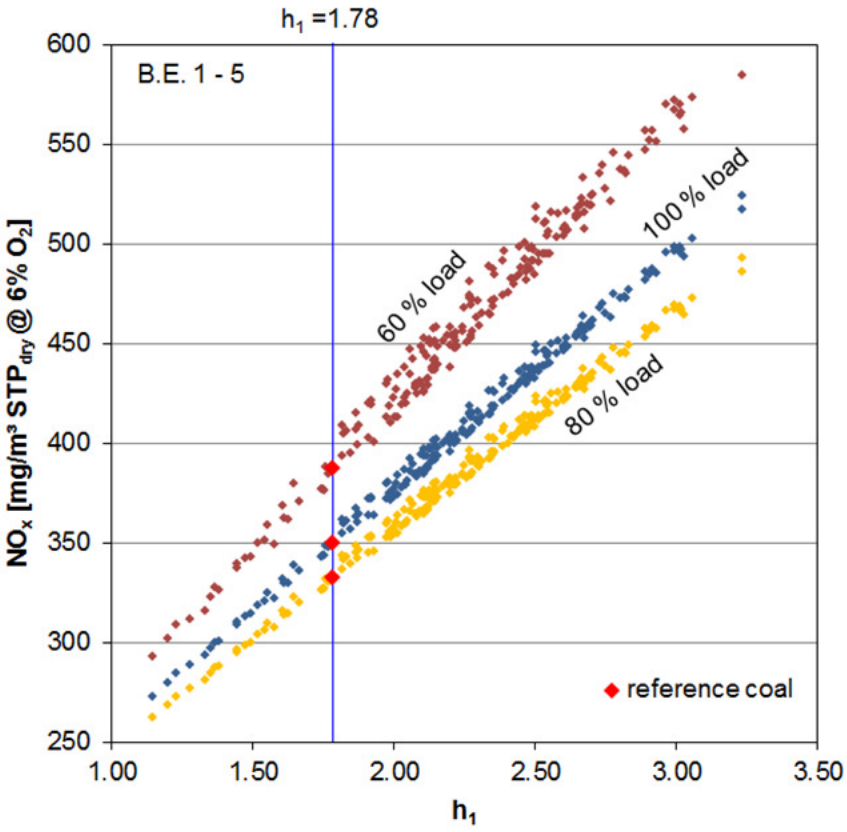

Figure 39. NO_{xPred} **vs.** h_1 **depending on load for FPP–2**

Figure 39 shows the predicted NO_x values as function of the coal influence factor $(\boldsymbol{h_1})$ for the selected coal properties (Table 15) for the three considered thermal loads. The single vertical line describes the reference coal scenario for 'Test 10B' of Hwang [202]. The scattering of the predicted NO_x values can be explained by the fact that all coals have been used under identical operation conditions. Especially the set burner air ratio $(\boldsymbol{n_{BZ}})$ is sometimes more, sometimes less far away from the optimal burner air ratio $(\boldsymbol{n_{OBZ}})$ depending on the coal volatile content (see Table 15).

Summarized it can be concluded that based on the furnace load influence $(\boldsymbol{h_5})$ the developed approach could be a helpful tool to operate pulverized coal–fired systems. Figure 38 and Figure 39 would allow making assumptions of a possible boiler load range under consideration of coal qualities and a specific emission limits. Furthermore these diagrams could give fast and easy predictions of the boiler emissions under consideration of coal qualities and boiler load which could be helpful for the purchasing strategy of a plant. Furthermore it can be said that the results obtained matches with those of other researcher. Bartok et al. [88], Lim et al. [91] and Boyd et al. [80] stated in general that NO_x emissions decrease with decreasing boiler load which can be confirmed as long as the excess oxygen level keeps constant. But in the end is the necessary operating load dictated by the grid demand, which makes this technique obviously not to a practical method of NO_x control except in several instances.

Preheat Air Temperature

Another found hint in the available literature regarding NO_x control possibilities due to a change in the operational settings of a boiler is to reduce the preheat temperature of the hot combustion air [5, 88, 91, 212, 218–220]. The theory is simple, since NO_x emissions are influenced by the effective peak temperature of the combustion process would any change in that temperature profile result in a change in NO_x emissions. For the developed model approach means that, a change in the furnace influence factor $(\boldsymbol{h_5})$ due to a change in the thermal energy fed to the furnace $(\dot{\boldsymbol{Q}}_{\boldsymbol{gas}})$ (equation (**VI–22**)).

In order to investigate the grade of influence of reducing the secondary air temperature a sensitivity analysis had been taken out on the above used reference case (‘Test 10B’). The secondary air temperature was reduced from 370 °C to 150 °C while all other parameter had been kept unchanged. Figure 40 shows the results.

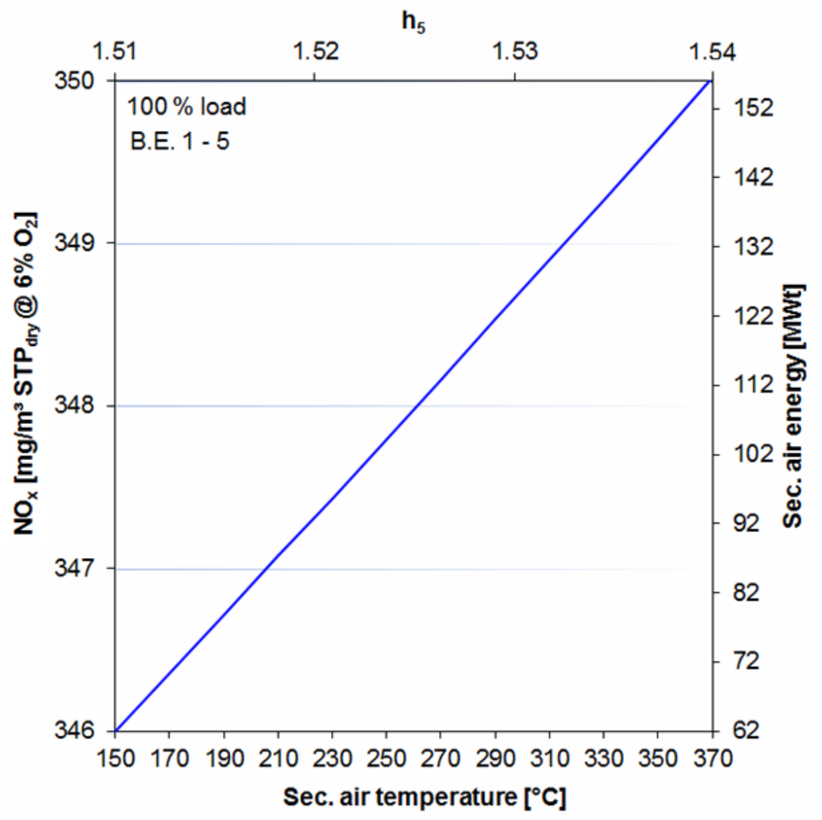

Figure 40. NO_{xPred} **vs. sec. air temperature for FPP–2**

This control strategy was originally established for natural gas–fired systems where in particular NO_x emissions were reduced by 15 % at full load with a 45 K reduction in combustion air temperature [218]. Principally the results in Figure 40 confirmed the general statement that with reducing the air preheat the NO_x formation can be suppressed also for pulverized coal–fired systems which had already been identified to have relatively small reduction potentials [221]. Based on Figure 40 this can be explained by the fact, that lowering the secondary air temperature will reduce the thermal energy supplied to the furnace and lowers the average energy density. That means, the influence referred mainly to the combustion temperature and thus influences the thermal–NO_x formation [91, 222, 223]. The grade of influence due to reduced air preheat on the NO_x generation is therefore even lower for low ranked coals as for high ranked coals because low ranked coals generate almost fuel–NO_x due to lower combustion temperatures in the primary combustion zone as usual for high ranked coals. For the reference scenario used here means that an almost negligible reduction in NO_x emissions.

Above all, if considering that lowering the secondary air down to 150 °C will significant rise the flue gas heat loss which would lead to a substantial reduction in the boiler efficiency. In addition, a reduction of the secondary air temperature is also limited by the necessary primary air temperature supplied to the pulverizer which is controlled by the water content of the coal, the required primary air–fuel ratio which ensured a continuous transport of the particles through the mill to the burners, and a defined classifier outlet temperature. Depending on these variables a certain temperature of the primary air is required for the grinding and drying process of the raw coal. Furthermore, reducing the air preheat temperature can be a critical issue for low ranked coals. A stable self–sustaining ignition of such coals is very sensitive and lowering the combustion air temperature can lead to combustion instabilities which would require the continuous use of support firing, e.g. oil or gas which would eliminate the effect of lower combustion temperatures on the NO_x emissions. From the capital– and operational expenditure (CAPEX and OPEX) site of view it can be concluded that this technique has initially low equipment costs, but due to high operating costs resulting from losses in unit efficiency, is the least desirable of the system evaluated. Therefore it seems not to be suitable for an effective NO_x suppression for coal–fired steam generators and should be carefully examined and weighed before bring to bear.

System Modifications

In the previous chapters the effect of coal properties and operational settings had shown to have a significant influence on the NO_x emission behavior of the reference boiler FPP–2. The following chapter dealt with the investigation on possible hardware combustion modifications and how changes in some design features of FPP–2 would theoretically change the NO_x generation of the whole boiler. It is important in this respect to distinguish retrofit amendment techniques and original design features. The effectiveness of boiler combustion control technologies depend on the extent of equipment already fitted. While switching the furnaces may not be an option for utilities, it should be clear that the following chapter focused on retrofit amendment techniques which will affect the boundary conditions as air staging and burner design.

Overfire Air Design

Overfire air (OFA) injection is a critical component of an air–staged low–NO_x firing system. Because how and where the OFA is introduced in an air–staged low–NO_x system have significant effects on NO_x, CO and loss of ignition (LOI), among other things. Therefore was a separate task devoted to this aspect of the air–staged process. The design of an overfire air system can vary significantly between different boilers depending on the state of the art of the respective manufacturer at the time the system was designed. In pulverized coal–fired boilers separate overfire air injectors (nozzles) are typically located at different elevations above the upper main burners. Older systems utilize a single elevation whereas newer systems or latest retrofits provide rather more levels depending on the space situation around the boiler and specifications made by the power plant owner. Generally the injection of the overfire air can be accomplished in a number of different methods depending on the equipment supplier but due to the fact that the objective of this research work was not to consider or to evaluate specific design or control philosophies, the present chapter focused on general combustion process related assumptions, e.g. amount of overfire air and injection elevation which can easily be transferred to other facilities instead of flow, stream velocities, distribution etc. For this background, sensitivity analyses were carried out on overfire air configurations that can be categorized in two groups, as follows:

1. The existing OFA system of FPP–2 is considered to be replaced, i.e. the location of the existing OFA register could be varied.
2. Additional separate OFA registers will be provided at a certain elevation, i.e. the location of the additional OFA register could be varied.

From a combustion point of view the OFA must be injected at an elevation that guaranteed sufficient residence time exists downstream of the point of OFA injection to largely complete combustion prior to entering the convective heating surfaces [217]. This specific time period is determined by the char reactivity, particle size, density and the combustion environment of the respective original equipment manufacturer (OEM). Especially the design philosophy of the OEMs depends on several individual design specifications which have been developed mainly through experience and well–kept corporate knowledge. But due to the comparisons of installed systems with its combustion parameters it can be postulated that this necessary time must be in between 1 second and 2 seconds.

Based on this, the maximum allowable residence time for the reactants in a sub–stoichiometric environment can be derived. If the approximately minimum time needed to complete the combustion process is at least 1 second than must the maximum allowable time for the burning particles less than 1 second in order not to interrupt the chemical reactions. Similar to the specific time frames described above a specific flue gas velocity of 8 to 9 meter / second has evolved to be most suitable over the years and experience. This range builds the perfect balance between combustion and thermodynamic process related issues. By the help of these assumptions the remaining furnace height above the main burners of the reference boiler FPP–2 can easily be allocated and divided according to minimum and maximum permissible OFA vertical spacing $(\boldsymbol{OFA_{VS}})$ between burners and OFA injection.

With the prerequisite that the existing closed–coupled overfire air (CCOFA) will be replaced to the system without any changings on design geometry or operational mode conditions the maximum distance between upper active burner elevation (B.E.) and OFA can be describe as follows:

$$\boldsymbol{OFA_{VS1_{Max}} = 1\,sec * 8.5\frac{m}{sec} = 8.5\,m \sim 8\,m} \qquad \text{(VII–5)}$$

The maximum available vertical distance between main burner top row and furnace exit is 23.5 m (see Figure 25). The lowest possible active burner elevation during full boiler load is according to B.E. 1 – 5 the fifth burner elevation. In this case the actual distance is already 5 m and the investigation is thus limited to the range between 5 m and 8 m. However, to a better impression of the relationship between NO_x emissions and vertical spacing of the OFA the range had been extended by additional 10 m. Figure 41 shows the course of the relationship based on Hwangs [202] test procedure ‘Test 10B’ (same as used during chapter ‘Overfire Air Mode’) extended by consideration of two main burner zone configurations. Consisting of the lowest– (B.E. 1 – 5) and highest primary NO_x emission level (B.E. 2 – 6).

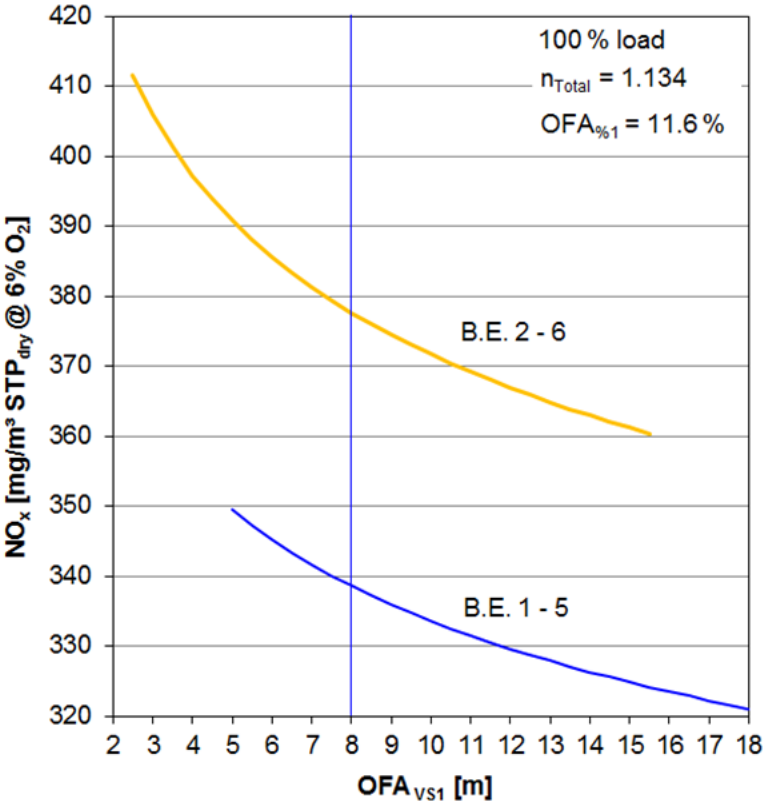

Figure 41. NO_{xPred} **vs.** OFA_{VS} **for FPP–2**

The vertical blue line given in Figure 41 represents the maximum permissible vertical spacing as described above (residence time between upper active burners and OFA < 1 sec, see equation (**VII–5**)). As shown NO_x emissions can be reduced as the distance between the staged air injector (OFA port) and the burner exit increases; however, if the distance exceeds a given value the loss of ignition (LOI) and CO emissions increase significantly. This circumstance decreases combustion efficiency because the residual concentration of oxygen turns out to be rather low at the end of primary combustion zone, and this substantially retards the burnout of the remaining fuel in burnout zone. Nevertheless, if assuming that these effects will only negligible increase within the permissible vertical spacing then shows up especially when burner elevation (B.E.) 2 – 6 is operating a significant influence on the boiler NO_x emissions.

Table 26. NO_{xPred} vs. OFA_{VS1} for FPP–2

B.E:	**Total air ratio (n_{total})**	$OFA_{\%1}$ [%]	**OFA_{VS1}** [m]	NO_{xPred} [mg / m³ STP_{dry} at 6 % O_2]
1 – 5	1.134	11.6	5	349.53
			8	338.60
2 – 6	1.134	11.6	2.5	411.47
			8	377.66

Table 26 summarized the results obtained from the sensitivity analysis. It shows for B.E. 1 – 5 and B.E. 2 – 6 a NO_x reduction potential of 3.1 % and 8.2 % respectively. It shall be remarked that this reduction belongs only to the increasing distance between burners and OFA register not the amount of air supplied to it. Although it is known that NO_x reduction efficiency grows with increasing the distance from the overfire air nozzle to the top pulverized coal nozzle have only limited research been done on the impact of these factors. Since the development of the OFA sub–model approach based on the only one available results published by Gwosdz [163] (Figure 14) can no further cross–comparison be made. Therefore additional investigations in that area would be appreciated.

As stated above, the air staging within the reference boiler FPP–2 could also be changed by a second variant, i.e. integration of a second separate OFA register (SOFA) at a specific elevation. The particular arrangement consist of the assumption that the existing close–coupled overfire air (CCOFA) elevation remains unchanged and one additional SOFA with variable distance ($\boldsymbol{OFA_{VS2}}$) downstream the CCOFA location will be added. Additionally it has been assumed that the OFA air share ($\boldsymbol{OFA_{\%}}$) remains constant but the OFA volume stream is uniform distributed to both registers. All other parameters unchanged. Figure 42 is a schematic of a possible OFA configuration for the reference boiler FPP–2. Details of the furnace dimensions can be found in Figure 25.

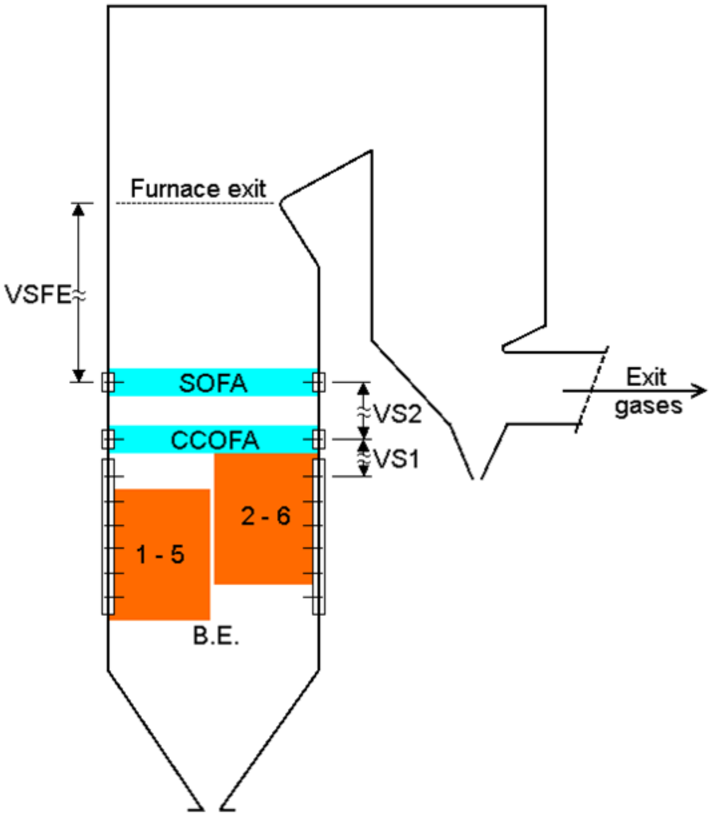

Figure 42. Schema of varying OFA elevation for FPP–2

To define the possible range in which a separate overfire air register (SOFA) could be allocated the conditions present at FPP–2 needs to be analyzed. As mentioned above a certain particle travel time is needed in order to largely complete combustion prior to entering the convective heating surfaces. Based on this fact, the required distance between SOFA elevation and furnace exit (VSFE) which guaranteed sufficient residence time can be calculated as follows:

$$\boldsymbol{OFA_{VSFE} = 1.5\,sec * 8.5\,\frac{m}{sec} = 12.75\,m \sim 13\,m} \qquad \text{(VII–6)}$$

The maximum available vertical distance between CCOFA and furnace exit is according to the dimensions given in Figure 25 approximately 21 m and thus is the possible remaining furnace height where OFA elevations could be allocated around 8 m. As stated in equation (**VII–5**) is the maximum permissible vertical spacing of air injection also 8 m. Why exactly one additional SOFA elevation had been considered for the sensitivity analysis shown in Figure 43.

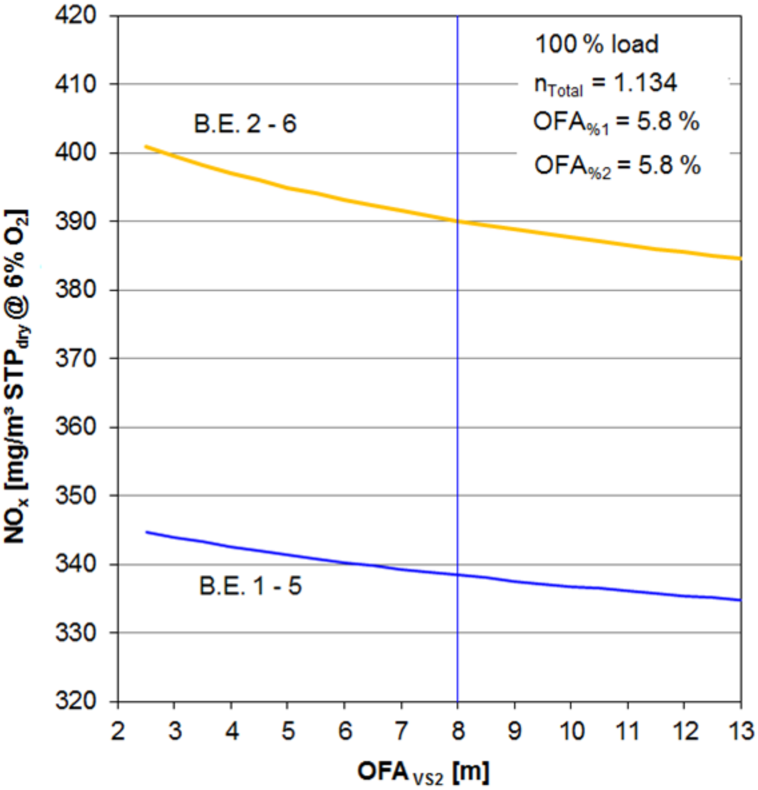

Figure 43. NO_{xPred} **vs.** OFA_{VS2} **(**$OFA_{\%2}$ **= 5.8 %) for FPP–2**

Figure 43 shows the results obtained from the sensitivity analysis extended by additional 5 m distance in order to get a better impression of the relationship between

NO_x emissions and vertical spacing of the SOFA, similar as done for Figure 41. Table 27 summarized the numbers of Figure 43.

Table 27. NO_{xPred} **vs.** OFA_{VS2} **(**$OFA_{\%2}$ **= 5.8 %) for FPP–2**

B.E:	**Total air ratio (n_{total})**	$OFA_{\%2}$ [%]	**OFA$_{VS2}$** [m]	NO_{xPred} [mg / m³ STP$_{dry}$ at 6 % O_2]
1 – 5	1.134	$\frac{11.6}{2}$	2.5	344.74
			8	338.42
2 – 6	1.134	$\frac{11.6}{2}$	2.5	400.92
			8	390.08

Table 27 shows for B.E. 1 – 5 and B.E. 2 – 6 a NO_x reduction potential of 6 mg and 10 mg (1.8 % and 2.7 %) respectively. It shall be remarked that this reduction belongs only to the increasing distance between CCOFA and SOFA register with equal amount of air supplied to both elevations. Based on the results and under consideration of the operational parameters chosen it can be quite clearly say that retrofitting of a separate overfire air elevation promises no appreciable success. This can mainly be explained by the fact that the OFA air portion per elevation of the total combustion air was reduced by half to keep the total OFA air portion constant. Therefore it can be concluded that the grade of influence is much more significant with the OFA air quantity instead of the injection elevation.

To proof the previous conclusion the reference operational settings for Figure 43 had been changed by the assumption, that every OFA elevation will supported by the same amount of combustion air while keeping the overall combustion oxygen level constant. That means, the necessary amount of combustion air has been taken from the burners and shifted to the additional SOFA elevation. The results are shown in Figure 44.

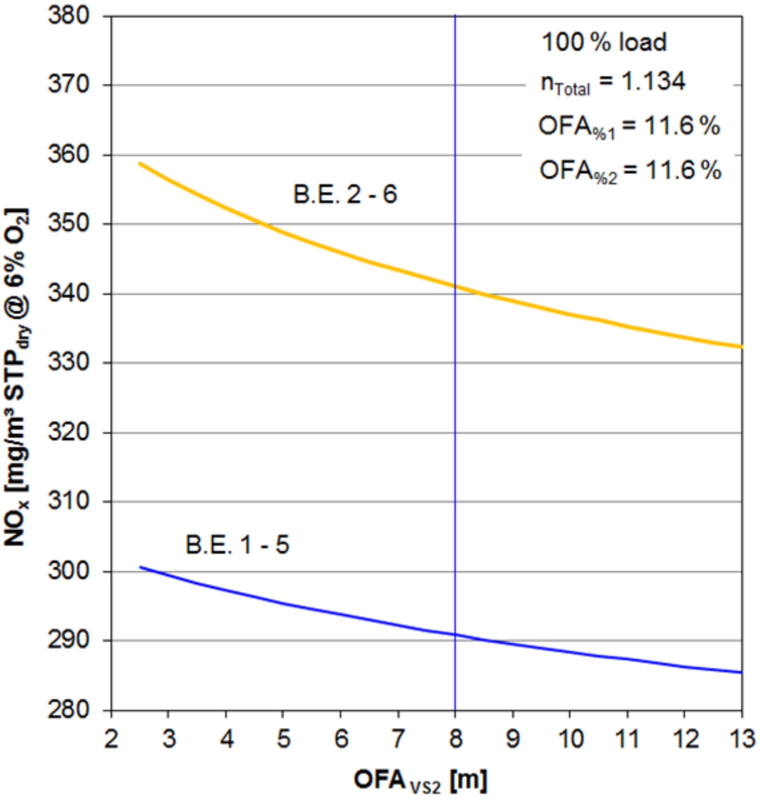

Figure 44. NO_{xPred} **vs.** OFA_{VS2} **(**$OFA_{\%2}$ **= 11.6 %) for FPP–2**

Table 28 summarized the numbers of Figure 44.

Table 28. NO_{xPred} **vs.** OFA_{VS2} **(**$OFA_{\%2}$ **= 11.6 %) for FPP–2**

B.E:	**Total air ratio (n_{total})**	$OFA_{\%2}$ [%]	**OFA**$_{VS2}$ [m]	NO_{xPred} [mg / m³ STP$_{dry}$ at 6 % O_2]
1 – 5	1.134	11.6	2.5	300.59
			8	290.87
2 – 6	1.134	11.6	2.5	358.79
			8	341.04

Table 28 shows for B.E. 1 – 5 and B.E. 2 – 6 a NO_x reduction potential of 3.2 % and 4.9 % respectively. That means, by doubling the amount of air per OFA elevation the reduction potential has almost doubled. Table 29 compared all obtained results.

Table 29. NO_x reduction potential trough OFA for FPP–2

Total air ratio (n_{total})	**B.E:**	$OFA_{\%1}$ [%]	**OFA_{VS1}** [m]	$OFA_{\%2}$ [%]	**OFA_{VS2}** [m]	**NO_x reduction potential** [%]
1.134	1 – 5	11.6	5 to 8	–	–	3.1
		5.8	2.5	5.8	2.5 to 8	1.8
		11.6	2.5	11.6	2.5 to 8	3.2
	2 – 6	11.6	2.5 to 8	–	–	8.2
		5.8	2.5	5.8	2.5 to 8	2.7
		11.6	2.5	11.6	2.5 to 8	4.9

It can be concluded that under the assumption made within this section the grade of influence regarding NO_x reduction potential is much more significant with the air quantity instead of the injection location. From the model point of view, the greatest NO_x reduction would be achieved when injecting the highest possible air amount to the highest possible OFA elevation. Unfortunately, this is not feasible in practice. As mentioned in the previous chapters the air staged combustion process is a complicated process that can quickly get out of balance. That means, the combustion process needs to be fed by the right amount of air at the right time in order to let the combustion reactions continuing until the flue gas leaves the furnace. What is reason, why nowadays it is preferred to install several OFA registers over the complete furnace height.

It is known that NO_x reduction efficiency increases with increasing stage–two air (OFA) rate. However not limitless, as described above leads too much burnout air to an increased in unburned carbon content in the fly ash, but also it increase the slagging and fouling behavior and high–temperature corrosion on the water wall in the burner belt due to the lack of oxygen. Furnace air–staged combustion can achieve high combustion efficiency if the burnout air position is optimized in combination with the air–staging rate. It shall be remarked, that from the model point of view, especially according to equation (**VI–10**), an OFA system can also has a negative effect on the NO_x formation. If the vertical distance between the upper active burners and the point of burnout air being injected becomes less than one meter the value of $\boldsymbol{h_3}$ will be getting greater than one, which causing an increase of the NO_x Indicator $(\boldsymbol{NI})$ according to equation (**VI–1**) and thus results in higher NO_x level prediction. This is mainly justified by the fact that in such case the residence times of the coal particles in the sub–stoichiometric zone becomes too low (less than 100 ms) and, thereby the particles devolatilization process extends well into secondary zone with higher oxygen concentrations. This is a critical issue about staged combustion because the fate of char–nitrogen which devolatilize in the late and oxidizing region is being exposed to further oxidation during final burnout and increase the NO_x level [151, 160]. Additionally the CO afterburning process could become such intensive that the reaction temperature rises over the critical value for thermal–NO_x generation and as a result, the total NO_x emission value will increase further. Objectively, it is questionable whether a OFA supplied such closed to the burner would be definable as overfire air or whether it is an upper air which should rather be assigned to the burner air streams directly.

From the NO_x emission perspective the developed prediction model can help to optimize any existing or new build boiler regarding lowest NO_x emissions but at any time must also the other factors to be considered in this context in order to establish a balanced mix with respect to availability, reliability and performance.

Permanent Burner–Out–of–Service

In case where no OFA elevations are installed can be the closure of the upper burner elevation an option to create air staging within the furnace with lowest cost [171]. This is accomplished by removing the coal supply from the upper burner row while keeping the air register open. The balance of the fuel is redirected to the lower burners, creating fuel–rich conditions in those burners. This technique is within the literature also known as burner–out–of–service (BOOS) but the major difference to the thesis at hand is that the system changed permanently. That means it become a system design modification instead of a changed operational setting. This possible system modification would combine two major system improvements. It creates an air staging environment and reduces the primary emission level due to the increased residence time of the particle within a sub–stoichiometric environment depended on the BOOS pattern selected.

Due to the fact that the initial conditions of such air–staging variant is absolutely identical with the principles of operation shown in the previous section the evaluation of this variant was dispensed. The results already achieved would only be repeated. What makes this method, however, a very cost effective way to reduce NO_x emissions efficiently.

Burner Design

The design of low–NO_x burners is even more critical than designing an overfire air system. Even minor changes in the discharge configuration of the nozzle design can result in a significant change in the emission behavior [172, 224]. As mentioned in chapter 'Burner Influence' it is recommendable not to focus only on burner details, rather than to consider the whole primary zone. Nakata et al. [97], Alfonso et al. [99] and Makino et al. [114] based their NO_x prediction techniques on describing different primary combustion conditions by the help of function coefficients which describes the boundary conditions based on a combination of variation possibilities (see Table 7). The analogy, to the approach presented in this thesis is, instead of various function coefficients the new approach described the primary zone conditions by the help of a burner index $(\boldsymbol{BI})$ (see equation (**VI–13**)). On the basis of the assumptions made in chapter 'Aerodynamic Effectiveness' and 'Furnace Influence' is the $\boldsymbol{BI}$ and the primary NO_x level $\left(\boldsymbol{NO_{x_{Prim}}}\right)$ directly related to the NO_x indicator $(\boldsymbol{NI})$. From this it follows, a change in $\boldsymbol{NO_{x_{Prim}}}$ will cause a change in the overall NO_x emission level $\left(\boldsymbol{NO_{x_{Ref}}}\right)$. In order to illustrate the correctness of this conclusion as well as to investigate the grade of influence, a sensitivity analysis had been carried out based on the reported experimental data of Hwang [202]. It shall be remarked that according to the findings obtained in chapter 'Operational Settings' every burner configuration of FPP–2 have different primary NO_x levels but it has been assumed that the primary NO_x level of all three known burner configurations (e.g. see Table 18) will decrease likewise. Figure 45 shows the relationship.

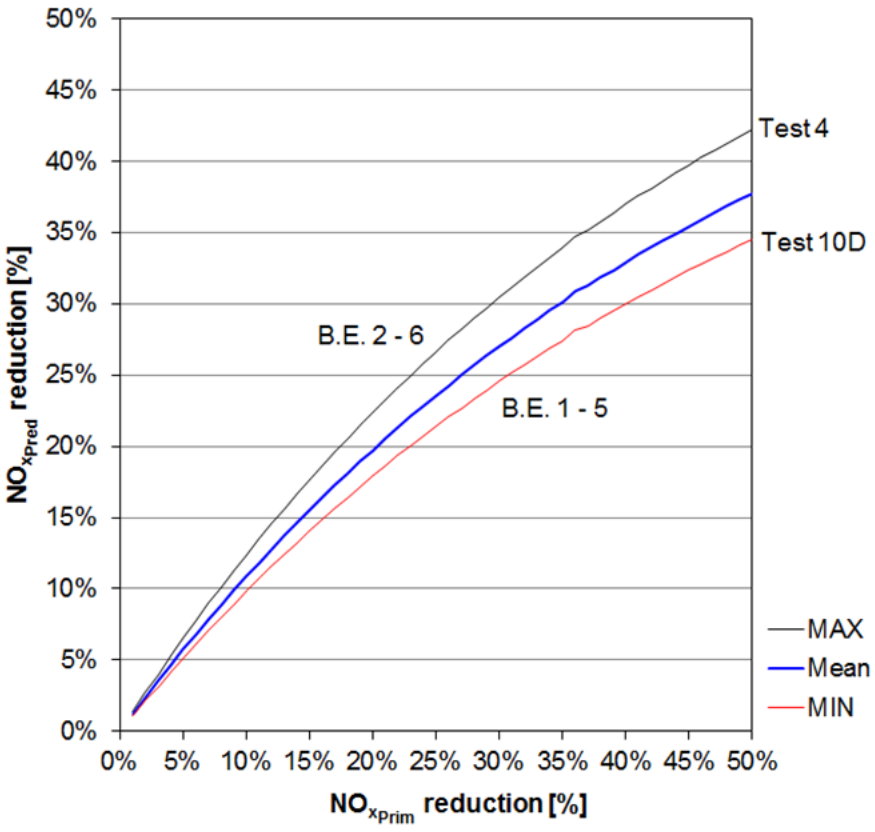

Figure 45. NO_{xPred} **vs.** NO_{xPrim} **reduction for FPP–2**

It has been shown that two sets of operational data represent the maximal and minimal possible relationship between $\boldsymbol{NO_{x_{Pred}}}$ and $\boldsymbol{NO_{x_{Prim}}}$. As Figure 45 suggest are the data available of Hwangs [202] ‘Test 4’ with active burner elevations (B.E.) 2 – 6 (black line in Figure 45) most susceptible for NO_x reductions whereas Hwangs [202] ‘Test 10D’ with active burner elevations (B.E.) 1 – 5 (red line in Figure 45) at least. It can be seen that the average grade of influence (blue line in Figure 45) of all data sets decrease as more the $\boldsymbol{NO_{x_{Prim}}}$ level will be reduced. Based on this, it can be concluded that higher $\boldsymbol{NO_{x_{Prim}}}$ levels and thus older and ineffective combustion systems seems to be more capable for NO_x reductions as newer low–NO_x systems with lower primary NO_x emission levels. What confirms the conclusions made in chapter ‘Burner Operation’.

This degree of dependence shall be illustrated by the following example. As mentioned in chapter ‘Aerodynamic Effectiveness’, there are two possible procedures to evaluate and define the primary emission level of a coal–fired furnace.

1. Reverse arithmetic via goal seek function according to a known target value, i.e. overall NO_x emission level $\left(\boldsymbol{NO_{x_{Ref}}}\right)$ as objective, primary NO_x level $\left(\boldsymbol{NO_{x_{Prim}}}\right)$ as variable.
2. Direct comparison with similar furnace conditions, i.e. matching parameters according to Table 7and Table 8.

Due to the fact that the research work done in this thesis based on real operational plant data, i.e. reference NO_x vales were available, the first procedure were used and thus a detailed description of the procedure is omitted since the equation (**VI–1**) has only one unknown. For that background the focus shall be on the second approach, especially since it can also provide information to which extent the underlying systems can be compared.

A comparison basement could be built on the basis of rough plant parameters which enabling to draw conclusions on expected primary emission levels after retrofit by the help of similar known parameter of other units. But even that is only possible with prudence. Because the design features of burners and its direct furnace condition can limit NO_x formation by controlling the stoichiometric and temperature profiles of the combustion process. These features influence the aerodynamic distribution and mixing of the fuel and air. Add to this, every boiler have individual load parameters (see Table 9) which define the average heat density within the furnace. Significant influence on the NO_x behavior of a boiler have the firing mode (wall– or tangential–fired) [97], the furnace size as well as type, burner configuration, and thermal capacity [197]. Referred to the assumptions made in chapter 'Furnace Influence' for the grade of the primary emission level respectively. Therefore it is recommendable not to compare every system with every system. Comparison criteria have to be defined in order to evaluate potential similarities of similar systems. Based on the reference unit used so far (FPP–2) means that, looking for tangential sub–bituminous coal–fired dry bottom boilers with similar thermal capacity. Table 30 shows such possible comparison done based on the reference units (see chapter 'Basis for Comparison').

Table 30. Primary emission levels of tangentially–fired units

Utility	**Thermal rating** MWt	**Design stage**	**Coal type**	**Active burner rows**	$\boldsymbol{BBVHR}$ MWt / m²	$\boldsymbol{NO_{x_{Prim}}}$ mg / m³ STP_{dry}[28]
Proprietary[29]	1,728	n.s.	High Vol. C Bit.	1 – 5	0.725	633
Fayette No. 2	1,567	1979	Sub–bit. C	1 – 5	0.428	785
Maasvlakte No. 2	1,300	1988	Medium Vol. Bit.	2 – 5	0.621	565

$\boldsymbol{BBVHR}$ is the burner belt volume heat release rate which is the quotient of the thermal capacity ($\dot{\boldsymbol{Q}}_{\boldsymbol{th}}$) and the burner belt volume ($\boldsymbol{BBV}$) according to equation (**VI–20**). All three boilers listed in Table 30 based on the tangential–fired concept and have been designed by Combustion Engineering Company (USA)[30]. In addition, the fuels used are not very far apart in terms of quality and thus these other two plants should be capable for

---

[28] Corrected to 6 % O_2

[29] Data based on the work of Zhou et al. [203].

[30] Since 2000 purchased by Alstom.

comparison. Unfortunately the design stage of the largest boiler is not specified but due to the relatively high $\boldsymbol{BBVHR}$ and the lower $\boldsymbol{NO_{x_{Prim}}}$ compared to FPP–2 it could be assumed to be somewhere in the middle or late 90's. Comparing the data given in Table 30 and taking into account that furnaces with larger dimensions are generally more capable for NO_x minimizing and completing carbon burnout [73, 123], than it could be assumed that a primary NO_x emission level of approximately 500 mg / m³ STP_{dry} at 6 % O_2 for the burner configuration (B.E.) 1 – 5 should be achievable even under conservative estimations. Nevertheless, in order to get a broader understanding three different reduction potentials have been investigated. Table 31 summarized the results obtained for primary NO_x level reductions of 25 %, 35 % and 45 % according to the relationship shown in Figure 45.

Table 31. Dependency of different NO_{xPrim} on NO_{xPred} for FPP–2

$\boldsymbol{NO_{x_{Prim}}}$ **reduction** %	**Reference acc. to Hwang [202]**	**B.E.**	$\boldsymbol{NO_{x_{Prim}}}$ mg / m³ STP_{dry}[31]	$\boldsymbol{NO_{x_{Pred}}}$ **reduction** %
25	Test 10D	1 – 5	589	21.40
	Test 4	2 – 6	645	26.65
35	Test 10D	1 – 5	510	27.42
	Test 4	2 – 6	559	33.89
45	Test 10D	1 – 5	432	32.37
	Test 4	2 – 6	473	39.74

---

[31] Corrected to 6 % O_2.

As stated above, even very minor changes in the discharge configuration of the burner tips can result in NO_x changes on the order of 25 – 30 % [172]. Nalbandian [225] reported that NO_x reduction potential of 30 – 50 % can be achieved with an acceptable content of unburnt carbon in the fly ash only by installation of new low–NO_x burners.

The results of the sensitivity analysis given in Figure 45 indicating that a burners retrofit would decrease the $\boldsymbol{NO_{x_{Prim}}}$ potential by 36.3 % (equivalent to 500 mg / m³ STP_{dry} at 6 % O_2 for 'Test 10D'). That means, the NO_x emissions at the economizer outlet would decrease by 30.9 % for the mean value. This result is in very good agreement with available literature also compared to other firing configuration, e.g. Douglas [226] reported 50 – 60 % reduction for wall–fired boilers with cell–burner arrangement. Normal wall–fired systems equipped with circular burners show a reduction efficiency of 35 – 40 % without overfire air [227].

In summary, low–NO_x burners appear very attractive, with potential NO_x reductions of up to 50 %, depending on its former design stage. A number of advanced burner designs are being developed and tested to reduce NO_x emissions of coal–fired utility boilers and although these research efforts focused on new installations but they can also be retrofitted to older units. Especially for retrofit applications, burner modifications have the advantage of requiring minor changes in current boiler design and operation why it might be the preferred combustion modification technique for coal–fired utility boilers.

Another cost effective alternative method which reduces the excess air available in the primary combustion zone is the biased–burner–firing technique (BBF) [91]. It consists of firing the lower rows of burners more fuel rich than the upper rows of burners.

This can be accomplished by adjusting the fuel flow so that a greater amount of fuel enters the furnace through the lower burner elevations than through the upper elevations while maintaining normal air distribution. An additional add–on could be to distribute the air vice versa. A portion of the combustion air is shifted away from the lower burners to the upper burners which reinforced the effect of firing air rich. This method should suppressed fuel– and thermal–NO_x formation.

Summary

NO_x formation during coal combustion is very complicated by the complexity of factors involved. Even with 40 years of effort to understand NO_x formation in coal combustion systems it remains quite difficult to predict the effectiveness of a low–NO_x combustion system. The major reason is that relationships between the constituents that comprise each single influence factor and NO_x emissions are masked by the impact of other factors. Each of these influence factors can consist of several sub–factors of more or less importance. The detailed understanding of their differences and their interactions within a specific furnace environment gain the possibility to optimize combustion systems with respect to efficiency and reliability under environmental awareness. Focused on the prediction of expected NO_x emissions means that the investigation on the influence of combustion variables and constraints with reasonable computational effort.

The chapter 'Comparison with the Literature' shows the theoretical application of the developed NO_x prediction approach on an existing coal–fired utility boiler. The chosen reference unit 2 of Fayette power plant stands exemplary for all dry bottom coal–fired units. On the basis on operational data documented by J. Hwang (1997) [202] during his full–scale experiments, sensitivity analysis were carried out by varying a parameter while holding the other parameter constant as far as that was plausible with respect to real operation conditions. The results show very good conformities of the model history and observations reported by other researchers which provide evidence concerning the applicability of the whole prediction model.

It can be concluded that the developed approach acts as good approximation, especially the strong statistical model correlation coefficient indicate that the developed interpolative NO_x prediction technique could serve a very useful tool in identifying key variables that affect NO_x formation and highlights general trends in order to achieve required NO_x emission levels. A number of potential problems due to superpositioning of different influence factors which cannot be decoupled in practical experiments were shown, at least in full–scale applications. Precisely for this reason, could the described relationships and illustration of superposition effects help for further investigations and experimental works to the understanding of NO_x formation in self–sustaining pulverized coal–fired utilities.

Furthermore it shall be remarked, that in 2004 the reference boiler FPP–2 was modified and shows now significant lower NO_x emissions with minimal effects on boiler performance [228]. This could be realized by changing the primary combustion zone conditions plus an additional modification on the overfire air system. Thanks to these efforts became FPP the first coal–fired facility in Texas to be recognized at the gold level by the Texas Commission on Environmental Quality Clean Texas Program for taking steps beyond regulatory requirements to reduce its impact on the environment in 2009 [229]. A prime example for the implementation of today's options regarding combustion system optimizations with respect to efficiency under environmental awareness.

VIII. SUMMARY, CONCLUSION AND RECOMMENDATIONS

Summary

Although, coal combustion generates high quantities of NO_x emissions which are a significant driver for photochemical smog and acid rain, is nearly every economic engine primarily fueled by coal. Coal will continue to be one of the major sources of electricity generation for the world for indefinite time but it needs to be reliable, economical and definitely ecological too in order to protect life, environment and ensure climate stability. Increasing competition and stricter emission legislation force power plant operators to improve the economic and combustion performance of their boilers.

The formation process of NO_x is a very complicated result of burning pulverized coal due to inherent nitrogen in both the coal particle and the combustion air. Fundamental investigations to determine the mechanism of NO_x formation during coal combustion has been done for many years but it is still an imperfectly understood phenomenon. At the same time NO_x emissions can be influenced by process modification more than any other pollutant. Practical testing is expensive and time consuming. Consequently numerical models which can predict various combustion performances under certain boundary conditions and individual input factors are becoming increasingly important. Many chemistry and physical aspects have to be coupled in a way that allows realistic prediction of NO_x formation of practical coal–fired boilers with reasonable computational effort.

For this background a comprehensive literature research focused on published NO_x prediction approaches from scientific publications based on fundamental quantitative relationships, empirical algorithms and statistical relationships were carried out in order to summarize all the efforts already undertaken and to show / take up possible synergy effects. It can be concluded that although, a considerable number of prediction techniques are available, these models usually related to a small part of fundamental combustion variables and do not consider significant boundary conditions described by the interplay between furnace design, operational settings and coal properties. Consequently, a more empirical approach had been developed in this study which is within a reasonable range independent of the previous mentioned conditions. The approach based on systematically targeted extending investigations under the requirement of objectivity and repeatability. Focused on the prediction of NO_x emissions means that, the investigation on the interaction of combustion variables and constraints, and possible relationships between collected available information and numerically calculated helping factors. The developed model shows a strong statistical significance with a coefficient of determination of 0.9876 and a standard error of 28 mg / m³ STP_{dry} at 6 % O_2 based on 142 observations coming from 28 utility units. Sensitivity analyses have been carried out and direct comparisons between model history and observations reported by other researchers have also shown very good conformities. Why this thesis forms a good basis for identifying individual factors which contributes to system related NO_x emissions in order to investigate how variations in the process parameters affect the emission level. Perhaps, as contribution to the understanding of NO_x formation during coal combustion, or as basis for possible process optimization which might find application on pulverized coal–fired boilers. It is noted that since the data base was limited, the model should only be examined for general trends. Indeed it should not be considered predictive, but interpolative. Nevertheless, the above described model accuracy should be more than sufficient, to interpretate and optimize the operation of any pulverized coal–fired furnace, to evaluate economical investigations for possible system improvements or modifications, and to assess the environmental impact of traded coals from geographically diverse sources, with respect to efficiency and reliability under environmental awareness.

Conclusion

Towards that end, the following conclusions can be made from the foregoing research regarding NO_x formation in dry bottom pulverized coal–fired systems:

- The performed literature research identified nineteen approaches established by other researcher between 1971 and 2004. Including the developed approach in this thesis results the register in twenty NO_x prediction techniques. Thus, this thesis includes the most comprehensive and completest register of NO_x prediction techniques based on fundamental quantitative relationships, empirical algorithms and statistical relationships at the present time.
- The developed model is the first model which considers changes in the magnitude of variables which belongs to all three major groups of NO_x influences (furnace design, operational parameter, coal properties) at the same time. The model key variables for staged–air low–NO_x firing systems are:
    - Coal volatile portion, fixed carbon hydrogen and nitrogen content.
    - Main burner zone stoichiometry.

- Primary zone mixing effectiveness.
- Furnace burner belt heat density.
- Overfire air portion.
- Overfire air elevation above main burners.
- Excess oxygen content.

Thus, this research work successfully attempted to combine experimental results of previous studies, operational field data, and scientific and industrial knowhow into one framework.

- The model consists of different sub–models which were developed mainly via multiple regression analysis. First and second orders as well as exponential growing sub–models were required to fit the NO_x emissions data compiled as discussed in chapter 'Model Basis'. Therefore it can be concluded that NO_x formation is usually nonlinear with fundamental combustion parameters. Which can be confirmed by the fact that first order model does not correlate the data successful.
- The model based on the assumption that for lowest NO_x combustion special attention needs to be done regarding the optimum oxygen concentration within the closed flame area (see chapter 'Ignition Behavior'). It has been postulated that lower ranked coals would need a higher oxygen concentration than higher ranked coals. This contradicts the general opinion that lower O_2 levels within the primary combustion zone leads always to lower NO_x production as rather that the right O_2 level for lowest NO_x emissions depends on the coal volatile content.

- The market for retrofit demands on existing coal–fired boilers will be significant for the next several years as plant owners have to comply with the Clean Air Act and Ambient Air Quality environmental regulations. The here presented model methodology allows every interested process engineer to draw conclusions on expected NO_x emission levels under given conditions. Especially the possibility to adjust coefficients of the sub–models according to any available field data makes the use of the model very flexible.
- The model includes a way of estimating coal properties regarding their NO_x emission behavior without the necessarily of a certain combustion environment. By using the first helping factor (equation (**VI–8**)) alone it is possible to estimate whether NO_x emissions will increase or decrease compared to the reference coal if assuming that all other process conditions remains unchanged.
- It has been stated by others that the contribution of char nitrogen under oxidizing conditions is lower than the contribution of volatile nitrogen [72, 214, 230] but higher pyrolysis temperatures during the devolatilization process leads to an additional release of nitrogen with the volatiles [103, 231–233]. Due to the fact that the real pyrolysis temperature during the devolatilization process deemed as an unknown variable most research works relies on the adiabatic flame temperature[32] as indicator for the activation energy. This adiabatic flame temperature depends mainly on the carbon and hydrogen content of the coal. Therefore tends a low volatile coal (high ranked) to much higher adiabatic flame temperatures as high volatile coals (low ranked) and for thus, the possibility of

---

[32] The adiabatic flame temperature results from a complete combustion process that occurs without any heat exchange or changes in kinetic or potential energy.

NO_x formation is smaller for coals containing more volatile matter, than for coals containing less volatile matter.

- The estimation of the effective volatile content based on proximate and ultimate analysis measurements which are usually fixed in contracts. A procurement strategy could be based on the decision whether a particular coal should be burned in a power plant of interest or not. Because the increased international trade in coal makes it essential that the environmental impact of traded coals from geographically diverse sources can be assessed accurately. Much has been published on coal switching as a method of meeting Clean Air Act compliance for sulfur dioxide, e.g. [234–236]. Very little has been published on NO_x.
- Although a detailed mechanistic explanation of volatile evolution has not been described so far, some certain influence factors are discernible. Volatile evolution depends on fuel–composition and heating rate. If the weight loss of a coal particle under real flame conditions exceeds the proximate volatile matter contents by 10 – 100 % [133] the test procedure of the standard test method for volatile matter in the analysis sample of coal and coke (ASTM D3175–11) needs to be overthought. The model includes a possible correction of the volatile matter content according to its burning and ignition characteristics. The new described effective volatile content based on the mass proportion of the key components carbon and hydrogen related to the mass of all volatile ingredients.

Recommendations

Even with 40 years of effort to understand NO_x formation in coal combustion systems, it remains difficult to predict the effectiveness of low–NO_x combustion systems.

A number of research recommendations were identified which could lead to a better understanding on NO_x production and could allow the coal industry to be able to respond effectively to trends in NO_x control technologies.

NO_x Formation Pathways for Pulverized Coal Flames

The principle NO_x formation pathways established by e.g. De Soete [237], Fiveland and Wessel [42], Bowman [38], Smoot [238], Visona and Stanmore [138], Daood et al. [175] during the coal pyrolysis and combustion under laboratory conditions based on the observation of previous prepared particles entering the furnace. That means, the research focused on the time when the coal devolatilization process of the particles starts due to the self–sustaining heat generation inside the combustion chamber. Thus, the formation process of NO_x is a result of inherent nitrogen in the coal particle and the combustion air reacting in the furnace. But under full–scale applications it can be postulated that the coal particles are being accompanied by already devolatilize nitrogen portions when entering the furnace due to the particle grinding process. Therefore the formation process of NO_x within a furnace at a very early point could be considered as a result of inherent nitrogen in the coal particle and in the combustion air extended by already existing volatile nitrogen which has been driven–off the particles during the grinding. The coal devolatilization process occurs in two steps. First the grinding process where the cool particles come in content with hot secondary air or / and hot flue gas which provides the thermal energy needed for the vaporization of the water and the heating of the coal, and second the extreme heating pyrolysis during the primary pyrolysis at the burner outlet inside the furnace. The coal particles are already preheated at temperature of around 80 to 170 °C during the grinding process and will be injected into the furnace with a specific amount of residual inherent moisture (typically ~ 2 – 3 %). It is therefore recommended to extent the NO_x formation pathway by third factor, i.e. existing volatile nitrogen.

Volatile Matter Content of Coals

Volatile evolution depends on fuel–composition and heating rate. Due to the fact that the heating rates under real furnace conditions are much higher than these occurring during the standard test method (ASTM D3175–11) it is recommended to overthink the test procedure in order to describe the effective volatile content of coals based on practical conditions. Therefore it is recommended to change to extremer heating rates for more realistic results.

Primary NO_x Value

Due to the variety of possible influence factors which determine the actual conditions of the primary combustion zone within utility boilers and the limited access to the required detailed information concerning the in Table 7 and Table 8 listed influence factors it was not possible to identify any reasonable relationship according to the estimated burner influence factors given in equation (**VI–13**). Future research in this area would certainly help to improve the presented NO_x prediction technique as well as to gain the understanding concerning major influence factors and relationships contributing to NO_x emissions.

Boiler Types

Due to the fact that there are several different utility boiler designs in widespread use would it be of great importance to extent, adjust or modify the developed NO_x

prediction approach according to other boiler applications which have been excluded within this thesis. In the area of pulverized coal–fired boilers, these are for example slag–tap firing systems (see Figure 4), e.g. U–shaped or W–shaped downshot–fired units. Furthermore, cyclone–fired or turbo–fired furnaces but also for utility boilers which work without burners as stoker–fired or fluidized–bed boilers, will be a need for simple models suitable for use by coal marketers and plant operators to allow the prediction of NO_x emissions from utility boilers for different coals.

CO Emissions and Loss of Ignition

As stated even small changings on an air–staged low–NO_x system can have significant effects on NO_x, CO emissions and loss of ignition (LOI). The developed approach focused exclusively on NO_x emissions but special attention needs to be made on CO and LOI when the NO_x level getting improved. The inclusion of CO emission and LOI predictions could be help to draw conclusions on the reverse acting factors which improve the optimization possibilities regarding more objectives. Any research focused on a model extension by these factors would be appreciated.

REFERENCES

1 DIN 1343:1990–01 (1990): *Reference conditions, normal conditions, normal volume, concepts and values*, Norm

2 BP p.l.c. (2010): *Statistical Review of World Energy 2010*, London, United Kingdom, June 2010

3 International Energy Agency (2011): *World Energy Outlook 2011*, IEA, 696 p, ISBN: 978 92 64 12413 4, November 2011

4 EIA, U.S. Energy Information Administration (2011): *International Energy Outlook 2011*, DOE/EIA–0484(2011)

5 Eddinger, J., Grano, D., William, V., Ravi, S. (1999): *Nitrogen Oxides (NOx) why and how they are controlled*, EPA–456/F–99–006R, 57 p

6 Directive 2010/75/EU of the European Parliament and of the Council of 24 November 2010 on industrial emissions (integrated pollution prevention and control) (Recast)

7 Munir, S., Akhtar, N.A., Nimmo, W., Gibbs, B.M. (2009): *NOx Formation During Combustion Process and in– Furnace Control Technologies*, Journal of Pakistan Institute of Chemical Engineers, Volume 37, pp 15–23

8 Li, Z.Q., Wie, F., Jin, Y. (2003): *Numerical simulation of pulverized coal combustion and NO formation*, Chemical Engineering Science 58, pp 5161–5171

9 BP p.l.c. (2013): *BP's Energy Outlook 2030*, January 2013

10 Yin, J., Ren, J., and Wei, D. (2008): *NOx control in large–scale power plant boilers through superfine pulverized coal technology*, Frontiers of Energy and Power Engineering in China, Volume 2, Issue 4, pp 461–465

11 Opaprakasit, P. (2003): *Interaction and the structures of coal*. The Pennsylvania State University, ProQuest Dissertations and Theses, 199 p

12 ASTM D388 (1998): *Standard Classification of Coal by Rank*, CFR Section: 40 CFR 60.251(b), American Society for Testing and Materials

13 U.S. Department of Energy (2008): *Coal Production and Preparation Report*, Energy Information Administration Form, EIA–7A

14 Skorupska, N.M. (1993): *Coal Specifications: Impact on Power Station Perfermonce*, IEA Coal Research, London, UK, IEACR/52, ISBN: 9789290292104, January 1993, 120 p

15 Unsworth, J.F., Barratt, D.J., Roberts, P.T. (1991): *Coal Quality and Combustion Performance*. Part A, Coal Science and Technology, Volume 19, Elsevier, Amsterdam

16 Miller, B.G., Tillman, D. (2008): *Combustion Engineering Issues for Solid Fuel Systems*. Elsevier Academic Press, San Diego, California, ISBN: 0–123736110, 528 p

17 ISO 562–2010 (2010): *Hard Coal and Coke – Determination of Volatile Matter*, Norm

18 Bragg, L.J., Oman, J.K., Tewalt, S.J., Oman, C.L., Rega, N.H., Washington, P.M., and Finkelman, R.B. (1998): *U.S. Geological Survey coal quality (COALQUAL) database*, version 2.0, U.S. Geological Survey Open–File Report 97–134

19 Slezak, S. E. (1984): *Combustion of coal dust–air mixtures (flammability, radiation, volatile)*. University of Illinois at Urbana–Champaign, ProQuest Dissertations and Theses, 310 p

20 Bose, A.C., Dannecker, K.M., Wendt, J.O.L. (1988): *Coal composition effects on mechanisms governing the destruction of nitric oxide and other nitrogenous species during fuel–rich combustion*, Energy Fuels, Volume 2, Issue 3, pp 301–308

21 Ohtsuka, Y., Mori, H., Nonaka, K., Watanabe, T., and Asami, K. (1993): *Selective Conversion of Coal Nitrogen to N_2 with Iron*, Energy and Fuels, Volume 7, Issue 6, pp 1095–1096

22 Mori, H., Asami, K., and Ohtsuka, Y. (1996): *Role of Iron Catalyst in Fate of Fuel Nitrogen during Coal Pyrolysis*, Energy and Fuels, Volume 10, Issue 4, pp 1022–1027

23 Leppälahti, J., Simell, P., and Kurkela, E. (1991): *Catalytic Conversion of Nitrogen Compounds in Gasification Gas*, Fuel Processing Technology, Volume 29, pp 43–56

24 Solomon, P.R., Hamblen, D.G., Carangelo, R.M., Serio, M.A., Deshpande, G.V. (1988): *General model of coal devolatilization*, Energy Fuels, Volume 2, Issue 4, pp 405–422

25 Essenhigh, R.H. (1981): *Fundamentals of Coal Combustion*. Chemistry Coal Utilization, ed. M. A. Elliott, 2nd suppl.. vol., J. Wiley, New York

26 Illerup, J.B., Dam–Johansen, K., Glarborg, P. (1994): *Characterization of a full–scale, single–burner pulverized coal boiler: Temperatures, gas concentrations and nitrogen oxides*, Fuel, Volume 73, Issue 4, pp 492–499

27 van der Lans, R.P., Glarborg, P., Dam–Johansen, K. (1997): *Influence of process parameters on nitrogen oxide formation in pulverized coal burners*, Progress in Energy and Combustion Science, Volume 23, Issue 4, pp 349–349

28 Chen, J.C., Castagnoli, C., Niksa, S. (1992): *Coal devolatilization during rapid transient heating. 2. Secondary pyrolysis*, Energy Fuels, Volume 6, Issue 3, pp 264–271

29 Sotirchos, S.V., Amundson, N.R. (1984): *Diffusion and reaction in a char particle and in the surrounding gas phase. A continuous model*, Industrial & Engineering Chemistry Fundamentals, Volume 23, Issue 2, pp 191–201

30 Pregermain, S. (1988): *Rank and maceral effects on coal combustion characteristics*, Fuel Processing Technology, Volume 20, pp 297–306

31 Morgan, P. A., Robertson, S.D., Unsworth, J.F. (1987): *Combustion studies by thermogravimetric analysis: 2. Char oxidation*, Fuel, Volume 66, Issue 2, pp 210–215

32 Hippo, E., Walker, P.L. Jr. (1975): *Reactivity of heat–treated coals in carbon dioxide at 900 °C*, Fuel, Volume 54, Issue 4, pp 245–248

33 Solomon, P.R., Colket, M.B. (1979): *Coal devolatilization*, Symposium (International) on Combustion, Volume 17, Issue 1, pp 131–143

34 Freihaut, J.D., Zabielski, M.F., Seery, D.J. (1982): *A parametric investigation of tar release in coal devolatilization*, Symposium (International) on Combustion, Volume 19, Issue 1, pp 1159–1167

35 Chen, J.C., Niksa, S. (1992): *Coal devolatilization during rapid transient heating. 1. Primary devolatilization*, Energy Fuels, Volume 6, Issue 3, pp 254–264

36 Miller, B.G. (2005): *Coal Energy Systems*, Elsevier Academic Press, San Diego, California, ISBN: 0–12–497451–1, 543 p

37 Rayaprolu, K. (2009): *Boilers for Power and Process*, CRC Press Taylor & Francis Group, pp 3, 6, 11–13, 27, 79, 97–98, 132

38 Bowman, C.T. (1992): *Control of combustion–generated nitrogen oxide emissions: Technology driven by regulation*, Symposium (International) on Combustion, Volume 24, Issue 1, 1992, pp 859–878

39 Lucka, K. (1996): *Contribution to the reduction of NOx emissions through systematic manipulation of the flow control in combustion*, RWTH Aachen University, Dissertations and Theses, 83 p

40 Goodger, A.M. (2004): *The formation of nitrogen oxides in a pulverized coal boiler*, The University of Southern Queensland, 130 p

41 Cox, R.A. (1982): *Chemical Transformation Process for NOx Species in the Atmosphere*, *Air Pollution by Nitrogen Oxides*, Proceedings of the US–Dutch International Symposium, pp 45–60

42 Fiveland. W.A., Wessel, R.A. (1991): *Model for predicting formation and reduction of NO sub (x) in three–dimensional furnaces burning pulverized fuel*, Journal of the Institute of Energy, Volume 64, pp 41–54

43 Hori, M. (1988): *Nitrogen dioxide formation by the mixing of hot combustion gas with cold air*, Symposium (International) on Combustion, Volume 22, Issue 1, pp 1175–1181

44 Wendt, J.O.L. (1980): *Fundamental coal combustion mechanisms and pollutant formation in furnaces*, Progress in Energy and Combustion Science, Volume 6, Issue 2, pp 201–222

45 Zeldovich, Ya.B. (1946): *The Oxidation of nitrogen in combustion explosions*, Acta Physiochimica USSR, Volume 21. Issue 4, pp 577–628

46 Fenimore, C.P., Jones, G.W. (1957): *The Water–Catalyzed Oxidation of Carbon Monoxide by Oxygen at High Temperature*, Journal of Physical Chemistry, Volume 61, Issue 5, pp 651–654

47 Fenimore, C.P. (1971): *Formation of nitric oxide in premixed hdrocarbon fames*, Symposium (International) on Combustion, Volume 13, The Combustion Institute, pp 373 379

48 Johnsson, J.E., Glarborg, P. & Dam–Johansen, K. (1992): *Thermal dissociation of nitrous oxide at medium temperatures*, Symposium (International) on Combustion, Volume 24, Issue 1, pp 917–923

49 Bowman, C.T. (1973): *Kinetics of nitric oxide formation in combustion processes*, Symposium (International) on Combustion, Volume 14, Issue 1, pp 729–738

50 Sarofim, A.F. & Pohl, J.H. (1973): *Kinetics of nitric oxide formation in premixed laminar flames*, Symposium (International) on Combustion, Volume 14, Issue 1, pp 739–754

51 Malte, P.C. & Pratt, D.T. (1977): *Hydroxyl radical and atomic oxygen concentrations in high–intensity turbulent combustion*, Symposium (International) on Combustion, Volume 16, Issue 1, pp 145–155

52 Fenimore, C.P. & Fraenkel, H.A. (1981): *Formation and interconversion of fixed–nitrogen species in laminar diffusion flames*, Symposium (International) on Combustion, Volume 18, Issue 1, pp 143–149

53 Miller, J.A., Branch, M.C., Mc Lean, W.J., Chandler, D.W., Smooke, M.D. & Kee, R.J. (1984): *The conversion of HCN to NO and N2 in H2−O2−HCN−Ar flames at low pressure*, Symposium (International) on Combustion, Volume 20, Issue 1, pp 673–684

54 Glarborg, P., Miller, J.A. & Kee, R.J. (1986): *Kinetic modeling and sensitivity analysis of nitric oxide formation in well–strirred reactors*, Combustion and Flame, Volume 65, Issue 2, pp 177–202

55 Fong, W.S., Peters, W.A. & Howard, J.B. (1996): *Kinetics of generation and destruction of pyridine extractables in a rapidly pyrolysing bituminous coal*, Fuel, Volume 65, Issue 2, pp 251–254

56 Niksa, S. (1988): *Modeling the devolatilization behavior of high volatile bituminous coal*, Symposium (International) on Combustion, Volume 22, Issue 1, 1989, pp 105–114

57 Cheng, M.T., Kirsch M.J. & Lester T.W. (1989): *Reaction of nitric oxide with bound carbon at flame at temperatures*, Combustion and Flame, Volume 77, Issue 2, pp 213–217

58 Miller, J.A., Bowman, C.T. (1989): *Mechanism and modeling of nitrogen chemistry in combustion*, Progress in Energy and Combustion Science, Volume 15, Issue 4, pp 287–338

59 Muzio, L.J., Montgomery, T.A., Samuelsen, G.S., Kramlich, J.C., Lyon, R.K. & Kokkinos, A. (1990): *Formation and measurement of N2O in combustion systems*, Symposium (International) on Combustion, Volume 23, Issue 1, pp 245–250

60 Glarborg, P., Lilleheie, N.I., Byggstøyl, S., Magnussen, B.F., Kilpinen, P. & Hupa, M. (1992): *A reduced mechanism for nitrogen chemistry in methane combustion*, Symposium (International) on Combustion, Volume 24, Issue 1, pp 889–898

61 Williams, A., Woolley, R. & Lawes, M. (1992): *The formation of NOx in surface burners*, Combustion and Flame, Volume 89, Issue 2, pp 157–166

62 Tomeczek, J. & Gradoń, B. (1997): *The role of nitrous oxide in the mechanism of thermal nitric oxide formation within flame temperature range*, Combustion Science and Technology, Volume 125, Issue 1–6, pp 159–180

63 Schnell, U., Epple, B., Spliethoff, H. (1991): *Modelling of pulverised coal combustion with special emphasis on NOx formation and mixing phenomena related NOx reduction*, Proceedings of the 2nd International Symposium on Coal Combustion Science and Technology, Beijing, China, 7–10 October 1991, Beijing, China, China Machine Press, pp 98–107

64 Visona, S.P., Stanmore, B.R. (1995): *Prediciton of nitric formation in a turbulent premixed pulverised coal flame*, In 2nd International Conference on Combustion and Emission Control, London UK, 4–5 December 1995, London, UK, Institute of Energy. pp 199–208

65 Förtsch, D., Kluger, F., Schnell, U., Spliethoff, H., Hein, K.R.G. (1998): *A kinetic model for the prediction of no emissions from staged combustion of pulverized coal*, Symposium (International) on Combustion, Volume 27, Issue 2, pp 3037–3044

66 Chui, E.H., Hughes, P.M.J. (1996): *Validation of Nox and Nox precursor predictions in coal flames*, Combustion Science and Technology, Volume 119, Issue 1/6, pp 51–75

67 Chui, E.H., Gao, H. (2010): *Estimation of NOx emissions from coal–fired utility boilers*, Fuel, Volume 89, Issue 10, pp 2977–2984

68 Bowman, C.T., Seery, D.J. (1972): *Investigation of NO Formation Kinetics in Combustion Processes: The Methane–Oxygen–Nitrogen Reaction*, Emissions from Continuous Combustion Systems, Plenum Press, NY, pp 123–139

69 Bowman, C.T. (1992): *Control of combustion–generated nitrogen oxide emissions: Technology driven by regulation*, Symposium (International) on Combustion, Volume 24, Issue 1, pp 859–878

70 Eddings, E.G., Molina, A., Pershing, D.W., Sarofim, A.F., Fletcher, T.H., Zhang, H., Davis, K.A., Dension, M., Shim, H. (2002): *Minimization of NO emissions from multi–burner coal–fired boilers*, U.S. Deptartment of Energy Grant No. DE–FG26–97FT97275, University of Utah, Brigham Young University, Brigham Young University, Report, 353 p

71 Niessen, W.R. (2002): *Combustion and Incineration Process, Applications in Environmental Engineering*, Marcel Dekker Inc. New York. 3rd Edition, ISBN: 0–8247–0629–3

72 Pershing, D.W., Wendt, J.O.L. (1977): *Pulverized coal combustion: The influence of flame temperature and coal composition on thermal and fuel NOx*, Symposium (International) on Combustion, Volume 16, Issue 1, pp 389–399

73 Nordin, J.S., Merriam, N.W. (1997): *NOx Emissions produced with combustion of Powder River Basin Coal in a Utility Boiler*, U.S. Dep. Of Energy DE–FC21–93MC30127 Task 9

74 Fenimore, C.P. (1974): *Effects of Dilutens and Mixing on Oxide from Fuel Nitrogen in Diffusion flames*, Symposium (International) on Combustion, Volume 16, pp 169–179

75 Bergsma, F. (1985): *Abatement of nitrogen oxide (NOx) from coal combustion. Chemical background and present state of technical development*, Industrial and Engineering Chemistry Process Design and Development, Volume 24, Issue 1, pp 1–7

76 Fenimore, C. P. (1976): *Reactions of fuel–nitrogen in rich flame gases*, Combustion and Flame, Volume 26, February–June 1976, pp 249–256

77 Michelfelder, S., Jacobs, J., (1979): *20 Years of Pulverized–Coal Firing Research of IFRFdVV and Actual Test Results of Pulverized–Coal Flames*, Combustion, Volume 51, Issue 6, December 1979, pp 7–17

78 Sloss, L. (1998): *Trends in NOx emissions from coal utilization*, IEA Coal Research, Report CCC/02, ISBN: 92–9029–302–0, pp 49

79 Reed, R.J. (1997): *Combustion Handbook,* North American Mfg. Co., Volume 2, 3rd Edition, ISBN: 0–9601596–3–0 (v.II)

80 Boyd, R.K., Nelson, P.F., McEwan, B.R., Nguyen, T.H. (2000): *Review of NOx Formation in PF Combustion*, University of Newcastle (N.S.W.), Advanced Technology Centre, Cooperative Research Centre for Black Coal Utilisation

81 Smith, R.D.C., Conroy, A., Stanmore, B. (1996): *Development of a NOx Predictor for pulverised Coal combustion. Impact of coal quality on thermal coal utilization*, CRC coal utilisation– A practical workshop, 1–4 September 1996, Brisbane, Australia

82 Zhou, L., Qiao, L., Zhang, J. (2003): *Simulation of NOx formation in turbulent swirling combusiton using a usm turbulence chemistry model*, ACTA Mechanica Sinicia, Volume 19, Issue 3

83 Fan, J., Sun, P., Zha, X., Cen, K. (1999): *Modeling of Combustion Process in 600 MW Utility Boiler Using Comprehensive Models and Its Experimental Validation*, Energy Fuels, Volume 13, Issue 5, pp 1051–1057

84 Zeng, L., Li, Zh., Zhao, G., Shen, Sh., Zhang, F. (2010): *Numerical Simulation of Combustion Characteristics and NOx Emissions in a 300 MWe Utility Boiler with Different Outer Secondary–Air Vane Angles*, Energy Fuels, Volume 24, Issue 10, pp 5349–5358

85 Chen, Zh., Li, Zh., Zhao, G., Shen, Sh., Zhang, F. (2011): *Gas/particle flow and combustion characteristics and NOx emissions of a new swirl coal burner*, Energy (Oxford), Volume 36, Issue 2, pp 709–723

86 Stanmore, B. R., Visona, S.P. (2000): *Prediction of NO emissions from a number of coal–fired power station boilers*, Fuel Processing Technology, Volume 64, Issues 1–3, pp 25–46

87 Gao, F., Han, P., Zhai, Y., & Lu, Y. (2012): *Computational intelligence in low NOx emission combustion for coal–fired power plants*, International Journal of Advancements in Computing Technology, Volume 4, Issuer 14, pp 69–75

88 Bartok, W., Crawford, A.R., Piegari, G.J. (1971): *Systematic field study of NOx emission control methods for utility boilers*, Linden, N.J., Esso Research and Engineering Co., Government Research Laboratory, 230 p

89 Crawford, A. R., Manny, E. H., Bartok, W. (1974): *Field Testing: Applications of Combustion Modifications to Control NOx Emissions from Utility Boilers*, U.S. Environmental Protection Agency, NTIS Report Pb–237 344, 151 p

90 Pershing, D. W. (1976): *Nitrogen–oxide formation in pulverized coal flames*, The University of Arizona, ProQuest Dissertations and Theses, 411 p

91 Lim, K.J., Waterland, L.R., Castaldini, C., Chiba, Z., Higginbotham, E.B. (1980): *Environmental Assessment of Utility Boiler Combustion Modification NOx Controls: Volume 1 – Technical Results*, U.S. Environmental Protection Agency, Office of Air Quality Planning and Standards, Research Triangle Park, N.C.,EPA–600/7–80–075a, 443 p

92 Chen, S.L., Heap, M.P., Pershing, D.W., & Martin, G.B. (1982): *Influence of coal composition on the fate of volatile and char nitrogen during combustion*, Symposium (International) on Combustion, Volume 19, Issue 1, pp 1271–1280

93 Nelson, P.F., Nancarrow, P.C., Bus, J., Nicholls, P.M.., Prokopiuk, A. (2001): *Improved techniques for the prediction of NO formation from char N*, Research Report 24, Cooperative Research Centre for Black Coal Utilisation, The University of Newcastle

94 Nakazawa, T., Kawamura, T. (1982): *Operating experience of Matsushima power station no. 1 and no. 2 coal fired boilers*, Thermal and nuclear power, Volume 3, Issue 4

95 Pohl, J.H., Chen, S.L., Heap, M.P., Pershing, D.W. (1983): *Correlation of NOx Emissions with Basic Physical and Chemical Characteristics of Coal*, Proceedings of the 1982 Joint Symposium on Stationary Combustion NOx Control, Palo Alto. July 1983, EPRI Report No. CS–3182, 36 p

96 Pohl, J.H., Dusatko, G.C., Orban, P.C., Mcgraw, R.W. (1987): *The influence of fuel properties and boiler design and operation on NOx Emissions*, Proceedings of the 1986 Joint Symposium on Stationary Combustion NOx Control. EPRI, New Orleans, March 1987

97 Nakata, T., Sato, M., Makino, H., Ninomiya, T. (1988): *Methods for predicting NOx emissions in coal combusiton and unburned carbon in fly ash – Effects of coal properties,* Criepo Report EW87003, Tokyo: Central Research Institute of Electric Power Industry, Yokosuka Research Laboratory

98 Shimizu, T., Sazawa, Y., Adschiri, T., Furusawa, T. (1992): *Conversion of char–bound nitrogen to nitric oxide during combustion*, Fuel, Volume 71, Issue 4, April 1992, pp 361–365

99 Alfonso, R., Dusatko, G.C., Pohl, J.H. (1993): *Measurements of NOx emissions from coal boilers*, Combustion Science and Technology, Volume 93, Issue 1, pp 41–51

100 Michelfelder, S., Heap, M.P., Lowers, T.M. (1977): *The Effect of Burner Construction and Burner Parameters on the Emission of NOx from Natural Gas, Heavy Fuel Oil, and Pulverized Coal Flames*, International Flame Research Document Number K20/a/90, Ijmuiden, The Netherlands, April 1977

101 Kambara, S., Takarada, T., Toyoshima, M., Kato, K. (1995): *Relation between functional forms of coal nitrogen and NOx emissions from pulverized coal combustion*, Fuel, Volume 74, Issue 9, pp 1247–1253

102 Rozendaal, C.M., Witcamp, J.G., van Vliet, H.N., Vissers, A.M.C. (1997): *Impact of coal quality and coal blending on NO emissions for two pulverized coal fired units*, EPRI–DOE–EPA Combined Utility Air Pollutant Control Symposium, The Mega Symposium, Volume 1, Washington, DC, Aug. 25–29, 1997, Electric Power Research Institute, EPRI–TR–108683–VI, Pleasant Hill, CA, USA

103 Rozendaal, C.M. (1999): *Impact of coal quality on nitrogen oxide emissions from power plant*s, Technische Universiteit Delft (The Netherlands), ProQuest Dissertations and Theses, 300 p

104 Van der Kooij et al (1997): *The effect of coal quality on NOx emissions*, Thermal Generation Study Committee, 20.03 THERNOX Ref.: 02003Ren9769, Paris, France, UNIPEDE, 50 p

105 Niksa, S., Kornfeld, A., Muzio, L., Fang, T., Hurt, R., Sun, J., Metha, A., Stallings, J., Gibb, W., Cloke, M., Lester, E. (1997): *Assess coal quality impacts on NOx and LOI with EPRI's NOx – LOI Predictor*, EPRI–DOE–EPA Combined utility air pollutant control symposium (The Mega Symposium), August 25–29, Washington D.C., USA, 1997

106 Niksa, S., Kerstein, A.R. (1991): *FLASHCHAIN Theory for Rapid Coal Devolatilization Kinetics. 1. Formulation*, Energy & Fuels 1991, Volume 5, Issue 5, pp 647–665

107 Niksa, S. (1991): *FLASHCHAIN Theory for Rapid Coal Devolatilization Kinetics. 2. Impact of operating conditions*, Energy & Fuels 1991, Volume 5, Issue 5, pp 665–673

108 Niksa, S. (1991): *FLASHCHAIN Theory for Rapid Coal Devolatilization Kinetics. 3. Modeling the behavior of various coals*, Energy & Fuels 1991, Volume 5, Issue 5, pp 673–683

109 Niksa, S. (1994): *FLASHCHAIN Theory for Rapid Coal Devolatilization Kinetics. 4. Predicting Ultimate Yields from Ultimate Analyses Alone*, Energy & Fuels 1994, Volume 8, Issue 3, pp 659–670

110 Niksa, S. (1994): *FLASHCHAIN Theory for Rapid Coal Devolatilization Kinetics. 5. Interpreting Rates of Devolatilization for Various Coal Types and Operating Conditions*, Energy & Fuels 1994, Volume 8, Issue 3, pp 671–679

111 Niksa, S. (1995): *FLASHCHAIN Theory for Rapid Coal Devolatilization Kinetics. 6. Predicting the Evolution of Fuel Nitrogen from Various Coals*, Energy & Fuels 1995, Volume 9, Issue 3, pp 467–478

112 Niksa, S. (1996): *FLASHCHAIN Theory for Rapid Coal Devolatilization Kinetics. 7. Predicting the Release of Oxygen Species from Various Coals*, Energy & Fuels 1996, Volume 10, Issue 1, pp 173–187

113 Schlessing, J. (1998): *Determination of operating parameters for the use of hard–to–burning coal in dry–deashed boilers*. VGB Kraftwerkstechnik, VGB Power Tech (VGB Technical Association of Large Power Plant Operators),Volume 78, Issue 8. August 1998, pp, 74–91

114 Makino, H., Matsuda, H. (1999): *Improvements of pulverized coal combustion technology for power generation*, Central Research Institute of Electric Power Industry (CRIEPI), 129 p

115 Makino, K. (1999): *The use of Australian coals as pulverized coal in Japan*, CRC for Black Coal Utilisation Seminar, The Future of Pulverized Coal Firing, Newcastle, March 1999

116 Jung, K.S., Keener, T.C., Khang, S.J. (2001): *Compositional factors affecting NOx emissions from Ohio coals*, Fuel Processing Technology, Volume 74, Issue 1, 26 November 2001, pp 49–61

117 Bennett, P.A. (2001): *NOx Prediction*, Research Report 20, Cooperative Research Centre for Black Coal Utilisation, The University of Newcastle

118 Badzioch, S., Hawksley, P.G.W. (1970): *Kinetics of thermal decomposition of pulverized coal particles*, Industrial & Engineering Chemistry Process Design and Development, Volume 9, Issue 4, pp 521–530

119 Kurose, R., Ikeda, M., Makino, H., Kimoto, M., Miyazaki, T. (2004): *Pulverized coal combustion characteristics of high–fuel–ratio coals*, Fuel, Volume 83, Issue 13, September 2004, pp 1777–1785

120 Kokkinos A., Lewis R.D., Borio R.W., McCartney, M.S. (1983): *Low–NOx firing system for tangentially fired boilers – preliminary testing*, Proceedings of the 1982 Joint Symposium on Stationary Combustion NOx Control, EPRI Report No. CS–3182

121 Stamey–Hall, S. (1992): *Evaluation of nitrogen oxide emissions data from TVA coal–fired boilers*, EPA–600/R–92–242, December 1992, U.S. Environmental Protection Agency

122 Eddings, E.G., Smith, P.J., Heap, M.P., Pershing, D.W., Sarofim, A.F. (1994): *The Use of Models to Predict the Effect of Fuel Switching on NOx Emissions, in Coal Blending and Switching of Western Low–Sulfur Coals*, R.W. Bryers and N.S. Harding (Eds.), ASME, New York, pp 169–184

123 Smouse, S.M., Wildman, D.J., Mcilvried, T.S., Harding, S. (1994): *Estimation of Nox Emissions from Pulverized Coal–fired Utility Boilers*, Proceedings of the 1993 Joint Symposium on Stationary Combustion NOx Control, CRADA PC94–005, Final Report, Bal Harbour, Florida, pp 24–27

124 Burgess, D. M., Hertzberg, M., Richmond, J. K., Liebman, I., Cashdollar, K. L., Lazzara, C. P. (1979): *Combustion, Extinguishment and Devolatilization in Coal Dust Explosions*, Western States Section, The Combustion Institute

125 Howard, J. B., Essenhigh, R. H. (1967): *Mechanism of solid particle combusiton with simutaneous gas–phase volatiles combustion*, Symposium (International) on Combustion, Volume 11

126 Beeston, G., Essenhigh, R. H. (1963): *Kinetics of coal combustion: The influence of oxygen concentration on the burning–out times of single particles*, The Journal of Physical Chemistry, Volume 67, 1349 p

127 Rozendaal, C.M., Witkamp, J.G., Meijer, R., Benneker, R.J.M., Hoogendoorn, A. (1998): *Laboratory and Full Scale Blending Studies*, KEMA, Contract No JOF3–CT95–0005, pp 361–408

128 Pershing, D. W., Wendt, J. O. L. (1976): *Pulverized coal combustion: The influence of flame temperature and coal combustion on thermal and fuel NOx*, Symposium (International) on Combustion, Volume 16, Pittsburgh, pp 389–399

129 Hill, S. C., Smoot, L. D. (2000): *Modeling of nitrogen oxides formation and destruction in combustion systems*, Progress in Energy and Combustion Science, Volume 26, Issues 4–6, pp 417–458

130 Baxter, L. L., Mitchell, R. E., Fletcher, T. H., Hurt, R. H. (1996): *Nitrogen Release during Coal Combustion*, Energy Fuels, Volume 10, Issue 1, pp 188–196

131 DIN 51720:2001–03 (2001): *Testing of solid fuels – Determination of volatile matter content*, Norm

132 ASTM D3175–02 (2002): *Standard Test Method for Volatile Matter in the Analysis Sample of Coal and Coke*, Norm

133 Niksa, S. (1998): *Assessing coal quality impacts on pc combustion behavior*, Fuel and Energy, Volume 39, Issue 1, January 1998, 44 p

134 Winkler, H., Neumann, M. (2007): *Advanced Analysis for the Choice of Importcoals and Other Fuels*, International Journal for Electricity and Heat Generation, VGB Power Tech Journal (VGB Technical Association of Large Power Plant Operators, Volume 87, Issue 7, July 2007, pp 62–66

135 Kluger, F., Greul, U., Spliethoff, H., & Hein, K. R. G. (1997): *Experimental study of C and N release at combustion of high and medium volatile hard coals*, In Flammentag 1997, Delft, Netherlands

136 Fisher, C.H. (1938): *Relation between Volatile Matter and Hydrogen–Carbon Ratio of Coal and Its Banded Constituents*, Industrial & Engineering Chemistry Analytical Edition 1938, Volume 10, Issue 7, pp 374–378

137 Wang, W. X., Thomas, K.M., Cai, H.Y., Dugwell, D.R., and Kandiyote, R., (1996): *NO Release and Reactivity of Chars During Combustion: The Effect of Devolatilization Temperature and Heating Rate*, Energy & Fuels, Volume 10, Issue 2, pp 409–416

138 Visona, S. P., Stanmore, B. R. (1996): *Modeling NOx release from a single coal particle I. Formation of NO from volatile nitrogen*, Combustion and Flame, Volume 105, Issues 1–2, pp 92–103

139 Boyd, R. K., Nelson, P. F., McEwan, B. R., Nguyen, T. H. (2000): *Review of NOx Formation in PF Combustion*, University of Newcastle (N.S.W.), Advanced Technology Centre, Cooperative Research Centre for Black Coal Utilisation

140 Zygarlicke, C.J., McCollor, D.P., Torrnan, D.L., Wall, T.F., Gupta, R.P., Raznei, H.. (1995): *A Comparison of Ash Produced under Conventional and Low–NOx Combustion Conditions*, Proceedings of the 1995 International Joint Power Generation Conference, American Society of Mechanical Engineers, Minneapolis, MN, pp 449–462

141 Okazaki, K., Shishido, H., Nishikawa, T. and Ohtake, K. (1985): *Separation of the basic factors affecting no formation in pulverized coal combustion*, Symposium (International) on Combustion, Volume 20, Issue 1, pp 1381–1389

142 Armento, W.J., Stage, W.L. (1975): *Effect of Design and Operation Variables on Nox Formation in Coal Fired Furnaces: Status Report*, AIChE Symposium, Series No. 148, Volume 71, 160 p

143 BoilerSpec (2010): *Boiler Emission Guide*, 3rd Edition, Cleaver Brooks, Thomasville, 41 p

144 Jin, J., Zhang, Z., & Li, R. (2007): *Study on the NOx release rule along the boiler during pulverized coal combustion*, Frontiers of Energy and Power Engineering in China, Volume 1, Issue 1, pp 91–95

145 Zhang, H. (2001): *Nitrogen evolution and soot formation during secondary coal pyrolysis*, Brigham Young University, ProQuest Dissertations and Theses, 210 p.

146 Hardgrove, R. M. (1962): *Method for Burning Fuel*, U.S. Patent 3,048,131, August 7, 1962

147 Straka, R., Makovicka, J., Benes, M. (2009): *Numerical model of air–staging and OFA in PC boiler*, Proceedings of Algoritmy, pp 350–361

148 Costa, M., Azevedo, J.L.T. (2007) *Experimental characterization of an industrial pulverized coal–fired under deep staging conditions*, Combustion Science and Technology Volume 179, Issue 9, pp 1923–1935

149 Man, C.K., Gibbins, J.R., Witkamp, J.G., Zhang, J. (2005): *Coal characterisation for NOx prediction in air–staged combustion of pulverised coals*, Fuel, Volume 84, Issue 17, December 2005, pp 2190–2195

150 Li, Z., Fan, S., Liu, G., Yang, X., Chen, Z., Su, W., Wang, L. (2010): *Influence of Staged–Air on Combustion Characteristics and NOx Emissions of a 300 MWe Down–Fired Boiler with Swirl Burners*, Energy Fuels, Volume 24 Issue 1, pp 38–45

151 Ribeirete, A., Costa, M. (2009): *Impact of the air staging on the performance of a pulverized coal fired furnace*, Symposium (International) on Combustion, Volume 32, Issue 2, pp 2667–2673

152 Fan, W., Lin, Z., Li, Z., Kuang, J., & Zhang, M. (2009): *Effect of Air–Staging on Anthracite Combustion and NOx Formation*, Energy Fuels, Volume 23, Issue 1, pp 111–120

153 Maier, H., Spliethoff, H., Kicherer, A., Fingerle, A., & Hein, K.R.G. (1994): *Effect of coal blending and particle size on NOx emission and burnout*, Fuel, Volume 73, Issue 9, pp 1447–1452

154 Backreedy, R.I., Jones, J.M., Ma, L., Pourkashanian, M., Williams, A., Arenillas, A., Arias, B., Pis, J.J., & Rubiera, F. (2005): *Prediction of unburned carbon and NOx in a tangentially fired power station using single coals and blends*, Fuel, Volume 84, Issue 17, pp 2196–2203

155 Spliethoff, H., Greul, U., Rüdiger, H., Hein, K.R.G. (1996): *Basic effects on NOx emissions in air staging and reburning at a bench–scale test facility*, Fuel, Volume 75, Issue 5, pp 560–564

156 Li, S., Xu, T., Hui, S., Zhou, Q., Tan, H. (2009): *Optimization of air staging in a 1 MW tangentially fired pulverized coal furnace*, Fuel Processing Technology, Volume 90, Issue 1, pp 99–106

157 Li, S., Xu, T.M., Sun, P., Zhou, Q.L., Tan, H.Z., Hui, S.E. (2008): *NOx and SOx emissions of a high sulfur self–retention coal during air–staged combustion*, Fuel, Volume 87, Issue 6, pp 723–731

158 Maier, H. (1997): *Experimentelle Untersuchungen der Kohlenstaubverbrennung unter Berücksichtigung der Brennstoffaufbereitung*; Translation: 'Experimental studies of pulverized coal combustion, taking into account the fuel treatment', PhD–thesis, Shaker Verlag, Aachen 1998, Berichte aus der Energietechnik, ISBN 3–8265–3295–3

159 Greul, U. (1998): *Experimentelle Untersuchung feuerungstechnischer NOx Minderungsverfahren bei der Kohlenstaubverbrennung*, VDI Fortschrittsberichte, Reihe6: Energietechnik, No. 388, ISBN 3–18–338806–5, Düsseldorf, Germany

160 Coda, B., Kluger, F., Förtsch, D., Spliethoff, H., Hein, K. R. G., Tognotti, L., (1998): *Coal–Nitrogen Release and NOx Evolution in Air–Staged Combustion*, Energy Fuels, Volume 12, Issue 6, pp 1322–1327

161 Liu, H., Zailani, R., Gibbs, B.M., (2005): *Comparisons of pulverized coal combustion in air and in mixtures of O2/CO2*, Fuel, Volume 84, Issues 7–8, ISSN 0016–2361, pp 833–840

162 Li, S., Xu, T., Hui, S., Zhou, Q., Tan, H. (2009): *Optimization of air staging in a 1 MW tangentially fired pulverized coal furnace*, Fuel Processing Technology, Volume 90, Issue 1, pp 99–106

163 Gwosdz, A. (2010): *Feuerungskomponenten*, Company Presentation of Hitachi Power Europe

164 Brown, R. A., Mason, H. B., Pershing, D. W., Wendt, J. O. L. (1979): *Investigation of first– and second–stage variables on control of NOx emissions using staged combustion in a pulverized coal wall–fired furnace*, American Institute of Chemical Engineers, Volume 75, Issue 188, pp 27–47

165 Glassman I. (1977): *Combustion*, London: Academic Press, New York– San Francisco– London, ISBN 10: 0122858506, 275 p

166 Steitz, T.H., Grusha, J., Cole, R. (1998): *Wall fired low NOx burner evolution for global NOx compliance*. In Proceedings of the 23rd International Technical Conference on Coal Utilization & Fuel Systems, Clearwater, Florida USA, March 9–13, 1998

167 Niksa, S., Cho, S., (1996): *Conversion of Fuel–Nitrogen in the Primary Zones of Pulverized Coal Flames*, Energy Fuels, Volume 10, Issue 2, pp 463–473

168 Heap, M.P., Lowes, T.M., Walmsley, R. (1972): *The effect of burner parameters on nitric oxide formation in natural gas and pulverized coal flames*, Paper presented at the American Flame Days Conference, American Flame Research Committee

169 Heap, M.P., Lowes, T.M., Walmsley, R., Bartelds, H., & LeVaguerese, P. (1976): *Burner criteria for NOx control, Volume 1, Influence of burner variables on NOx in pulverized coal flames*, U.S. Environmental Protection Agency, Air and Energy Engineering Research Laboratory, EPA Report No. EPA/600/2–76/061a

170 Heap, M.P., Tyson, T.J., Lowes, T.M. (1975): *Burner design and nitric oxide formation in pulverized coal flames*, Paper presented at the 68th annual AIChE Meeting, Los Angelas, California, November 16–20, 1975

171 Stamey–Hall, S. (1994): *Alternative Control Techniques Document – NOx Emissions from Utility Boilers*, United States Environmental Protection Agency, EPA–453/R–94023, March 1994

172 Steitz, T.H., Cole, R.W. (1996): *Field Experience in Over 30,000 MW of Wall Fired Low NOx Installations*, ASME International Joint Power Generation Conference, Houston, TX

173 Cai, H.–Y., Güell, A.. J., Dugwell, D.R., and Kandiyoti, R. (1993): *Heteroatom Distribution in Pyrolysis Products as a Function of Heating Rate and Pressure*, Fuel, Volume 72, Issue 3, pp 321–327

174 Schlessing, J., Benesch, W., Franitza, W. (1997): *Primärmaßnahmen zur NOx–Minderung an Staubfeuerungen für Stein– und Braunkohle*, (VGB–Erfahrungsbericht) – Translation: 'Primary measures for NOx reduction for hard and lignite firing systems (VGB Experience Report)', VGB Technical Association of Large Power Plant Operators, VGB Kraftwerkstechnik TW 216, 1997, 119 p

175 Daood, S.S., Nimmo, W., Edge, P., & Gibbs, B.M. (2012), *Deep–staged, oxygen enriched combustion of coal*, Fuel, Volume 101, pp 187–196

176 Tarelho, L.A.C., Matos, M.A.A., Pereira, F.J.M.A. (2004) *Axial concentration profiles and no flue gas in a pilot–scale bubbling fluidized bed coal combustor*, Energy & Fuels, Volume 18, Issue 6, pp 1615–1624

177 Law, C.K. (2006): *Combustion physics*, New York: Cambridge University Press, 2006, ISBN–10 0–521–87052–6

178 Chen, L., Yong, S. Z., & Ghoniem, A. F. (2012): *Oxy–fuel combustion of pulverized coal: Characterization, fundamentals, stabilization and CFD modeling*, Progress in Energy and Combustion Science, Volume 38, Issue 2, April 2012, pp 156–214

179 Shaddix, C.R., Molina, A. (2009): *Particle imaging of ignition and devolatilization of pulverized coal during oxy–fuel combustion*, Symposium (International) on Combustion, Volume 32, Issue 2, pp 2091–2098

180 Khatami, R., Stivers, C., Levendis, Y.A. (2012): *Ignition characteristics of single coal particles from three different ranks in O2/N2 and O2/CO2 atmospheres*, Combustion and Flame, Volume 159, Issue 12, December 2012, pp 3554–3568

181 Bejarano, P.A., Levendis, Y.A. (2008): *Single–coal–particle combustion in O2/N2 and O2/CO2 environments*, Combustion and Flame, Volume 153, Issues 1–2, pp 270–287

182 Bradley J, Bool L, Kobayashi S. (2004): *NOx reduction from a 125–MW wall fired boiler utilizing oxygen enhanced combustion*, In: Proceedings of the 29th international technical conference on coal utilization and fuel systems clear water, Florida, USA, 2004

183 Bool L, Kobayashi H. (2003): *NOx reduction from a 44–MW wall fired boiler utilizing oxygen enhanced combustion*, In: Proceedings of the 28th international technical conference on coal utilization and fuel systems clear water, Florida, USA, 2003

184 WRI 06–R019. Task 49 final report DE–FC26–98FT40323 (2006): *Reduction of NOx emission from coal combustion through oxygen enrichment*, Western Research Institute, Laramie, Wyoming, July 2006

185 Wang, J., Fan, W., Li, Y., Xiao, M., Wang, K., & Ren, P. (2012): *The effect of air staged combustion on NOx emissions in dried lignite combustion*, Energy (Oxford), Volume 37, Issue 1, pp 725–736

186 Yang, J., Mestl, G., Herein, D., Schlögl, R., Find, J. (2000): *Reaction of NO with carbonaceous materials: 2. Effect of oxygen on the reaction of NO with ashless carbon black*, Carbon, Volume 38, Issue 5, pp 729–740

187 Aarna, I., Suuberg, E.M. (1997): *A review of the kinetics of the nitric oxide–carbon reaction*, Fuel, Volume 76, Issue 6, pp 475–491

188 Rodriguez–Mirasol, J., Ooms, A.C., Pels, J.R., Kapteijn, F., Moulijn, J.A. (1994): *NO and N2O decomposition over coal char at fluidized–bed combustion conditions*, Combustion and Flame, Volume 99, Issues 3–4, pp 499–507

189 Matsuoka, K., Orikasa, H., Itoh, Y., Chambrion, P., Tomita, A. (2000): *Reaction of NO with soot over Pt–loaded catalyst in the presence of oxygen*, Applied Catalysis B: Environmental, Volume 26, Issue 2, 24 pp 89–99

190 Chambrion, P., Kyotani, T., Tomita, A. (1998): *C–NO reaction in the presence of O2*, Symposium (International) on Combustion, Volume 27, Issue 2, pp 3053–3059

191 Tsai, K.–C., Chung, W.–T. (2011): *Clarifying the mechanism of flashover from the view of unburned fuel volatiles and secondary fuels*, Symposium (International) on Combustion, Volume 33. Issue 2, pp 2649–2656

192 Fan, W.D., Lin, Z.C., Kuang, J.G., Li, Y.Y.(2010): *Impact of air staging along furnace height on NOx emissions from pulverized coal combustion*, Fuel Processing Technology, Volume 91, Issue 6, pp 625–634

193 Greul, U., Spliethoff, H., Magel, H.C., Schnell, U., Ruediger, H., Hein, K.R.G., Li, C., Nelson, P.F. (1996): *Impact of temperature and fuel–nitrogen content on fuel–staged combustion with coal pyrolysis gas*, Symposium (International) on Combustion, Volume 26, Issue 2, pp 2231–2239

194 Lawn, C. J. (1987): *Principles of Combustion Engineering for Boilers*, Academic Press Inc (Mai 1988), ISBN: 0124390358, 628 p

195 Ogden, G. E. (2002): *Pulverized coal combustion: Flame attachment and nitrogen oxide emissions*, The University of Arizona, ProQuest Dissertations and Theses, pp 318–318

196 Beér, J. M. (1994): *Minimizing NOx emissions from stationary combustion, reaction engineering methodology*, Chemical Engineering Science, Volume 49, Issue 24, Part A, pp 4067–4083

197 Soud, H., Fukasawa, K. (1996): *Developments in NOx Abatement and Control*, IEA Coal Research, Report IEACR/89, London, UK, August 1996, ISBN: 92–9029–273–3. 123 p

198 Cherry, S.S. (1984): *Analysis Of Low NOx Operation Of Two Pulverized–coal–fired Utility Boilers*, U.S. Environmental Protection Agency, Industrial Environmental Research Laboratory, Research Triangle Park, N.C.,EPA–600/S7–83–056

199 Thring, M.W. (1962): *The science of flames and furnaces*, 2nd Edition, New York, Wiley, 1962. 625 p

200 Sankey, H.R. (1896): *The Thermal Efficiency of Steam–Engines*. Minutes of Proceedings of the Institution of Civil Engineers, Volume 125, Issue 1896, pp 182–212

201 Latta, C. A., Weston, R. F. (1998): *Methods for reducing NOx emissions*, Plant Engineering, Volume 52, Issue 10, pp 105–112

202 Hwang, Y. (1997): *Three–dimensional model studies of a pulverized coal corner–fired utility furnace and comparisons with local furnace data and boiler exhaust NO(x)*, The University of Texas at Austin, ProQuest Dissertations and Theses, 216 p

203 Zhou, H., Cen, K., Fan, J. (2004): *Modeling and optimization of the NOx emission characteristics of a tangentially fired boiler with artificial neural networks*, Energy, Volume 29, Issue 1, January 2004, pp 167–183

204 Makansi, J. (1996): *Process Optimization Aims for Closed–loop Control*, Power, Volume 140, Issue 2, pp 26–28

205 Arenillas, A., Backreedy, R.I., Jones, J.M., Pis, J.J., Pourkashanian, M., Rubiera, F., Williams, A. (2002): *Modeling of NO formation in the combustion of coal blends*, Fuel, Volume 81, Issue 5, March 2002, ISSN 0016–2361, pp 627–636

206 Rodriguez, G., Needler, R. (2006): *Audit Report, Fayette Power Project Scrubber Costs*, Austin City Council, Audit No. AU06113, 13 p

207 Kremer, H., Grigoleit, H., Jacobs, J. (1990): *Neigung von Kraftwerkskohlen zur NOx Bildung* (Ergebnisse des VGB–Forschungsprojektes 89), VGB Kraftwerkstechnik 70, VGB Technical Association of Large Power Plant Operators, Heft 7, 1990, pp 566–573

208 Hesselmann, G., Hepburn, P., Fish, S. (1997): *Effect of coal quality on in–furnace nox reduction efficiency*, ETSZ–COAL–R–075, Energy Technology Support Unit, Department of Trade and Industry, Harwell, United Kingdom

209 Jones, A.R., Gibb, W.H., Irons, R.M.A., Price, H.J., Stallings, J.W., and Mehta, A.K., (1995): *An integrated full, pilot and laboratory scale study of the effect of coal quality on NOx and unburnt carbon formation*, In Joint EPA/EPRI Symposium on Stationary Combustion NOx Control, 27 p

210 British Coal Utilisation Research Association., & Field, M. A. (1967): *Combustion of pulverised coal*, Leatherhead Sy.: B.C.U.R.A., London, England

211 Saji, K. (1954): *Combustion rate of pulverized coal in a jet stream*, Symposium (International) on Combustion, Volume 5, Issue 1, pp 252–260

212 Wood, G.H., Davenport, M. (1978): *Control Techniques for Nitrogen Oxides Emissions from Stationary Sources*, EPA 450/ 1–78–001, January 1979. 400 p

213 Appleton, J.P., Heywood, J.B. (1973): *The effects of imperfect fuel–air mixing in a burner on NO formation from nitrogen in the air and the fuel*, Symposium (International) on Combustion, Volume 14, Issue 1, pp 777–786

214 Muzio, L. J., Quartucy, G. C. (1997): *Implementing NOx control: Research to Application*, Progress in Energy and Combustion Science, Volume 23, Issue 3, pp 233–266

215 Allen, J.W., Brooks, W.J.D., Burdett, N.A., Clarke, F., Foley, G. (1987): *Reductions in NOx emissions from a 500 MW comer–fired boiler*, In: Proceedings of the joint EPRI/IEPA 1987 symposium on stationary combustion NOx control, New Orleans, LA, USA, 23–26 Mar 1987

216 Botsford, C. W. (2001): *The two faces of NOx control*, Chemical Engineering, Volume 108, Issue 7, pp 66–71

217 Richards, G.H., Maney, C.Q., Borio, R.W., Lewis, R.D. (2002): *Ultra low NOx Integrated System for NOx Emission Control from Coal–fired Boiler*, U.S. Department of Energy, National Energy Technology Laboratory Pittsburgh, Pennsylvania

218 Bagwell, F.A. Rosentha, K.E., Teixeira, D.P., Breen, B.P., Bayardde, N., Kerho, S. (1971): *Utility Boiler Operating Modes for Reduced Nitric Oxide Emissions*, Journal of the Air Pollution Control Association, Volume 21, Issue: 11, pp 702–708

219 U.S. Environmental Protection Agency (1992): *Summary of NOx Control Technologies and their Availability and Extent of Application*, Office of Air Quality Planning and Standards, Research Triangle Park, N.C., EPA–450/3–92–004

220 Blakeslee, C.E., Selker, A.P. (1973): *Program for Reduction of NOx From Tangential Coal–Fired Boilers: Phase I*, U.S. Environmental Protection Agency, Office of Research and Development, Washington D.C. EPA–650/2–73–005

221 Goodwin, D.R. (1978): *Electric utility steam generating units. Electric utility steam generating units: background information for proposed NOx emission standards*, EPA 450/2–78–005a, NTIS–PB 286 155, 200 p

222 Brown, R. A., Mason, H. B., & Schreiber, R. J. (1974): *Systems analysis requirements for nitrogen oxide control of stationary sources*, NTIS Report Pb–237 367

223 U.S. Environmental Protection Agency (1976): *Guideline Series Sip Preparation Manual For NOx*, Office of Air Quality Planning and Standards, Research Triangle Park, N.C., OAQPS NO. 1.2–048, 169 p

224 Thompson, E.E., Shiomoto, G.H., Haumesser, F.P. (1996): *Post–Retrofit Operating and NOx Emission Experience on Five Tangentially–fired Units*, ASME International Joint Power Generation Conference, Housten, TX, October 1996

225 Nalbandian, H. (2009): *NOx control for coal–fired plant*, IEA Coal Research, Report CCC/157, ISBN: 978–92–9029–477–1, 51 p

226 Douglas, J. (1987): *Retrofit strategies for NOx control*, Electric Power Research Institute Journal, Volume 12, Issue 2, pp 26–31

227 Ekman, I., Asikainen, A., Lepikko, J. (1990): *Desulphurization with limestone injection combined with low–NOx combustion*, Paper presented at the Gen–Upgrade 90 international symposium on performance improvement, retrofitting and repowering of fossil fuel power plants, Washington, DC, USA, May 6–9 1990, 15 p

228 Pargac, G., Kirkland, R., Ohnheiser, L., Mathis, J.D., Matus, S.A., Hart, D., Veenema, R.J., Bailey, W. (2005): *An Update on Achieving NOx Emission Levels Less Than 0.10 lb/mmBtu for Tangentially Fired Boilers Burning PRB Coal at the LCRA Fayette Facility*

229 Lower Colorado River Authority (2009): *Fayette Power Project Fact Sheet*, Retrieved from www.lcra.org

230 Pershing, D.W., Wendt, J.O.L. (1979): *Relative Contributions of Volatile Nitrogen and Char Nitrogen to NOx Emissions from Pulverized Coal Flames*, Industrial & Engineering Chemistry Process Design and Development, Volume 18, Issue 1, pp 60–67

231 Man, C.K., Pendlebury, K.J., Gibbins, J.R. (1993): *Laboratory measurement of N release under combustion conditions and comparison with plant NOx formation*, Fuel Processing Technology, Volume 36, Issues 1–3, pp 117–122

232 Blair, D.W., Wendt, J.O.L., Bartok, W. (1977): *Evolution of nitrogen and other species during controlled pyrolysis of coal*, Symposium (International) on Combustion, Volume 16, Issue 1, pp 475–489

233 Pohl, J.H., Sarofim, A.F. (1976): *Devolatilization and oxidation of coal nitrogen.* Symposium (International) on Combustion, Volume 16, August 15–20, 1976. Cambridge, Massachusetts

234 Makansi, J. (1994): *SO2/NOx Control: Fine Tuning for Phase I Compliance*, Power, Volume 138, Issue 3, pp 18–28

235 McComas, M., Morris, C. (1995): *Fuel Switch Meets Clean Air Act and Reduces Power Cost 17%*, Proceedings of the American Power Conference, 57–II, Chicago, IL. pp 1627–1632

236 Krameric, B.A., Rupinskas, R.L. (1995): *Experience Modifying Power Plant Systems for Switching to Power River Basin (PRB) Coal*, Proceedings of the American Power Conference, 58–II, Chicago, IL. pp 842–852

237 De Soete, G.G. (1975): *Overall reaction rates of NO and N2 formation from fuel nitrogen*, Symposium (International) on Combustion, Volume 15, Issue 1, pp 1093–1102

238 Smoot, L.D. (1993): *Fundamentals of Coal Combustion for Clean and Efficient Use*, Elsevier, ISBN: 9780444896438, New York, 755 p

APPENDIX 1 – NOTATION

ACIRL	Australian Coal Industry Research Laboratories
AE	Austin Energy
APH	Air preheater
ar	As received
ASTM	The American Society for Testing and Materials
b	burner design factor
B.E.	Burner elevation
BI	Burner index
BMCR	Boiler maximum continuous rating
BOOS	Burner–out–of–service
C	Carbon
CAPEX	Capital expenditure
CCOFA	Closed–coupled overfire air
CFD	Computational fluid dynamic
CHx	Hydrocarbons radicals
CO	Carbon monoxide
CO_2	Carbon dioxide
CQIM	Coal Quality Impact Model
CR	Conversion ratio
daf	Dry ash free

db	Dry basis
DCS	Distributed control system
DIN	Deutsches Institut für Normung (German Institute for Standardization)
dmmf	dry–mineral–matter–free
ECON	Economizer
EPA	US Environmental Protection Agency
EPRI	Electric Power Research Institute
FC	Fixed carbon
$FeCl_3$	Iron(III) chloride
FF	Fuel factor
FFW	Furnace firing wall
FGR	Flue gas recirculation
FR	Fuel ratio
H	Hydrogen
h	helping factor
H_2O	Water
HCN	Hydrogen cyanide
HR	Heat release
HRBZ	Heat release per burner area
HRBZA	Heat release per burner zone area
HRI	Heat release impact
HTWM	High temperature wire mesh
IEA	The International Energy Agency
ISO	The International Organization for Standardization

LCRA	Lower Colorado River Authority
LHV	Lower heating value
LOI	Loss of ignition
M	Atomic weight
MM	Mineral matter
mmf	Mineral–matter–free
moist, mmf	Moisture, mineral–matter–free
N	Nitrogen
n.s.	Not specified
N_2	Molecular nitrogen
N_2O	Nitrous oxide
N_2O_2	Dinitrogen dioxide
N_2O_3	Dinitrogen trioxide
N_2O_4	Dinitrogen tetroxide
N_2O_5	Dinitrogen pentoxide
NAAQS	National Ambient Air Quality Standards
n_{BB}	Air ratio at the burner belt exit
n_{BZ}	Air ratio for the closed burner zone
n_{OFA}	Air ratio for the overfire air
NH_3	Ammonia
NI	NO_x Indicator
NL	The Netherlands
NO	Nitrogen oxide
No.	Number
NO_2	Nitrogen dioxide

NO_x	Nitrogen oxides
NSPS	New Source Performance Standards
O_2	Molecular oxygen
O_3	Trioxygen (ozone)
OECD	Organization for Economic Co–operation and Development
OEM	Original equipment manufacturer
OFA	Overfire air
OPEX	Operational expenditure
OSC	Off–stoichiometric combustion
PA	Primary air
PdN	Pyridinic nitrogen
PF	Pulverized fuel
PRB	Southern Powder River Basin
PrN	Pyrrolic nitrogen
QN	Quaternary nitrogen
R	Coefficient of correlation
R^2	Coefficient of determination
R^2(adj)	Adjusted coefficient of determination
RH	Reheater
S	Residual standard deviation
SA	Secondary air
SGR	Separate gas recirculation
SH	Super heater
SI	International System of Units
SO_2	Sulfur dioxide

SOFA	Separate overfire air
SO_x	Sulfur oxides
SR	Stoichiometric ratio
STP	Standard temperature and pressure
SWA	Side wall air system
UBC	Unburnt carbon content
UK	United Kingdom
US	United States
USA	United States of America
USGS	US Geological Survey
V	Gas volume
VBA	Visual Basic for Applications
VM	Volatile matter content
VOC	Volatile organic compounds
VSFE	Vertical spacing until furnace exit
waf	Water–ash–free basis
wf	Water–free basis
XPS	X–ray photoelectron spectroscopy

APPENDIX 2 – REFERENCE DATA

Table A2–1. Reference data of boiler 1

Opposed–fired boiler with partition wall, Western Europe (bituminous coal)		
Fuel rating (BMCR)	1,073.00	MWt
Primary NO_x level	585	mg / m^3 STP_{dry} at 6 % O_2
System design		
Burner installed	32	–
Burner elevations (B. E.)	4	–
Partition wall surface (inside burner belt)	562	m^2
Furnace depth (furnace side walls)	12.806	m
Furnace width (burner walls, hopper trapezia)	19.286	m
Furnace height (without hopper)	34.700	m
B. E. vertical spacing	4.305	m
Distance between lower B. E. and hopper edge	1.617	m
Distance between upper B. E. and OFA	7.000	m
Hopper height	12.915	m
Hopper angle	55	°

Table A2–2. Reference data of boiler 2 and 3 (pre– and post–retrofit)

Allwall–fired boiler, Western Europe (bituminous coal)

	Pre–	**Post–**	**retrofit**
Fuel rating (BMCR)	730.00	799.00	MWt
Primary NO_x level	495	475	mg / m³ STP_{dry} at 6 % O_2
System design			
Burner installed	12		–
Burner elevations (B. E.)	3		–
Furnace depth (furnace side walls)	12.086		m
Furnace width	12.086		m
Furnace height (without hopper)	31.380		m
B. E. vertical spacing	5.742		m
Distance between lower B. E. and hopper edge	1.914		m
Distance between upper B. E. and OFA	4.454		m
Hopper height	7.070		m
Hopper angle	52		°

Table A2–3. Reference data of boiler 4 and 5 (pre– and post–retrofit)

Front–fired boiler, Western Europe (bituminous coal)

	Pre–	**Post–**	**retrofit**
Fuel rating (BMCR)	90.00	90.00	MWt
Primary NO_x level	537	465	mg / m³ STP_{dry} at 6 % O_2
System design modifications			
Distance between upper B. E. and OFA 1	–	1.800	m
Distance between upper OFA 1 and OFA 2	–	1.550	m
System design			
Burner installed		6	–
Burner elevations (B. E.)		3	–
Furnace depth (furnace side walls)		6.960	m
Furnace width (burner wall, hopper trapezia)		6.000	m
Furnace height (without hopper)		13.000	m
B. E. vertical spacing		2.850	m
Distance between lower B. E. and hopper edge		1.600	m
Hopper height		2.142	m
Hopper angle		55	°

Table A2–4. Reference data of boiler 6

Opposed–fired boiler with partition wall, Western Europe (bituminous coal)		
Fuel rating (BMCR)	1,712.00	MWt
Primary NO_x level	630	mg / m³ STP_{dry} at 6 % O_2
System design		
Burner installed	48	–
Burner elevations (B. E.)	4	–
Partition wall surface (inside burner belt)	1,130	m²
Furnace depth (furnace side walls)	19.548	m
Furnace width (burner wall, hopper trapezia)	15.319	m
Furnace height (without hopper)	50.238	m
B. E. vertical spacing	4.486	m
Distance between lower B. E. and hopper edge	1.647	m
Distance between upper B. E. and OFA	9.967	m
Hopper height	10.082	m
Hopper angle	55	°

Table A2–5. Reference data of boiler 7 and 8 (pre– and post–retrofit)

Opposed–fired boiler, Western Europe (bituminous coal)			
	Pre–	**Post–**	**retrofit**
Fuel rating (BMCR)	1,190.00	1,190.00	MWt
Primary NO_x level	610	535	mg / m³ STP_{dry} at 6 % O_2
System design			
Burner installed		12	–
Burner elevations (B. E.)		3	–
Furnace depth (furnace side walls)		12.086	m
Furnace width (burner walls, hopper trapezia)		16.086	m
Furnace height (without hopper)		50.000	m
B. E. vertical spacing		11.000	m
Distance between lower B. E. and hopper edge		2.800	m
Distance between upper B. E. and OFA		5.294	m
Hopper height		11.170	m
Hopper angle		56	°

Table A2–6. Reference data of boiler 9 and 10 (pre– and post–retrofit)

Opposed–fired boiler with partition wall, Western Europe (bituminous coal)			
	Pre–	**Post–**	**retrofit**
Fuel rating (BMCR)	1,240.00	1,240.00	MWt
Primary NO_x level	640	430	mg / m^3 STP_{dry} at 6 % O_2
System design modifications			
Distance between upper B. E. and OFA 1	–	3.000	m
Distance between OFA 1 and OFA 2	–	3.408	m
Distance between OFA 2 and OFA 3	–	2.592	m
System design			
Burner installed		32	–
Burner elevations (B. E.)		4	–
Partition wall surface (inside burner belt)		760	m^2
Furnace depth (furnace side walls)		14.486	m
Furnace width (burner walls, hopper trapezia)		19.286	m
Furnace height (without hopper)		35.230	m
B. E. vertical spacing		4.028	m
Distance between lower B. E. and hopper edge		1.615	m
Hopper height		12.915	m
Hopper angle		55	°

Table A2–7. Reference data of boiler 11

Allwall–fired boiler, Central Asia (bituminous coal)		
Fuel rating (BMCR)	414.00	MWt
Primary NO_x level	460	mg / m^3 STP_{dry} at 6 % O_2
System design		
Burner installed	8	–
Burner elevations (B. E.)	2	–
Furnace depth (furnace side walls)	11.370	m
Furnace width (hopper trapezia)	11.260	m
Furnace height (without hopper)	21.000	m
B. E. vertical spacing	4.000	m
Distance between lower B. E. and hopper edge	1.820	m
Distance between upper B. E. and OFA 1	3.700	m
Distance between OFA 1 and OFA 2	4.000	m
Hopper height	6.000	m
Hopper angle	50	°

Table A2–8. Reference data of boiler 12

Opposed–fired boiler with partition wall, Northwestern Europe (bituminous coal)		
Fuel rating (BMCR)	1,550.00	MWt
Primary NO_x level	725	mg / m³ STP_{dry} at 6 % O_2
System design		
Burner installed	48	–
Burner elevations (B. E.)	5	–
Partition wall surface (inside burner belt)	450	m²
Furnace depth (furnace side walls, hopper trapezia)	12.120	m
Furnace width (Burner walls)	25.600	m
Furnace height (without hopper)	21.500	m
B. E. vertical spacing	2.300	m
Distance between lower B. E. and hopper edge	1.600	m
Distance between upper B. E. and OFA	5.580	m
Hopper height	7.300	m
Hopper angle	53	°

Table A2–9. Reference data of boiler 13

Opposed–fired boiler, Northwestern Europe (bituminous coal)		
Fuel rating (BMCR)	1,330.00	MWt
Primary NO_x level	755	mg / m^3 STP_{dry} at 6 % O_2
System design		
Burner installed	48	–
Burner elevations (B. E.)	4	–
Furnace depth (furnace side walls, hopper trapezia)	9.220	m
Furnace width (Burner wall)	29.600	m
Furnace height (without hopper)	23.485	m
B. E. vertical spacing	2.946	m
Distance between lower B. E. and hopper edge	1.316	m
Distance between upper B. E. and OFA 1	4.389	m
Distance between OFA 1 and OFA 2	4.237	m
Hopper height	5.588	m
Hopper angle	54	°

Table A2–10. Reference data of boiler 14

Opposed–fired boiler, Western Europe (bituminous coal)		
Fuel rating (BMCR)	1545.00	MWt
Primary NO_x level	502	$mg / m^3 STP_{dry}$ at 6 % O_2
System design		
Burner installed	36	–
Burner elevations (B. E.)	3	–
Furnace depth (furnace side walls, hopper trapezia)	14.600	m
Furnace width (Burner walls)	21.200	m
Furnace height (without hopper)	36.500	m
B. E. vertical spacing	4.000	m
Distance between lower B. E. and hopper edge	4.300	m
Distance between upper B. E. and OFA 1	6.100	m
Distance between OFA 1 and OFA 2	3.000	m
Hopper height	8.100	m
Hopper angle	50	°

Table A2–11. Reference data of boiler 15

Tangentially–fired boiler, Western Europe (bituminous coal)			
Fuel rating (BMCR)		1,300.00	MWt
Primary NO_x level	B. E. 1–3&5 B. E. 2–5	585 565	mg / m³ STP_{dry} at 6 % O_2
System design			
Burner installed (corner registers)		4	–
Pulverized fuel injectors installed		24	–
Burner elevations (B. E.)		6	–
Furnace depth (furnace side walls, hopper trapezia)		14.600	m
Furnace width		17.300	m
Furnace height (without hopper)		29.400	m
B. E. vertical spacing		2.200	m
Distance between lower B. E. and hopper edge		4.300	m
Distance between upper B. E. and OFA 1		1.300	m
Distance between OFA 1 and OFA 2		0.430	m
Distance between OFA 2 and OFA 3		0.430	m
Distance between OFA 3 and OFA 4		0.430	m
Hopper height		10.081	m
Hopper angle		56	°

Table A2–12. Reference data of boiler 16

Opposed–fired boiler with partition wall, South Africa (bituminous coal)		
Fuel rating (BMCR)	1,486.50	MWt
Primary NO_x level	1,150.00	$mg / m^3 STP_{dry}$ at 6 % O_2
System design		
Burner installed	24	–
Burner elevations (B. E.)	3	–
Partition wall surface (inside burner belt)	750	m^2
Furnace depth (furnace side walls)	20.186	m
Furnace width (Burner walls, hopper trapezia)	17.186	m
Furnace height (without hopper)	39.000	m
B. E. vertical spacing	7.287	m
Distance between lower B. E. and hopper edge	3.589	m
Hopper height	11.000	m
Hopper angle	54	°

Table A2–13. Reference data of boiler 17

Tangentially–fired boiler, East Asia (bituminous coal)		
Fuel rating (BMCR)	1,728.00	MWt
Primary NO_x level	633	mg / m³ STP_{dry} at 6 % O_2
System design		
Burner installed (corner registers)	4	–
Pulverized fuel injectors installed	20	–
Burner elevations (B. E.)	5	–
Furnace depth (furnace side walls)	19.558	m
Furnace width (hopper trapezia)	16.433	m
Furnace height (without hopper)	47.567	m
B. E. vertical spacing	1.608	m
Distance between lower B. E. and hopper edge	4.986	m
Distance between upper B. E. and OFA 1	2.724	m
Distance between OFA 1 and OFA 2	0.642	m
Hopper height	7.716	m
Hopper angle	45	°

Table A2–14. Reference data of boiler 18

Tangentially–fired boiler, East Asia (sub–bituminous coal)		
Fuel rating (BMCR)	2,860.00	MWt
Primary NO_x level	865	mg / m³ STP_{dry} at 6 % O_2
System design		
Burner installed (corner registers)	12	–
Pulverized fuel injectors installed	48	–
Burner elevations (B. E.)	3	–
Furnace depth (furnace side walls)	25.080	m
Furnace width (hopper trapezia)	25.080	m
Furnace height (without hopper)	66.114	m
B. E. vertical spacing	8.653	m
Distance between lower B. E. and hopper edge	7.835	m
Distance between upper B. E. and OFA 1	11.280	m
Hopper height	16.434	m
Hopper angle	54	°

Table A2–15. Reference data of boiler 19

Opposed–fired boiler, Southeast Asia (sub–bituminous coal)		
Fuel rating (BMCR)	1,315.00	MWt
Primary NO_x level	617.4	mg / m³ STP_{dry} at 6 % O_2
System design		
Burner installed	24	–
Burner elevations (B. E.)	3	–
Furnace depth (furnace side walls, hopper trapezia)	16.032	m
Furnace width (Burner walls)	22.214	m
Furnace height (without hopper)	35.500	m
B. E. vertical spacing	5.000	m
Distance between lower B. E. and hopper edge	4.000	m
Distance between upper B. E. and OFA 1	10.000	m
Distance between OFA 1 and OFA 2	5.190	m
Distance between OFA 2 and OFA 3	3.000	m
Hopper height	10.300	m
Hopper angle	55	°

Table A2–16. Reference data of boiler 20

Tangentially–fired boiler, North America (sub–bituminous coal)			
Fuel rating (BMCR)		1,567.32	MWt
Primary NO_x level	B. E. 1–5 B. E. 1–4&6 B. E. 2–6	785 850 860	mg / m³ STP_{dry} at 6 % O_2
System design			
Burner installed (corner registers)		4	–
Pulverized fuel injectors installed		24	–
Burner elevations (B. E.)		6	–
Furnace depth (furnace side walls, hopper trapezia)		16.050	m
Furnace width		19.810	m
Furnace height (without hopper)		45.300	m
B. E. vertical spacing		2.500	m
Distance between lower B. E. and hopper edge		6.000	m
Distance between upper B. E. and OFA 1		2.500	m
Hopper height		10.600	m
Hopper angle		55	°

Table A2–17. Reference data of boiler 21

Tangentially–fired boiler, Southern Europe (lignite)		
Fuel rating (BMCR)	995.00	MWt
Primary NO_x level	1,085	mg / m^3 STP_{dry} at 6 % O_2
System design		
Burner installed (with vapor separation)	16	–
Pulverized fuel injectors installed	16	–
Burner elevations (B. E.)	2	–
Furnace depth (furnace side walls, hopper trapezia)	17.280	m
Furnace width	17.280	m
Furnace height (without hopper)	36.500	m
B. E. vertical spacing	8.570	m
Distance between lower B. E. and hopper edge	4.500	m
Distance between upper B. E. and OFA	10.000	m
Hopper height	11.000	m
Hopper angle	54	°

Table A2–18. Reference data of boiler 22 and 23 (pre– and post–retrofit)

Tangentially–fired boiler, Southeastern Europe (lignite)

	Pre–	**Post–**	**retrofit**
Fuel rating (BMCR)	660.00	660.00	MWt
Primary NO_x level	965	185	mg / m³ STP_{dry} at 6 % O_2
System design modifications			
Distance between upper B. E. and OFA 1	–	16.750	m
Distance between OFA 1 and OFA 2	–	2.000	m
Distance between OFA 2 and OFA 3	–	1.500	m
System design			
Burner installed (with vapor separation)		8	–
Pulverized fuel injectors installed		16	–
Burner elevations (B. E.)		2	–
Furnace depth (furnace side walls, hopper trapezia)		12.240	m
Furnace width		14.620	m
Furnace height (without hopper)		36.730	m
B. E. vertical spacing		6.690	m
Distance between lower B. E. and hopper edge		1.780	m
Hopper height		8.512	m
Hopper angle		55	°

Table A2–19. Reference data of boiler 24

Tangentially–fired boiler, Central Europe (lignite)		
Fuel rating (BMCR)	635.00	MWt
Primary NO_x level	1,020	mg / m³ STP_{dry} at 6 % O_2
System design		
Burner installed (with vapor separation)	16	–
Pulverized fuel injectors installed	8	–
Burner elevations (B. E.)	2	–
Furnace depth (furnace side walls, hopper trapezia)	12.000	m
Furnace width	10.200	m
Furnace height (without hopper)	23.030	m
B. E. vertical spacing	5.600	m
Distance between lower B. E. and hopper edge	1.600	m
Distance between upper B. E. and OFA 1	5.750	m
Distance between OFA 1and OFA 2	5.050	m
Hopper height	5.960	m
Hopper angle	54	°

Table A2–20. Reference data of boiler 25 and 26 (pre– and post–retrofit)

Tangentially–fired boiler, Western Europe (lignite)			
	Pre–	**Post–**	**retrofit**
Fuel rating (BMCR)	1,770.00	1,770.00	MWt
Primary NO_x level	886.4	793.4	mg / m³ STP_{dry} at 6 % O_2
System design modifications			
Distance between upper B. E. and OFA 1	11.860	18.273	m
Distance between OFA 1 and OFA 2	21.350	8.783	m
System design			
Burner installed (without vapor separation)		16	–
Pulverized fuel injectors installed		32	–
Burner elevations (B. E.)		2	–
Furnace depth (furnace side walls)		20.000	m
Furnace width (hopper trapezia)		20.000	m
Furnace height (without hopper)		48.930	m
B. E. vertical spacing		6.668	m
Distance between lower B. E. and hopper edge		5.000	m
Hopper height		13.567	m
Hopper angle		55	°

Table A2–21. Reference data of boiler 27

Opposed–fired boiler, Central Europe (lignite)		
Fuel rating (BMCR)	196.00	MWt
Primary NO_x level	535	mg / m³ STP_{dry} at 6 % O_2
System design		
Burner installed (without vapor separation)	12	–
Pulverized fuel injectors installed	24	–
Burner elevations (B. E.)	2	–
Furnace depth (furnace side walls, hopper trapezia)	8.125	m
Furnace width	9.125	m
Furnace height (without hopper)	16.155	m
B. E. vertical spacing	1.200	m
Distance between lower B. E. and hopper edge	0.965	m
Distance between upper B. E. and OFA 1	7.042	m
Hopper height	5.875	m
Hopper angle	56	°

Table A2–22. Reference data of boiler 28

Opposed–fired boiler, East Asia (lignite)		
Fuel rating (BMCR)	1,523.25	MWt
Primary NO_x level	1,110	mg / m³ STP_{dry} at 6 % O_2
System design		
Swirl–burner installed (without vapor separation)	35	–
Burner elevations (B. E.)	4	–
Furnace depth (furnace side walls, hopper trapezia)	16.840	m
Furnace width	22.187	m
Furnace height (without hopper)	34.451	m
B. E. vertical spacing	3.620	m
Distance between lower B. E. and hopper edge	3.414	m
Distance between upper B. E. and OFA 1	7.129	m
Hopper height	10.832	m
Hopper angle	54	°

Table A2–23. Reference coal compositions

Coal No.	LHV	Analysis results in wt.–% on a as received basis							
		Proximate			Ultimate				
	MJ / kg	VM	W	Ash	C	H	S	O	N
1	23.762	31.59	13.70	11.21	61.00	4.06	0.67	8.13	1.23
2	16.100	14.67	4.61	43.00	42.50	2.90	0.54	5.70	0.75
3	25.100	32.90	13.50	7.10	64.10	4.40	0.60	8.95	1.35
4	24.709	26.36	8.90	13.69	63.54	3.77	0.62	8.00	1.48
5	29.740	29.08	6.64	5.44	77.20	4.78	0.49	4.21	1.24
6	23.123	26.45	12.09	16.92	58.64	3.69	2.19	5.08	1.39
7	28.252	28.73	8.50	8.20	70.50	4.50	3.30	3.80	1.20
8	28.750	25.13	10.10	6.13	72.40	4.41	0.82	4.79	1.35
9	25.690	22.60	7.00	14.00	67.72	3.60	0.50	5.45	1.73
10	25.300	32.70	13.80	6.10	65.80	4.14	0.68	8.11	1.37
11	25.290	27.50	10.60	10.40	65.51	3.76	0.56	7.68	1.49
12	25.960	35.50	12.20	3.70	66.36	4.17	0.35	11.94	1.28
13	25.050	28.30	10.70	9.70	64.41	3.92	0.52	9.40	1.35
14	25.790	25.00	6.90	12.20	65.62	3.98	0.88	9.29	1.13
15	25.750	32.20	10.90	8.70	66.64	4.54	0.60	7.41	1.21
16	25.660	28.50	9.50	10.60	66.00	4.10	0.70	7.90	1.20
17	22.496	27.01	14.00	12.00	59.42	3.61	0.43	9.83	0.71
18									
19	28.070	31.23	8.21	7.96	71.56	4.56	0.91	5.59	1.21
20	23.620	30.26	12.89	12.27	62.19	4.26	0.70	6.47	1.22
21	17.720	21.06	6.00	27.92	53.17	2.61	0.83	8.24	1.23

Coal No.	LHV MJ / kg	Analysis results in wt.–% on a as received basis							
		Proximate			Ultimate				
		VM	W	Ash	C	H	S	O	N
22	16.830	18.15	6.90	31.56	49.99	2.39	1.18	6.89	1.09
23	17.150	18.94	6.60	31.03	50.67	2.44	1.13	7.02	1.11
24	25.231	24.22	7.57	13.49	65.99	3.66	0.31	7.39	1.59
25	25.807	30.17	11.27	8.61	67.30	4.46	1.36	5.43	1.57
26	26.100	31.60	9.50	8.80	68.20	4.50	0.90	6.50	1.60
27	25.054	27.98	12.61	9.39	65.08	3.83	1.28	6.41	1.40
28	5.310	20.58	51.49	17.41	19.51	1.44	0.69	8.94	0.52
29	5.266	19.97	51.17	18.20	19.07	1.42	0.56	9.07	0.51
30	5.521	19.94	52.45	16.69	19.49	1.44	0.57	8.84	0.52
31	24.720	18.92	9.40	17.54	64.14	3.63	0.99	3.11	1.19
32	19.092	31.47	27.39	5.16	51.47	2.65	0.30	12.34	0.69
33	19.014	31.48	27.61	5.13	50.86	2.58	0.30	12.84	0.68
34	19.317	30.90	26.88	5.42	52.77	2.27	0.35	11.64	0.67
35	18.848	30.73	27.63	5.14	51.85	2.65	0.24	11.82	0.67
36	18.610	30.85	28.88	4.99	50.44	2.61	0.33	11.99	0.76
37	18.429	30.77	30.18	4.62	49.71	2.58	0.32	11.90	0.69
38	18.728	30.63	28.14	4.85	51.21	2.58	0.27	12.21	0.74
39	19.014	31.22	28.10	4.96	51.80	2.67	0.33	11.44	0.70
40	18.801	30.99	28.54	5.11	51.74	2.56	0.32	11.05	0.68
41	18.760	30.58	29.55	5.18	50.15	2.56	0.30	11.63	0.63
42	18.754	31.48	28.39	5.17	51.29	2.47	0.30	11.64	0.74
43	18.938	31.18	27.88	4.77	52.64	2.52	0.30	11.23	0.66

Coal No.	**LHV**	**Analysis results in wt.–% on a as received basis**							
		Proximate			**Ultimate**				
	MJ / kg	VM	W	Ash	C	H	S	O	N
44	18.524	29.98	28.91	4.87	51.94	2.52	0.29	10.76	0.71
45	18.876	30.62	27.45	5.24	53.13	2.66	0.31	10.53	0.68
46	25.000	29.90	11.00	9.00	65.50	3.50	0.32	9.16	1.52
47	24.800	28.70	11.80	8.60	65.50	3.26	0.39	8.99	1.46
48	26.100	30.50	8.90	9.00	65.00	3.59	0.47	11.91	1.13
49	24.500	31.30	13.60	7.30	62.50	3.98	0.41	11.29	0.92
50	26.900	24.50	8.10	11.00	70.00	3.67	0.41	5.58	1.24
51	24.200	30.80	13.50	8.40	61.50	3.99	0.41	11.03	1.17
52	24.700	29.90	13.90	7.80	63.00	3.94	0.48	9.71	1.17
53	25.100	28.60	11.80	9.50	64.50	3.72	0.47	8.82	1.19
54	25.800	29.70	8.50	11.00	66.50	3.63	0.61	8.56	1.20
55	26.900	29.20	7.50	9.90	68.00	4.20	0.66	8.20	1.54
56	24.600	25.80	9.00	14.10	63.00	3.57	0.57	8.21	1.55
57	25.600	26.40	9.00	12.30	65.00	3.57	0.55	7.94	1.64
58	24.200	31.10	12.80	9.50	66.00	3.80	0.53	5.97	1.40
59	25.200	35.60	13.30	5.00	70.00	4.10	0.40	6.10	1.10
60	24.500	28.20	9.90	12.00	64.87	4.00	0.66	7.07	1.50
61	26.000	26.80	7.50	12.20	64.87	4.00	0.53	9.30	1.60
62	27.500	29.40	6.90	10.30	65.50	3.90	1.15	10.73	1.52
63	27.100	28.10	7.00	11.20	65.58	3.82	1.05	9.85	1.50
64	27.200	29.30	7.30	10.60	65.50	3.90	1.20	10.10	1.40
65	26.800	32.80	8.00	11.10	65.58	3.82	1.14	9.06	1.30

Coal No.	LHV	Analysis results in wt.–% on a as received basis							
		Proximate			Ultimate				
	MJ / kg	VM	W	Ash	C	H	S	O	N
66	25.900	28.70	9.70	10.60	65.50	3.90	0.97	8.03	1.30
67	25.000	31.00	13.90	7.00	68.00	3.50	0.40	6.00	1.20
68	25.500	34.60	12.10	8.20	66.71	3.63	0.59	7.57	1.20
69	24.600	23.80	8.00	15.40	64.11	3.49	0.68	6.79	1.53
70	25.100	29.20	10.00	11.80	65.58	3.82	0.63	6.80	1.37
71	8.569	19.14	51.70	11.70	25.95	2.04	1.16	7.21	0.24
72	8.479	19.02	52.30	11.10	25.69	2.08	1.20	7.41	0.22
73	8.625	19.21	52.00	10.80	25.89	2.06	1.08	7.95	0.22
74	8.504	19.06	52.90	10.20	25.60	2.05	1.16	7.87	0.22
75	9.164	19.91	51.80	9.20	27.23	2.17	1.01	8.37	0.22
76	8.453	18.99	51.30	12.50	25.32	2.01	1.14	7.51	0.22
77	24.541	19.74	12.53	14.22	64.00	4.00	0.92	2.81	1.54
78	7.033	18.55	54.18	13.86	21.17	1.77	1.85	6.80	0.37
79	6.698	18.05	54.48	14.75	20.34	1.70	1.84	6.53	0.36
80	6.899	18.35	53.42	14.81	20.78	1.74	1.88	7.00	0.37
81	26.069	28.11	15.00	8.00	64.51	3.99	0.41	6.53	1.56
82	23.667	24.75	17.00	10.00	57.89	3.17	1.00	9.98	0.96
83	14.070	25.08	31.10	17.08	37.33	2.74	0.56	10.49	0.70
84	14.370	25.21	31.90	15.87	38.50	2.76	0.52	9.75	0.70
85	13.780	24.85	32.50	15.98	35.00	2.72	0.50	12.60	0.70
86	26.495	33.50	3.00	16.20	66.29	4.61	1.97	6.87	1.06
87	19.467	34.29	26.00	4.06	52.08	3.10	0.89	12.82	1.05

Coal No.	**LHV**	**Analysis results in wt.–% on a as received basis**							
		Proximate			**Ultimate**				
	MJ / kg	VM	W	Ash	C	H	S	O	N
88	8.931	21.40	55.39	4.77	27.60	1.97	0.30	9.66	0.31
89	18.153	80.00	7.10	0.30	51.50	7.40	0.20	33.20	0.30
90	14.500	28.04	26.04	21.06	36.78	3.12	0.91	11.65	0.44
91	5.464	21.50	49.93	17.85	18.00	1.37	0.64	11.73	0.48

Table A2–24. Reference NO$_x$ emissions

Ref. No.	Boiler No.	Coal No.	Fuel rating MWt	Active B. E.	Air temp. °C		PA/ PF ratio	$NO_{x_{Ref}}$ mg/m³ STP$_{dry}$ (at 6 % O$_2$)
					SA	PA		
1	1	5	1,073.00	1–4	330.0	90.0	2.20	489.000
2	2	19	730.00	1–3	340.0	90.0	1.80	304.000
3	2	24	708.10	1–3	340.0	90.0	1.79	425.000
4	3	1	798.40	1–3	340.0	90.0	1.80	321.000
5	5	7	90.00	1–3	300.0	87.0	2.51	380.000
6	6	8	1,712.00	1–4	300.0	70.0	1.80	396.000
7	7	3	1,190.00	1–3	344.0	85.0	1.65	319.000
8	11	2	414.00	1–2	324.0	110.0	1.80	320.000
9	10	4	1,242.00	1–4	330.0	90.0	1.26	303.000
10	14	9	1,520.00	1–3	300.0	90.0	2.08	364.620
11	14	9	1,520.00	1–3	300.0	90.0	2.22	397.580
12	14	9	1,520.00	1–3	300.0	90.0	2.00	441.870
13	14	10	1,520.00	1–3	300.0	90.0	1.97	266.770
14	14	10	1,520.00	1–3	300.0	90.0	1.97	269.860
15	14	10	1,520.00	1–3	300.0	90.0	2.00	290.460
16	14	11	1,520.00	1–3	300.0	90.0	2.00	320.330
17	14	11	1,520.00	1–3	300.0	90.0	2.00	329.600
18	14	11	1,520.00	1–3	300.0	90.0	2.00	364.620
19	14	12	1,520.00	1–3	300.0	90.0	2.05	202.910
20	14	12	1,520.00	1–3	300.0	90.0	2.05	211.150
21	14	12	1,520.00	1–3	300.0	90.0	2.00	224.540

Ref. No.	**Boiler No.**	**Coal No.**	**Fuel rating** MWt	**Active B. E.**	**Air temp.** °C		**PA/ PF ratio**	$NO_{x_{Ref}}$ mg/m³ STP_{dry} (at 6 % O_2)
					SA	PA		
22	14	13	1,520.00	1–3	300.0	90.0	1.93	300.760
23	14	13	1,520.00	1–3	300.0	90.0	1.93	311.060
24	14	13	1,520.00	1–3	300.0	90.0	2.00	317.240
25	3	1	799.00	1–3	340.0	90.0	1.96	300.000
26	3	20	799.00	1–3	340.0	90.0	1.99	385.000
27	3	25	799.00	1–3	340.0	90.0	1.97	395.000
28	3	26	799.00	1–3	340.0	90.0	1.90	355.000
29	10	4	1,240.00	1–4	330.0	90.0	2.79	350.000
30	10	27	1,240.00	1–4	330.0	90.0	2.98	390.000
31	10	4	1,240.00	1–4	330.0	90.0	2.88	310.000
32	9	4	1,240.00	1–4	330.0	90.0	2.14	1.110.000
33	16	21	1,402.00	1–3	290.0	104.0	1.64	1.654.282
34	16	22	1,430.00	1–3	290.0	104.0	1.57	1.788.667
35	16	23	1,430.00	1–3	290.0	104.0	1.46	2.100.781
36	7	31	1,329.12	1–3	336.0	85.0	1.39	525.000
37	4	7	90.00	1–3	300.0	87.0	2.51	682.000
38	12	6	1,550.17	1–5	294.4	88.2	2.05	606.540
39	12	6	1,117.30	1–5	276.7	85.2	2.11	533.500
40	20	32	1,567.32	2–6	370.7	65.4	2.15	435.437
41	20	33	1,567.32	2–6	370.7	65.4	2.15	425.472
42	20	33	1,567.32	2–6	370.7	65.4	2.15	504.343
43	20	34	1,567.32	2–6	370.7	65.4	2.15	459.446

Ref. No.	Boiler No.	Coal No.	Fuel rating MWt	Active B. E.	Air temp. °C		PA/ PF ratio	$NO_{x_{Ref}}$ mg/m³ STP$_{dry}$ (at 6 % O$_2$)
					SA	PA		
44	20	35	1,567.32	1–5	370.7	65.4	2.14	304.627
45	20	36	1,567.32	1–5	370.7	65.4	2.15	336.412
46	20	37	1,569.90	1–4&6	370.7	65.4	2.15	389.755
47	20	38	1,567.32	1–4&6	370.7	65.4	2.15	410.082
48	20	39	1,500.00	1–5	370.7	65.4	2.15	316.640
49	20	40	1,575.06	1–5	370.7	65.4	2.15	372.887
50	20	41	1,567.32	1–5	370.7	65.4	2.15	355.922
51	20	42	1,572.48	1–5	370.7	65.4	2.15	459.676
52	20	43	1,572.48	1–5	370.7	65.4	2.15	314.436
53	20	41	1,575.06	1–5	370.7	65.4	2.15	330.320
54	20	41	1,572.48	2–6	370.7	65.4	2.15	465.719
55	20	42	1,569.90	1–5	370.7	65.4	2.15	309.301
56	20	43	1,569.90	1–5	370.7	65.4	2.15	396.811
57	20	43	1,567.32	1–5	370.7	65.4	2.15	322.422
58	20	44	1,567.32	1–5	370.7	65.4	2.15	327.079
59	20	45	1,505.24	1–5	370.7	65.4	2.15	319.763
60	15	14	1,300.00	1–3&5	300.0	80.0	2.00	440.000
61	15	14	1,302.50	1–3&5	300.0	80.0	2.00	468.000
62	15	14	1,300.00	1–3&5	300.0	80.0	2.00	440.000
63	15	14	1,327.50	1–3&5	300.0	80.0	2.00	462.000
64	15	14	1,300.00	2–5	300.0	80.0	2.00	514.000
65	15	16	1,300.00	1–3&5	300.0	80.0	2.00	421.000

Ref. No.	**Boiler No.**	**Coal No.**	**Fuel rating** MWt	**Active B. E.**	**Air temp.** °C		**PA/ PF ratio**	$NO_{x_{Ref}}$ mg/m³ STP$_{dry}$ (at 6 % O_2)
					SA	PA		
66	15	16	1,300.00	1–3&5	300.0	80.0	2.00	417.000
67	15	16	1,300.00	1–3&5	300.0	80.0	2.00	401.000
68	15	16	1,300.00	1–3&5	300.0	80.0	2.00	427.000
69	15	16	1,312.50	2–5	300.0	80.0	2.00	425.000
70	15	15	1,300.00	1–3&5	300.0	80.0	2.00	398.000
71	15	15	1,300.00	1–3&5	300.0	80.0	2.00	407.000
72	15	15	1,302.50	1–3&5	300.0	80.0	2.00	392.000
73	15	15	1,300.00	1–3&5	300.0	80.0	2.00	396.000
74	15	15	1,300.00	2–5	300.0	80.0	2.00	452.000
75	15	46	1,300.00	1–3&5	300.0	80.0	2.00	389.000
76	15	46	1,300.00	1–3&5	300.0	80.0	2.00	414.000
77	15	46	1,300.00	1–3&5	300.0	80.0	2.00	468.000
78	15	47	1,300.00	1–3&5	300.0	80.0	2.00	418.000
79	15	47	1,300.00	1–3&5	300.0	80.0	2.00	442.000
80	15	47	1,300.00	1–3&5	300.0	80.0	2.00	479.000
81	15	48	1,300.00	1–3&5	300.0	80.0	2.00	405.000
82	15	48	1,300.00	1–3&5	300.0	80.0	2.00	435.000
83	15	48	1,300.00	1–3&5	300.0	80.0	2.00	485.000
84	15	49	1,300.00	1–3&5	300.0	80.0	2.00	323.000
85	15	49	1,300.00	1–3&5	300.0	80.0	2.00	357.000
86	15	50	1,300.00	1–3&5	300.0	80.0	2.00	478.000
87	15	50	1,300.00	1–3&5	300.0	80.0	2.00	495.000

Ref. No.	Boiler No.	Coal No.	Fuel rating MWt	Active B. E.	Air temp. °C		PA/ PF ratio	$NO_{x_{Ref}}$ mg/m³ STP_{dry} (at 6 % O_2)
					SA	PA		
88	15	50	1,300.00	1–3&5	300.0	80.0	2.00	539.000
89	15	51	1,300.00	1–3&5	300.0	80.0	2.00	413.000
90	15	51	1,300.00	1–3&5	300.0	80.0	2.00	442.000
91	15	51	1,300.00	1–3&5	300.0	80.0	2.00	511.000
92	15	52	1,300.00	1–3&5	300.0	80.0	2.00	387.000
93	15	52	1,300.00	1–3&5	300.0	80.0	2.00	439.000
94	15	52	1,300.00	1–3&5	300.0	80.0	2.00	483.000
95	15	53	1,300.00	1–3&5	300.0	80.0	2.00	392.000
96	15	53	1,300.00	1–3&5	300.0	80.0	2.00	428.000
97	15	53	1,300.00	1–3&5	300.0	80.0	2.00	478.000
98	15	54	1,300.00	1–3&5	300.0	80.0	2.00	422.000
99	15	54	1,300.00	1–3&5	300.0	80.0	2.00	464.000
100	15	55	1,300.00	1–3&5	300.0	80.0	2.00	442.000
101	15	55	1,300.00	1–3&5	300.0	80.0	2.00	472.000
102	15	55	1,300.00	1–3&5	300.0	80.0	2.00	483.000
103	15	56	1,300.00	1–3&5	300.0	80.0	2.00	482.000
104	15	56	1,300.00	1–3&5	300.0	80.0	2.00	530.000
105	15	57	1,300.00	1–3&5	300.0	80.0	2.00	453.000
106	15	57	1,300.00	1–3&5	300.0	80.0	2.00	513.000
107	15	57	1,300.00	1–3&5	300.0	80.0	2.00	551.000
108	21	30	994.77	1–2	275.0	175.0	0.00	350.270
109	21	28	795.82	1–2	275.0	175.0	0.00	275.130

Ref. No.	Boiler No.	Coal No.	Fuel rating MWt	Active B. E.	Air temp. °C		PA/ PF ratio	$NO_{x_{Ref}}$ mg/m³ STP_{dry} (at 6 % O_2)
					SA	PA		
110	21	29	596.86	1–2	275.0	175.0	0.00	325.007
111	18	17	2,859.24	1–3	350.0	75.0	1.62	420.000
112	24	71	586.70	1–2	285.3	130.0	0.00	373.000
113	24	72	560.20	1–2	282.6	140.0	0.00	390.000
114	24	73	529.20	1–2	281.9	136.0	0.00	439.000
115	24	74	500.70	1–2	279.2	95.0	0.00	387.000
116	24	75	471.90	1–2	283.6	110.0	0.00	429.000
117	24	76	454.30	1–2	274.5	111.0	0.00	478.000
118	8	77	1,190.00	1–3	336.0	85.0	1.54	470.000
119	23	78	651.72	1–2	254.0	125.0	0.00	147.000
120	23	79	514.16	1–2	245.0	125.0	0.00	155.000
121	23	80	431.38	1–2	230.0	125.0	0.00	150.000
122	22	78	653.00	1–2	254.0	125.0	0.00	367.000
123	17	81	1,727.80	1–5	300.0	100.0	2.25	746.340
124	17	81	1,716.93	1–5	300.0	100.0	2.25	732.940
125	17	81	1,677.83	1–5	300.0	100.0	2.29	777.870
126	17	81	1,685.07	1–5	300.0	100.0	2.22	906.530
127	17	81	1,656.11	1–5	300.0	100.0	2.34	784.640
128	17	82	1,580.43	1–5	300.0	100.0	2.30	644.750
129	17	82	1,594.89	1–5	300.0	100.0	2.23	620.170
130	17	82	1,584.37	1–5	300.0	100.0	2.25	713.910
131	17	82	1,581.74	1–5	300.0	100.0	2.26	671.720

Ref. No.	**Boiler No.**	**Coal No.**	**Fuel rating** MWt	**Active B. E.**	**Air temp.** °C		**PA/ PF ratio**	$NO_{x_{Ref}}$ mg/m³ STP$_{dry}$ (at 6 % O$_2$)
					SA	PA		
132	17	81	1,308.52	1–5	300.0	100.0	2.54	638.760
133	17	81	1,035.52	1–5	300.0	100.0	3.21	632.940
134	17	82	1,572.54	1–5	300.0	100.0	2.27	659.320
135	28	83	1,396.80	1–3	369.0	65.0	2.51	458.400
136	28	84	1,142.84	1–3	319.0	65.0	2.56	698.200
137	28	85	761.89	1–3	306.0	65.0	2.62	771.300
138	13	86	1,330.05	1–4	280.0	85.0	2.45	386.000
139	19	87	1,315.00	1–3	325.0	70.0	2.00	250.000
140	25	88	1,770.39	1–2	337.0	155.0	0.50	223.000
141	26	88	1,770.39	1–2	337.0	155.0	0.52	230.000
142	27	90	196.00	1–2	350.0	150.0	1.27	306.000

Table A2–25. Reference Air ratios

Ref. No.	n_{BZ}	n_{BB}	n_{OFA2}	n_{OFA2}	n_{OFA3}	n_{OFA4}	n_{Total}	O_2 Vol.–%, dry
1	0.932	1.117	0.081	–	–	–	1.198	3.549
2	0.750	0.950	0.250	–	–	–	1.200	3.576
3	0.780	0.980	0.220	–	–	–	1.200	3.557
4	0.906	1.070	0.150	–	–	–	1.220	3.859
5	0.905	1.011	0.145	0.052	–	–	1.208	3.698
6	0.826	0.826	0.354	–	–	–	1.180	3.273
7	0.752	0.964	0.216	–	–	–	1.180	3.262
8	0.753	0.847	0.170	0.170	–	–	1.188	3.385
9	0.848	1.033	0.051	0.051	0.051	–	1.186	3.348
10	0.800	0.800	0.183	0.183	–	–	1.165	3.027
11	0.800	0.800	0.208	0.208	–	–	1.216	3.789
12	0.800	0.800	0.221	0.221	–	–	1.242	4.163
13	0.800	0.800	0.172	0.172	–	–	1.143	2.688
14	0.800	0.800	0.195	0.195	–	–	1.191	3.432
15	0.800	0.800	0.231	0.231	–	–	1.263	4.449
16	0.800	0.800	0.180	0.180	–	–	1.160	2.942
17	0.800	0.800	0.194	0.194	–	–	1.188	3.372
18	0.800	0.800	0.230	0.230	–	–	1.261	4.413
19	0.800	0.800	0.173	0.173	–	–	1.145	2.706
20	0.800	0.800	0.193	0.193	–	–	1.186	3.348
21	0.800	0.800	0.236	0.236	–	–	1.271	4.550
22	0.800	0.800	0.183	0.183	–	–	1.167	3.055

Ref. No.	n_{BZ}	n_{BB}	n_{OFA2}	n_{OFA2}	n_{OFA3}	n_{OFA4}	n_{Total}	O_2 Vol.–%, dry
23	0.800	0.800	0.205	0.205	–	–	1.210	3.699
24	0.800	0.800	0.231	0.231	–	–	1.262	4.427
25	0.900	1.030	0.150	–	–	–	1.180	3.268
26	0.930	1.060	0.150	–	–	–	1.210	3.725
27	0.930	1.060	0.120	–	–	–	1.180	3.276
28	0.930	1.060	0.120	–	–	–	1.180	3.273
29	0.860	1.010	0.057	0.057	0.057	–	1.180	3.259
30	0.860	1.010	0.057	0.057	0.057	–	1.180	3.264
31	0.843	0.973	0.069	0.069	0.069	–	1.181	3.274
32	1.300	1.300	–	–	–	–	1.300	4.921
33	1.145	1.245	–	–	–	–	1.245	4.180
34	1.136	1.236	–	–	–	–	1.236	4.060
35	1.265	1.365	–	–	–	–	1.365	5.670
36	0.769	0.988	0.236	–	–	–	1.224	3.937
37	1.160	1.260	–	–	–	–	1.260	4.427
38	0.971	0.971	0.182	–	–	–	1.153	2.841
39	1.011	1.011	0.178	–	–	–	1.189	3.411
40	1.022	1.072	0.065	–	–	–	1.137	2.560
41	1.015	1.065	0.068	–	–	–	1.133	2.490
42	1.091	1.141	0.005	–	–	–	1.146	2.700
43	1.015	1.065	0.071	–	–	–	1.135	2.519
44	0.872	0.922	0.212	–	–	–	1.135	2.519
45	0.937	0.987	0.160	–	–	–	1.147	2.710

Ref. No.	**n_{BZ}**	**n_{BB}**	**n_{OFA2}**	**n_{OFA2}**	**n_{OFA3}**	**n_{OFA4}**	**n_{Total}**	**O_2** Vol.–%, dry
46	0.922	0.972	0.164	–	–	–	1.136	2.530
47	0.949	0.999	0.142	–	–	–	1.141	2.620
48	0.879	0.929	0.207	–	–	–	1.136	2.540
49	0.932	0.982	0.153	–	–	–	1.135	2.520
50	0.953	1.003	0.131	–	–	–	1.134	2.503
51	1.053	1.103	0.037	–	–	–	1.140	2.595
52	0.839	0.889	0.240	–	–	–	1.128	2.411
53	0.869	0.919	0.218	–	–	–	1.137	2.559
54	1.033	1.083	0.055	–	–	–	1.138	2.570
55	0.834	0.884	0.250	–	–	–	1.134	2.500
56	1.047	1.097	0.110	–	–	–	1.207	3.630
57	0.840	0.890	0.267	–	–	–	1.157	2.870
58	0.888	0.938	0.223	–	–	–	1.161	2.940
59	0.833	0.883	0.264	–	–	–	1.147	2.720
60	0.770	0.770	0.109	0.109	0.109	0.109	1.207	3.665
61	0.770	0.770	0.125	0.125	0.125	0.125	1.268	4.514
62	0.770	0.770	0.104	0.104	0.104	0.104	1.186	3.346
63	0.770	0.770	0.111	0.111	0.111	0.111	1.214	3.772
64	0.770	0.770	0.106	0.106	0.106	0.106	1.193	3.452
65	0.770	0.770	0.111	0.111	0.111	0.111	1.215	3.788
66	0.770	0.770	0.121	0.121	0.121	0.121	1.253	4.321
67	0.770	0.770	0.104	0.104	0.104	0.104	1.186	3.361
68	0.770	0.770	0.113	0.113	0.113	0.113	1.223	3.895

Ref. No.	n_{BZ}	n_{BB}	n_{OFA2}	n_{OFA2}	n_{OFA3}	n_{OFA4}	n_{Total}	O_2 Vol.–%, dry
69	0.770	0.770	0.115	0.115	0.115	0.115	1.230	4.002
70	0.770	0.770	0.113	0.113	0.113	0.113	1.223	3.918
71	0.770	0.770	0.121	0.121	0.121	0.121	1.254	4.345
72	0.770	0.770	0.104	0.104	0.104	0.104	1.187	3.381
73	0.770	0.770	0.113	0.113	0.113	0.113	1.223	3.918
74	0.770	0.770	0.112	0.112	0.112	0.112	1.216	3.811
75	0.770	0.770	0.091	0.091	0.091	0.091	1.132	2.493
76	0.770	0.770	0.110	0.110	0.110	0.110	1.208	3.668
77	0.770	0.770	0.140	0.140	0.140	0.140	1.328	5.255
78	0.770	0.770	0.108	0.108	0.108	0.108	1.201	3.556
79	0.770	0.770	0.131	0.131	0.131	0.131	1.294	4.827
80	0.770	0.770	0.151	0.151	0.151	0.151	1.374	5.773
81	0.770	0.770	0.096	0.096	0.096	0.096	1.152	2.811
82	0.770	0.770	0.111	0.111	0.111	0.111	1.216	3.770
83	0.770	0.770	0.140	0.140	0.140	0.140	1.329	5.250
84	0.770	0.770	0.094	0.094	0.094	0.094	1.147	2.744
85	0.770	0.770	0.120	0.120	0.120	0.120	1.249	4.252
86	0.770	0.770	0.089	0.089	0.089	0.089	1.124	2.367
87	0.770	0.770	0.098	0.098	0.098	0.098	1.164	3.007
88	0.770	0.770	0.126	0.126	0.126	0.126	1.274	4.594
89	0.770	0.770	0.105	0.105	0.105	0.105	1.189	3.396
90	0.770	0.770	0.124	0.124	0.124	0.124	1.265	4.470
91	0.770	0.770	0.155	0.155	0.155	0.155	1.388	5.957

Ref. No.	n_{BZ}	n_{BB}	n_{OFA2}	n_{OFA2}	n_{OFA3}	n_{OFA4}	n_{Total}	O_2 Vol.–%, dry
92	0.770	0.770	0.094	0.094	0.094	0.094	1.147	2.741
93	0.770	0.770	0.118	0.118	0.118	0.118	1.241	4.141
94	0.770	0.770	0.140	0.140	0.140	0.140	1.332	5.312
95	0.770	0.770	0.097	0.097	0.097	0.097	1.159	2.934
96	0.770	0.770	0.117	0.117	0.117	0.117	1.239	4.111
97	0.770	0.770	0.142	0.142	0.142	0.142	1.338	5.383
98	0.770	0.770	0.084	0.084	0.084	0.084	1.107	2.055
99	0.770	0.770	0.100	0.100	0.100	0.100	1.172	3.125
100	0.770	0.770	0.084	0.084	0.084	0.084	1.107	2.063
101	0.770	0.770	0.095	0.095	0.095	0.095	1.151	2.815
102	0.770	0.770	0.107	0.107	0.107	0.107	1.200	3.562
103	0.770	0.770	0.081	0.081	0.081	0.081	1.095	1.847
104	0.770	0.770	0.101	0.101	0.101	0.101	1.172	3.135
105	0.770	0.770	0.081	0.081	0.081	0.081	1.094	1.843
106	0.770	0.770	0.100	0.100	0.100	0.100	1.172	3.129
107	0.770	0.770	0.125	0.125	0.125	0.125	1.268	4.509
108	0.953	1.050	0.170	–	–	–	1.220	3.810
109	0.955	1.075	0.151	–	–	–	1.226	3.890
110	1.173	1.283	0.194	–	–	–	1.477	6.800
111	0.910	1.000	0.200	–	–	–	1.200	3.557
112	0.870	1.170	0.080	0.120	0.027	–	1.397	6.060
113	0.905	1.205	0.080	0.120	0.027	–	1.432	6.430
114	0.976	1.276	0.080	0.120	0.027	–	1.503	7.120

Ref. No.	n_{BZ}	n_{BB}	n_{OFA2}	n_{OFA2}	n_{OFA3}	n_{OFA4}	n_{Total}	**O_2** Vol.–%, dry
115	1.028	1.328	0.080	0.120	0.027	–	1.555	7.590
116	1.103	1.403	0.080	0.120	0.027	–	1.630	8.210
117	1.174	1.474	0.080	0.120	0.027	–	1.701	8.750
118	0.769	0.959	0.239	–	–	–	1.198	3.568
119	0.800	0.950	0.060	0.060	0.060	–	1.129	2.445
120	0.850	1.000	0.064	0.064	0.064	–	1.192	3.447
121	0.850	1.000	0.062	0.062	0.062	–	1.185	3.329
122	1.050	1.150	–	–	–	–	1.150	2.788
123	1.000	1.010	0.103	0.069	–	–	1.182	3.295
124	1.000	1.010	0.082	0.092	–	–	1.184	3.327
125	1.000	1.010	0.145	0.009	–	–	1.164	3.019
126	1.105	1.115	0.047	0.004	–	–	1.165	3.031
127	1.058	1.068	0.053	0.027	–	–	1.148	2.760
128	1.000	1.010	0.096	0.064	–	–	1.170	3.099
129	1.000	1.010	0.095	0.064	–	–	1.169	3.078
130	1.100	1.110	0.036	0.024	–	–	1.170	3.090
131	1.050	1.060	0.072	0.048	–	–	1.180	3.240
132	1.000	1.010	0.248	0.016	–	–	1.274	4.602
133	0.950	0.960	0.305	0.019	–	–	1.284	4.729
134	1.050	1.060	0.066	0.044	–	–	1.170	3.089
135	0.861	0.891	0.300	–	–	–	1.191	3.411
136	1.103	1.133	0.100	–	–	–	1.233	4.026
137	1.301	1.326	0.050	–	–	–	1.376	5.800

Ref. No.	$\mathbf{n_{BZ}}$	$\mathbf{n_{BB}}$	$\mathbf{n_{OFA2}}$	$\mathbf{n_{OFA2}}$	$\mathbf{n_{OFA3}}$	$\mathbf{n_{OFA4}}$	$\mathbf{n_{Total}}$	$\mathbf{O_2}$ Vol.–%, dry
138	0.890	0.905	0.090	0.209	–	–	1.203	3.630
139	0.820	0.970	0.115	0.058	0.058	–	1.200	3.538
140	0.800	0.850	0.210	0.290	–	–	1.350	5.495
141	0.900	0.950	0.100	0.140	–	–	1.190	3.390
142	0.950	1.000	0.120	–	–	–	1.120	2.295

APPENDIX 3 – INPUT DATA SET FOR REGRESSION ANALYSIS

Table A3–1. Results obtained from the field data

Ref. No.	h_1	h_2	h_3	h_4	h_5	NI	mg / m³ STP$_{dry}$ at 6 % O$_2$	
							$NO_{x_{Pred}}$	$NO_{x_{Ref}}$
1	4.450	1.945	0.877	1.812	1.325	18.216	489.108	489.000
2	3.629	1.950	0.733	1.269	1.375	9.046	314.882	304.000
3	5.448	1.950	0.760	1.285	1.362	14.139	411.649	425.000
4	3.002	1.997	0.832	1.295	1.422	9.183	317.470	321.000
5	4.089	1.969	0.885	1.330	1.315	12.466	379.862	380.000
6	5.424	1.900	0.502	1.835	1.407	13.342	396.501	396.000
7	3.244	1.899	0.737	1.703	1.226	9.476	323.037	319.000
8	4.064	1.919	0.619	1.251	1.544	9.318	320.044	320.000
9	4.495	1.915	0.802	1.145	1.357	10.716	346.609	303.000
10	6.453	1.860	0.533	1.342	1.548	13.287	395.453	364.620
11	6.453	1.987	0.503	1.342	1.547	13.398	397.564	397.580
12	6.453	2.044	0.489	1.342	1.548	13.409	397.763	441.870
13	3.378	1.798	0.547	1.289	1.548	6.631	268.997	266.770
14	3.378	1.928	0.517	1.289	1.548	6.724	270.748	269.860
15	3.378	2.084	0.479	1.289	1.548	6.729	270.845	290.460
16	4.446	1.845	0.536	1.301	1.547	8.855	311.240	320.330
17	4.446	1.919	0.519	1.301	1.547	8.918	312.442	329.600

Ref. No.	h_1	h_2	h_3	h_4	h_5	NI	mg / m³ STP_{dry} at 6 % O_2	
							$NO_{x_{Pred}}$	$NO_{x_{Ref}}$
18	4.446	2.080	0.480	1.301	1.547	8.934	312.739	364.620
19	2.921	1.803	0.546	1.291	1.546	5.738	252.022	202.910
20	2.921	1.916	0.520	1.291	1.546	5.809	253.364	211.150
21	2.921	2.099	0.475	1.291	1.546	5.813	253.438	224.540
22	3.997	1.865	0.532	1.297	1.547	7.951	294.071	300.760
23	3.997	1.973	0.507	1.297	1.547	8.014	295.264	311.060
24	3.997	2.082	0.479	1.297	1.547	8.001	295.021	317.240
25	3.002	1.900	0.827	1.286	1.419	8.611	306.611	300.000
26	3.244	1.974	0.831	1.365	1.423	10.337	339.408	385.000
27	4.224	1.900	0.859	1.376	1.424	13.508	399.660	395.000
28	4.019	1.900	0.859	1.363	1.424	12.724	384.758	355.000
29	4.495	1.900	0.781	1.162	1.349	10.456	341.655	350.000
30	4.203	1.900	0.781	1.141	1.350	9.598	325.370	390.000
31	4.495	1.902	0.739	1.138	1.347	9.692	327.153	310.000
32	4.495	2.145	1.000	3.872	1.364	50.920	1.110.487	1.110.000
33	4.139	2.050	1.000	7.780	1.231	81.249	1.686.725	1.654.282
34	4.373	2.032	1.000	7.879	1.235	86.503	1.786.563	1.788.667
35	4.242	2.220	1.000	8.721	1.239	101.734	2.075.952	2.100.781
36	6.186	2.005	0.725	1.743	1.257	19.709	517.470	525.000
37	4.089	2.078	1.000	2.521	1.324	28.375	682.124	682.000
38	3.950	1.825	0.762	2.578	1.600	22.662	573.580	606.540
39	3.950	1.924	0.773	2.710	1.403	22.325	567.180	533.500

Ref. No.	h_1	h_2	h_3	h_4	h_5	NI	mg / m³ STP_{dry} at 6 % O_2	
							$NO_{x_{Pred}}$	$NO_{x_{Ref}}$
40	1.840	1.780	0.949	3.370	1.544	16.163	450.094	435.437
41	1.799	1.768	0.947	3.347	1.542	15.530	438.061	425.472
42	1.799	1.806	0.996	3.559	1.548	17.820	481.573	504.343
43	1.871	1.774	0.944	3.362	1.543	16.262	451.984	459.446
44	1.901	1.772	0.740	2.623	1.534	10.026	333.486	304.627
45	1.953	1.808	0.799	2.674	1.537	11.598	363.355	336.412
46	1.839	1.774	0.876	3.115	1.430	12.741	385.071	389.755
47	1.981	1.791	0.892	3.155	1.432	14.297	414.639	410.082
48	1.891	1.776	0.746	2.625	1.506	9.893	330.962	316.640
49	1.868	1.772	0.805	2.673	1.541	10.988	351.777	372.887
50	1.785	1.769	0.830	2.698	1.537	10.870	349.532	355.922
51	1.870	1.787	0.949	2.906	1.549	14.285	414.418	459.676
52	1.858	1.752	0.711	2.614	1.534	9.275	319.217	314.436
53	1.785	1.780	0.734	2.619	1.534	9.372	321.062	330.320
54	1.785	1.782	0.957	3.401	1.546	15.996	446.927	465.719
55	1.870	1.769	0.701	2.615	1.530	9.289	319.485	309.301
56	1.858	1.967	0.863	2.905	1.549	14.198	412.771	396.811
57	1.858	1.837	0.690	2.614	1.531	9.427	322.119	322.422
58	2.026	1.849	0.734	2.635	1.536	11.129	354.451	327.079
59	1.969	1.808	0.690	2.614	1.507	9.686	327.043	319.763
60	4.329	1.967	0.795	1.594	1.643	17.740	480.064	440.000
61	4.329	2.093	0.780	1.594	1.645	18.531	495.081	468.000

Ref. No.	h_1	h_2	h_3	h_4	h_5	NI	mg / m³ STP_{dry} at 6 % O_2	
							$NO_{x_{Pred}}$	$NO_{x_{Ref}}$
62	4.329	1.915	0.801	1.594	1.643	17.390	473.413	440.000
63	4.329	1.984	0.793	1.594	1.661	18.039	485.732	462.000
64	4.329	1.932	0.799	1.517	1.861	18.863	501.397	514.000
65	3.764	1.986	0.793	1.587	1.644	15.466	436.856	421.000
66	3.764	2.066	0.783	1.587	1.644	15.893	444.962	417.000
67	3.764	1.916	0.801	1.587	1.644	15.068	429.293	401.000
68	3.764	2.003	0.791	1.587	1.644	15.558	438.602	427.000
69	3.764	2.019	0.789	1.509	1.873	16.956	465.171	425.000
70	3.220	2.005	0.791	1.587	1.646	13.338	396.426	398.000
71	3.220	2.068	0.783	1.587	1.646	13.624	401.862	407.000
72	3.220	1.918	0.801	1.587	1.648	12.931	388.691	392.000
73	3.220	2.005	0.791	1.587	1.646	13.338	396.426	396.000
74	3.220	1.988	0.793	1.510	1.864	14.287	414.462	452.000
75	3.962	1.765	0.817	1.587	1.643	14.884	425.788	389.000
76	3.962	1.970	0.795	1.587	1.643	16.171	450.250	414.000
77	3.962	2.182	0.766	1.587	1.643	17.275	471.228	468.000
78	4.087	1.952	0.797	1.586	1.643	16.569	457.814	418.000
79	4.087	2.136	0.774	1.586	1.643	17.605	477.493	442.000
80	4.087	2.227	0.757	1.586	1.643	17.956	484.165	479.000
81	3.213	1.824	0.811	1.587	1.640	12.365	377.938	405.000
82	3.213	1.987	0.793	1.587	1.640	13.179	393.396	435.000
83	3.213	2.183	0.766	1.587	1.640	13.992	408.842	485.000

Ref. No.	h_1	h_2	h_3	h_4	h_5	NI	mg / m³ STP$_{dry}$ at 6 % O$_2$	
							$NO_{x_{Pred}}$	$NO_{x_{Ref}}$
84	2.738	1.809	0.812	1.590	1.642	10.505	342.591	323.000
85	2.738	2.057	0.784	1.590	1.642	11.539	362.242	357.000
86	4.943	1.740	0.819	1.599	1.645	18.529	495.058	478.000
87	4.943	1.856	0.807	1.599	1.645	19.481	513.138	495.000
88	4.943	2.104	0.778	1.599	1.645	21.295	547.610	539.000
89	3.134	1.923	0.800	1.589	1.642	12.582	382.049	413.000
90	3.134	2.088	0.781	1.589	1.642	13.326	396.186	442.000
91	3.134	2.237	0.754	1.589	1.642	13.796	405.132	511.000
92	3.357	1.808	0.812	1.587	1.643	12.855	387.253	387.000
93	3.357	2.041	0.787	1.587	1.643	14.050	409.941	439.000
94	3.357	2.186	0.766	1.587	1.643	14.653	421.398	483.000
95	3.632	1.844	0.808	1.586	1.643	14.106	411.023	392.000
96	3.632	2.037	0.787	1.586	1.643	15.172	431.263	428.000
97	3.632	2.194	0.764	1.586	1.643	15.867	444.477	478.000
98	3.498	1.682	0.825	1.586	1.643	12.646	383.281	422.000
99	3.498	1.878	0.805	1.586	1.643	13.778	404.788	464.000
100	4.353	1.682	0.825	1.586	1.644	15.752	442.280	442.000
101	4.353	1.821	0.811	1.586	1.644	16.766	461.551	472.000
102	4.353	1.950	0.797	1.586	1.644	17.647	478.296	483.000
103	4.691	1.642	0.829	1.590	1.643	16.671	459.755	482.000
104	4.691	1.879	0.805	1.590	1.643	18.529	495.060	530.000
105	4.883	1.641	0.829	1.589	1.642	17.335	472.359	453.000

Ref. No.	h_1	h_2	h_3	h_4	h_5	NI	mg / m³ STP$_{dry}$ at 6 % O$_2$	
							$NO_{x_{Pred}}$	$NO_{x_{Ref}}$
106	4.883	1.878	0.805	1.589	1.642	19.266	509.051	513.000
107	4.883	2.094	0.780	1.589	1.642	20.806	538.319	551.000
108	0.893	1.998	0.726	5.607	1.245	9.040	314.760	350.270
109	0.828	2.010	0.753	5.606	1.193	8.389	302.393	275.130
110	0.843	2.254	0.739	6.259	1.145	10.063	334.202	325.007
111	2.769	1.950	0.668	3.332	1.213	14.576	419.945	420.000
112	1.153	2.242	0.704	4.720	1.627	13.975	408.523	373.000
113	1.136	2.255	0.710	4.750	1.594	13.776	404.749	390.000
114	1.136	2.244	0.722	4.858	1.556	13.914	407.372	439.000
115	1.142	2.206	0.730	4.976	1.523	13.935	407.772	387.000
116	1.162	2.106	0.740	5.201	1.490	14.048	409.918	429.000
117	1.101	1.962	0.750	5.556	1.471	13.236	394.486	478.000
118	7.015	1.945	0.717	1.440	1.227	17.297	471.643	470.000
119	1.078	1.754	0.629	0.589	1.362	0.955	161.139	147.000
120	1.042	1.932	0.624	0.588	1.276	0.944	160.933	155.000
121	1.073	1.912	0.634	0.588	1.225	0.938	160.822	150.000
122	1.078	1.817	1.000	4.435	1.358	11.797	367.134	367.000
123	4.478	1.905	0.854	2.151	2.065	32.348	757.604	746.340
124	4.478	1.910	0.849	2.151	2.056	32.109	753.063	732.940
125	4.478	1.857	0.874	2.151	2.022	31.617	743.718	777.870
126	4.478	1.859	0.957	2.552	2.043	41.541	932.277	906.530
127	4.478	1.811	0.928	2.354	2.011	35.607	819.534	784.640

Ref. No.	h_1	h_2	h_3	h_4	h_5	NI	mg / m³ STP_{dry} at 6 % O_2	
							$NO_{x_{Pred}}$	$NO_{x_{Ref}}$
128	3.553	1.874	0.862	2.170	1.933	24.067	600.273	644.750
129	3.553	1.871	0.863	2.170	1.945	24.202	602.829	620.170
130	3.553	1.873	0.946	2.558	1.948	31.363	738.896	713.910
131	3.553	1.899	0.896	2.347	1.940	27.512	665.737	671.720
132	4.478	2.104	0.810	2.151	1.730	28.400	682.599	638.760
133	4.478	2.120	0.774	2.012	1.537	22.716	574.606	632.940
134	3.553	1.873	0.903	2.347	1.932	27.250	660.750	659.320
135	1.789	1.927	0.610	5.897	1.441	17.853	482.201	458.400
136	1.837	2.025	0.853	6.473	1.357	27.848	672.112	698.200
137	1.747	2.228	0.931	7.463	1.227	33.189	773.589	771.300
138	2.706	1.958	0.616	2.517	1.557	12.789	386.000	386.000
139	2.090	1.950	0.613	1.728	1.305	5.632	250.011	250.000
140	1.184	2.206	0.327	3.399	1.448	4.209	222.971	223.000
141	1.184	1.926	0.518	2.676	1.449	4.579	229.997	230.000
142	1.190	1.726	0.811	1.528	3.370	8.579	305.998	306.000

APPENDIX 4 – REFERENCE DATA OF FPP–2

Table A4–1. General FPP–2 reference data

Tangential–fired boiler (606 MWe) located in USA, Texas		
System design		
Burner elevations	6	–
Furnace depth	16.05	m
Furnace width	19.81	m
Furnace height	45.30	m
Burner elevation vertical spacing	2.50	m
Distance between burner elevation 1 and hopper	6.00	m
Distance between burner elevation 6 and CCOFA	2.50	m
Width of slagging slot	1.20	m
Hopper height	10.604	m
General operational settings		
Primary NO_x level (BE 1– 5, BE 1–4&6, BE 2–6)	785, 850, 860	mg / m³ STP_{dry}[1]
Air ratio (miscellaneous)	0.05	–
Secondary air temperature	370.65	°C
Classifier outlet temperature	65.35	°C
Air / coal ratio	2.15	–
Average combustion temperature	1,400	°C

---

[1] Corrected at 6 % O_2.

Table A4–2. FPP–2 reference coal compositions

Reference test No. acc. to Hwang [202]	LHV	Analysis results in wt.–% on a as received basis							
		Proximate			Ultimate				
	MJ / kg	VM	W	Ash	C	H	S	O	N
2	19.092	31.47	27.39	5.16	51.47	2.65	0.30	12.34	0.69
3A	19.014	31.48	27.61	5.13	50.86	2.58	0.30	12.84	0.68
3C	19.014	31.48	27.61	5.13	50.86	2.58	0.30	12.84	0.68
4	19.317	30.90	26.88	5.42	52.77	2.27	0.35	11.64	0.67
5	18.848	30.73	27.63	5.14	51.85	2.65	0.24	11.82	0.67
6	18.610	30.85	28.88	4.99	50.44	2.61	0.33	11.99	0.76
7	18.429	30.77	30.18	4.62	49.71	2.58	0.32	11.90	0.69
8	18.728	30.63	28.14	4.85	51.21	2.58	0.27	12.21	0.74
9	19.014	31.22	28.10	4.96	51.80	2.67	0.33	11.44	0.70
10A	18.801	30.99	28.54	5.11	51.74	2.56	0.32	11.05	0.68
10B	18.760	30.58	29.55	5.18	50.15	2.56	0.30	11.63	0.63
10C	18.754	31.48	28.39	5.17	51.29	2.47	0.30	11.64	0.74
10D	18.938	31.18	27.88	4.77	52.64	2.52	0.30	11.23	0.66
11A	18.760	30.58	29.55	5.18	50.15	2.56	0.30	11.63	0.63
11B	18.760	30.58	29.55	5.18	50.15	2.56	0.30	11.63	0.63
12	18.754	31.48	28.39	5.17	51.29	2.47	0.30	11.64	0.74
13A	18.938	31.18	27.88	4.77	52.64	2.52	0.30	11.23	0.66
13B	18.938	31.18	27.88	4.77	52.64	2.52	0.30	11.23	0.66
14	18.524	29.98	28.91	4.87	51.94	2.52	0.29	10.76	0.71
15	18.876	30.62	27.45	5.24	53.13	2.66	0.31	10.53	0.68

Table A4–3. FPP–2 reference NO_x emissions for all tests

Reference test No. acc. to Hwang [202]	Burner elevation	Boiler load	Fuel rating	Oxygen level	NO_x economizer outlet	
		MWe	MWt	%, dry	ppm	mg / m³ STP_{dry}[2]
2	2 – 6	607	1,567.32	2.56	261	435.437
3A	2 – 6	607	1,567.32	2.49	256	425.472
3C	2 – 6	607	1,567.32	2.70	300	504.343
4	2 – 6	607	1,567.32	2.52	276	459.446
5	1 – 5	607	1,567.32	2.52	183	304.627
6	1 – 5	607	1,567.32	2.71	200	336.412
7	1 – 4& 6	608	1,569.90	2.53	234	389.755
8	1 – 4& 6	607	1,567.32	2.62	245	410.082
9	1 – 5	579	1,500.00	2.54	190	316.640
10A	1 – 5	610	1,575.06	2.52	224	372.887
10B	1 – 5	607	1,567.32	2.50	214	355.922
10C	1 – 5	609	1,572.48	2.60	275	459.676
10D	1 – 5	609	1,572.48	2.42	190	314.436
11A	1 – 5	610	1,575.06	2.56	198	330.320
11B	2 – 6	609	1,572.48	2.57	279	465.719
12	1 – 5	608	1,569.90	2.50	186	309.301
13A	1 – 5	608	1,569.90	3.63	224	396.811
13B	1 – 5	607	1,567.32	2.87	190	322.422
14	1 – 5	607	1,567.32	2.94	192	327.079
15	1 – 5	582	1,505.24	2.72	190	319.763

---

[2] Corrected at 6 % O_2.

Table A4–4. FPP–2 air volume flow according to damper opening[3]

Reference test No. acc. to Hwang [202]	Damper opening		Air volume flow		OFA share of total air	Air ratio	
	Aux. air	OFA	Aux. air	OFA		OFA	Total
2	72.5 %	80 %	94 %	96 %	5.8 %	0.065	1.137
3A	72.0 %	100 %	94 %	100 %	6.0 %	0.068	1.133
3C	100.0 %	10 %	99 %	45 %	0.5 %	0.005	1.146
4	71.6 %	80 %	94 %	96 %	6.2 %	0.071	1.136
5	54.2 %	80 %	81 %	96 %	18.7 %	0.212	1.135
6	58.6 %	80 %	86 %	96 %	13.9 %	0.160	1.147
7	58.3 %	80 %	85 %	96 %	14.4 %	0.164	1.136
8	60.7 %	80 %	87 %	96 %	12.5 %	0.142	1.141
9	54.5 %	80 %	81 %	96 %	18.2 %	0.207	1.136
10A	59.7 %	80 %	86 %	96 %	13.4 %	0.153	1.135
10B	59.2 %	50 %	87 %	89 %	11.6 %	0.131	1.134
10C	70.3 %	10 %	93 %	46 %	3.2 %	0.037	1.14
10D	51.5 %	80 %	78 %	96 %	21.1 %	0.240	1.134
11A	53.9 %	80 %	80 %	96 %	19.2 %	0.218	1.137
11B	74.4 %	80 %	95 %	96 %	4.8 %	0.055	1.138
12	51.0 %	80 %	77 %	96 %	22.1 %	0.250	1.134
13A	67.0 %	80 %	91 %	96 %	9.1 %	0.110	1.207
13B	50.8 %	80 %	76 %	96 %	23.0 %	0.267	1.157
14	53.8 %	80 %	80 %	96 %	19.2 %	0.223	1.161
15	50.0 %	80 %	76 %	96 %	23.0 %	0.264	1.147

---

[3] According to Figure 34.

CURRICULUM VITAE

Name	Niko Hachenberg
Address	Neichener Str. 26 51491 Overath, Germany
DOB	Bergisch Gladbach, Germany – September 28, 1981
Marital Status	married since 2008, 1 child (2010)
Education	University of Louisville, 2014 Ph.D. Industrial Engineering
	University of Louisville, 2011 M.S. Industrial Engineering
	University of Applied Science Cologne, 2007 Dipl.–Wirt.–Ing. (FH) Business Engineering
	University of Applied Science Cologne, 2006 Dipl.–Ing. (FH) Mechanical Engineering
Professional Career	Steinmueller Engineering GmbH (since 2009) Applications Manager
	Steinmueller Engineering GmbH (2007 – 2009) Project Manager, Plant Planning
	Postel Pressure Casting GmbH (2005 – 2007) Process Engineer
	Bläsius Bedachungen GmbH (1998 – 2001) Professional Roofer